ROLE OF THE CTLA-4 C-TERMINUS IN REGULATING ITS INTRACELLULAR TRAFFICKING

SATDIP KAUR

A thesis submitted to the
University of Birmingham
for the degree of
DOCTOR OF PHILOSOPHY

School of Immunity and Infection
College of Medical and Dental Sciences
The University of Birmingham
Edgbaston
B15 2TT

March 2014

ABSTRACT

CTLA-4 is an important inhibitor of T cell immune responses. The location of CTLA-4 in intracellular vesicles is the most dominating aspect of its biology, yet the significance of this at the functional level remains to be completely understood. I have therefore investigated the role of the CTLA-4 cytoplasmic domain in the intracellular trafficking of the receptor with particular emphasis on sorting signals encoded within this domain.

We found that CTLA-4 was located in punctate intracellular vesicles in transfected cells, activated T cells and in regulatory T cells. CTLA-4 internalisation from the cell surface was clathrin dependent and was driven by the YVKM motif encoded within the cytoplasmic domain. Post-internalisation CTLA-4 co-localised with markers of late endosomes. Since the degradation process may serve as one of the mechanisms to regulate CTLA-4 expression we investigated this further and found that ubiquitination of intracellular lysine residues targets CTLA-4 to lysosomes. The ability of CTLA-4 to recycle was dependent on the YVKM motif and subtle changes in this motif reduced recycling efficiency. Moreover, in the absence of lysine residues CTLA-4 recycling was enhanced. CTLA-4 transendocytosis was conserved through evolution but the exact sorting signals required for this function remain to be identified. Overall this thesis emphasises the importance of the CTLA-4 cytoplasmic domain in regulating its intracellular trafficking.

DEDICATION

This thesis is dedicated to my family and friends for their invaluable support and inspiration throughout the four years of this PhD.

ACKNOWLEDGEMENTS

I would like to thank my supervisor Professor David Sansom for the support and guidance he provided throughout the four years of my PhD. A huge thank you to members of the Sansom lab past and present who have made this an enjoyable experience and without whom this would not have been possible. In particular I would like to thank Dr Omar Qureshi for helping me design experiments and learn how to use a confocal microscope. His regular insight and input into my project really helped me to stay motivated and has further strengthened my ambition to pursue a career in the cell biology field. I would also like to take this opportunity to thank all the girls in the IBR who started their PhD at the same time as me. We all have shared this experience together and it is finally coming to an end. I would also like to thank the College of Medical and Dental Sciences at the University of Birmingham for funding my project.

Finally I would like to thank my mum, dad, my sisters Vicky and Randip, my brother Amanjit and a new member of our family my nephew Avi. They have been there for me during the highs and lows of my PhD and never gave up on me. Their love and support has turned this dream into a reality and I am forever grateful.

CONTENTS PAGE

LIST OF FIGURES

LIST OF TABLES

ABBREVIATIONS

1MT	1-methyltryptophan
Ab	Antibody
Ag	Antigen
AP	Adaptor Protein
APC	Antigen-presenting cells
ARF1	ADP-ribosylation factor 1
BTLA	B and T Lymphocyte Activator
Cbl-b	Casitas B-lineage lymphoma proto-oncogene b
CCV	Clathrin-coated vesicle
CDC42	Cell division cycle 42
CHO	Chinese hamster ovary
CHX	Cycloheximide
CoRs	Co-stimulatory receptors
CoLs	Co-stimulatory ligands
cSMAC	Central supramolecular activation cluster
CTLA-4	Cytotoxic T Lymphocyte Associated-4
DC	Dendritic Cells
DP	Double positive
DN	Double negative
E1	Ubiquitin-activating enzymes
E2	Ubiquitin-conjugating enzymes
E3	Ubiquitin ligases

EEA1	Early endosome antigen 1
EGFR	Epidermal Growth Factor Receptor
Eps15	Epidermal growth factor receptor substrate 15
ESCRT	Endosomal sorting complex required for transport
FOXP3	Forkhead box P3
GFP	Green fluorescent protein
GLUT4	Glucose transporter type 4
GPCR	G-protein coupled receptor
GPI	Glycosphosphatidylinositol
GRAIL	Gene related to anergy in lymphocytes
GDP	Guanosine Diphosphate
GEF	GDP/GTP exchange factor
GTP	Guanosine Triphosphate
HECT	Homologous to E6-AP carboxyl terminus
Hrs	Hepatocyte growth-factor regulated tyrosine kinase substrate
ICOS	Inducible T cell co-stimulator
IDO	Indoleamine 2,3-dioxygenase
IFNAR1	Interferon-α receptor 1 subunit
IgSF	Immunoglobulin superfamily
IgG	Immunoglobulin G
IL	Interleukin
ILV	Intraluminal vesicles
IPEX	Immunodysregulation Polyendocrinopathy Enteropathy X- linked syndrome
ITAM	Immunoreceptor Tyrosine Based Activation Motif

ITCH	Itchy homologue E3 ubiquitin E3 ligase
LAMP1	Lysosomal-associated membrane protein 1
LAP	Lysosomal acid phosphatase
LDL	Low-density lipoprotein
MHC	Major histocompatibility complex
MTOC	Microtubule organising centre
MVBs	Multivesicular bodies
NH_4Cl	Ammonium chloride
NMDA	N-methyl-D-aspartate receptor
NF-AT	Nuclear Factor of Activated T cell
NFκB	Nuclear Factor Kappa B
PAR	Protease-activated receptor
PBMC	Peripheral Blood Mononuclear Cells
PD-1	Programmed Cell Death-1
$PtdIns(3,5)P_2$	Phosphatidylinositol-4,5-bisphosphate
$PtdIns(3,4,5)P_3$	Phosphatidylinositol-3,4,5-triphosphate
RA	Rheumatoid arthritis
RING	Really interesting new gene
SCID	Severe combined immunodeficiency
SP	Single positive
TCR	T Cell Receptor
Tf	Transferrin
TfR	Transferrin receptor
TGF-β	Transforming growth factor-β

TGN	Trans-Golgi network
Treg	Regulatory T cell
TSG101	Tumor susceptibility gene 101
USP8	Ubiquitin-specific protease 8
VpS4	Vacuolar protein sorting 4
WBCs	White blood cells
WT	Wild-type
ZAP70	Zeta-chain associated protein kinase

PUBLICATIONS

Appendix

Kaur S, Qureshi OS, Sansom DM. Comparison of the Intracellular Trafficking Itinerary of CTLA-4 Orthologues. PLOS 2013;8(4).

Jeffery LE, Wood AM, Qureshi OS, Hou TZ, Gardner D, Briggs Z, **Kaur S**, Raza K, Sansom DM. Availability of 25-hydroxyvitamin D(1) to APCs controls the balance between regulatory and inflammatory T cell responses. J Immunol 2012;189(11):5155-5164.

Qureshi OS, **Kaur S**, Hou TZ, Jeffery LE, Poulter NS, Briggs Z, Kenefeck R, Willox AK, Royle SJ, Rappoport JZ, Sansom DM. Constitutive clathrin-mediated endocytosis of CTLA-4 persists during T cell activation. J Biol Chem 2012;287(12):9429-9440.

Qureshi OS, Zheng Y, Nakamura K, Attridge K, Manzotti C, Schmidt EM, Baker J, Jeffery LE, **Kaur S**, Briggs Z, Hou TZ, Futter CE, Anderson G, Walker LS, Sansom DM. Trans-endocytosis of CD80 and CD86: a molecular basis for the cell-extrinsic function of CTLA-4. Science 2011;332(6029):600-603.

1.0 INTRODUCTION

1.1 Introduction to immune regulation

The immune system is made up of a variety of effector cells and molecules that protect the body from infectious agents and the damage they cause, and from other harmful substances (Delves and Roitt, 2000a; Murphy, 2008). The immune system fulfills four tasks to protect an individual against disease. The first task is immunological recognition. The key players to detect the infection are the white blood cells (WBCs) of the innate immune system, which provide an immediate response, and the lymphocytes of the adaptive immune system. The second task is to control the infection, and if at all possible eliminate it. This involves immune effector functions such as the complement system, antibodies (Abs), lymphocytes, and other WBCs. The third task is self-regulation. The immune response must be kept under control so as to prevent any damage to the body, as a failure to regulate contributes to conditions such as autoimmune disease and allergy (Murphy, 2008). The fourth task is to provide the individual with protection against disease caused by the same pathogen. The ability of the adaptive immune system to generate immunological memory allows an individual to make an immediate and stronger response after re-exposure to the same infectious agent (Murphy, 2008). In the following sections I will consider the major aspects of the adaptive immune system as it pertains to T cell regulation, which is the topic of this thesis.

1.1.1 T lymphocyte development

T lymphocytes, also known as T cells, develop from a common progenitor in the bone marrow and migrate through the blood to the thymus (Schwarz and Bhandoola, 2006). The thymus provides a

specialised and organised microenvironment for mature T cell development (Gray et al., 2005). Most steps in T cell development take place in the thymic cortex, whereas the medulla mainly contains mature T cells. T cell receptors (TCR) are encoded by TCR genes assembled by somatic recombination (Murphy, 2008). The TCR is composed of two disulphide-linked polypeptide chains, an α-chain and a β-chain (**figure 1.1**) (Jones and Zhuang, 2007). At the CD4 and CD8 double-negative (DN) stage, TCR gene rearrangement gives rise to $\alpha\beta$ or $\gamma\delta$ progenitors. A small proportion of the $\alpha\beta$ CD4 and CD8 DN thymocytes expand to give a large number of CD4 and CD8 double positive (DP) thymocytes. Each of these thymocytes undergoes somatic recombination of the TCR genes generating a broad repertoire of distinct $\alpha\beta$ TCRs with random specificity (Chien et al., 1984). DP cells undergo selection for their ability to recognise self-peptides in association with self-major histocompatibility complex (MHC) molecules. If successful, the cells are rescued from programmed cell death and mature into single positive (SP) CD4 or CD8 cells (Goodnow et al., 2005; Murphy, 2008).

1.1.2 Antigen presentation to T cells

T cells encounter and respond to antigen (Ag) in the peripheral lymphoid organs – the lymph nodes, spleen, and the mucosal lymphoid tissues. Lymphocyte recirculation through these tissues ensures contact with pathogen Ags. The TCR recognises Ag in the form of a processed foreign peptide bound to a self-MHC molecule on the surface of antigen-presenting cells (APCs) such as dendritic cells (DCs) (Inaba et al., 1983), B cells (Chen and Jensen, 2008) and macrophages (Davis et al., 1998). There are two different classes of MHC: MHC class I that activate $CD8^+$ T cells, and MHC class II that activate $CD4^+$ T cells. MHC class I molecules present peptides derived from proteins synthesised in the cell cytoplasm and display fragments of viral proteins. MHC class II molecules present peptides derived from phagocytosed proteins and display fragments of Ags engulfed by professional APCs such as DCs.

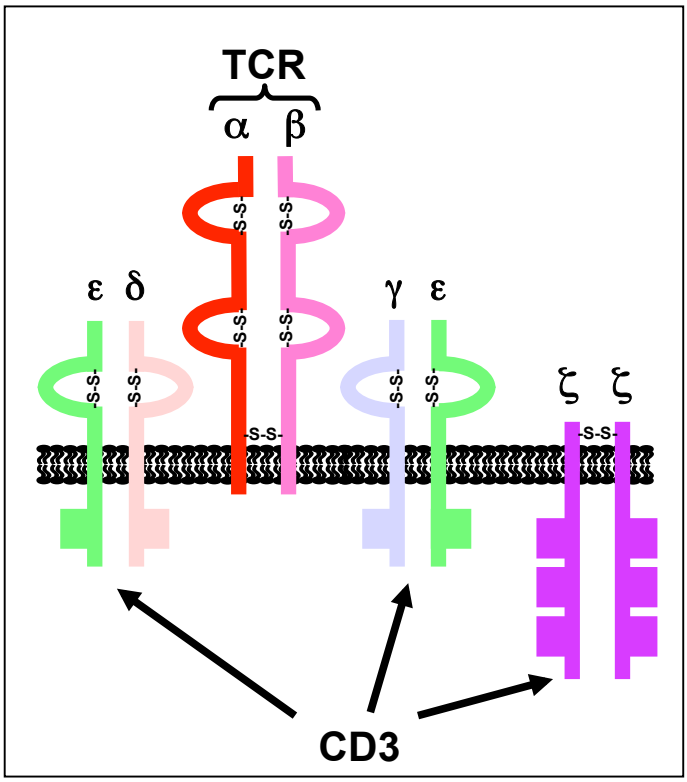

Figure 1.1 The TCR/CD3/ζ complex. The TCR complex consists of the TCR-α and -β chains, ζ-chain accessory molecule and the CD3 signal transduction complex. The α and β chain each contain two ITAM (immunoreceptor tyrosine-based activation motif) domains. The CD3 T cell co-receptor consists of four chains, a CD3γ chain, a CD3δ chain and two CD3ε chains. Taken from (de Felipe, 2004).

1.1.3 Two signal model of T cell activation

T cells require two signals for optimal activation (**figure 1.2**). Signal one is provided by the TCR binding to peptide-MHC complexes presented on the surface of APCs. Since the TCR has a short cytoplasmic domain it lacks the signalling motifs required to activate downstream signalling pathways, which ultimately lead to T cell activation (Delves and Roitt, 2000b). In order to achieve this, the TCR associates with the CD3 co-receptor (Clevers et al., 1988). This association leads to the activation of the transcription factors AP-1 (Baier-Bitterlich et al., 1996), Nuclear factor of activated T cells (NF-AT) (Shaw et al., 1988) and Nuclear factor Kappa B (NF-κB) (Schwartz, 1992). Importantly this results in the production of cytokines of which interleukin-2 (IL-2) is required to initiate and maintain T cell proliferation. Signal two is best known as the co-stimulatory signal. This signal is just as important as signal one, and is provided by the cell surface co-stimulatory CD28 receptor binding to CD80 or CD86 ligands on the surface of APCs. CD28 co-stimulation increases IL-2 production, leads to T cell proliferation and prevents cell apoptosis. The importance of CD28 co-stimulation is highlighted by the phenotype of CD28 knockout mice. Such mice have decreased sensitivity to antigen, reduced IL-2 production and are unable to maintain T cell proliferation (Shahinian et al., 1993). A different outcome however can result if the T cell only receives signal one in the absence of signal two. In such circumstances T cells become unresponsive (anergic) or can undergo apoptosis (Schwartz, 1996). The ligation of co-stimulatory receptors alone also fails to result in T cell activation since signal two is dependent on signal one.

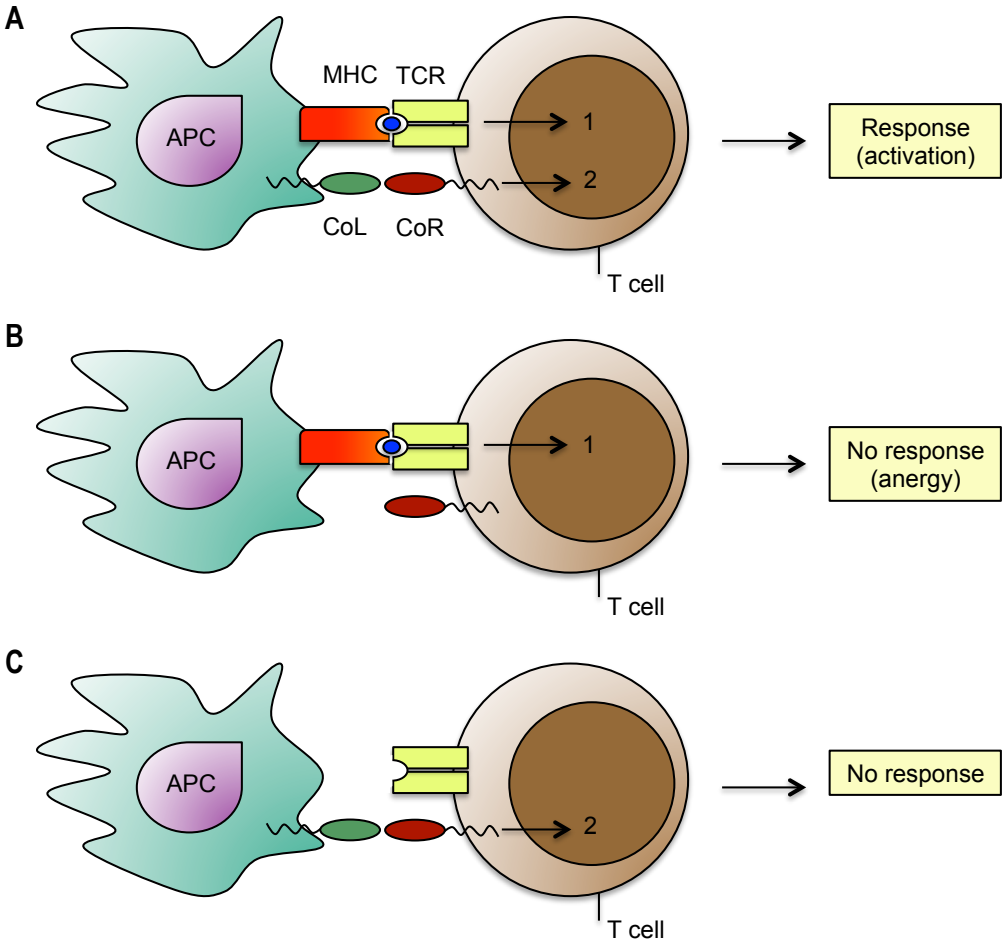

Figure 1.2 The two signal model of T cell activation. **(A)** The TCR recognises Ag in the form of a peptide-MHC complex presented on the surface of APCs (signal 1). T cells require a second signal provided by co-stimulatory receptors (CoRs) and ligands (CoLs). Both signals are required for efficient T cell activation, proliferation, differentiation and cytokine production. **(B)** In the absence of co-stimulation, T cells become anergic or undergo apoptosis. **(C)** In the absence of TCR ligation T cells fail to respond.

1.1.4 Central tolerance

The immune system must distinguish between self-reactive and non-reactive lymphocytes to generate a state of self-tolerance (Murphy, 2008; Xing and Hogquist, 2012). T cell tolerance is important, not only because T cells recognising self-Ag can cause enormous damage of healthy tissue, but T cell tolerance has an impact on B cell tolerance, as B cells require T cell help in Ab responses (Xing and Hogquist, 2012). Thus, a failure or breakdown of T cell tolerance can result in autoimmune disease. T cell tolerance begins in the thymus once a T cell progenitor forms and expresses a TCR. This is referred to as "central tolerance'. Ultimately, the fate of the thymocyte is determined by the affinity of the TCR for self-peptide:self-MHC complexes. Thymocytes that do not recognise self-peptide:self-MHC complexes die by neglect, thymocytes with a weak affinity TCR undergo positive selection and those with a high affinity TCR undergo negative selection (Laufer, 2008; Murphy, 2008; Xing and Hogquist, 2012).

1.1.5 Peripheral tolerance: Role of Regulatory T cells (Tregs)

Since the thymus does not express all self-Ags required to eliminate self-reactive T cells, additional tolerance mechanisms exist in the periphery. This is referred to as "peripheral tolerance". Anergy and deletion have long been recognised as the primary mechanisms used in the periphery to eliminate self-reactive T and B cells. However evidence is now emerging that the thymic $CD4^+$ $CD25^+$ Tregs play an important role in maintaining self-tolerance. Tregs are characterised by the expression of CD4, CD25, the transcription factor Forkhead box P3 (FOXP3) and by the constitutive expression of cytotoxic T lymphocyte antigen-4 (CTLA-4).

Thymic Tregs encode TCRs that recognise self-peptides and studies suggest that recognition of self is central to their role in preventing other T cells from attacking self (Toda and Piccirillo, 2006). Such ideas stem from observations that autoimmunity can result if nude mice, which lack T cells, are given $CD4^+CD25^-$ T cells without a $CD25^+$ regulatory population (Sakaguchi et al., 2007). Moreover, a mutation in the Treg transcription factor FOXP3 causes the disease scurfy in mice. Such mice have pathology suggestive of poor $CD4^+$ T cell regulation where $CD4^+$ cells are over-proliferative and cause multi-organ infiltration again highlighting the central role Tregs play in preventing autoimmune disease. A similar phenotype is also seen in humans with Immunodysregulation, Polyendocrinopathy, and Enteropathy X-linked (IPEX) syndrome, a disease resulting from mutations in the FOXP3 gene. The importance of the CTLA-4 receptor in preventing autoimmune disease is illustrated in mice genetically deficient in *CTLA-4*. Such mice develop a lymphoproliferative disease, where T cells accumulate in peripheral lymphoid organs and the mice die 3-5 weeks after birth (Tivol et al., 1995; Waterhouse et al., 1995). In humans, type 1 diabetes, Grave's disease and celiac disease are a few of many autoimmune diseases associated with CTLA-4 deficiency (Ueda et al., 2003).

1.1.5.1 Role of Immunosuppressive Cytokines

The role of the immunosuppressive cytokines, IL-10 and transforming growth factor-β (TGF-β) in Treg-mediated suppression in the periphery remains to be completely understood. The importance of IL-10 in Treg mediated suppression has been shown using inflammatory disease models, where severe combined immunodeficiency (SCID) mice developed inflammatory bowel disease after transfer of $CD4^+CD25^-CD45RB^{high}$ T cells. However the co-transfer of $CD4^+CD25^+$ or $CD4^+CD45RB^{low}$ T cells prevented disease development. Moreover when the mice were injected with a neutralising anti-IL-10 receptor monoclonal Ab they developed inflammatory bowel disease (Annacker et al., 2003). In this

situation, IL-10 production by Tregs compensated for the lack of IL-10 production by the $CD4^{+}CD25^{-}CD45RB^{high}$ T cells in order to regulate immune homeostasis, an effect that was abolished by the anti-IL-10 receptor monoclonal Ab.

Mice deficient in TGF-β1 develop T cell mediated autoimmune disease within a few weeks of birth (Li et al., 2006), similar to that observed in CTLA-4 knockout mice. Tregs produce copious amounts of both membrane-bound and soluble TGF-β. The importance of this cytokine in Treg mediated suppression has been demonstrated in human T cells where by blocking TGF-β suppression T cell proliferation was partially abrogated (Levings et al., 2002). However, data presented by other groups failed to demonstrate a role for TGF-β in Treg mediated suppression (Godfrey et al., 2005; Oberle et al., 2007), suggesting that a combination of suppression mechanisms may operate at one time, which could be influenced by factors such as the site of the immune response and the activation status of the Treg (Schmidt et al., 2012).

1.2 The B7-1/B7-2-CD28/CTLA-4 pathway

CD28 and CTLA-4 are glycoproteins that belong to the immunoglobulin superfamily (IgSF) (Sharpe and Freeman, 2002). Both are expressed on T cells and are important in shaping immune responses. CD28 and CTLA-4 share 30% homology at the amino acid level and use a conserved MYPPPY motif located in the extracellular domain to interact with CD80 (B7-1) and CD86 (B7-2) expressed on the surface of APCs (Sharpe and Freeman, 2002, Peggs et al., 2008). However the two molecules differ in terms of their function. While CD28 is important in promoting T cell responses, CTLA-4 acts as an inhibitor (Carreno and Collins, 2002; Peggs et al., 2008; Sansom and Walker, 2006; Sharpe and Freeman, 2002).

CD28 and CTLA-4 expression on T cells is highly distinct (Malmstrom et al., 2005; Murphy, 2008). While CD28 is constitutively expressed on the plasma membrane of both naïve and activated T cells, (Gross et al., 1990), CTLA-4 expression is induced after TCR signaling (Lindsten et al., 1993). CTLA-4 expression can be detected after 6hours of TCR engagement and levels peak around 36hours. Moreover, both CD28 and IL-2 can further upregulate CTLA-4 levels. Staining for CTLA-4 expression reveals that it is predominantly located in intracellular vesicles and it is trafficked from these compartments to the cell surface upon TCR activation. As such, CTLA-4 expression at the cell surface appears to be dependent on the strength of the TCR signal as opposed to resulting from new protein synthesis. This situation provides the best mechanism to balance both stimulatory and inhibitory signals, where although CD28 binding to ligand stimulates T cell activation, once activated the T cells upregulate CTLA-4, which acts to inhibit T cell activation.

1.2.1 Other B7 and CD28 family co-stimulatory systems

Although the B7-1/B7-2-CD28/CTLA-4 represents the best and most recognised co-stimulatory pathway new members of the B7-CD28 family have been discovered. These include the CD28 family members ICOS (inducible T cell co-stimulator), PD-1 (programmed death-1) and B and T lymphocyte attenuator (BTLA) that interact with their respective B7 ligands ICOS-L (B7-H2), PD-L1 (B7-H1), PD-L2 (B7-DC), B7-H3 and B7-H4 (Carreno et al., 2005). The receptors have been found on leukocytes whilst both hematopoietic and non-hematopoietic cells express the ligands. Studies in knockout mice have been key in identifying whether these receptor-ligand pairs regulate T cell activation and whether they have a stimulatory or inhibitory effect. In the absence of these molecules, mice develop autoimmune disease or an immunosuppressive disorder. The importance of these receptor-ligand pairs on the basis of their function and requirement is ongoing but there are differences between their expression patterns when

compared to the B7-1/B7-2-CD28/CTLA-4 (Carreno et al., 2005). For instance ICOS is upregulated rapidly after T cell activation suggesting that co-stimulation is provided to activated T cells and not to naïve T cells. Thus, these differences may allow for finer tuning of T cell activation.

1.2.2 Interactions between CD28, CTLA-4 and their ligands

CD28 and CTLA-4 are homodimers; however whereas CD28 has a single ligand-binding site, CTLA-4 has two. Crystallisation studies of CTLA-4 reveal that the ligand-binding site is distal to the homodimerisation domain of CTLA-4 and CD80/CD86 (Alegre et al., 2001; Schwartz et al., 2001; Stamper et al., 2001). The binding of a CTLA-4 dimer to a CD80 or CD86 dimer creates a stable zipper-like structure (Schwartz et al., 2001; Stamper et al., 2001). Structural studies suggest that CD80 is a homodimer whereas CD86 is monomeric (Collins et al., 2002; Sansom and Walker, 2006). This complexity supports a model where the different receptor-ligand interactions may generate a difference in the balance of co-stimulatory and inhibitory actions (Sansom and Walker, 2006). So although CD80 is a potent co-stimulator of CD28, the increased affinity of CTLA-4 for CD80 suppresses its stimulatory capacity; while CD86 is a poor CD28 co-stimulator, the decreased affinity of CTLA-4 for CD86 only weakly impairs its co-stimulatory capacity. Therefore, in situations where CTLA-4 is present, CD86 may function as a better co-stimulator than CD80 (Sansom and Walker, 2006).

The view that CD80 and CD86 have overlapping functions (Borriello et al., 1997; McAdam et al., 1998) has been challenged in recent years using mice deficient in either CD80 or CD86, with suggestions that both molecules differ in affinity, valency and in the structural organisation of receptor-ligand interactions (Collins et al., 2002; Ikemizu et al., 2000). Compared to CD28, CTLA-4 has a 20- to 100-fold higher

affinity for CD80 and CD86 (Collins et al., 2002; Sansom and Walker, 2006); yet both receptors have a higher affinity for CD80 compared to CD86 (**figure 1.3**) (Borriello et al., 1997). The significance of this finding is not known but may have implications at the functional level. The 10-fold higher affinity of CD28 for CD80 could imply this interaction makes CD80 a more effective co-stimulator of CD28 function.

1.2.3 Blocking CD28-B7 pathway: CTLA-4 Ig

For the treatment of autoimmune disease, it has long been anticipated that by blocking the CD28-B7 pathway T cells that respond to self-Ags could be selectively targeted without affecting resting T cells. The fact that CTLA-4 has a higher affinity for both CD80 and CD86 has allowed investigators to take advantage of this mechanism and block CD28 signalling. To this end, the fusion protein CTLA-4 Ig, which consists of the CTLA-4 extracellular domain fused to the constant region of IgG (immunoglobulin G), was developed and ultimately this fusion protein blocks CD28-B7 interactions (Linsley et al., 1991). In mice CTLA-4 Ig has been shown to facilitate organ transplantation, block T cell responses and inhibit the differentiation of B cells into plasma cells (Lenschow et al., 1992; Lin et al., 1993; Milich et al., 1994). Moreover in models of autoimmune disease, treatment with CTLA-4 Ig has been shown to prevent the production of autoantibodies and to reduce the severity of lupus nephritis.

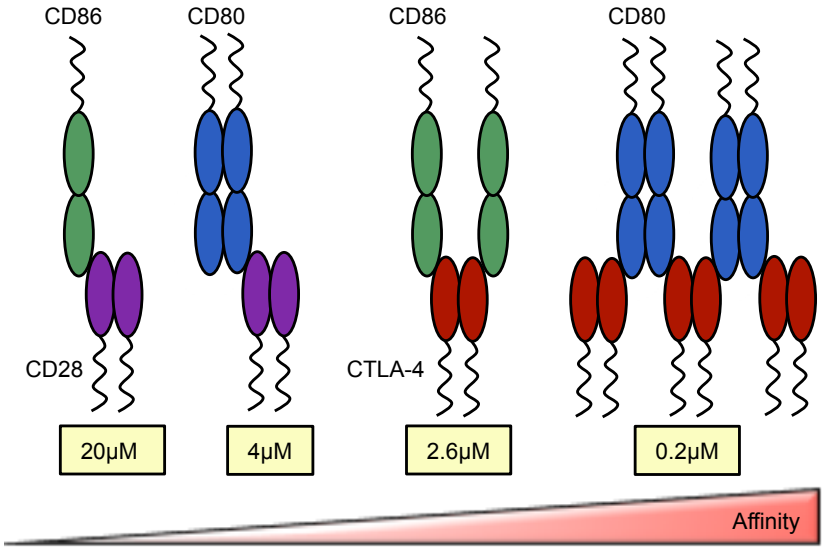

Figure 1.3 Interactions between co-stimulatory receptors and their ligands. CD28, CTLA-4 and CD80 are dimers, whilst CD86 is a monomer. Both receptors interact with both ligands and so four interactions are possible. The interactions vary according to affinity. Interactions between CD28 and either CD80 or CD86 are weaker than those for CTLA-4 and either ligand. The monovalent solution dissociation constant (K_d) for each interaction, as reported by Collins et al., (2002), is shown.

With the encouraging results from animal models of autoimmune disease, attention has now been directed at using CTLA-4 Ig for treating patients with autoimmune disease. The drug Abatacept consists of the CTLA-4 extracellular domain and the Fc fragment of human IgG1 (Davis et al., 2007). The drug has been shown to improve the signs and symptoms of rheumatoid arthritis (RA) at different stages of disease ranging from early stage RA to refractory disease (Genovese et al., 2005; Kremer et al., 2005). Moreover Abatacept has been used successfully in the treatment of patients with juvenile idiopathic arthritis and in patients with systemic lupus erythematosus (Merrill et al., 2010; Ruperto et al., 2008). Another human CTLA-4 Ig in phaseI/II clinical trials is Belatacept (LEA29Y). Although a difference of two amino acids distinguishes Belatacept from Abatacept, this difference allows Belatacept to bind B7 molecules with a higher avidity (Larsen et al., 2005). As such Belatacept has a greater inhibitory effect on T cell activation. The preliminary efficacy of Belatacept in RA treatment has been shown in phaseI/II clinical trials (Watanabe and Nakajima, 2012).

1.3 CTLA-4 function

The concept of CTLA-4 actively inhibiting T cell activation is widely accepted. However, the mechanisms and circumstances under which CTLA-4 inhibition becomes dominant remain to be identified. CTLA-4 function has long been defined as the delivery of an inhibitory signal into cells. However, a number of studies now dispute the existence of this model and have proposed alternative models of CTLA-4 function that could have cell-intrinsic or cell-extrinsic effects on T cells. Walker & Sansom (2011) have reviewed these proposed functions and it is now becoming clear that in fact CTLA-4 exerts its effects through other cells (cell-extrinsic) (Walker and Sansom, 2011).

1.3.1 Ligand Competition

The preferential affinity of CD80 and CD86 for CTLA-4 compared with CD28 provides the basis for the first model of ligand competition (**figure 1.4A**). It can be argued that in situations where ligand expression is limited and CTLA-4 is highly expressed, the ligands will preferentially bind to CTLA-4 (Sansom and Walker, 2006). The lack of CD28 signalling results in depriving T cells of essential co-stimulatory signals and results in decreased responses. Moreover, the administration of CTLA-4 Ig blocks T cell activation and furthermore transgenic mice with high surface CTLA-4 expression do not respond to Ag stimulation (Saito and Yamasaki, 2003). Taken together, these results support the concept that high surface CTLA-4 expression may outcompete CD28 to bind ligands. However, this could be due to increased negative signalling by CTLA-4 but further support for the ligand competition model comes from transgenic CTLA-4 knockout mice that express CTLA-4 without a cytoplasmic tail (Masteller et al., 2000). Although these mice were long lived and did not encounter multi-organ infiltration, they accumulated large numbers of activated T cells, and eventually suffered from lymphadenopathy. These results suggest that ligand competition could contribute to the inhibitory effects of CTLA-4, and the cytoplasmic domain may also confer inhibitory function.

1.3.2 Inhibitory signalling

The second model of CTLA-4 function suggests that CTLA-4 delivers a cell-intrinsic negative signal, acting either at the level of the TCR or by directly antagonising CD28 signalling (**figure 1.4B)**. This possibility is supported by several studies in which Abs to CTLA-4 inhibit IL-2 production and T cell proliferation (Krummel and Allison, 1995; Walunas et al., 1996). A number of signalling models have been proposed that account for the inhibitory actions of CTLA-4. Amongst these include the recruitment of phosphatases to the TCR, and the reduction of lipid raft formation. Studies have also shown that

CTLA-4 has the potential to remove TCR signalling components, such as TCRξ, from lipid rafts, while other studies propose that CTLA-4 acts to reduce ZAP70 (Zeta-chain associated protein kinase 70) microcluster formation thereby reducing the phosphorylation of TCR substrates (Chikuma et al., 2003; Darlington et al., 2002; Martin et al., 2001).

The observation that negative signalling by CTLA-4 can occur in the absence of ligand binding has raised the possibility that this level of signalling might be a constitutive event regulated by CTLA-4 expression levels and not by a ligand-generated signal (Chikuma et al., 2005). However, the functional events that occur in the absence of the cytoplasmic domain do not appear to be explained by this negative signalling model. Moreover CTLA-4 mediated inhibition of T cell proliferation during primary T cell responses has been consistently difficult to demonstrate, particularly using natural ligands (Chambers et al., 1998).

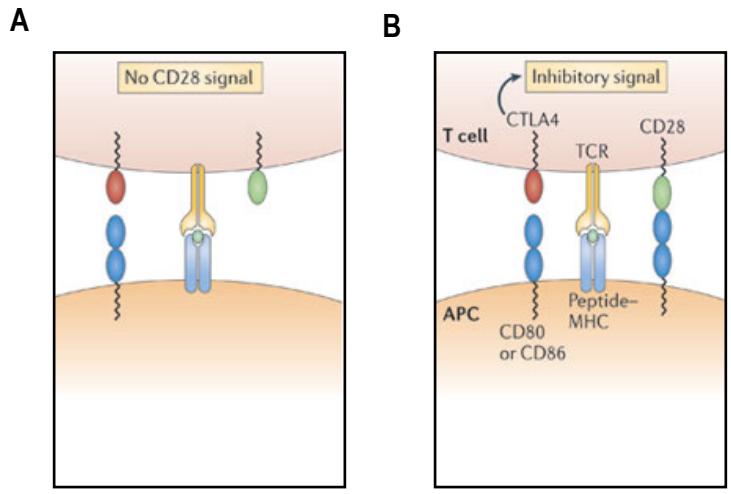

Figure 1.4 Cell-intrinsic models of CTLA-4 function. (A) Representation of the ligand competition model. CTLA-4 has a higher affinity for both CD80 and CD86 and so can outcompete CD28 for binding the ligands. **(B)** Representation of the model where CTLA-4 delivers an inhibitory signal. CTLA-4 can impair lipid raft formation following its co-ligation with the TCR and can therefore raise the threshold for TCR signalling. Additionally, CTLA-4 could impair TCR signalling by reducing ZAP70 microcluster formation. Taken from (Walker and Sansom, 2011).

1.3.3 Indoleamine 2,3-dioxygenase (IDO) and tryptophan metabolism

A third model of CTLA-4 function has been the suggested ability of CTLA-4 to induce the expression of the enzyme IDO on DCs by initiating a reverse signal. In this model CTLA-4 functions in a cell-extrinsic manner and indirectly inhibits T cell activation (**figure 1.5A**) (Gough et al., 2005; Munn et al., 1999). IDO is the rate-limiting enzyme that catalyses the breakdown of the essential amino acid tryptophan required for T cell proliferation. In doing so, IDO suppresses T cell mediated immunity.

Numerous studies have now indicated that the immune tolerance resulting from the interaction between co-stimulatory ligands on DCs and CTLA-4 on T cells is mediated by IDO (Grohmann et al., 2002; Mellor et al., 2004; Munn et al., 2004). CTLA-4 is an important receptor expressed on Tregs and IDO has been identified to have an important downstream effector role in CTLA-4-mediated immune tolerance (Boasso et al., 2005). In fact IDO induction was suggested to be a potential function of CTLA-4 Ig, where CTLA-4 Ig stimulates the upregulation of IDO activity in APCs as opposed to acting as a blockade of CD80 and CD86 function (Orabona et al., 2005). Support for this idea was provided in a study where the IDO inhibitor 1-methyltryptophan (1MT) prevented the long-term survival of pancreatic islet allografts that was induced by CTLA-4 Ig (Grohmann et al., 2002). Likewise Tregs, which constitutively express CTLA-4, have been shown to upregulate the activity of IDO in DCs via a CTLA-4-dependent mechanism (Oderup et al., 2006). However if IDO induction is the primary function of CTLA-4, why does the phenotype of IDO deficient mice differ from the phenotype of CTLA-4 deficient mice? Since CTLA-4 plays an important role in regulating peripheral T cell tolerance, CTLA-4 knockout mice die within a couple of weeks of birth from fatal lymphoproliferation (Waterhouse et al., 1995), yet IDO-knockout mice have not been observed to show signs of spontaneous autoimmune disease (Mellor and Munn, 2004). These observations therefore suggest that IDO is not an absolute requirement for

homeostatic maintenance of central or peripheral tolerance to self-Ags. Furthermore, CD80 or CD86 Abs are reported to drive IDO production so a further question that remains to be answered is how the DC integrates the opposing signal from CTLA-4 Ig?

1.3.4 Regulatory T cells

A further proposed model of CTLA-4 function is for CTLA-4 to inhibit T cell activation through Tregs. In mice and humans, Tregs constitute 2-10% of peripheral $CD4^+$ T cells (Sakaguchi, 2000). The importance of CTLA-4 in Tregs has been demonstrated in studies where CTLA-4 blockade inhibits the regulatory function of Tregs. Moreover, Bachmann et al., (1999) demonstrated the ability of CTLA-4 expressing cells to regulate disease caused by CTLA-4 negative cells by generating chimeric animals, which were reconstituted with bone marrow from CTLA-4 knockout and CTLA-4 wild-type (WT) mice (Bachmann et al., 1999). Cross-linking CTLA-4 with Abs has been shown to drive the production of the inhibitory cytokine TGF-β in $CD4^+$ T cells. This results in an inhibition of T cell proliferation and IL-2 production. In doing so, the TGF-β production by the CTLA-4 positive cell compensates for the lack of TGF-β production by the CTLA-4 negative cell and therefore prevents disease development (**figure 1.5B**) (Chen et al., 1998)**.** Moreover, adoptive transfer experiments have revealed that WT cells are less responsive to antigenic stimulation than CTLA-4 deficient cells, thus demonstrating a cell-autonomous mechanism of CTLA-4 inhibition (Egen et al., 2002). These experiments reveal the ability of CTLA-4 to regulate not only the cell in which it is expressed on, but also to regulate bystander cells.

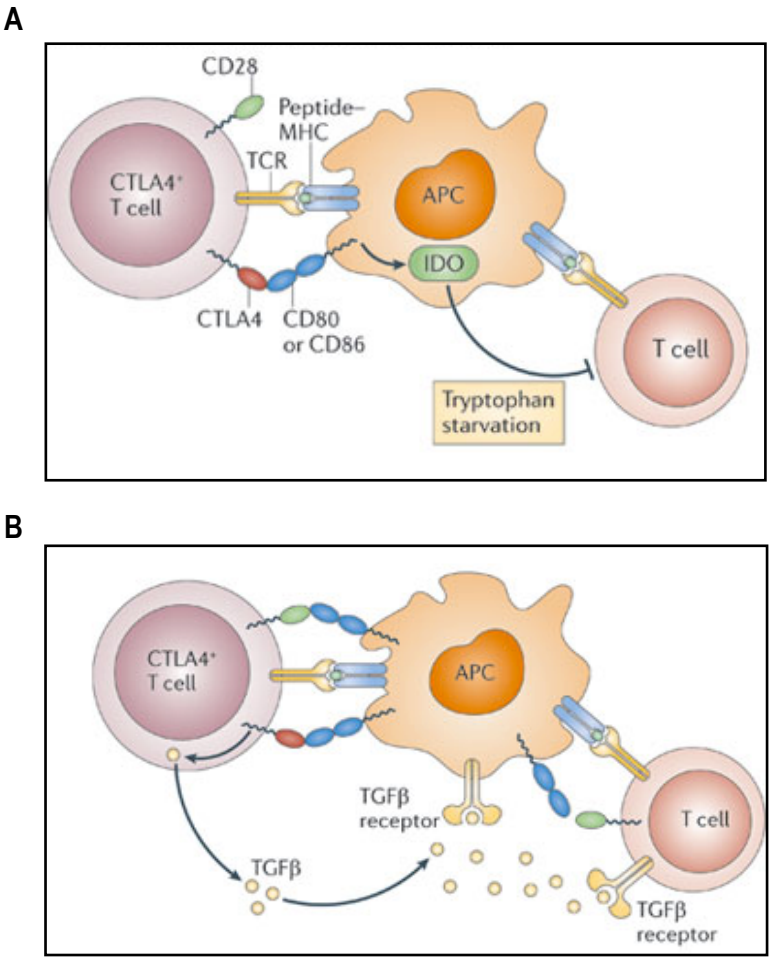

Figure 1.5 Cell-extrinsic models of CTLA-4 function. (A) CTLA-4 induces the production of IDO, the tryptophan metabolising enzyme, by APCs. IDO catalyses the breakdown of tryptophan, an essential amino acid required for T cell proliferation. **(B)** CTLA-4 in Tregs stimulates the production of the inhibitory cytokine TGF-β, which acts to inhibit T cell proliferation and IL-2 production. Taken from (Walker and Sansom, 2011).

1.3.5 Transendocytosis

Treg suppression in vitro can proceed in the absence of accessory cells. However, in vivo Treg suppression operates via an APC. In lymph nodes, it has been shown that a Treg can alter the ability of a DC bound to Ag to form stable contacts with T cells (Tadokoro et al., 2006; Tang et al., 2006). Furthermore, Tregs have been demonstrated to impair the stimulatory capacity of human DCs in vitro (Misra et al., 2004). This raises the possibility for the existence of a model where the expression of CTLA-4 by Tregs can function to modify APCs. In both mouse and human systems, there is evidence for Tregs to downregulate CD80 and CD86, to inhibit the upregulation of ligand during APC maturation, and to downregulate ligands on mature DCs (Onishi et al., 2008; Wing et al., 2008).

Our lab has now identified a further model of CTLA-4 function where CTLA-4 in activated T cells and in Tregs, alters APC phenotype by removing ligand from the APC and thus suppresses T cell responses (**figure 1.6)** (Qureshi et al., 2011). This phenomenon is called transendocytosis. In this case, CTLA-4 traffics to the plasma membrane, and binds and rips it ligand from the surface of the APC. CTLA-4 then internalises the ligand and targets it for degradation in lysosomes. Such a model clears up some unexplained features of the CD28/CTLA-4 system. Firstly, this model could explain why CD28 and CTLA-4 share ligands, as without this CD28 stimulation cannot be inhibited by CTLA-4. Secondly, this model requires CTLA-4 to be internalised from the plasma membrane, which currently is seen as the most dominating aspect of CTLA-4 biology.

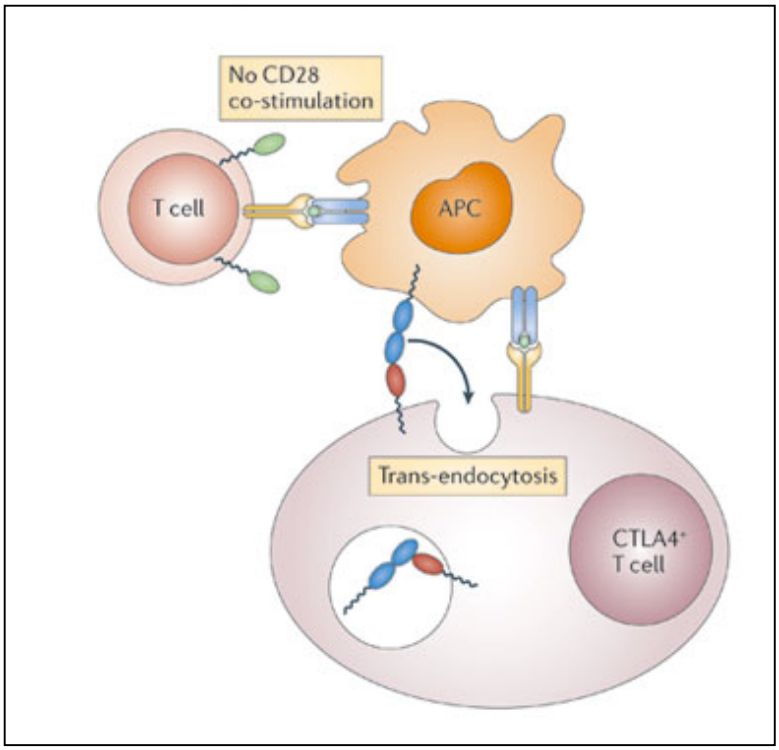

Figure 1.6 CTLA-4 captures ligands and alters APC phenotype. CTLA-4 binds its ligand and internalises the entire molecule from the surface of the APC. This reduces the amount of ligand available to bind CD28 and therefore CTLA-4 inhibits T cell activation in a cell-extrinsic manner. Taken from (Walker and Sansom, 2011).

1.4 The evolutionary biology of CTLA-4

The genetic and molecular similarities between CD28 and CTLA-4 suggest the evolution of CTLA-4 is a duplication event of an ancient co-stimulatory gene (Bernard et al., 2007; Teft et al., 2006). Interestingly the CD28 and CTLA-4 receptor have been reported in fish, amphibians and birds. The conservation of the ligand-binding site (L/MYPPPY) in the CTLA-4 extracellular domain suggests the CTLA-4 ligand competition model dates back to teleost fish. The amino acid sequence of CTLA-4 in mammalian species shows an increasing degree of conservation from the extracellular domain to the cytoplasmic domain. In fact the 100% conservation in the mammalian CTLA-4 cytoplasmic domain suggests there is a selective pressure to conserve the functional mechanisms mediated through this region (Teft et al., 2006). This is also true for the conserved cysteine residue located in the extracellular domain required for CTLA-4 dimerisation. The cysteine residue forms a covalent bond between individual CTLA-4 chains (Teft et al., 2006).

The CTLA-4 cytoplasmic domain varies considerably in non-mammals (**figure 1.7**). As a lab we have shown that the specialised intracellular trafficking itinerary of CTLA-4 is key for its ability to remove ligand from APCs and to target the ligand for degradation in lysosomes (Qureshi et al., 2011). This raises questions as to whether this feature of CTLA-4 has developed through evolution. Importantly, the YVKM motif required for CTLA-4 internalisation is absent in fish. However trout CTLA-4 does encode YxxF motif further downstream the cytoplasmic domain, which is also found in several fish species including salmon (Bernard et al., 2007; Walker and Sansom, 2011). Although the significance of this motif in fish CTLA-4 remains to be identified, this motif could represent the initial emergence of CTLA-4 endocytosis.

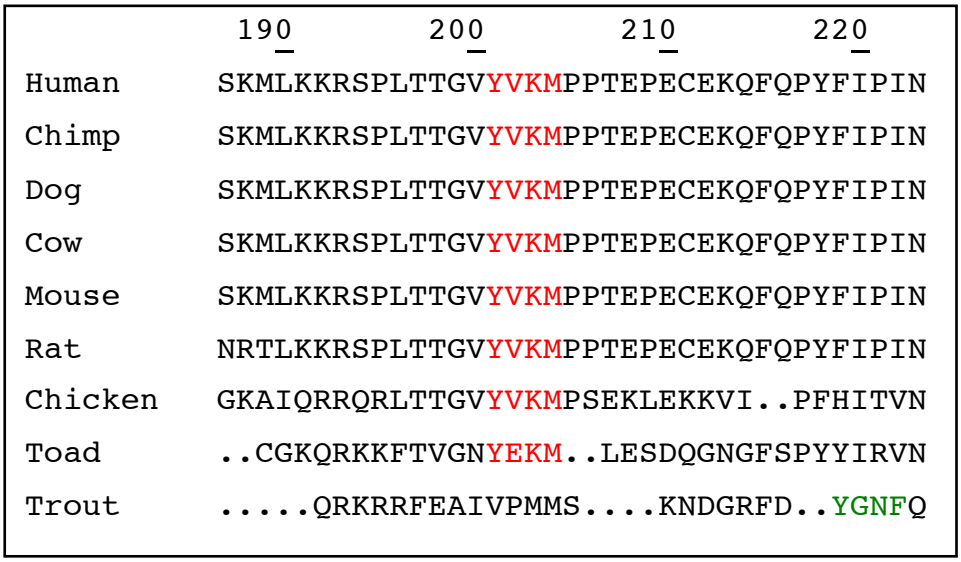

Figure 1.7 Evolution of CTLA-4 molecules. The CTLA-4 cytoplasmic domain is conserved amongst mammalian species suggesting there is selective pressure to maintain this region. Importantly the YVKM motif required for internalisation (red) is not evident until after birds. Trout CTLA-4 lacks this conserved endocytic motif but does possess a YxxF motif (green) the significance of which remains to be determined. Adapted from (Bernard et al., 2007).

1.5 Receptor Protein Trafficking

1.5.1 Endocytic Pathways

There are different types of endocytic pathways, which vary according to the size of the endocytic vesicle, the mechanism of vesicle formation and the nature of the cargo (Conner and Schmid, 2003; Wing et al., 2008). Endocytosis is divided into two categories: phagocytosis and pinocytosis. Phagocytosis takes place in specialised mammalian cells. Pinocytosis, however, takes place in all cells by four basic mechanisms: macropinocytosis, clathrin-mediated endocytosis, caveolae-mediated endocytosis, and clathrin- and caveolae-independent endocytosis (Conner and Schmid, 2003).

1.5.2 Phagocytosis

Phagocytosis is an active and regulated process. In mammals phagocytosis takes place in specialised cells such as neutrophils, macrophages and monocytes (Aderem and Underhill, 1999). The main function of this process is to clear cell debris, apoptotic cells and microorganisms and involves cell surface receptors and signalling cascades (Doherty and McMahon, 2009; Nichols and Lippincott-Schwartz, 2001). For example, in macrophages Abs bound to surface Ags are recognised by the surface Fc receptor. This activates a signalling cascade, which in turn activates cell division cycle 42 (CDC42) and Rac. This process triggers the assembly of actin and cell surface extensions (Hall and Nobes, 2000). These extensions then facilitate the engulfment of the Ab-coated pathogen into a phagosome. The bacteria are then destroyed once the cell's inflammatory responses are activated and finally an immune response is elicited once the regurgitated bacterial peptides are presented on the macrophage surface.

1.5.3 Macropinocytosis

Pinocytosis involves the internalisation of large volumes of extracellular fluid. The efficiency of endocytosis is often greater when solutes bind non-specifically to the cell membrane. In certain cells, growth factor stimulation or other types of stimulation induces membrane ruffling, which is accompanied by macropinocytosis (Swanson and Watts, 1995). Similar to phagocytosis the Rho-family GTPases are activated by signalling cascades, which triggers actin assembly and membrane protrusions. However, unlike phagocytosis the protrusions fuse with the plasma membrane and generate large endocytic vesicles called macropinosomes, which move into the cytosol (Doherty and McMahon, 2009; Nichols and Lippincott-Schwartz, 2001).

1.5.4 Caveolin-mediated endocytosis

Caveolae is one of the most common clathrin-independent pathways studied (Le Roy and Wrana, 2005). They are small flask-shaped invaginations and their appearance, function and composition are cell-type dependent. For long, caveolae have been suggested to be involved in internalisation and cell signalling (Pelkmans and Helenius, 2002). The internalisation of caveolae is triggered by a signalling cascade, which results in the tyrosine phosphorylation of caveolae constituents by Src kinases (Li et al., 1996). The process seems to require dynamin and actin rearrangement, since the overexpression of dominant-negative dynamin or the disruption of actin assembly can block caveolin-mediated endocytosis (Pelkmans and Helenius, 2002). Recent studies have shown that caveolae are important in the internalisation of non-enveloped viruses such as Simian virus 40, bacterial toxins such as cholera toxin, extracellular ligands such as albumin, and membrane components such as glycosphingolipids (Pelkmans and Helenius, 2002; van der Aa et al., 2007).

1.5.5 Clathrin- and caveolin-independent endocytosis

A number of lipids, toxins, viruses and proteins can be internalised into cells via non-clathrin mediated pathways (Sandvig and van Deurs, 2002). Lipid rafts, like caveolae, are cholesterol-rich microdomains that diffuse freely on the cell surface (Anderson and Jacobson, 2002; Edidin, 2001). Whilst dynamin is not an absolute requirement for this pathway, cholesterol plays a crucial role in cargo internalisation. For example glycophosphatidylinositol (GPI)-anchored proteins are internalised by a raft-dependent pinocytic route, which is dynamin-independent but dependent on CDC42 (Mayor and Pagano, 2007; Sabharanjak et al., 2002). By contrast on lymphocytes the IL-2 receptor, which is associated with lipid microdomains, is internalised in a clathrin- and caveolin-independent way (Lamaze et al., 2001). While dominant-negative dynamin mutants inhibit the internalisation of IL-2 receptors, dominant-negative mutants of Epidermal growth factor receptor substrate 15 (Eps15), which is an AP-2 binding partner and inhibits clathrin-mediated endocytosis, fails to inhibit IL-2 receptor internalisation. How clathrin- and caveolae-independent endocytosis is regulated is not clear. Nevertheless, the existence of such pathways could suggest they mediate unique functions in the cell, which vary according to which cargo is being transported, where it is being transported to and how entry into these compartments is regulated. For example tetanus toxins, which are internalised via the clathrin pathway, require cholesterol-dependent clustering to facilitate their internalisation by clathrin (Deinhardt et al., 2006).

1.5.6 Clathrin-mediated endocytosis

In mammalians cells, clathrin-mediated endocytosis is the major mechanism used to regulate cell surface traffic (Brodsky et al., 2001; Kibbey et al., 1998). A number of receptors including transferrin receptor (TfR), epidermal growth factor receptor (EGFR) and low-density lipoprotein (LDL) use clathrin-

mediated endocytosis to internalise ligand (Clague and Hammond, 2006). Receptors become concentrated in clathrin-coated pits, which bind to the clathrin adaptor protein 2 (AP-2) directly or indirectly via sorting motifs encoded in the cytoplasmic domain of the receptor (**figure 1.8**). Clathrin is then recruited to the plasma membrane by binding to AP-2 (Kirchhausen et al., 1997). When many clathrin triskelions interact at the membrane they form a polyhedral lattice, which pulls the membrane into a bud. Changes in membrane curvature, resulting from localised changes in phospholipid composition, facilitate this membrane invagination. A protein that is thought to play an important role in altering the membrane curvature is Endophylin (Verstreken et al., 2002). The completion of the inward budding of the membrane is then followed by fission of the forming vesicle resulting from the interactions between AP-2 and the GTPase dynamin (Wang et al., 1995).

Following on from the invagination and pinching off of the coated pits, the vesicles are released into the cytoplasm, and deliver their cargo to a tubovesicular compartment known as the early or sorting endosome (Sorkin, 2000). From here the receptors can either be recycled back to the plasma membrane or they can be targeted for lysosomal degradation. Vesicles containing receptors destined for lysosomes bud from the limiting membrane into the lumen of multivesicular bodies (MVBs) (Madshus and Stang, 2009), whilst the recycling components are removed in recycling vesicles, and are sorted from lysosomally targeted components. Thus, the number of receptors at the cell surface is a balance between the rate of internalisation and the rate of replacement (recycling and new synthesis) (Goh and Sorkin, 2013).

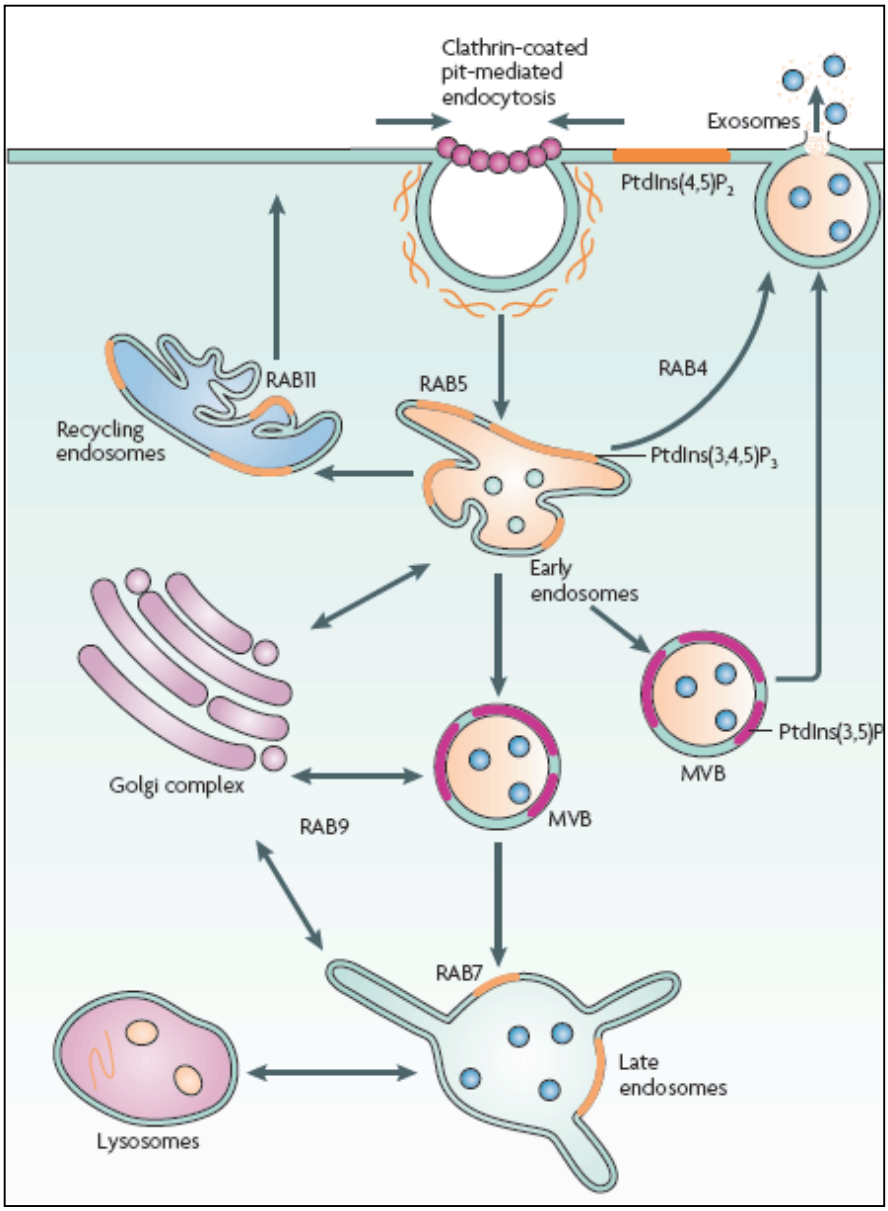

Figure 1.8 Clathrin-mediated endocytosis. Proteins that internalise by the clathrin (orange) and dynamin (pink circle) pathway are sorted in early endosomes. Rab5 is the marker for early endosomes. The conversion of Rab5 and Rab7 marks the point when early endosomes are converted into late endosomes. In most cases, there is an intermediate organelle that mediates cargo transfer called MVBs. Fusion of MVBs with the plasma membrane allows protein and lipids, which are sorted in the intraluminal vesicles (blue circles) of MVBs, to be released into the extracellular space as exosomes. Proteins targeted for degradation are sorted from late endosomes to lysosomes. Rab4 mediates recycling of proteins and lipids directly from early endosomes to the plasma membrane. Other proteins are recycled to the plasma membrane via recycling endosomes mediated by Rab11. Rab9 is associated with the transfer of cargo from late endosomes to the Golgi complex. Intracellular organelles can also be distinguished by Phosphoinositide phosphates such as phosphatidylinositol-4,5-bisphosphate ($PtdIns(3,5)P_2$) and phosphatidylinositol-3,4,5-triphosphate ($PtdIns(3,4,5)P_3$) (coloured arcs on endosomes). Taken from (Rajendran et al., 2010).

1.5.6.1 Clathrin and AP Complexes

Clathrin and AP complexes are the two fundamental building blocks of the clathrin coat. The clathrin protein was first discovered in 1975 (Pearse, 1976) and forms a triskelion shape, which is composed of three heavy chains and three light chains. The AP complex family in mammals has six members (Robinson, 2004), however, two of these members, AP-5 and AP-6, have only been recently identified (Hirst et al., 2011; Ohno, 2006b). AP-1 and AP-2 were the first two complexes to be discovered and these complexes are important in the sorting of cargo into clathrin-coated vesicles (CCVs) (Robinson, 2004). AP-3 and AP-4 on the other hand can function in the absence of clathrin (Boehm and Bonifacino, 2001). The AP complexes are heterotetramers that consist of two large subunits and two small subunits, for AP-1 γ, β1, μ1 and σ1; for AP-2 α, β2, μ2 and σ2; for AP-3 δ, β3, μ3 and σ3 and for AP-4 ε, β4, μ4 and σ4 (Owen et al., 2004).

The AP complexes have specialised functions in distinct transport pathways. AP-1 is important in trafficking cargo between early endosomes, the trans-Golgi network (TGN) and the plasma membrane. However the direction of transport remains to be determined (Owen et al., 2004; Traub, 2005). AP-2 is important in clathrin-dependent endocytosis where it facilitates CCV formation from the plasma membrane, which eventually fuse with early endosomes (Owen et al., 2004; Traub, 2005). AP-3 is important in trafficking cargo from early endosomes to late endosomes and/or lysosomes (Owen et al., 2004). AP-4 is important in the delivery of lysosomal proteins from the TGN to lysosomes (Ohno, 2006a) and has recently been identified to have a role in the transport of the amyloid precursor protein from the TGN to endosomes (Burgos et al., 2010).

1.5.7 Sequences of Receptor Internalisation

1.5.7.1 YXXΦ motif

A number of short-linear sequences important for clathrin-dependent internalisation have been identified using models where critical amino acid residues important for internalisation have been deleted or substituted in the cytoplasmic domain of the receptor (Kozik et al., 2010; Pandey, 2009). The first and most common internalisation signal is the bulky tyrosine-based hydrophobic YXXΦ motif (Kozik et al., 2010; Le Roy and Wrana, 2005; Traub, 2003). This motif contains the critical tyrosine residue that binds directly to μ2 subunit in AP-2 and drives clathrin-dependent endocytosis. The use of the tyrosine-based motif is not restricted to internalisation and in fact roles have been identified in other sorting events such as targeting of receptors from the endosome to lysosomes (Pandey, 2009). Further studies have revealed that the location of the tyrosine residue in the cytoplasmic domain of receptors is critical to the movement of the receptor into coated pits (Lazarovits and Roth, 1988). For example the influenza virus hemagglutinin does not move into coated pits but when a key cysteine residue was substituted to tyrosine, the receptor moved into coated pits (Lazarovits and Roth, 1988). Importantly the distance of the tyrosine residue from the transmembrane domain was a key factor in this movement.

1.5.7.2 Dileucine motif

The second internalisation signal is the dileucine motif DxxxLL that interacts with the β1 subunit of AP-1 (Owen and Evans, 1998). Dileucine based motifs were discovered using chimeras of Tac antigen and the cytoplasmic domain of CD3-γ and δ (Letourneur and Klausner, 1992). The study revealed that both CD3 chains contained a dileucine motif that was responsible for internalisation. Moreover the dileucine motif played an important role in the lysosomal targeting of the chimeras. Both tyrosine-based and

dileucine based signals have been implicated in the internalisation of a variety of receptors including neurotransmitter receptors such as N-methyl-D-aspartate (NMDA) receptors, GPCRs (G-protein coupled receptors), TfR and EGFR. Importantly, there is no preference as to which motif is used to drive receptor internalisation. For example whilst the subunit NR2B requires YXXΦ motif for internalisation, NR2A shows some dependency on a dileucine based signal for internalisation and can internalise in the absence of YXXΦ motif (Lavezzari et al., 2004).

1.5.7.3 FXNPXY motif

The third internalisation signal is the FXNPXY motif that interacts with the phosphotyrosine-binding domains of the 'alternative adaptors' such as ARH, Dab1, Dab2 and Numb (Kozik et al., 2010). In fact a NPXY motif has been identified to be important in driving the rapid internalisation of the LDL receptor. By generating a range of truncated LDL receptor mutants, Chen et al., 1990 demonstrated that LDL receptor internalisation is markedly reduced when N, P or Y are substituted to alanine and this reduces the clustering of the receptor into coated pits (Chen et al., 1990). The occurrence of this motif in tyrosine kinase-linked receptors such as EGFR and insulin receptor family is far more frequent than to be present by chance alone suggesting it has some underlying importance. However in the case of EGFR, a role for this motif in ligand-dependent internalisation has been ruled out by deletion experiments (Glenney et al., 1988), but a role in ligand-independent internalisation may be possible (Chen et al., 1990).

1.5.8 Endosomal sorting of receptors

There are three types of endosomes: early endosomes, late endosomes and recycling endosomes (Mellman, 1996). Each endosome is specialised to perform distinct functions and markers such as Rabs can distinguish them (Stenmark, 2009). Cargo internalised from the cell surface first reaches early endosomes. Early endosomes are sorting organelles that are located in the periphery of the cell and consist of a tubular-vesicular network (Huotari and Helenius, 2011). The mildly acidic pH of the lumen facilitates ligand dissociation from receptors as is well described for EGFR and TfR. This process then enables the receptor to recycle back to the cell surface via tubules or the receptor can be targeted for degradation (Mellman, 1996; Mukherjee et al., 1997). Markers that distinguish early endosomes are EEA1 (Early Endosome Antigen 1), transferrin and TfR, Rab5A and Rab4. Late endosomes are spherical and consist of luminal vesicles but can be distinguished by the lack of tubules. They are acidic (pH 5.5) and receive material prior to degradation in lysosomes (Huotari and Helenius, 2011). This includes material from the TGN in the biosynthetic pathway and internalised material from early endosomes in the endocytic pathway. Markers including LAMP1 (Lysosomal associated membrane protein 1), Rab7, Rab9 and mannose-6-phosphate receptor are used to distinguish late endosomes from early endosomes (Russell et al., 2006). Recycling endosomes consist of a tubular network and are concentrated mainly at the microtubule organising centre (MTOC). Rab11 is the main marker of recycling endosomes (Ullrich et al., 1996). The final compartment of the endocytic pathway is the lysosomes. The primary function of lysosomes is to break down cellular waste into simple compounds that can be used as new cell-building material once the compounds are returned to the cytoplasm (Luzio et al., 2000). Lysosomes consist of large vacuoles that contain electron dense material. Lysosomes are acidic (pH 4.8) and contain active lysosomal hydrolases and lysosomal membrane proteins (Gruenberg and Maxfield, 1995; Luzio et al., 2000). The lack of mannose 6-phosphate receptor distinguishes lysosomes from late endosomes.

1.5.9 Degradation of trafficking receptors

Cell surface proteins have different rates of degradation, ranging from minutes to days, but any changes in their stability can form the underlying basis for certain forms of cancer and disease (Hare and Taylor, 1991; Vendruscolo et al., 2003). Different reasons could account for why certain receptors are degraded more rapidly than others (Cooper, 2000). Most regulatory proteins such as transcription factors are degraded rapidly so as to allow their levels to change rapidly in response to external factors. Other proteins however are degraded rapidly in response to specific signals or if the protein is damaged, thus providing an additional regulatory mechanism of intracellular enzyme activity (Cooper, 2000). For many signalling receptors lysosomal targeting is used as a mechanism to downregulate the receptor and switch off the signal (Sorkin and von Zastrow, 2009).

Cell surface expressed proteins, in most cases, must internalise to undergo degradation since their proteolysis is dependent on trafficking through endosomes and lysosomes (Cooper, 2000). The receptors most often encode sorting motifs, which facilitate their transport to lysosomal compartments (Sorkin and von Zastrow, 2009). The susceptibility for their selective removal from the membrane results from a structural feature of the protein that controls its protease sensitivity, diffusion rate or some other physical characteristic (Hare and Taylor, 1991). A recycling protein, on the other hand, is either degraded more frequently, or since a greater proportion of their life span is spent inside the cell, they show a greater likelihood to interact with lysosomes or intracellular proteolytic enzymes (Hare and Taylor, 1991). Support for the latter is provided in studies using surface-labeling methodologies. These reveal that a protein recycling frequently between the cell surface and endosomes has a rapid degradation rate (t½ 2-20h), when compared to other surface glycoproteins (t½ >50) (Baumann and Doyle, 1978; Chu and Doyle, 1985).

1.5.10 Ubiquitin-Proteasome Pathway

Destruction is a major cellular regulatory pathway that controls protein half-life. There are two major destruction pathways in cells: the first is the collection of proteolytic enzymes within the lysosome, and the second is the multi-catalytic proteolytic core of the ubiquitin-proteasome pathway (Urbanowski and Piper, 2001). Proteins targeted for degradation are marked by the covalent attachment of multiple ubiquitin molecules. This provides a signal for the 26S proteasome. The process is divided into two steps: the first step is a specific recognition system that uses the ubiquitin conjugation cascade, and the second is the destruction process mediated by the proteasome (proteolytic) core (Myung et al., 2001).

1.5.11 Ubiquitin Conjugation Cascade

Ubiquitination is the process where protein receptors undergo post-translational modification through the attachment of ubiquitin proteins to intracellular lysine residues. Most commonly, a carboxypeptide bond is formed between the carboxylic acid group of the glycine 76 residue in ubiquitin and the amino group of the lysine residue. The ubiquitin conjugation cascade uses three different sets of enzymes to link ubiquitin to the protein substrate (**figure 1.9**). These are the ubiquitin activating enzymes (E1), ubiquitin-conjugating enzymes (E2) and ubiquitin ligases (E3). The unique degradation signal of a substrate protein is recognised by a different combination of E2 or E3 or both. This confers specificity for the ubiquitination of protein substrates (Huang et al., 2004a; Huang et al., 2004b).

There are three types of ubiquitin modifications: monoubiquitination where a single ubiquitin is attached to a lysine residue, multi-ubiquitination where single ubiquitin proteins are attached to several lysine residues and polyubiquitination where chains of ubiquitin proteins are formed on a single lysine residue

(Sadowski and Sarcevic, 2010). Importantly, ubiquitin contains seven lysine residues and all of these can serve as targets for ubiquitination. Depending on the type of modification, different cellular processes are affected, from membrane trafficking and endocytosis to protein degradation. Several receptor proteins use ubiquitination modification as their targeting signal to lysosomes including EGFR and PAR2 (Protease-activated receptor 2) (Berlin et al., 2010; Jacob et al., 2005). To date proteomics have been used to identify the lysine residues that serve as targets for ubiquitin attachment in a protein receptor and in identifying the E3 ubiquitin ligase. For most receptors including GPCRs and EGFR such a technique has been useful in understanding the post-endocytic sorting of the receptors to lysosomes (Marotti et al., 2002; Miranda and Sorkin, 2007). Moreover, deubiquitination of a receptor provides a further level of regulation where ubiquitinated receptors can escape degradation and undergo recycling. This has been well described for EGFR that is deubiquitinated by ubiquitin-specific protease 8 (USP8) and in doing so this ultimately helps regulate EGFR signalling (Berlin et al., 2010).

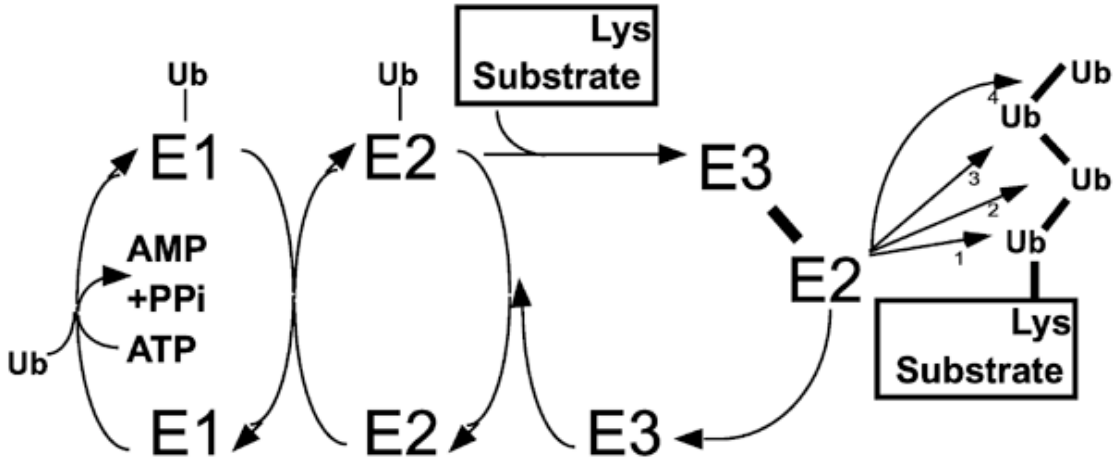

Figure 1.9 Ubiquitin Conjugation Cascade. E1 activates ubiquitin, a reaction that involves the hydrolysis of ATP. Following activation, ubiquitin is transferred to E2. E2, by itself or in cooperation with E3, shuttles ubiquitin to a protein substrate and is attached to internal lysine residues. Following the mono-ubiquitination of the protein substrate, a polyubiquitin chain can be formed through the same ubiquitination conjugation cascade (Huang et al., 2004b). Taken from (Huang et al., 2004b).

1.5.12 Endosomal sorting complex required for transport (ESCRT) complex

Receptors destined for lysosomal degradation are ubiquitinated and are subsequently sorted into MVBs by members of the ESCRT complex (Vardhana et al., 2010; Wollert and Hurley, 2010). Localisation of internalised receptors to MVBs was shown 30 years ago by Haigler et al., (1979) who monitored the post-internalisation fate of the EGF:receptor complex in human cells, using EGFR:ferritin conjugates that bind to cell surface EGFR. Within minutes stimulated EGFR was shown to localise to MVBs, and contents were degraded in lysosomes. In fact, it has been identified that this is the same pathway used in yeast to downregulate cell surface receptors and transporters (Babst et al., 2002; Katzmann et al., 2001).

The hallmark of MVBs is the presence of intraluminal vesicles (ILVs) that are formed by inward budding of the endosomal limiting membrane (Haigler et al., 1979; Piper and Luzio, 2001). There are five ESCRT complexes 0, I, II, III and the AAA-ATPase vacuolar protein sorting 4 (VpS4) complex (Schmidt and Teis, 2012). The complexes function to co-ordinate receptor sorting to ILVs of MVBs as is well described for EGFR (Katzmann et al., 2002). The ESCRT-0 component Hepatocyte growth-factor regulated tyrosine kinase substrate (Hrs) binds ubiquitinated cargo using a ubiquitin interaction motif and concentrates the cargo at the perimeter of the membrane (Razi and Futter, 2006; Wollert and Hurley, 2010). Hrs then recruits the ubiquitin-binding subunit of ESCRT-I, Tumor susceptibility gene 101 (TSG101), which recognises ubiquitinated cargo through an ubiquitin E3 variant domain. ESCRT-I in co-operation with ESCRT-II regulates ILV formation and the sorting of ubiquitinated cargo in ILVs. The depletion of TSG101 inhibits MVB formation and subsequent sorting of protein receptors into MVBs, thus highlighting the important role played by TSG101 in this process (Bache et al., 2006; Doyotte et al., 2005). ESCRT-III is then recruited to deubiquitinate the ubiquitinated cargo. The VpS4 complex then

catalyzes membrane scission releasing the ESCRT III subunits, which are recycled to allow another round of MVB formation (Wollert et al., 2009).

1.5.13 Recycling of trafficking receptors

Recycling pathways are used as a mechanism to regulate the transport of essential molecules to organelles, which are required for their function, and to maintain the lipid and protein composition of other organelles. There are two types of recycling pathways: fast recycling and slow recycling (Grant and Donaldson, 2009; Sheff et al., 1999). The fast recycling route has been well described for the TfR and is associated with receptor recycling back to the plasma membrane from early endosomes. The slow recycling route, on the other hand, follows an indirect path through recycling endosomes.

Rab11 is the key regulator of recycling endosomes (Green et al., 1997). Rab proteins exist in two states the active form, which is bound to GTP (guanosine triphosphate) and the inactive form, which is bound to GDP (guanosine diphosphate) (Seabra and Wasmeier, 2004). Thus the activity of Rab proteins is regulated by the phosphorylation status of the bound GDP by GDP/GTP exchange factor (GEF). In fact, overexpression of WT or mutant rab11 proteins can modulate the traffic through recycling endosomes (Ren et al., 1998; Ullrich et al., 1996). Studies of the TfR demonstrated that overexpression of the dominant-negative rab11S25N, which is unable to bind GTP, slowed down the recycling of trafficking receptors from early endosomes to the cell surface and further inhibited the delivery of transferrin to recycling endosomes (Ren et al., 1998). Moreover, overexpression of the constitutively active Rab11 rab11Q70L resulted in transferrin accumulation in recycling endosomes. Rab11 has been implicated in

the recycling of many trafficking receptors including EGFR (Chi et al., 2011) and a number of GPCRs (Drake et al., 2006).

Previously it has been documented that Rab4 is important for the recycling of the TfR from early endosomes but recent studies have questioned the precise role of Rab4 in this process. Studies have shown that fast recycling is inhibited when a dominant-negative Rab4 is expressed whilst other studies have shown an increase in fast recycling when short-interfering RNA is used to knockdown Rab4 (Deneka et al., 2003; Yudowski et al., 2009). Rab35 on the other hand is now emerging as an important regulator of rapid recycling in particular for the mammalian TfR (Kouranti et al., 2006). Rab35 has been shown to localise to early endosomes and to the plasma membrane. Depletion of Rab35 or the overexpression of an inhibitor of Rab35 (EP164C) has been shown to impair the formation of the immunological synapse and TfR recycling (Patino-Lopez et al., 2008).

1.6 CTLA-4 receptor trafficking

1.6.1 CTLA-4 Internalisation

The phosphorylation status of the YVKM motif in the CTLA-4 cytoplasmic domain has long been established as the regulator of its function. Tyrosine phosphorylation has been suggested to stabilise the cell surface expression of CTLA-4 following T cell stimulation (Bradshaw et al., 1997; Chuang et al., 1997). In fact, such a mechanism overcomes the issue of how the highly endocytic CTLA-4 receptor interacts with cell surface ligands on APCs. When the tyrosine residue is phosphorylated, this blocks the interaction of the YVKM with the clathrin adaptor AP-2 thereby preventing CTLA-4 endocytosis. A question recently addressed by our lab was whether CTLA-4 endocytosis is inhibited in T cells following

stimulation. We found that T cell stimulation does increase CTLA-4 trafficking to the plasma membrane, which is in agreement with previous studies (Egen and Allison, 2002; Linsley et al., 1996). However, the ratio of surface to internalised CTLA-4 demonstrated that the amount of CTLA-4 at the T cell surface at any given time remains the same (Qureshi et al., 2012), suggesting the receptor is not stabilised at the cell surface.

The importance of tyrosine 201 for CTLA-4 internalisation was initially demonstrated using mutational analysis (Leung et al., 1995), and in later studies, an interaction between the cytoplasmic tail of CTLA-4 and the medium subunit (μ2) AP-2 clathrin-adaptor complex was determined (Chuang et al., 1997; Shiratori et al., 1997). Using immunoprecipitation and cells transfected with HA-tagged μ2 and GST-tagged CTLA-4, it was confirmed the tyrosine 201 residue within the YVKM motif was important for this interaction (Chuang et al., 1997; Zhang and Allison, 1997). The importance of clathrin-mediated endocytosis was further verified by incubating cells in potassium-depleted medium that has been shown to block assembly of CCVs (Chuang et al., 1997). CTLA-4 internalisation was indeed inhibited suggesting clathrin is required in CTLA-4 endocytosis.

Our lab has further shown that CTLA-4 internalisation is dynamin-dependent. Using confocal microscopy, we found that CTLA-4 internalisation was inhibited when CTLA-4-transfected chinese hamster ovary (CHO) cells were incubated with the dynamin inhibitor dynasore (Qureshi et al., 2012). Post-internalisation CTLA-4 has also been shown to co-localise with markers of early endosomes and with TfR (Mead et al., 2005). Although the post-internalisation fate of CTLA-4 is poorly understood, as a lab we have shown that CTLA-4 can recycle back to the plasma membrane or is targeted for degradation in lysosomes (**figure 1.10**).

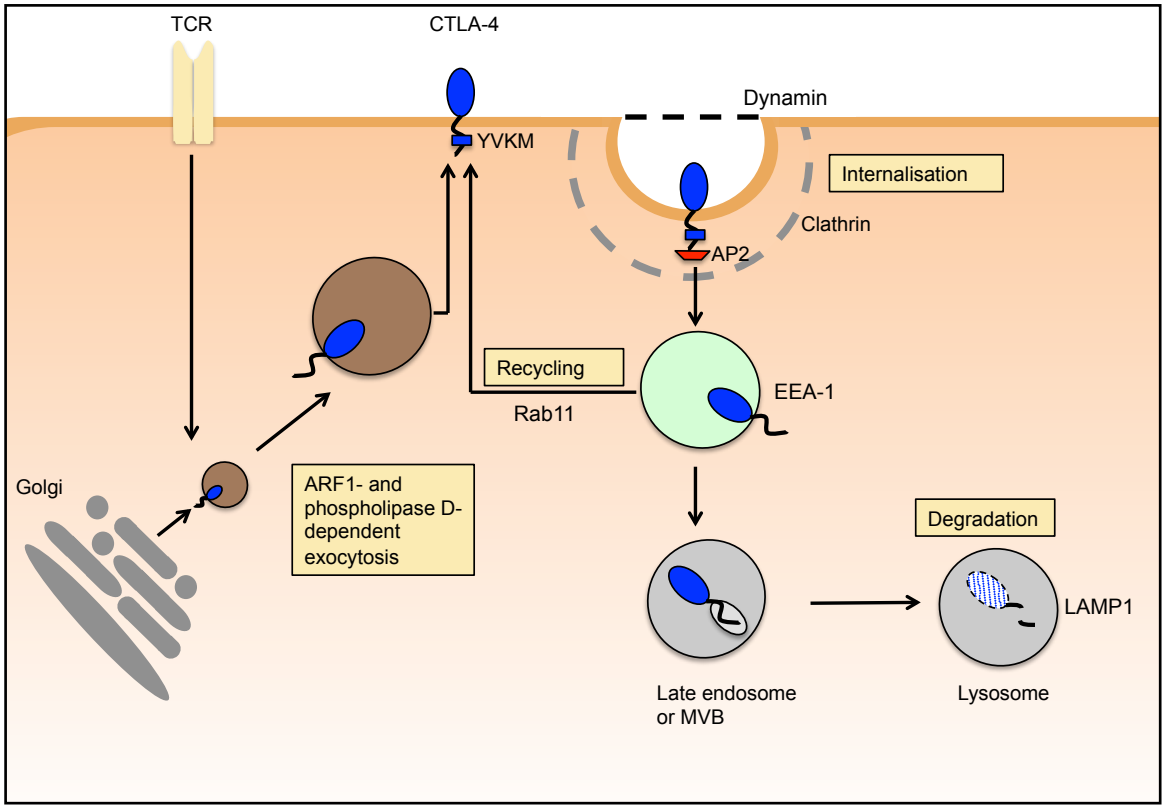

Figure 1.10 CTLA-4 intracellular trafficking. CTLA-4 is exported to the plasma membrane from the golgi in an ARF1- and phospholipase D-dependent manner. CTLA-4 internalises into clathrin-coated pits via the association of the YVKM motif located in the cytoplasmic domain and the clathrin adaptor AP-2. Scission of the vesicle is mediated by the GTPase dyanmin. Once internalised CTLA-4 has been found to co-localise with EEA-1 a marker of early endosomes. From here, CTLA-4 has been shown to co-localise with Rab11 a marker of recycling endosomes, which suggests the receptor recycles back to the plasma membrane. CTLA-4 has also been shown to co-localise with LAMP1, which suggests the receptor is targeted for degradation in lysosomes. Prior to entry into lysosomes CTLA-4 has been identified in late endosomes or MVBs. ARF1, ADP-ribosylation factor 1; LAMP1, Lysosomal-associated membrane protein 1).

1.6.2 CTLA-4 degradation

Several groups have reported that CTLA-4 is degraded in lysosomal compartments and that this could serve as a potential mechanism by which a T cell could regulate the expression of CTLA-4. Co-localisation of CTLA-4 with lysosomal markers has been variable and in fact we also observed little co-localisation of CTLA-4 with Lysosomal-associated membrane protein 1 (LAMP1) in primary T cells (Qureshi et al., 2012). This data rules out the possibility that CTLA-4 is stored in secretory lysosomes as if this was the case substantial co-localisation of CTLA-4 with lysosomal markers should be observed at steady state. In a study where T cells were treated with Cycloheximide (CHX), the half-life of CTLA-4 protein turnover was revealed to be approximately 2 hours (Egen and Allison, 2002). Moreover, total CTLA-4 expression was increased following treatment with Ammonium chloride (NH_4Cl), an inhibitor of lysosomal degradation, further suggesting that lysosomes are used to degrade CTLA-4 and are not being used as a storage compartment. For transendocytosis function, we have demonstrated using lysosomal inhibitors that CTLA-4 targets the ligand for degradation in lysosomes thus providing a purpose for this trafficking pathway (Qureshi et al., 2011).

The mechanism required for CTLA-4 targeting to lysosomes remains to be identified. Most trafficking receptors use ubiquitin as a sorting signal to be trafficked to lysosomes. In fact, in T cells the TCR is downregulated after ligand binding and the internalised receptor is trafficked to lysosomes for degradation (Valitutti et al., 1997). It has been suggested that ubiquitination of the TCR could serve as the signal regulating its targeting to lysosomes a process performed by the most likely candidate E3 ligase Casitas B-cell lymphoma-b (Cbl-b) (Naramura et al., 2002). Recently, Vardhana et al., (2010) have demonstrated that in TCR downregulation the recognition of ubiquitin by TSG101 is essential for central supramolecular activation cluster (cSMAC) formation and function, the site identified to be

concentrated in MVB markers. A model is therefore proposed that ESCRT-I sorts the TCR into MVB-like structures within the cSMAC and targets the TCR for degradation. This is suggested to be dependent upon strong agonist engagement with the TCR (Vardhana et al., 2010). Thus, it is interesting to speculate whether CTLA-4 uses a similar pathway to be targeted for lysosomal degradation.

1.6.3 CTLA-4 recycling

The well-characterised TfR, which also internalises by clathrin-mediated endocytosis, can recycle constitutively back to the cell surface. In both murine splenocytes and activated human T cell blasts, CTLA-4 has been found to co-localise with TfR (Chuang et al., 1997; Leung et al., 1995), and thus this led to the hypothesis that following internalisation, CTLA-4 could recycle back to the plasma membrane (Chuang et al., 1997; Leung et al., 1995). As a lab, we have confirmed these findings by providing direct evidence of CTLA-4 co-localising with the recycling marker Rab11 (Qureshi et al., 2012). Although this data provides further understanding to CTLA-4 intracellular trafficking, it does not explain why the CTLA-4 receptor needs to recycle. Moreover, the motifs encoded in the CTLA-4 cytoplasmic domain that could possibly mediate such intracellular sorting remain to be identified.

1.7 Aims and Objectives

The foregoing introduction highlights the role of CTLA-4 as a potent negative regulator of T cell immune responses. The location of CTLA-4 in intracellular vesicles is the most dominating aspect of its biology, yet the significance of this at the functional level remains to be understood. The models of CTLA-4 function to date include a competition model, the delivery of a cell-intrinsic negative signal, IDO production in DCs, and inhibition of T cell responses via Tregs. However, these models assume CTLA-4 is arrested at the plasma membrane, and fail to take the constitutive internalisation of the receptor into account. In our lab, we have identified an unusual biological feature of CTLA-4 that could potentially explain some features of the CD28/CTLA-4 system. This phenomenon is called transendocytosis, where CTLA-4 in Tregs and activated T cells may modify the phenotype of APCs by removing ligand and targeting it for degradation. Central to the understanding of CTLA-4 function is an appreciation of how the expression and function of this protein has adapted through evolution. Therefore, an awareness of the intracellular trafficking pathways used by CTLA-4 and an understanding of how these trafficking events are regulated is essential.

To date, majority of the studies have emphasised that the internalisation of CTLA-4 occurs via the clathrin-dependent pathway. This requires the association of the YVKM motif encoded in the CTLA-4 cytoplasmic domain with the clathrin adaptor AP-2. However, mutations of the tyrosine residue in this motif can still facilitate CTLA-4 internalisation but at a slower rate suggesting other residues in the cytoplasmic tail may contribute to inclusion into clathrin pits. Moreover, the fate of the CTLA-4 receptor post-internalisation is poorly understood. As a lab we have shown that CTLA-4 is recycled and degraded but the intracellular trafficking pathways and sorting motifs required for such trafficking remain to be identified.

Therefore the aim of this project was to investigate the role of the CTLA-4 cytoplasmic domain in the intracellular trafficking of the receptor. My main objectives were as follows:

1. To investigate the steady state localisation of CTLA-4 in CTLA-4 transfected cells and in T cells.
2. To generate CTLA-4 chimeras and address whether CTLA-4 intracellular trafficking is conserved through evolution.
3. To use site-directed mutagenesis to address role of the CTLA-4 cytoplasmic domain in regulating CTLA-4 recycling and degradation.
4. To use site-directed mutagenesis to address the role of the CTLA-4 cytoplasmic domain in transendocytosis of ligand and to understand whether CTLA-4 function has changed through evolution.

2.0 MATERIALS AND METHODS

2.1 General Methods

All tissue culture work was carried out under sterile conditions in Class II laminar flow hoods. Vented 75m^2 tissue culture flasks, 6-well, 24-well flat bottom, 96-well round bottom and 96-well flat bottom tissue culture plates were purchased from Sarstedt. Cell lines were incubated at 37°C, 95% humidity, 5% CO_2 in a MCO-17A1C Sanyo CO_2 incubator. Following passage, cells were transferred into 30ml sterile universal tubes (Sterillin). Cells were counted using a haemocytometer (Neubauer B.S 748; Fison Scientific equipments).

For flow cytometric analysis on the FACSCalibur flow cytometer (BD Biosciences – Oxford, UK) cells were placed in non-sterile 12x75mm, 5ml round bottom polystyrene tubes (Falcon). For flow cytometric analysis on the Dako Cyan flow cytometer, cells were placed in non-sterile 12x75mm, 5ml round bottom polypropylene tubes (Falcon). For cell sorting, cells were placed in sterile 12x75mm, 5ml round bottom polypropylene tubes with snap caps (Falcon). Using a sterile 0.22μm filter (Millex), samples were filtered prior to sorting. For confocal analysis, glass slides and cover slips were purchased from VWR International.

2.1.1 Antibodies and reagents

Table lists antibodies used for flow cytometry, confocal microscopy and western blotting.

Specificity	Clone	Dilution	Source
Primary Antibodies			
CTLA-4-PE	BN13	1:100*	BD Biosciences
Mouse IgG_{2a}, κ	G155-178	1:100*	BD Biosciences
Unlabelled anti-CTLA-4	11G1	0.3mg/ml	Dr J. Allison
Ticililmumab		1μg/ml	Pfizer
Unlabelled anti-CTLA-4	Az1172/272	1:100	AstraZeneca
C-19	Polyclonal	0.5μg/ml	Santa Cruz
Ub (P4D1)	Monoclonal	1μg/ml	Santa Cruz
CD80-PE	L307.4	1:100*	BD Biosciences
CD86-PE	2331	1:100*	BD Biosciences
Secondary Antibodies			
AlexaFluor Donkey anti-mouse 488	-	1:500	Invitrogen
AlexaFluor Donkey anti-mouse 555	-	1:500	Invitrogen
AlexaFluor Donkey anti-mouse 647	-	1:200	Invitrogen
AlexaFluor Donkey anti-human 488	-	1:500	Invitrogen
AlexaFluor Donkey anti-human 565	-	1:500	Invitrogen
Polyclonal Goat anti-Mouse Immunoglobulins/HRP	-	1:7500	Dako
Polyclonal Rabbit anti-Goat Immunoglobulins/HRP	-	1:7500	Dako
IRDye 800CW Goat anti-Mouse IgG	-	1:10000	LI-COR

Table 2.1 List of antibodies used in flow cytometry, confocal microscopy and western blotting.

* BD Biosciences do not give concentration of Abs they sell as test format. Abs were titrated to find the best concentration required for a volume of 100μl.

The following reagents were purchased from Invitrogen: Dulbecco's Modified Eagle Medium (DMEM); Roswell Park Memorial Institute (RPMI); Trypsin-EDTA (ethylenediamine tetraacetic acid); Dimethyl sulphoxide (DMSO); PureLink™ HiPure Plasmid Filter Purification Kit; PureLink HiPure Precipitator Module; Tris-EDTA (TE) buffer; 100% Methanol; Penicillin and Streptomycin; Geneticin Selective Antibiotic (G418); Protein-G-Sepharose beads; Tranferrin from human serum, AlexaFluor 633 conjugate; Wheat Germ Agglutinin (WGA) - tetramethylrhodamine conjugate; Sybr safe DNA gel stain (10,000 concentration); pcDNA™3.3 TOPO Mammalian Expression Vector; One Shot TOP10 Chemically Competent *E.coli*; CellTrace Violet; Neon Transfection System; CD3/CD28 T Cell Expander Dynabeads. Prestained Protein Marker, Broad Range (7-175 kDa); BglII and SacII restriction enzymes; 1kb DNA ladder and 6X loading dye were purchased from New England Biosciences (NEB). QIAprep Spin Miniprep Kit was purchased from QIAGEN. The following reagents were purchased from Sigma: Hepes; Ampicillin; Select Agar; Sodium-Dodecyl-Sulphate (SDS); L-glutamine; Saponin; Paraformaldehyde (PFA); N,N,N′,N′-Tetramethylethylenediamine (TEMED); poly-L-lysine; Sodium azide; Ethanol; Protease Cocktail Inhibitor; MG132; Ammonium chloride (NH_4Cl). Fetal Bovine Serum (FBS) was purchased from Harlan Sera-Lab Ltd, UK. QuikChange Lightning Site-Directed Mutagenesis kit was purchased from Agilent Technologies. The following reagents were purchased from Thermo Fisher Scientific: Pierce Cell Surface Protein Isolation Kit; Pierce Spin Columns (Snap Cap); Precise Protein Gels 8-16% and 4-20%, 12-well; Pierce ECL (enhanced chemiluminescence) Western Blotting Substrate. The following reagents were purchased from Geneflow: Electroblotting Buffer Tris-glycine (10X); TAE buffer (50X); Protein Loading Buffer (2X); Protogel Resolving Buffer (4X); Protogel Stacking Buffer; ProtoGel 30%. The following reagents were purchased from Fisher Scientific: Tween20; Tris Base; Ethylenediaminetetraacetic acid (EDTA); Triton; Ammonium persulphate (APS). Immobilon-FL Polyvinylidene Fluoride (PVDF) was purchased from Millipore. *Pfu* DNA polymerase (recomb.) 100 units was purchased from Fermentas. X-gal/IPTG solution was purchased from Bioline. Amersham Hybond

ECL Nitrocellulose membrane was purchased from GE Healthcare Life Sciences. Amaxa Cell Line Nucleofector Solution Kit T was purchased from Lonza. Circlegrow was purchased from Q-biogene. Phosphate buffered saline (PBS) tablets were purchased from Oxoid. Cycloheximide (CHX) was purchased from Calbiochem. Bafilomycin A1 (BafA) was purchased from Tocris Biosciences. Unmodified oligonucleotide DNA primers were synthesised by Eurofins MWG and purified by High purity salt free (HPSF) purification. Unmodified oligonucleotide DNA primers required for QuikChange Lightning Site-Directed Mutagenesis were purified by High-performance liquid chromatography (HPLC).

2.2 Cell culture

2.2.1 Culture and passage of cell lines

Adherent chinese hamster ovary (CHO) transfectants were cultured in glutamine free DMEM medium supplemented with 2mM L-glutamine, 10% FBS and 1% penicillin and streptomycin. Cells were grown in vented 75cm^2 sterile tissue culture flasks as a monolayer culture and upon confluence were passaged every 2-3 days. To passage the cells, those in suspension were aspirated using glass Pasteur pipettes (Appleton Woods) and the flasks washed once in 10ml sterile PBS. Adherent cells were removed by incubation with 2ml Trypsin-EDTA for 5minutes at 37°C. Trypsin was inactivated with the addition of 8ml fresh medium. Up to 80% of the cell suspension was removed from the flask and fresh medium added to a total of 20ml.

Jurkat T cells were cultured in RPMI medium supplemented with 2mM L-glutamine, 10% FBS and 1% penicillin and streptomycin. Cells were grown in vented 75m^2 sterile tissue culture flasks.

2.2.2 Cryogenic preservation and storage of cell lines

To maintain a permanent stock, transfected CHO cells were stored in liquid nitrogen. Following cell passage, 5ml of the cell suspension was washed at 490 *g* for 5minutes to pellet the cells and re-suspended in 500µl 80% FBS in DMEM volume/volume (v/v) followed by 500µl 20% DMSO in DMEM (v/v). The cell suspension was transferred into cryotube vials and incubated at -80°C for 24hours before indefinite storage in liquid nitrogen.

2.2.3 Isolation of Peripheral Blood Mononuclear Cells (PBMC)

Leukocyte reduction system cones (LC) were provided by the Birmingham National Blood Service and used to isolate primary cells from PBMC. The Ficoll-Paque PLUS method of density gradient centrifugation was used for PBMC isolation.

LCs were diluted in PBS at a ratio of 1:4. 25ml of the diluted cell suspension was layered over 15ml Ficoll-Paque PLUS in a 50ml Falcon tube. The cell suspension was centrifuged at 1060 *g* without brake for 25minutes. The upper layer was aspirated and the mononuclear cell layer was transferred to a new 50ml Falcon tube using a Pasteur pipette. The cell suspension was made up to 50ml using PBS and centrifuged at 1060 *g* with brake for 10minutes. The supernatant was aspirated and the cells were washed in 50ml PBS at 260 *g* for 5minutes. This was followed by two washes in MACS® buffer (2mM EDTA, 0.5% Bovine Serum Albumin (BSA) in PBS). The cells were counted after each wash and the number of washes adjusted according to the efficiency of platelet removal.

2.2.3.1 Isolation of $CD4^+$ T cells using EASYSEP™ Human $CD4^+$ T cell Enrichment Kit

$CD4^+$ T cells were isolated from PBMCs using the EASYSEP™ Human $CD4^+$ T cell enrichment kit by negative selection. The cocktail contains Tetrametric Antibody Complexes that recognise CD8, CD14, CD16, CD19, CD20, CD36, CD56, CD66b, CD123, TCRγ/δ, glycophorin A and dextran-coated magnetic particles.

PBMCs were resuspended in MACS buffer at a concentration of $100x10^6$/ml in a 15ml Falcon tube. $CD4^+$ T cell enrichment cocktail was added to the cells at a concentration of 50µl/ml and the mixture was incubated at room temperature for 10minutes. EasySep™ magnetic particles were vortexed to ensure the aggregates were in a uniform suspension and added to the cells at a concentration of 100µl/ml. The tube was inverted to ensure the cells and particles were mixed well and incubated at room temperature for 5minutes. The total volume in the tube was adjusted to 9ml using MACS® buffer and the tube was placed into an EasySep™ magnet with the cap removed. After 5minute incubation, the magnet and tube were inverted for 2-3 seconds to pour off the negative selected cells into a fresh 15ml Falcon tube. To increase purity the magnetic removal step was repeated and the negative selected cells were finally transferred to a 30ml universal tube. The cells were counted, centrifuged at 490 *g* for 5minutes and resuspended at a concentration of $100x10^6$/ml in MACS® buffer.

2.2.3.2 Isolation of $CD4^+$ $CD25^+$ Tregs

$CD4^+$ T cells isolated as described in section **2.2.3.1** were resuspended in MACS buffer at a concentration of $1x10^8$/ml in a 15ml Falcon tube. The Tetrametric Antibody Complexes recognises non-$CD4^+$ T cells, $CD127^{high}$, $CD49d^+$ cells and dextran-coated magnetic particles.

EasySep™ Human $CD4^+CD127^{low}CD49d^-$ Regulatory T Cell Enrichment cocktail was added at a concentration of 50µl/ml and the mixture was incubated for 10minutes at room temperature. EasySep™ D2 Magnetic particles were vortexed to ensure the aggregates were in a uniform suspension and added to the cells at a concentration of 100µl/ml. The tube was inverted to ensure the cells and particles were mixed well and incubated at room temperature for 5minutes. The total volume in the tube was adjusted to 7ml using MACS® buffer and the tube was placed into an EasySep™ magnet with the cap removed. After 5minute incubation, the magnet and tube were inverted for 2-3 seconds to pour off the negative selected cells into a fresh 15ml Falcon tube. 70µl EasySep™ Dextran Selection Cocktail was added to the cells and the mixture was incubated at room temperature for 10minutes. EasySep™ D2 Magnetic particles were vortexed and 70µl of the particles were added to the mixture. The tube was inverted to ensure the cells and particles were mixed well and the mixture was incubated at room temperature for 5minutes. The tube was placed into an EasySep™ magnet with the cap removed. After 5minute incubation, the magnet and tube were inverted for 2-3 seconds to remove the negative selected cells, which were transferred into a fresh 30ml universal tube. The cells were counted and resuspended in RPMI at a concentration of $1x10^6$/ml.

2.2.3.3 T cell stimulation assays

T cell stimulation assays were performed in 96-well flat bottom plates. $1x10^5$ T cells were plated out per well in a total volume of 200µl. T cells were stimulated with CD3/CD28 T Cell Expander Dynabeads. 0.5µl of the beads were added to each well to achieve a 1:4 bead to cell ratio.

$CD4^+CD25^+$ T cells were supplemented with IL-2 (100U/ml).

2.3 Molecular Biology

2.3.1 Generation of CTLA-4-CD86 chimera

Oligonucleotide primers were designed to fuse the extracellular domain of CTLA-4 and the transmembrane and cytoplasmic domain (TMCY) of CD86 by PCR amplification, using CTLA-4 (5µg/ml) and CD86 (5µg/ml) plasmid DNA (Deoxyribonucleic acid) as templates (**table 2.2**). The volumes required for a single *Pfu* PCR are listed in **table 2.3**. PCR was performed by predenaturation at 95°C for 5minutes followed by 25 cycles at 95°C for 1minute, annealing at 55°C for 1minute and extension at 72°C for 1minute 30seconds. The programme ended with a period of extension at 72°C for 10minutes before cooling to 4°C for storage. Following amplification, 2µl of sample loading buffer was added to 10µl of digested samples to analyse product size by electrophoresis on 1% agarose TAE gel set with 10µl Sybr Safe DNA gel stain. 1kb DNA ladder was prepared by adding 1µl of DNA ladder to a microcentrifuge tube with 9µl of water and 2µl of loading buffer.

Construct	Plasmid DNA	Primers	Product length
CTLA-4-CD86	CTLA-4	[F]ATGGCTTGCCTTGGATTTCAGCGG	509bp
		[R]GGAAGTACAGCTGTAATCCAAGGAATGTCAGAA TCTGGGCACGGTTC	
	CD86	[F]GAACCGTGCCCAGATTCTGACATTCCTTGGATTA CAGCTGTACTTCC	276bp
		[R]TTAAAAACATGTATCACTTTTGTCGC	

Table 2.2 Forward and reverse primer sequences used for the amplification of regions within the transcripts of CTLA-4 and CD86. [F], Forward; [R], Reverse; bp, base pair.

Reagents	Volume (µl)
H_2O	44
dNTP (2.5mM)	10
$MgCl_2$ (5mM)	5
10X *Pfu* buffer with $MgSO_4$	10
Forward primer (10µM)	10
Reverse primer (10µM)	10
Target DNA	10
Pfu DNA polymerase	1
Total	**100**

Table 2.3 Volumes of reagents required for one *Pfu* reaction.

The reverse primers used to amplify CTLA-4 protein was designed to recognise the 5' transmembrane region of CD86 and the forward primer of CD86 was designed to recognise the 3' extracellular domain of CTLA-4. 15µl of CTLA-4 extracellular domain and 15µl of CD86 TMCY were added to a microcentrifuge tube with 2.5µl $MgCl_2$ and 17.5µl 10X *Pfu* buffer with $MgSO_4$. The amplicons were heated to 100°C for 2minutes to denature the DNA, and cooled to 55°C on ice to anneal the target DNA. A PCR was setup to amplify the construct using 10µl of target DNA and using the oligonucleotides designed to recognise the 5' extracellular domain of CTLA-4 and 3' cytoplasmic domain of CD86 under standard PCR conditions. The size of the amplicons were analysed by TAE (Tris-acetate EDTA) gel electrophoresis and visualised by ultraviolet transillumination.

2.3.2 Addition of 3' A-Overhangs Post-Amplification

Due to the proof reading capacity of *Pfu*, 3'A overhangs necessary for the direct cloning of the PCR fragments by the TOPO-TA method are not created. Prior to setting up the TOPO cloning reaction, 3' A-overhangs were added post-amplification. 1unit of Taq polymerase was added to each PCR tube and heated to 72°C for 10minutes. The DNA amplification product was used directly in the TOPO cloning reaction.

2.3.3 TOPO Cloning

2µl of the PCR product from section **2.3.2** were mixed with 1µl salt solution, 1µl H_2O and 1µl pcDNA™3.3 TOPO vector provided in the TOPO TA cloning kit from Invitrogen. The reaction mix was incubated at room temperature (25°C) for 10minutes, placed on ice and then used for the transformation of One Shot TOP10 Chemically Competent E.*coli* cells.

2.3.4 Bacterial Transformation

One vial of One Shot TOP10 Chemically Competent E.*coli* cells was thawed on ice. 2µl of the TOPO cloning reaction prepared in section **2.3.3** was added to the vial, mixed gently and incubated on ice for 30minutes. The cells were then heat shocked at 42°C for exactly 30seconds, and transferred to ice for 2minutes. 250µl of room temperature SOC medium was added to the vial, which was then shaken horizontally for 1hour at 37°C at 250RPM in a shaking incubator. 100µl of each transformation was spread onto a pre-warmed LB plate containing 50µg/ml ampicillin. Plates were inverted and incubated overnight at 37°C. The vectors contained an Ampicillin resistance gene and the presence of the antibiotic in the agar resulted in selective growth of transformed cells.

2.3.5 Quik-change lightning site-directed mutagenesis

Two complimentary oligonucleotides were synthesised for each desired mutation, flanked by unmodified nucleotide sequence and purified by HPLC (**table 2.4**). The volumes required for a single mutant strand synthesis reaction are listed in **table 2.5**. The control reaction was prepared as listed in **table 2.6**. PCR was performed by pre-denaturation at 95°C for 2minutes followed by 18 cycles at 95°C for 20seconds,

annealing at 60°C for 10seconds and extension at 68°C for 30seconds/kb of plasmid length. The programme ended with a period of extension at 68°C for 10minutes. The amplification products were mixed with 2µl of the *Dpn* I restriction enzyme. The reaction mixtures were gently vortexed and immediately incubated at 37°C for 5minutes to digest the parental supercoiled double stranded DNA. The reaction mixtures were transferred to ice and then used for transformation of XL-Gold ultracompetent cells.

2.3.6 Transformation of XL-Gold Ultracompetent Cells

The XL10-Gold ultracompetent cells were thawed on ice. 45µl of the ultracompetent cells were aliquoted into pre-chilled 15-ml BD Falcon polypropylene round-bottom tubes for each control and sample reaction. 2µl of the 2-Mercaptoethanol (β-ME) mix provided with the kit was added to the cells. The contents were swirled and the cells were incubated on ice for 2minutes. 2µl of the *Dpn* I-treated DNA from each control and sample reactions were added to the separate aliquots of the ultracompetent cells, gently mixed and the reactions were incubated on ice for 30minutes. The tubes were heat-pulsed in a 42°C water bath for 30seconds, and transferred to ice for 2minutes. 500µl of preheated (42°C) NZY^+ broth was added to each tube, which was then shaken for 1hour at 37°C at 250 rotations per minute (RPM) in a shaking incubator. 100µl of each transformation was spread onto a pre-warmed LB plate containing 50µg/ml Ampicillin. 100µl of the control reaction was spread onto LB-ampicillin plate containing 80µg/ml 5-Bromo-4-chloro-3-indoyl β-D-galactopyranoside (X-gal) and 20mM Isopropyl β-D-1-thiogalactopyranoside (IPTG). Plates were inverted and incubated overnight at 37°C. The vectors contained an Ampicillin resistance gene and the presence of the antibiotic in the agar resulted in selective growth of transformed cells.

Plasmid DNA	Construct	Primer	pmoles of oligo (125ng)*
CTLA-4	ATEP	[F]GTGAAAATGCCCGCAACAGAGCCAGAATGTGAA (33bp) [R]TTCACATTCTGGCTCTGTTGCGGGCATTTTCAC (33bp)	11.5µl
	AVKM	[F]CTTACAACAGGGGTCGCTGTGAAAATGCCCCCAACA (36bp) [R]TGTTGGGGGCATTTTCACAGCGACCCCTGTTGTAAG (36bp)	10.5µl
	AFIP	[F] GCAATTTCAGCCTGCTTTTATTCCCATCAATTGA (34bp) [R]TCAATTGATGGGAATAAAAGCAGGCTGAAATTGC (34bp)	11.1µl
AVKM	AVKM-AFIP	[F] GCAATTTCAGCCTGCTTTTATTCCCATCAATTGA (34bp) [R]TCAATTGATGGGAATAAAAGCAGGCTGAAATTGC (34bp)	11.1µl
CTLA-4	K191R	[F]GAGCAAAATGCTAAGGAAAAGAAGCCCTC (29bp) [R]GAGGGCTTCTTTTCCTTAGCATTTTGCTC (29bp)	13.1µl
	K192R	[F]GCAAAATGCTAAAGAGGAGAAGCCCTCTTAC (31bp) [R]GTAAGAGGGCTTCTCCTCTTTAGCATTTTGC (31bp)	12.2µl
	K203R	[F]CAGGGGTCTATGTGAGGATGCCCCCAACAG (30bp) [R]CTGTTGGGGGCATCCTCACATAGACCCCTG (30bp)	12.6µl
	K213R	[F]CCAGAATGTGAAAGGCAATTTCAGCC (26bp) [R]GGCTGAAATTGCCTTTCACATTCTGG (26bp)	14.6µl
K203R	K203,213R	[F]CCAGAATGTGAAAGGCAATTTCAGCC (26bp) [R]GGCTGAAATTGCCTTTCACATTCTGG (26bp)	14.6µl

Table 2.4 Forward and reverse primer sequences synthesised for each desired mutation. [F], Forward; [R], Reverse; bp, base pair.

* *X* pmoles of oligo = $\frac{\text{125ng of oligo}}{\text{330 x \# of bases in oligo}}$ x 1000

Reagents	Volume (µl)
10X reaction buffer	5
dsDNA (5ng/µl)	5
Oligonucleotide primer 1	125ng
Oligonucleotide primer 2	125ng
dNTP	1
QuikSolution Reagent	1.5
ddH_2O	To a final volume of 50µl
QuikChange Lightning Enzyme	1
Total	**50**

Table 2.5 Volume of reagents required for 1 QuikChange Lightning Site-Directed Mutagenesis reaction.

Reagents	Volume (µl)
10X reaction buffer	5
pWhitescript 4.5kb control plasmid (5ng/µl)	5
Oligonucleotide primer 1	1.25
Oligonucleotide primer 2	1.25
dNTP	1
QuikSolution Reagent	1.5
ddH_2O	34
QuikChange Lightning Enzyme	1
Total	**50**

Table 2.6 Volume of reagents required for the control QuikChange Lightning Site-Directed Mutagenesis reaction.

2.3.7 Mini Plasmid Preparations

Plates were analysed for the presence of bacterial colonies. Ten 5ml aliquots of Ampicillin broth (consisting of circle grow supplemented with 50µg/ml of Ampicillin) were each inoculated with one colony picked from the selection plates. The cultures were incubated for 8-12hours at 37°C under continual shaking at 250RPM in a shaking incubator. The QIAGEN plasmid mini kit was used to extract the plasmid from 2ml of the cultures for restriction digestion analysis prior to Maxi plasmid preparation. The bacterial pellet was resuspended in 250µl of Buffer P1 with RNAse, 250µl Buffer P2 to lyse the cells and inverted 6 times before the addition of Buffer N3 to precipitate proteins. The eppendorf was inverted 6 times and centrifuged for 10minutes. The supernatant was loaded onto the spin column, centrifuged for 1minute and supernatant discarded. The DNA was washed with 750µl of Wash Buffer with Ethanol for 1minute and to ensure removal of residual Ethanol, the column was centrifuged for a further minute. The collection tube was discarded and column transferred to a fresh eppendorf to elute the DNA with 30µl of Elution buffer. The column was left to stand for 1minute and centrifuged for a further minute. The concentration of plasmid was measured by a nanodrop using 1µl of the sample and using Elution buffer as the blank. Tubes were stored at 4°C. Unless otherwise indicated all centrifuge steps were carried out at 16.1 *g*.

2.3.8 Restriction Digest Analysis of Plasmid Extracts

To confirm the orientation of the chimera, restriction digest analysis was used as a screening method. The reactions were prepared by mixing 2µl of the plasmid DNA with 2µl of 10X restriction enzyme buffer, 2µl of restriction enzyme and 14µl of H_2O, and incubated at 37°C for 1hour and 30minutes. The reaction was stopped by the addition of 4µl of 6X loading buffer and separation by gel electrophoresis

against a 1kb ladder. The culture for the hybrid in the correct orientation was transferred into a large conical flask containing 500ml of Ampicillin broth and left overnight to grow at 250RPM and 37°C.

2.3.9 Maxi Plasmid Preparations

Large-scale preparations of plasmid DNA were performed using the PureLink™ HiPure Plasmid Filter DNA Purification Kit, according to the manufacturer's protocol. Cultures set up for maxiprep were centrifuged for 10minutes at 5000 *g* and 17°C using a JLA 162.50 rotor to pellet the cells. The pellet was resuspended in 10ml Resuspension Buffer with RNase A and transferred to a 50ml centrifuge tube, followed by addition of 10ml Lysis buffer to lyse the cells. 10ml of Precipitation Buffer was added to precipitate proteins. The supernatant was loaded onto the equilibrated column, washed with 50ml of Wash buffer and the flow-through was discarded. 15ml of Elution buffer was added to the column to elute the DNA and the column was discarded.

DNA was precipitated using the PureLink™ HiPure Precipitator Module. 10.5ml of Isopropanol was added to the elution tube and mixed. The plunger of a 30ml syringe was removed, and a PureLink HighPure™ Precipitator Module was attached through the luer lock inlet of the syringe. The precipitated DNA mixture was loaded into the syringe, placed over a waste container and the plunger was re-inserted into the syringe. A slow, constant force was used to push the plunger to pass the DNA mixture through the precipitator. The flow-through was discarded. The precipitator was detached from the syringe, the plunger removed and the precipitator was re-attached to the syringe. To wash the precipitated DNA, 5ml of 70% Ethanol was added to the syringe, plunger re-inserted and pushed to pass the Ethanol through the precipitator. The precipitator was detached from the syringe, the plunger

removed and the precipitator was re-attached to the syringe. To dry the precipitator membrane, the plunger was re-inserted and a slow, constant force was used to push the plunger to pass air through the precipitator. The precipitator was detached from the 30ml syringe. The plunger from a 5ml syringe was removed, and the precipitator module was attached to the syringe. To elute the DNA, 1ml TE buffer was added to the 5ml syringe. The plunger was reinserted and placed over a clean, sterile microcentrifuge tube. The plunger was pushed to elute the DNA into the new tube. The concentration of plasmid was measured by a nanodrop using 1µl of the sample and using TE buffer as the blank. Tubes were stored at 4°C.

2.3.10 Sequencing of amplified fragments

Following on plasmid preparation, samples of the DNA were then prepared for sequencing. Two reactions were prepared per DNA extract: one using the forward primer (CMV forward) and one using the reverse primer (BgH for pcDNA™3.1/V5-His vector and TKpolyA for pcDNA™3.3 vector). 500ng of DNA as determined by the Nanodrop were mixed with 1.5pmols of forward or reverse primer and H_2O added to give a final volume of 15µl. The Value Read Sequencing Service offered by Eurofins MWG Operon was used to sequence the DNA. The returned sense and antisense sequences were aligned with the expected sequence adapted from the NCBI database using the program DNA strider for confirmation of mutant plasmid generation.

2.4 Transfection

2.4.1 Transfection using the Amaxa Nucleofector

Stable cultures of CHO cells were transfected transiently with the CTLA-4 constructs by electroporation using an Amaxa Nucleofector device for CHO cell transfections, according to the manufacturer's protocol. Cells ($1x10^6$) were electroporated in 100µl of pre-warmed Nucleofector™ Solution T with 2µg of plasmid. The nucleofection sample was transferred into an amaxa certified cuvette. The program U-23 (for high transfection efficiency) was selected. Plastic pipettes were used to transfer the sample into a 6-well plate containing 2ml DMEM and incubated in a humidified 37°C/5% CO_2 incubator. Gene expression was analysed after 48-72hours.

Untransfected CHO cells and CHO cells previously transfected with WT CTLA-4, KLESS CTLA-4 (synthesised by Stratagene), green fluorescent protein (GFP) tagged CD80 and CD86 plasmid DNA were utilised in the experiments and maintained as described in section **2.2.1**.

2.4.2 Transfection using the Neon Transfection System

Stable cultures of CHO cells expressing CTLA-4 constructs were transfected with CD63-GFP plasmid using the Neon Transfection System under the following conditions: 1600mV, 20ms, 1 pulse. Briefly, cells were counted, spun down (5minute at 490 *g*), and resuspended in DMEM (containing 10% FBS only) at a concentration of $1x10^6$ cells/100µl. 10µg of plasmid DNA was transferred into a fresh eppendorf and combined with 100µl of cells. The cells and plasmid DNA was transferred into the Neon Pipette tip and the pipette was plugged into the pipette holder, which contained 3ml of DMEM alone.

The start button was selected. The transfected cells were transferred onto cover slips and left overnight in a 37°C incubator.

2.4.3 Selection of transfected cells

2.4.3.1 Antibiotic Resistance

G418 was used to select transfected cells that expressed the required vectors. G418 was added to the medium of transfected CHO cells at a concentration of 500µg/ml each time the cells were passaged.

2.4.3.2 Fluorescence Activated Cell Sorting (FACS)

Following passage, 5ml of the transfected cells were centrifuged at 490 *g* for 5minutes, resuspended in 100µl of DMEM and labelled with 3µl of PE-conjugated anti-CTLA-4 Ab at 4°C for 30minutes in a universal tube. Cells were washed in 5ml ice-cold DMEM at 870 *g* for 2minutes, filtered, and sorted using a MoFlo cell sorter to select cells expressing low levels of surface CTLA-4. Flow cytometry was used to screen the cells to obtain a clone of cells expressing the desired level of protein.

2.5 Flow Cytometric Analysis

2.5.1 Preparation for flow cytometric analysis

Staining of cells was performed using PE-conjugated anti-CTLA-4 (primary Ab) for 30minutes and where indicated this was followed by detection using Alexa647 anti-mouse secondary Ab for 30minutes.

Unless otherwise indicated following the incubation with the primary Ab, cells were washed once in 2ml ice-cold DMEM and supernatant discarded. Where indicated following the incubation with the secondary Ab, cells were washed once in excess ice-cold DMEM and supernatant was discarded. Cells were resuspended in 200µl ice-cold PBS and kept on ice until FACs analysis. Unless otherwise indicated all washes were performed at 870 *g* for 2minutes. Control samples were stained using the same protocol using a PE-labelled isotype control Ab, PE-conjugated anti-CTLA-4 alone or Alexa647 anti-mouse secondary Ab alone. CHX was used at a final concentration of 10µg/ml, NH_4Cl was used at a final concentration of 10mM, BafA was used at a final concentration of 50nM, MG132 was used at a final concentration of 5µM and UBEI-41 was used at a final concentration of 20µM.

2.5.2 Staining different pools of CTLA-4

A total of $2x10^5$ cells suspended in 100µl of medium were incubated at 4°C (surface CTLA-4) or 37°C (endocytosed CTLA-4) with PE-conjugated anti-CTLA-4 Ab. Cells were washed, resuspended in ice-cold PBS and kept on ice.

Total CTLA-4 expression was determined by fixing cells in 500µl of 3% PFA for 10minutes at room temperature. Cells were washed in PFA, supernatant discarded, and cells were resuspended and washed in 500µl of 0.1% saponin (PBS/sap). Supernatant was discarded and the cells were incubated with PE-conjugated anti-CTLA-4 Ab at room temperature for 30minutes in the dark. Cells were washed in 500µl PBS/sap, resuspended in 200µl of PBS and kept on ice. All washes were performed at 490 *g* for 5minutes.

Where indicated, cells were pre-incubated with MG132 at 37°C before analysing the effect of this chemical on CTLA-4 localisation.

2.5.3 CTLA-4 Internalisation

A total of $2x10^5$ cells suspended in 100µl of medium or 0.45M sucrose were incubated with PE-conjugated anti-CTLA-4 Ab at 4°C. Cells were washed, resuspended and raised to 37°C for 1minute, 5minutes, 15minutes, and 30minutes followed by incubation with Alexa647 anti-mouse secondary Ab at 4°C. Cells were washed, resuspended in ice-cold PBS and kept on ice (**figure 2.1A**).

2.5.4 CTLA-4 Recycling

A total of $2x10^5$ cells suspended in 100µl of medium were incubated with PE-conjugated anti-CTLA-4 Ab at 37°C. Cells were washed, resuspended and incubated with Alexa647 anti-mouse secondary Ab at 4°C or raised to 37°C for 2minutes, 4minutes, 8minutes, 16minutes and 30minutes. Cells were washed, resuspended in ice-cold PBS and kept on ice (**figure 2.1B**).

Where indicated, cells were pre-incubated with MG132 or UBEI-41 for 2hours at 37°C before analysing the effect of these chemicals on CTLA-4 recycling.

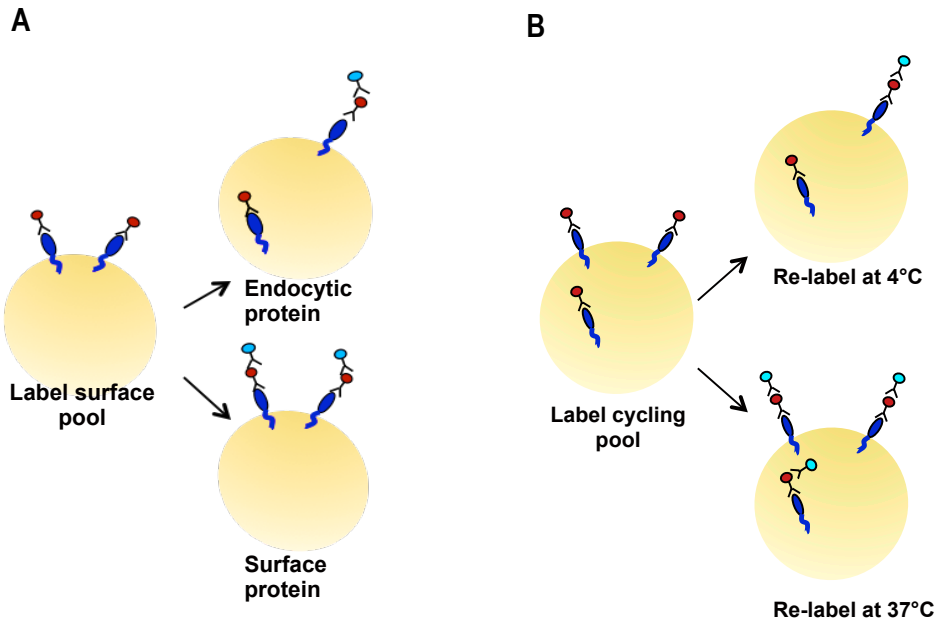

Figure 2.1 Diagrammatic representations of the internalisation and recycling assay performed by FACs. (A) CHO cells expressing CTLA-4 were labelled at 4°C with PE-conjugated anti-CTLA-4 Ab to label surface CTLA-4. Cells were then warmed to 37°C to allow endocytosis. Cells were placed on ice and any remaining surface CTLA-4 detected with Alexa647 anti-mouse secondary Ab. In the case of an endocytic protein, the loss of the secondary Ab signal indicates protein endocytosis. In the case of a surface protein, little or no loss of secondary Ab should be observed. **(B)** CHO cells expressing CTLA-4 were labelled with PE-conjugated anti-CTLA-4 Ab at 37°C to detect cycling CTLA-4, washed and any recycling primary Ab detected by addition of Alexa647 anti-mouse secondary Ab at either 4°C or 37°C.

There are two factors to consider when analysing the recycling FACs plots. Firstly how well the receptor internalises after the primary Ab label (**figure 2.2A, orange line)** and secondly the efficiency of recycling as determined by how fast the internalised receptor recycles back to the cell surface (**figure 2.2A, black line)**. For a highly endocytic receptor the control re-staining at 4°C with Alexa647 would reveal no signal, as all the PE-labelled receptor would have internalised. If the receptor recycles as efficiently as it internalises, incubation at 37°C with Alexa647 should result in a 1:1 relationship between the primary and secondary Ab indicating that all the internalised receptor has recycled back to the cell surface. For some receptors, complete endocytosis is not achieved but the internalised protein is able to recycle back to the cell surface producing a 1:1 relationship between the primary and secondary Ab (**figure 2.2B)**. For other receptors, complete endocytosis is not achieved and not all of the internalised protein is able to recycle back to the cell surface (**figure 2.2C**). In the case of a surface receptor the amount of protein at the surface should remain the same after a 4°C or 37°C incubation with Alexa647 (**figure 2.2D**).

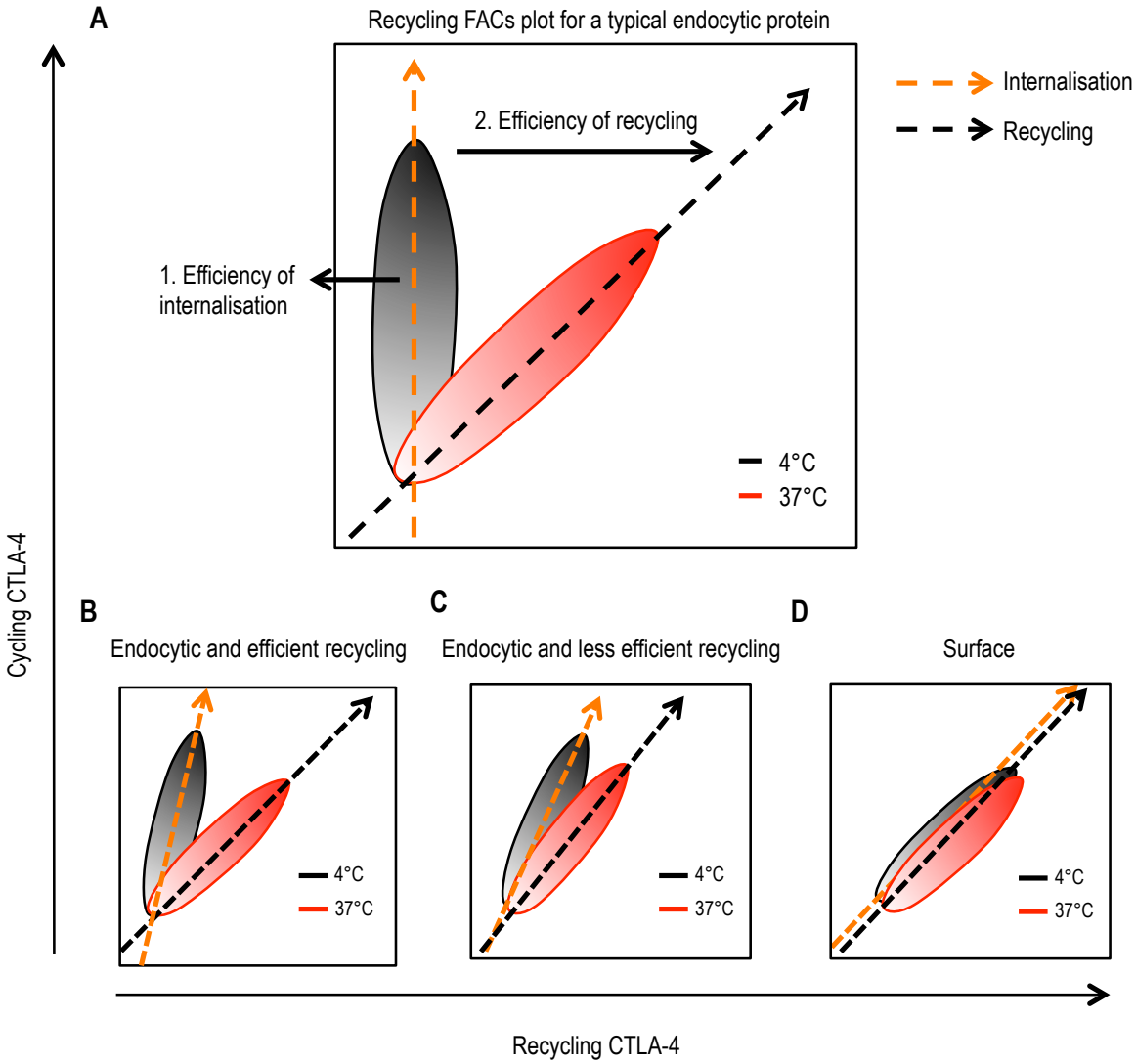

Figure 2.2 Analysis of recycling FACs plots. FACS plots are shown for PE-label (cycling CTLA-4) vs Alexa647 label (recycling CTLA-4). **(A)** FACs plot for a typical endocytic protein. In the 4°C control, there is no CTLA-4 remaining at the surface to be detected by Alexa647. However after a 37°C incubation, all the internalised protein recycles back to the surface producing a 1:1 relationship between the primary and secondary Ab. **(B)** In the 4°C control, the endocytic protein does not clear all the protein from the cell surface, however after incubation at 37°C with Alexa647 all the internalised protein has efficiently recycled back to the cell surface. **(C)** In the 4°C control, the endocytic protein does not clear all the protein from the cell surface. After incubation at 37°C with Alexa647 not all of the internalised protein recycles back to the cell surface. **(D)** FACs plot for a typical surface protein. The level of protein at the surface remains the same in the 4°C control and after 37°C incubation with Alexa647.

2.5.5 CTLA-4 Degradation

A total of $2x10^5$ cells suspended in 200µl of medium alone or medium supplemented with CHX, BafA, NH_4Cl, BafA and CHX or NH_4Cl and CHX were incubated at 37°C for 3hours in a 96-well round bottom plate. Cells were fixed and permeabilsed as described in section **2.5.2** and stained for total CTLA-4 with PE-conjugated anti-CTLA-4 Ab for 1hour at room temperature in the dark.

2.5.6 Transendocytosis assay

A total of $5x10^6$ CD80-GFP or CD86-GFP transfected CHO cells were violet labeled with CellTrace Violet in 1ml PBS for 10minutes at room temperature. Cells were washed in 5ml PBS at 490 *g* for 5minutes and resuspended in DMEM at a concentration of $2x10^6$/ml. CTLA-4 transfected CHO cells were counted and resuspended at a concentration of $2x10^6$/ml. CTLA-4 transfected CHO cells were then incubated with violet labeled CD80-GFP or CD86-GFP at a 1:1 ratio in the presence or absence of NH_4Cl for 3hours at 37°C in a 96-well round bottom plate. Cells were washed in 2ml ice-cold PBS and kept on ice. GFP transfer was quantified by gating single expressing CTLA-4 cells that were negative for Violet dye staining. CTLA-4 expressing cells were stained for cycling CTLA-4 to quantify the efficiency of capture. To obtain capture efficiency the percentage of cells that have acquired GFP was multiplied by the mean fluorescence intensity (MFI) of this population. This was divided by the percentage of positive CTLA-4 expressing cells (cycling) by the MFI of this population. Cells were analysed on the Dako cyan as shown in **figure 2.3**.

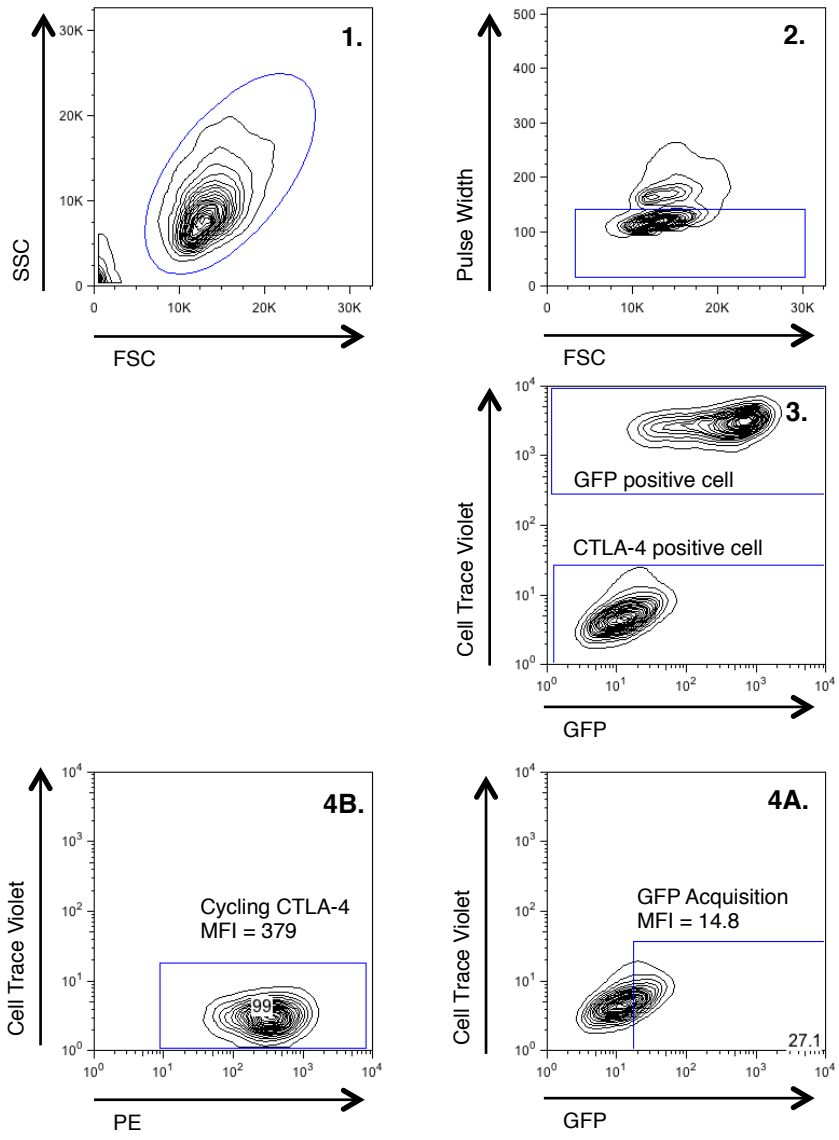

Figure 2.3 Gating strategy used for GFP acquisition and efficiency of capture by CTLA-4 expressing CHO cells. 1. FSC vs SSC was used to gate live cells. **2.** A low pulse width was used to gate single cells. **3.** Cell trace violet labelled CHO-CD80/CD86-GFP cells were excluded. **4A.** Percentage of CTLA-4 expressing cells that have acquired GFP was multiplied by the MFI of this population. **4B.** The MFI of CTLA-4 expressing cells (cycling) was multiplied by the percentage of CTLA-4 expressing cells that have acquired GFP shown in 4A.

2.5.7 Sample Acquisition and Analysis

Flow cytometry was carried out using a FACSCalibur flow cytometer and acquired using CellQuest software. For each sample, data for 10,000 cells within a gated region was collected. For transendocytosis flow cytometry was carried out using a Dako Cyan flow cytometer and acquired using Summit software. Analysis was performed using FlowJo software.

2.5.8 Statistical Analysis

Significance was calculated by a two-tailed Mann Whitney U test, as indicated in the figure legends, using GraphPad Prism4 software. This test allows two groups or conditions to be compared without making the assumption that the values are normally distributed.

2.6 Confocal Microscopy Analysis

2.6.1 Preparation of Cells for confocal microscopy

Cover slips were coated with an excess of poly-L-lysine for 1hour at room temperature, washed twice in excess PBS and plated into a 24-well plate. PBS was aspirated to allow the cover slips to dry completely. A total of $1.5x10^5$ cells suspended in 1ml of medium were grown on cover slips overnight at 37°C. Staining of cells was performed using unlabelled anti-CTLA-4 Ab for 1hour and an AlexaFluor secondary Ab for 1hour. Unless otherwise indicated Ab incubations were performed in the dark at room temperature. For live cells, Ab dilutions and washes were performed in 1ml ice-cold DMEM. For cells fixed and permeabilised in Methanol, Ab dilutions and washes were performed in PBS. For cells fixed

and permeabilised in 3% PFA and PBS/sap, Ab dilutions and washes were performed in PBS/sap. All washes were performed three times. Following staining, cover slips were removed and dried at 37°C for 10minutes. Cover slips were inverted and mounted onto microscope slides containing 1.8µl of Vectashield (Vector Laboratories, CA) as a mounting medium.

2.6.2 Staining different pools of CTLA-4

Surface expression was detected by incubating cells in 200µl of unlabelled anti-CTLA-4 Ab at 4°C for 1hour, and cycling CTLA-4 was detected by incubation at 37°C. Cells were fixed in 1ml 100% Methanol at -20°C for 30minutes. Cells were washed and incubated in 200µl Alexa555 anti-mouse secondary Ab. Cells were washed in PBS and cover slips mounted as described in section **2.6.1**.

Total CTLA-4 expression was determined by fixing cells in 100% Methanol at -20°C for 30minutes, prior to incubation in unlabelled anti-CTLA-4 Ab and Alexa555 anti-mouse secondary Ab. Untransfected CHO cells were stained using the same protocol and used as a negative control.

2.6.3 CTLA-4 chimera localisation

For analysis of localisation, CHO cells expressing CTLA-4 chimeras were plated overnight on a poly-L-lysine coated coverslip in a 24-well plate. For surface expression, cells were incubated with WGA - tetramethylrhodamine conjugate at 4°C for 45minutes. Cells were fixed in 500µl of 3% PFA for 15minutes in the dark at room temperature prior to incubation in 200µl of unlabelled anti-CTLA-4 Ab,

washed and then incubated in 200µl Alexa488 anti-human secondary Ab at room temperature. Cells were washed in PBS/sap and cover slips mounted as described in section **2.6.1**.

2.6.4 Surface vs Internalised CTLA-4

For analysis of surface vs internalised CTLA-4, cells were incubated at 37°C with unlabelled anti-CTLA-4 Ab for 1hour, washed and then placed on ice. Surface receptors were labeled with Alexa555 anti-mouse secondary Ab. Cells were then washed and fixed in 100% Methanol at -20°C for 30minutes. Internalised receptors were then detected by incubation with Alexa488 anti-mouse secondary Ab. Cells were washed in PBS and cover slips mounted as described in section **2.6.1**.

2.6.5 CTLA-4 Recycling

Cells suspended in 200µl and labelled with unlabelled anti-CTLA-4 Ab at 37°C for 1hour. Cells were washed and incubated at 4°C with Alexa488 anti-mouse secondary Ab to label surface CTLA-4 for 1hour. Cells were washed and incubated at 37°C with Alexa555 anti-mouse secondary Ab to label recycled CTLA-4. To ensure surface receptors were completely blocked, Alexa555 anti-mouse secondary Ab was applied to the 4°C control. Cells were washed in PBS and cover slips mounted as described in section **2.6.1**.

2.6.6 CTLA-4 Degradation

A total of $2x10^5$ cells suspended in 200µl of medium alone or medium supplemented with CHX, BafA, NH_4Cl, BafA and CHX or NH_4Cl and CHX were incubated at 37°C for 3hours. Cells were fixed in 500µl of 3% PFA for 15minutes in the dark at room temperature prior to incubation in 200µl of unlabelled anti-CTLA-4 Ab, washed and then incubated in 200µl Alexa488 anti-mouse secondary Ab at room temperature. Cells were washed in PBS/sap and cover slips mounted as described in section **2.6.1**.

2.6.7 Transferrin Uptake

A total of $2x10^5$ cells were serum-starved at 37°C for 45minutes. Cells were resuspended in 250µl of serum-starved medium and labeled with transferrin AlexaFluor633 conjugate and PE-conjugated anti-CTLA-4 at 37°C for 45minutes. Cells were fixed in 500µl of 3% PFA for 15minutes in the dark at room temperature. Cells were washed in PBS and cover slips mounted as described in section **2.6.1**.

2.6.8 Co-localisation with CD63-GFP

CTLA-4 chimeras transiently transfected with CD63-GFP were suspended in 200µl of medium alone or medium supplemented with NH_4Cl and incubated at 37°C for 3hours. Cells were fixed in 500µl of 3% PFA for 15minutes in the dark at room temperature prior to incubation in 200µl of unlabelled anti-CTLA-4 Ab and Alexa555 anti-human secondary Ab. Cells were washed in PBS/sap and cover slips mounted as described in section **2.6.1**.

2.6.9 Visualisation of fluorescence

Imaging was carried out using a Zeiss Axiovert LSM510 confocal microscope and Zeiss LSM 780 inverted laser scanning confocal microscope using a 100X oil-immersion objective with excitation at 488nm, 543nm and 633nm. Constant laser powers and acquisition parameters were maintained throughout individual experiments for analysis. For quantitation, cells were outlined and MFI measured using ImageJ (Wayne Rasband, NIH). All confocal images shown are representative of at least 40 cells taken from at least three independent experiments.

2.7 Protein Analysis

2.7.1 Sodium-Dodecyl-Sulphate Polyacrylamide Gel Electrophoresis (SDS-PAGE)

Proteins were analysed by SDS-PAGE. Briefly, protein was mixed with Protein Loading Buffer (2X) and samples were heat-denatured at 100°C for 5minutes prior to separation. 10% polyacrylamide gels were run in Tris-glycine-SDS electrophoresis buffer (230.3g Tris, 144g Glycine and 10g SDS) at a constant current of 125volts for 1hour 30minutes, alongside a protein marker. Precast gradient gels (4-20%) were used (Thermo Fisher Scientific, USA) to achieve better resolution of bands and samples were separated in Tris-HEPES-SDS electrophoresis buffer (100 mM Tris Base (pH 8.3), 100 mM HEPES (electrophoresis grade) and 3 mM SDS).

Prior to casting the gel, glass plates were wiped down with 70% Ethanol and a glass plate sandwich was setup in a gel-casting stand (Bio-rad Mini PROTEAN 3 Electrophoresis System). The following components were mixed to make two 10% polyacrylamide gels: separating gel - 9.9ml distilled H_2O,

8.3ml Protogel 30%, 6.5ml Resolving buffer (2X), 100µl APS (0.1g/ml) and 20µl TEMED; stacking gel – 6.3ml distilled H_2O, 1.3ml Protogel 30%, 2.5ml Stacking buffer (2X), 50µl APS and 10µl TEMED. TEMED was added to the mix in the fume cupboard. The separating gel was pipetted into the glass sandwich until the solution was ¾ of the way to the top. This was overlayed with 1ml dH_2O to allow polymerisation for 30minutes. After the gel had polymerised the water was removed by placing a paper towel in the corner of the sandwich. The stacking gel was pipetted into the glass sandwich until the gel reached the very top of the glass plate and a 1.5mm comb was inserted. The stacking gel was left to polymerise for 30minutes.

2.7.2 CTLA-4 Immunoprecipitation

Cells were pelleted and lysed in 1ml 1% Triton X-100 (1% Triton, 20mM Tris pH7.5, 150nM NaCl, 1mM EDTA and 0.02% Sodium azide) at 4°C for 30minutes containing protease cocktail inhibitor (1:100). Cells were centrifuged at 15.7 *g* for 10minutes at 4°C to remove cell debris. 50µl of cleared lysate was taken and added to an equal volume of Protein Loading buffer (2X) to make a whole cell lysate (WCL). For immunoprecipitation studies, 50µl of protein-G-sepharose beads were pre-coated with 2.5µg anti-human CTLA-4 Ab suspended in 750µl of 1% Triton X-100 overnight at 4°C. The bead-Ab complex was pelleted by centrifugation at 2.3 *g* for 20seconds. The pellet was then washed three times in 1ml 1% Triton X-100. Prior to the final wash, the 1ml bead-Ab complex was divided into two clean, eppendorf tubes, centrifuged and supernatant aspirated. 925µl of the lysate was added to the complex, vortexed and incubated at 4°C for 1hour and 30minutes. Following this, the beads were pelleted by centrifugation at 2.3 *g* for 20seconds and washed four times in 1ml 1% Triton X-100. Prior to the final wash the beads resuspended in 1ml 1% Triton X-100 were transferred to a clean eppendorf tube and centrifuged at 2.3 *g* for 10 seconds. Supernatant was aspirated leaving behind 50µl of 1% Triton X-100. The beads were

centrifuged for a further 10 seconds, supernatant was aspirated and the beads were resuspended in 40µl Protein Loading Buffer (2X).

2.7.3 Immunoblotting

Immunoblot analysis was performed using 10% polyacrylamide gels or precast gradient gels. Proteins were electrophoretically transferred to Immobilon-FL PVDF transfer membranes in transfer buffer at 350mA (100volts) for 1hour using a wet transfer system (Mini Trans-Blot Electrophoretic Transfer Cell, BIO-RAD). Membranes were activated for 1minute in Methanol. Gels and membranes were equilibrated in 1X transfer buffer (100ml Electroblotting Buffer Tris-glycine (10X), 200ml Methanol and 800ml dH_2O) for 30minutes. A transfer sandwich was set up as follows: a cassette was placed on a clean surface with the gray side up, pre-wetted fiber pad, sheet of filter paper, equilibrated gel, pre-wetted membrane, sheet of filter paper and pre-wetted fiber pad. A glass roller was used to remove any air bubbles. Membranes were blocked for 1hour at room temperature in 50ml of 5% milk/TBS with gentle shaking. Membranes were incubated overnight at 4°C with the desired Ab (1µg/ml) diluted in Tris-buffered-saline with 0.1% Tween (TBST) containing 3% BSA and 0.1% Sodium azide. Membranes were then washed three times in high salt TBST over a 30minute period. Following this, membranes were incubated with IRDye 800 secondary Ab (goat anti-mouse 1:10000) diluted in TBST containing 3% BSA and 0.1% Sodium azide for 1hour. Membranes were subsequently washed five times in high salt TBST over a 25minute period, followed by a final wash in Tris-buffered-saline (TBS) for 1minute. Membranes were then dried on filter paper and analysed using the Odyssey Infrared Imaging System (LI-COR Biosciences, Lincoln, NE).

For blots developed using the Pierce ECL Western Blotting Substrate, proteins were electrophoretically transferred to nitrocellulose membrane. The substrate solution was prepared by mixing equal parts of Detection Reagent 1 and 2. The membrane was transferred onto a clear plastic wrap and substrate solution applied. Following 1minute incubation, paper tissue was used to remove excess liquid and any bubbles present between the blot and membrane protector. The protected membrane was placed in a film cassette with the protein side facing up. X-ray film was placed on top of the membrane and film was developed in the dark room. Exposure time was varied to achieve optimal results.

2.7.4 Biochemical quantification of CTLA-4 internalisation

For analysis of internalisation, CTLA-4 transfected CHO cells were grown overnight in 6cm tissue culture petri dishes. Cells were transferred to ice and were surface labelled at 4°C with NHS-SS-biotin in PBS for 25minutes. Biotin was removed and cells re-labelled with NHS-SS-biotin for 25minutes. Cells were washed three times in ice-cold PBS and biotin quenched in 500µl Quenching solution at 4°C for 10minutes. Cells were washed three times in ice-cold PBS and transferred immediately to pre-warmed medium at 37°C to allow internalisation. At the indicated times the cells were rapidly transferred to ice, medium aspirated and washed twice with ice-cold PBS. Biotin was removed from proteins remaining at the cell surface by Sodium 2-mercaptoethanesulphonate (MesNa) prepared in cell surface reduction buffer (50mM Tris and 100mM NaCl adjusted to pH8.6). Reduction proceeded for 25minutes at 4°C with gentle rocking. Cells were washed three times in ice-cold PBS before lysis in 150µl 1% Triton X-100 (1% Triton, 20mM Tris pH7.5, 150nM NaCl, 1mM EDTA and 0.02% Sodium azide) at 4°C for 1hour containing protease cocktail inhibitor (1:100). 40µl of whole cell lysate (WCL) was removed prior to the addition of the sample to a neutravidin gel. Briefly, 100µl neutravidin gel was added to a column, centrifuged and supernatant discarded. The column was washed and then capped before addition of the

remaining sample for overnight end-to-end mixing at 4°C. Next day, the cap was removed, column centrifuged and supernatant discarded. 100µl Dithiothreitol (DTT) prepared in 2X Protein Loading Buffer (70mM) was added to the capped tube and the column was incubated at room temperature with end-to-end mixing for 1hour. The cap was removed and column transferred to an eppendorf before centrifuging for 2minutes. Proteins were analysed by SDS-PAGE and western blotting. Unless otherwise indicated all centrifuge washes were performed at 3.3 *g*.

2.7.5 CTLA-4 Degradation

A total of $4x10^6$ cells suspended in 4ml of medium alone or medium supplemented with CHX, NH_4Cl, or NH_4Cl and CHX were incubated at 37°C for 3hours. Cells were lysed and immunoprecipitated as described in section **2.7.2**. Immunoblotting was performed as described in section **2.7.3** using the Odyssey Infrared Imaging System. CTLA-4 was blotted using the C-19 C-terminus anti-CTLA-4 Ab.

2.7.6 CTLA-4 Ubiquitination

CTLA-4 transfected CHO were stained for total CTLA-4 expression as described in section **2.5.2**. Cell numbers with equivalent CTLA-4 protein were suspended in 5ml of medium alone or medium supplemented with BafA and incubated at 37°C for 3hours in a universal tube. Cells were lysed and immunoprecipitated as described in section **2.7.2**. Immunoblotting was performed as described in section **2.7.3** using ECL. CTLA-4 was blotted using the C-19 C-terminus anti-CTLA-4 Ab and ubiquitin was blotted using an anti-ubiquitin Ab.

3.0 CHARACTERISING THE CELL BIOLOGY OF THE CTLA-4 RECEPTOR

3.1 Introduction

CTLA-4 surface expression has been difficult to demonstrate by flow cytometry. One model used to explain this lack of surface expression is the constitutive internalisation of CTLA-4 from the cell surface mediated by the YVKM motif located in the cytoplasmic tail associating with the clathrin adaptor AP-2 (Chuang et al., 1997; Leung et al., 1995; Shiratori et al., 1997). Following T cell stimulation, however, CTLA-4 expression is upregulated and the receptor is trafficked to the cell surface. It has been proposed that this event is accompanied by tyrosine phosphorylation of the YVKM motif, which leads to CTLA-4 stabilisation at the plasma membrane (Miyatake et al., 1998; Shiratori et al., 1997). Theoretically tyrosine phosphorylation should block any association of YVKM with AP-2 and ultimately result in predominant cell surface accumulation of CTLA-4. However, when T cells are stained for total CTLA-4 expression there is predominant localisation of CTLA-4 in intracellular vesicles (Qureshi et al., 2012; Walker and Sansom, 2011). This therefore suggests that CTLA-4 endocytosis is a more complex process than initially thought. Moreover little is known about how the receptor is sorted in intracellular compartments. In this chapter I have therefore investigated the mechanisms that regulate the trafficking of the CTLA-4 receptor.

3.2 CTLA-4 is an endocytic receptor and is located in intracellular vesicles

In our lab, stable lines of CTLA-4 transfected CHO cells were established previously as a manipulable model of how CTLA-4 expression is controlled in T cells. Such a model has overcome the potential

drawbacks of using T cells including the time-consuming purification from PBMCs, several hours of stimulation to induce CTLA-4 expression for detection at the cell surface, and the large cytoplasm of CHO cells has eased co-localisation studies. The levels of CTLA-4 can be monitored and adjusted using cell sorting, and further the genetic analyses of the role of candidate trafficking proteins can be determined by co-transfecting additional plasmids into these cell lines. CTLA-4 transfected CHO cells were therefore used to further elucidate the intracellular trafficking of CTLA-4 and establish whether findings from CHO model systems were valid in CTLA-4 transfected Jurkat T cells and activated T cells.

To characterise the trafficking of CTLA-4 in CTLA-4 transfected CHO cells and activated T cells, CTLA-4 expression was compared using three different staining protocols. CTLA-4 transfected CHO cells were labelled with PE-conjugated anti-CTLA-4 Ab at 4°C, 37°C or were fixed and permeabilised before analysis by flow cytometry. In live cells staining at 4°C labelled all surface expressed CTLA-4 since at this temperature all metabolic processes, including protein trafficking, was inhibited. Staining at 37°C labelled all surface expressed CTLA-4 that was present during Ab staining, as well as protein that had been endocytosed from the cell surface. Finally, in cells that were fixed and permeabilised the total pool of CTLA-4 protein was measured before Ab staining. This included CTLA-4 within the endocytic pathway, newly synthesised CTLA-4 within the secretory pathway, and CTLA-4 within storage compartments. As shown in **figure 3.1A,** CHO cells expressing human CTLA-4 had a 5-fold lower cell surface expression at 4°C compared to cells stained for endocytosed CTLA-4 at 37°C. Moreover, the level of CTLA-4 expression in fixed and permeabilised cells was comparable to that identified in cells stained at 37°C further suggesting CTLA-4 is predominantly located in endocytic compartments (**figure 3.1B**).

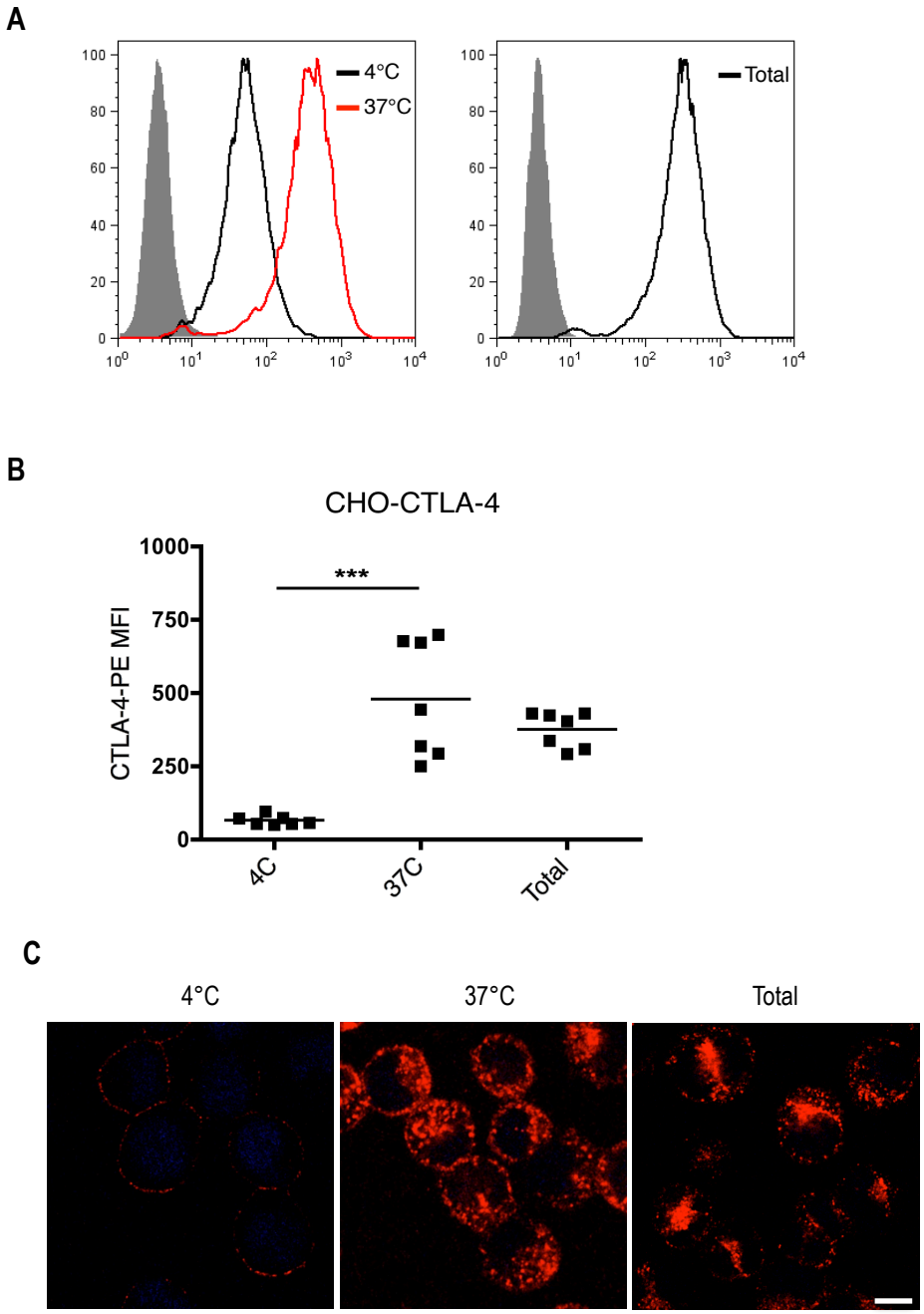

Figure 3.1 Human CTLA-4 is located in punctate intracellular vesicles with limited cell surface expression. (A) CHO cells expressing human CTLA-4 were stained for surface CTLA-4 expression at 4°C; endocytosed CTLA-4 expression at 37°C; or were fixed and permeabilised prior to staining for total CTLA-4 expression with PE-conjugated anti-CTLA-4 Ab. Cells were analysed by flow cytometry. Representative FACs plots of one independent experiment of n=7. **(B)** Horizontal lines indicate median values. Significance was tested by two-tailed Mann Whitney U test. (***, p<0.001). **(C)** CHO cells expressing human CTLA-4 were stained as described in A. with an unlabelled anti-CTLA-4 Ab and Alexa555 anti-mouse secondary Ab (n=5). Bar indicates scale of 10µm.

To validate CTLA-4 localisation in endocytic compartments as identified by flow cytometry, the staining of surface, cycling and total human CTLA-4 expression in CHO cells was repeated and analysed by confocal microscopy. Consistent with flow cytometry, staining at 4°C revealed little or no human CTLA-4 at the plasma membrane, whilst staining at 37°C revealed CTLA-4 to be located predominantly in intracellular vesicles (**figure 3.1C**). This is consistent with the concept that CTLA-4 was being exported to the plasma membrane and then rapidly endocytosed, contributing to the low steady-state level seen at the cell surface. In fixed and permeabilised cells, a perinuclear compartment was observed containing high levels of CTLA-4, representing either newly synthesised protein or protein that had been endocytosed and targeted back to this compartment.

The pattern of CTLA-4 expression was reproducible in CTLA-4 transfected Jurkat T cells where CTLA-4 expression was higher at 37°C compared to 4°C (**figure 3.2**). However, total CTLA-4 expression in Jurkat T cells was higher than the combined surface and cycling pool of the receptor. To characterise CTLA-4 expression in human T cells, $CD4^{+}CD25^{-}$ T-cells were stimulated with anti-CD3 and anti-CD28 beads for 3 days or 5 days. In keeping with literature, CTLA-4 was upregulated in activated T cells and levels peaked after 3 days of stimulation (**figure 3.3A** and **B**). CTLA-4 expression decreased after 5 days of stimulation but was still detectable (**figure 3.3C** and **D**). Importantly similar to CTLA-4 transfected Jurkat T cells, total CTLA-4 expression in activated T cells was higher when compared to cells stained at 37°C. This data suggests that only a fraction of total CTLA-4 is trafficking at any given time and that the vast majority of the protein may be stored in a storage compartment as is described for Glucose transporter type 4 (GLUT4) (Slot et al., 1991a; Slot et al., 1991b).

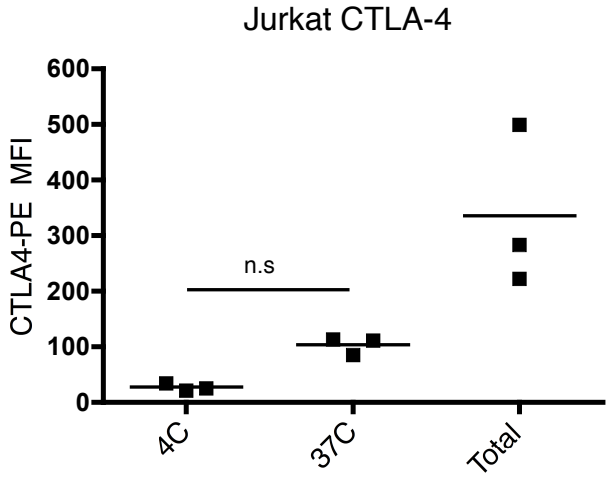

Figure 3.2 The pattern of human CTLA-4 expression in CTLA-4 transfected Jurkat T cells is comparable to CTLA-4 transfected CHO cells. Jurkat T cells expressing human CTLA-4 were stained for surface CTLA-4 expression at 4°C; endocytosed CTLA-4 expression at 37°C; or were fixed and permeabilised prior to staining for total CTLA-4 expression at room temperature with PE-conjugated anti-CTLA-4 Ab. Cells were analysed by flow cytometry. Horizontal lines indicate median values. Significance was tested by two-tailed Mann Whitney U test (n=3). (n.s, not significant).

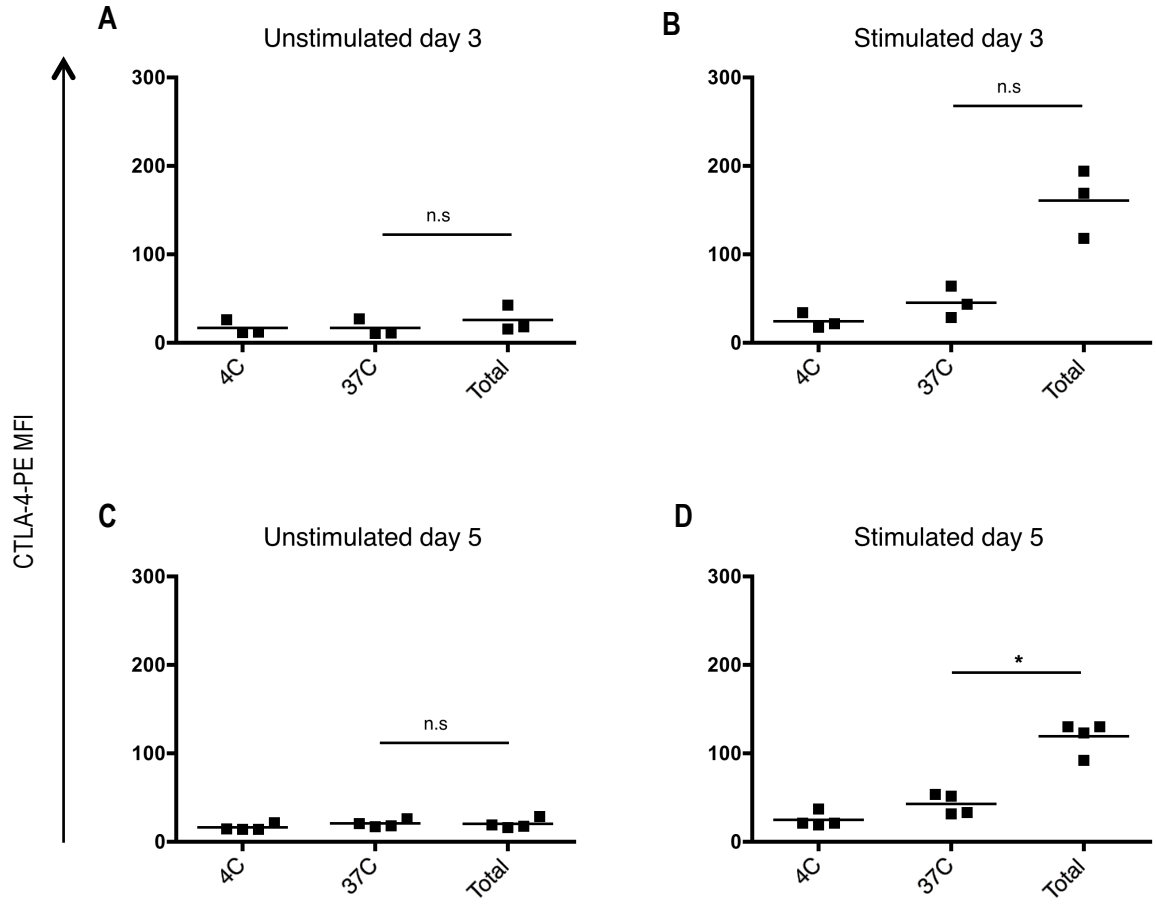

Figure 3.3 The pattern of human CTLA-4 expression in activated T cells is comparable to CTLA-4 transfected CHO cells and Jurkat T cells. $CD4^{+}CD25^{-}$ T cells were left untreated (unstimulated) or stimulated with anti-CD3/CD28 beads. At three days **(A** and **B)** and five days **(C** and **D)** cells were stained for surface CTLA-4 expression at 4°C; endocytosed CTLA-4 expression at 37°C; or were fixed and permeabilised prior to staining for total CTLA-4 expression at room temperature with PE-conjugated anti-CTLA-4 Ab. Cells were analysed by flow cytometry. Horizontal lines indicate median values. Significance was tested by two-tailed Mann Whitney U test (n≥3). (n.s, not significant; *, $p<0.05$).

In contrast to $CD4^+CD25^-$ T cells, Tregs constitutively express CTLA-4, which raises questions as to whether there is a difference in the turnover and trafficking of the receptor in the two cell types. To address this, $CD4^+CD25^+$ T cells were stimulated with anti-CD3/CD28 beads and IL-2 prior to staining for CTLA-4 localisation. In contrast to $CD4^+CD25^-$ T cells, total CTLA-4 expression was detectable in unstimulated Tregs (**figure 3.3A** and **C** vs **3.4A**). Comparable to stimulated T cells however, CTLA-4 expression in Tregs was upregulated after stimulation (**figure 3.3B** and **D** vs **3.4B**). Importantly, a 3-fold increase was observed in total CTLA-4 (unstimulated Tregs vs stimulated Tregs), again suggesting at steady state CTLA-4 could be stored and mobilised from storage compartments (**figure 3.4A** vs **3.4B**).

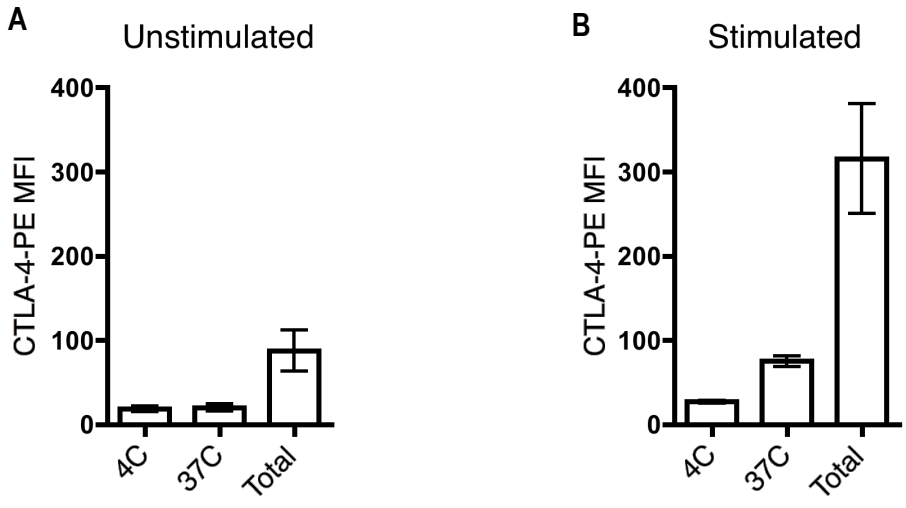

Figure 3.4 The pattern of CTLA-4 expression in $CD4^+CD25^+$ Tregs is comparable to $CD4^+CD25^-$ activated T cells. $CD4^+CD25^+$ T cells were unstimulated **(A)** or stimulated overnight with IL-2 and anti-CD3/CD28 beads **(B)**. Cells were stained for surface CTLA-4 expression at 4°C; endocytosed CTLA-4 expression at 37°C; or were fixed and permeabilised prior to staining for total CTLA-4 expression at room temperature with PE-conjugated anti-CTLA-4 Ab. Cells were analysed by flow cytometry. Error bars show standard error (n=3).

3.3 CTLA-4 endocytosis is clathrin-dependent

CTLA-4 localisation in intracellular vesicles questions the role of the tyrosine based hydrophobic motif (YVKM) located in the cytoplasmic tail driving its constitutive internalisation from the cell surface. To directly measure endocytosis CTLA-4 transfected CHO cells were stained for surface CTLA-4 expression at 4°C with PE-conjugated anti-CTLA-4 Ab. Cells were warmed to 37°C for various times to allow any internalisation of surface CTLA-4 to take place. Cells were then placed on ice and any remaining CTLA-4 at the surface detected with Alexa647 anti-mouse secondary Ab. Accordingly in this assay loss of Alexa647 staining over time reflects endocytosis of CTLA-4. **Figure 3.5A** shows that in the 4°C control there was a linear relationship between CTLA-4-PE (y-axis) and Alexa647 (x-axis). However after 30minute incubation at 37°C a curved plot was generated where the initial PE-labelled surface CTLA-4 internalised resulting in a minimal surface Alexa647 label, typical of an endocytic protein. **Figure 3.5B** shows that human CTLA-4 has a fast rate of endocytosis with 50% of the protein internalising within 5minutes. Since internalisation of CTLA-4 occurs in an AP-2 mediated, clathrin-dependent manner (Chuang et al., 1997; Shiratori et al., 1997), treatment with sucrose can be used to inhibit the formation of CCVs (Heuser and Anderson, 1989). Accordingly the rapid internalisation of human CTLA-4 was prevented by sucrose treatment (**figure 3.5B**).

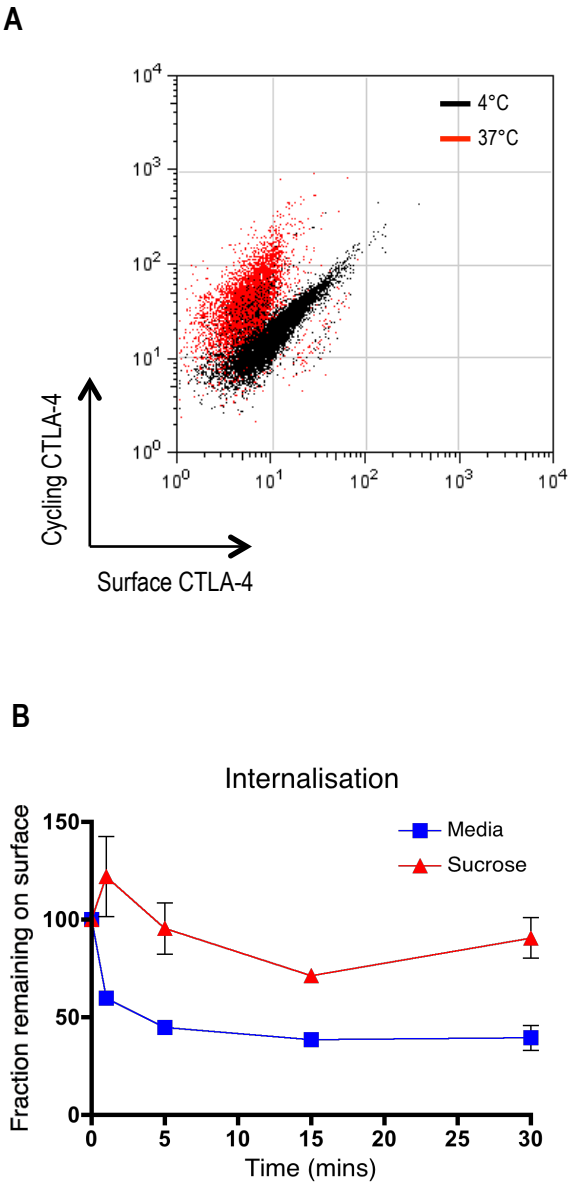

Figure 3.5 Human CTLA-4 has a fast rate of internalisation. (A) CHO cells expressing human CTLA-4 were labelled at 4°C with PE-conjugated anti-CTLA-4 Ab. Cells were then warmed to 37°C to allow endocytosis for the times indicated. Cells were then placed on ice and any remaining surface CTLA-4 detected with Alexa647 anti-mouse secondary Ab. Representative FACs plot of one experiment showing remaining surface CTLA-4 after maximum 37°C incubation (red) compared to 4°C (black). **(B)** The 647 signal was plotted against time as a fraction remaining compared to 4°C in medium or medium supplemented with sucrose. Error bars show standard error (n≥3).

To confirm that antibody binding is not inducing receptor endocytosis, CTLA-4 internalisation was measured by western blotting. Cell surface CTLA-4 was biotinylated at 4°C. Cells were then either kept on ice or warmed to 37°C for the indicated time-points and any remaining surface biotin was cleaved off by reducing agent. Cells were lysed and internalised CTLA-4 was concentrated by immunoprecipitating biotin using a neutravidin gel. Membranes were then probed for CTLA-4 using a C-19 C-terminus anti-CTLA-4 Ab. For human CTLA-4 maximal protection of biotinylated protein was seen after 15minutes (**figure 3.6**). However after 30minutes this protected pool of internalised CTLA-4 decreased, which could be suggestive of degradation. The difference in internalisation rate as detected by flow cytometry and western blotting could be due to the sensitivity of the assays.

The TfR is well characterised and internalises by clathrin-dependent endocytosis using signals encoded in the cytoplasmic tail (Iacopetta et al., 1988). Using transferrin as a marker for the clathrin pathway, the co-localisation of CTLA-4 with transferrin was compared. Cells were incubated with transferrin AlexaFluor633 and PE-conjugated anti-CTLA-4 Ab at 37°C for 45minutes and subsequently fixed and analysed by confocal microscopy. This revealed that human CTLA-4 co-localised with transferrin in intracellular vesicles suggesting that the internalisation pathway used by CTLA-4 overlaps with the pathway used by the TfR (**figure 3.7**). Taken together, this data confirms that CTLA-4 internalisation is clathrin-dependent and is not induced by Ab binding.

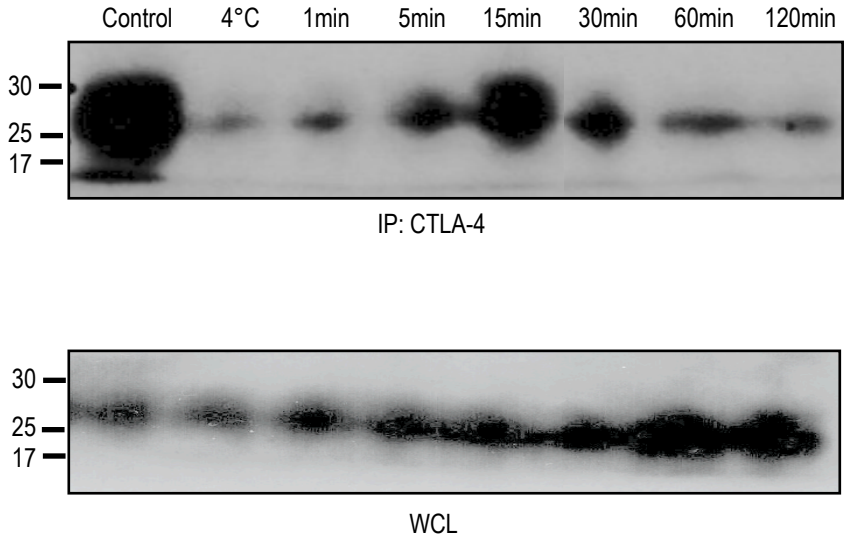

Figure 3.6 Antibody binding does not induce human CTLA-4 endocytosis. Cell surface CTLA-4 was biotinylated at 4°C. Cells were then either kept on ice or warmed to 37°C for the indicated time-points and any remaining surface biotin was reduced. Cells were lysed and internalised CTLA-4 was concentrated by immunoprecipitating biotin using a neutravidin gel. Membranes were then probed for CTLA-4 using a C-19 C-terminus anti-CTLA-4 Ab. CTLA-4 has a molecular weight of ~ 30kDa. IP, immunoprecipitated CTLA-4 - bands represent CTLA-4 that was internalised and protected. WCL, whole cell lysate - bands represent total amount of CTLA-4 protein present in each condition. This is representative of 3 independent experiments.

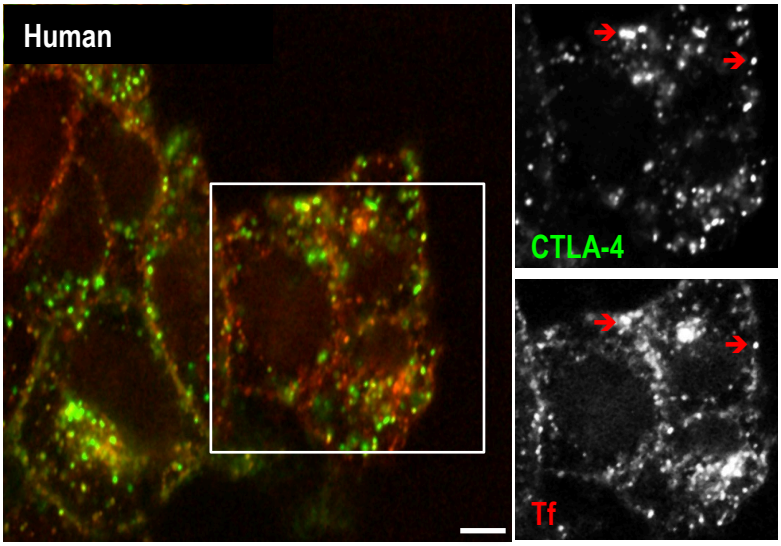

Figure 3.7 Human CTLA-4 co-localises with TfR. CTLA-4 transfected CHO cells were incubated with a transferrin AlexaFluor633 conjugate and PE-conjugated anti-CTLA-4 Ab at 37°C for 45minutes. Cells were subsequently fixed and analysed by confocal microscopy. The red arrows indicate co-localisation. This is representative of 3 independent experiments. Bar indicates scale of 10μm.

3.4 CTLA-4 is recycled back to the cell surface

The path taken by CTLA-4 post-internalisation is poorly understood. Despite studies suggesting that CTLA-4 co-localises with TfR in murine splenocytes and activated human T cells (Chuang et al., 1997; Leung et al., 1995), it is not clear if CTLA-4 like TfR also recycles back to the cell surface. To address CTLA-4 recycling, cells were incubated with an unlabelled anti-CTLA-4 Ab at 37°C for 1hour to label the cycling pool of CTLA-4. Cells were then placed on ice and any remaining cell surface CTLA-4 labelled with Alexa488 anti-mouse secondary Ab. Cells were then further stained at 37°C with Alexa555 anti-mouse secondary Ab. This detects any internalised receptor that subsequently recycled back to the plasma membrane. Labeling at 37°C with the Alexa555 anti-mouse secondary Ab revealed a clear population of recycling CTLA-4 receptor (**figure 3.8A top panel**). In contrast, control staining at 4°C did not show any additional red surface labeling with the Alexa555 anti-mouse secondary Ab (**figure 3.8A bottom panel**).

To validate that the CTLA-4 receptor does indeed recycle as identified by confocal microscopy, the assay was repeated using flow cytometry. Cells were incubated at 37°C with a PE-conjugated anti-CTLA-4 Ab for 30 minutes to label the cycling pool of CTLA-4. Cells were then incubated further at 37°C for various times with an Alexa647 anti-mouse secondary Ab to label any of the primary Ab recycling back to the cell surface. Accordingly, recycling CTLA-4 is seen as an increase in the Alexa647 signal over time. As shown in **figure 3.8B** and **C**, after 30minute incubation at 37°C the control re-staining at 4°C revealed only in a small percentage of cells does CTLA-4 protein remain at the surface to be detected by Alexa647. However, when cells are stained at 37°C with Alexa647, a greater pool of CTLA-4 was seen. This data suggests the Alexa647 signal could only increase if the internalised PE-labelled CTLA-4 recycled back to the plasma membrane (**figure 3.8C**). Data was reproducible in CTLA-4

transfected Jurkat T cells further verifying the reliability of this assay (**figure 3.9**). Taken together this data suggests one path taken by CTLA-4 post-internalisation is to be recycled back to the cell surface.

3.5 CTLA-4 is degraded in lysosomes

CTLA-4 has been reported to interact with the lysosomal adaptor AP-1 and undergo degradation in a lysosomal compartment (Iida et al., 2000; Schneider et al., 1999). To measure the stability of the CTLA-4 protein, CTLA-4 transfected CHO cells were incubated in medium or medium supplemented with CHX, NH_4Cl or BafA, at 37°C for 3hours. CHX is an inhibitor of new protein synthesis and NH_4Cl and BafA are inhibitors of lysosomal degradation. After treatment, cells were fixed and permeabilised prior to staining for total CTLA-4 expression. Degradation was analysed by both confocal microscopy and flow cytometry (**figure 3.10** and **3.11A-B**). In the absence of new protein synthesis, rapid loss of human CTLA-4 was observed indicating that CTLA-4 was degraded rapidly. Moreover, NH_4Cl and BafA resulted in an accumulation of CTLA-4 suggesting that blocking lysosomal function prevents CTLA-4 degradation. These results were also consistent with biochemical analysis of CTLA-4 by western blotting, indicating that CTLA-4 protein was indeed degraded rather than a loss of signal being due to loss of fluorescence (**figure 3.11C**). To validate the findings in CHO cells, the assay was repeated in CTLA-4 transfected Jurkat T cells and in activated T cells. The analysis in these cells revealed strong similarities in the pattern of CTLA-4 degradation observed in CHO cells (**figure 3.12** and **3.13**).

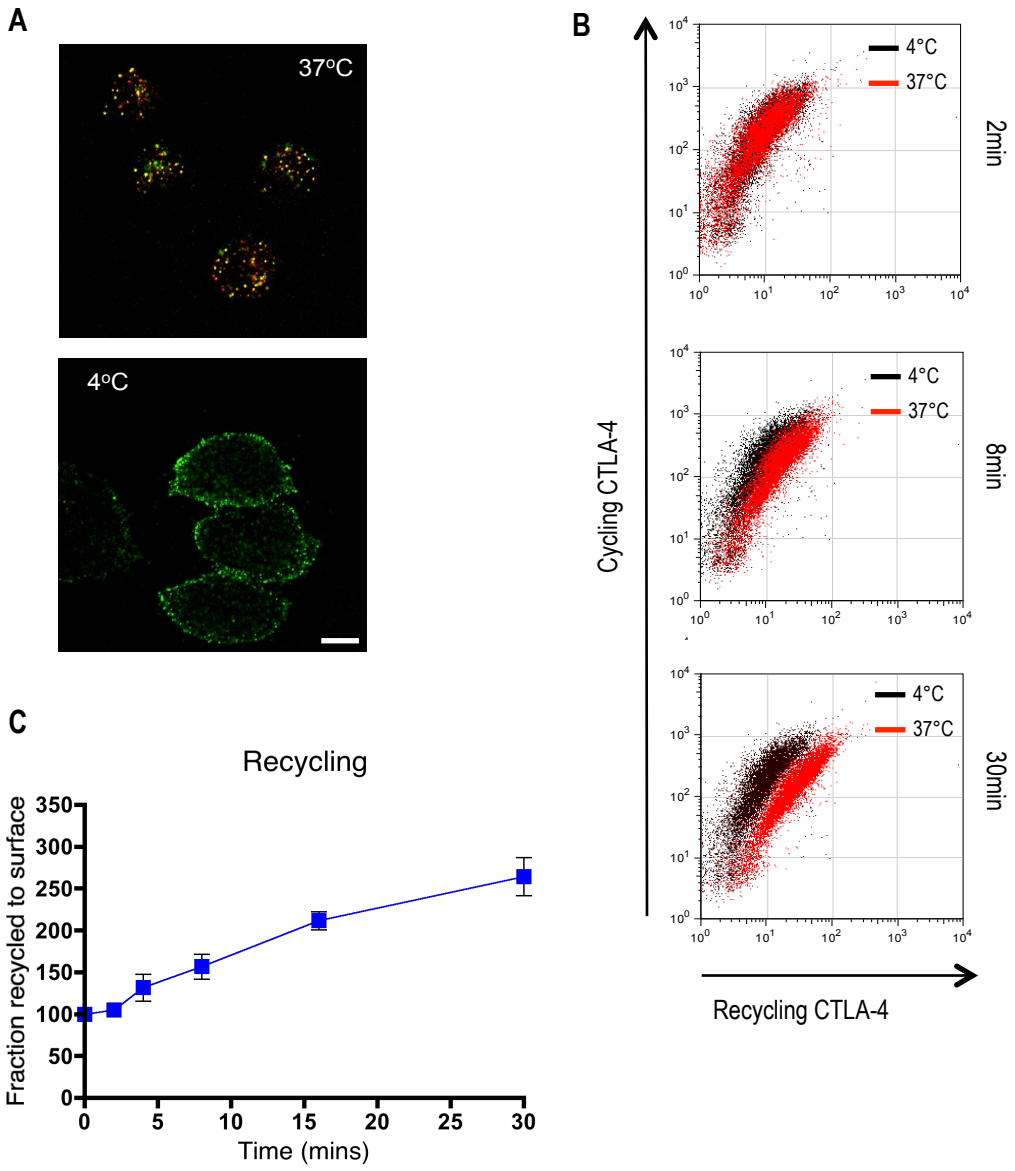

Figure 3.8 Human CTLA-4 recycles back to the cell surface after internalisation. (A) CHO cells expressing human CTLA-4 were labeled at 37°C with unlabelled anti-CTLA-4 Ab and then placed on ice to label surface CTLA-4 with Alexa488 anti-mouse secondary Ab (green). To observe recycling receptors, cells were labeled with Alexa555 anti-mouse secondary Ab (red) at 37°C and fixed before confocal analysis. Control conditions are shown where the Alexa555 Ab was incubated at 37°C (top) compared with incubation at 4°C (bottom). This is representative of 3 independent experiments. Bar indicates scale of 10μm. **(B)** CHO cells expressing human CTLA-4 were labeled with PE-conjugated anti-CTLA-4 Ab at 37°C to detect cycling CTLA-4, washed and any recycling primary Ab detected by addition of Alexa647 anti-mouse secondary Ab at either 4°C or 37°C. Representative FACS plots are shown for PE-label (cycling CTLA-4) vs Alexa647 label (recycling CTLA-4) at the indicated time points. **(C)** Recycling rates are plotted for human CTLA-4 as normalised to the 4°C control. Error bars show standard error (n=3).

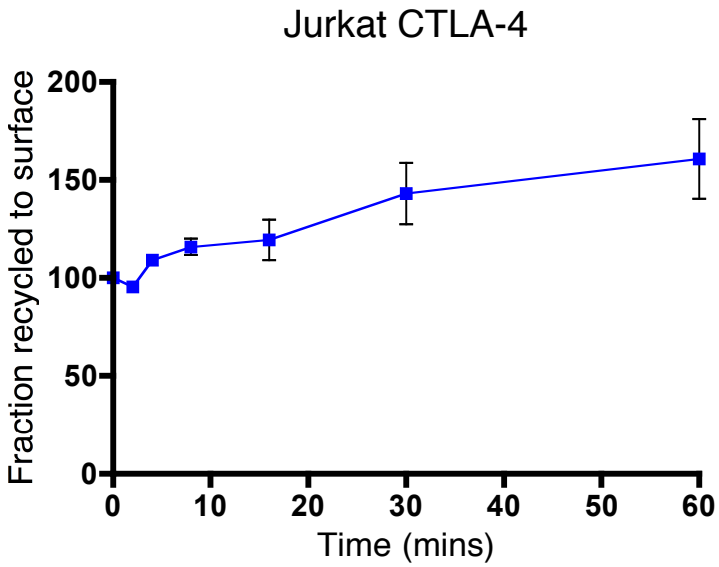

Figure 3.9 Human CTLA-4 recycling in CTLA-4 transfected Jurkat T cells is comparable to CTLA-4 transfected CHO cells. Jurkat T cells expressing human CTLA-4 were labelled with PE-conjugated anti-CTLA-4 Ab at 37°C to detect cycling CTLA-4, washed and any recycling primary Ab detected by addition of Alexa647 anti-mouse secondary Ab at either 4°C or 37°C. Recycling rates are plotted for human CTLA-4 as normalised to the 4°C control. Error bars show standard error (n=3).

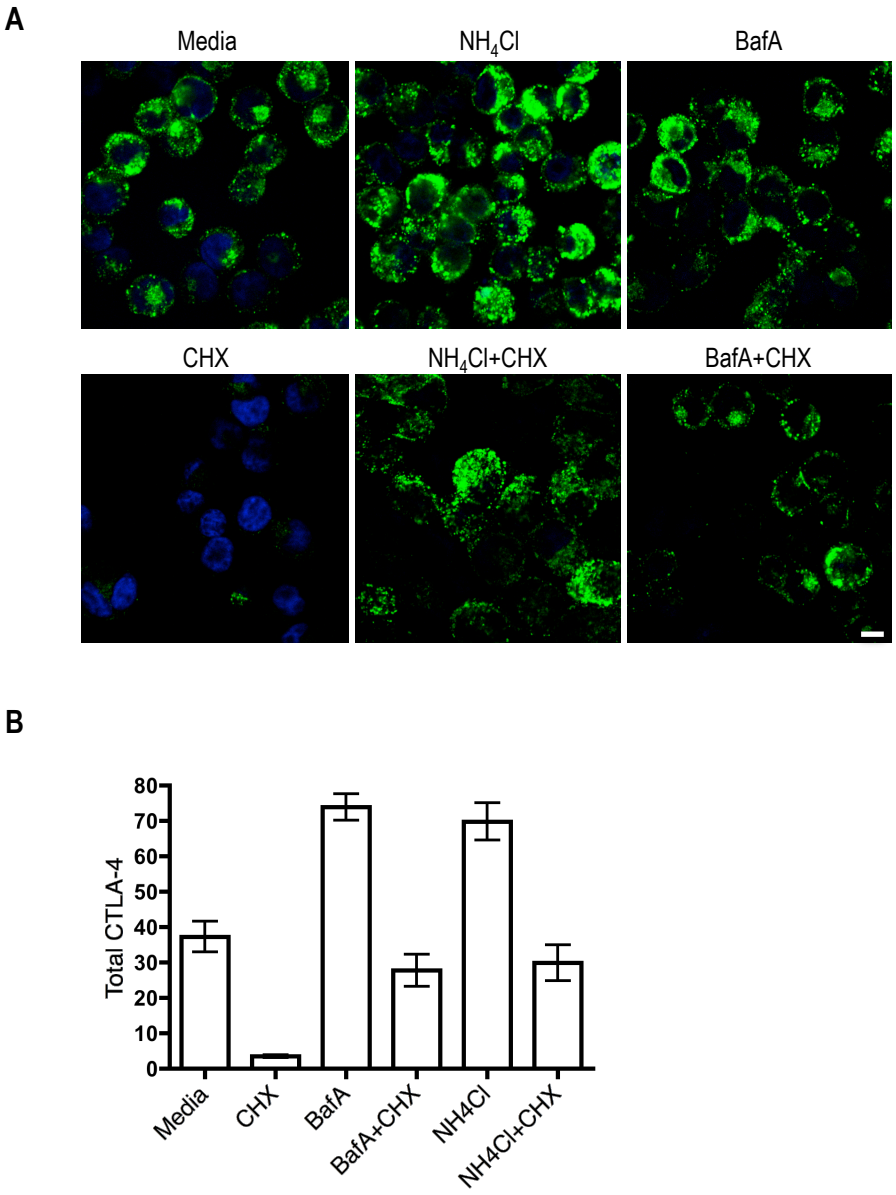

Figure 3.10 Human CTLA-4 is degraded in lysosomal compartments. (A) CHO cells expressing human CTLA-4 were incubated in medium or medium supplemented with CHX, NH_4Cl or BafA at 37°C for 3hours. Cells were stained for total CTLA-4 expression with an unlabelled anti-CTLA-4 Ab and Alexa488 anti-mouse secondary Ab and analysed by confocal microscopy. Bar indicates scale of 10µm. **(B)** Total CTLA-4 was quantified by outlining cells in ImageJ and MFI plotted**.** Error bars show standard error (n>3). MFI, mean fluorescence intensity.

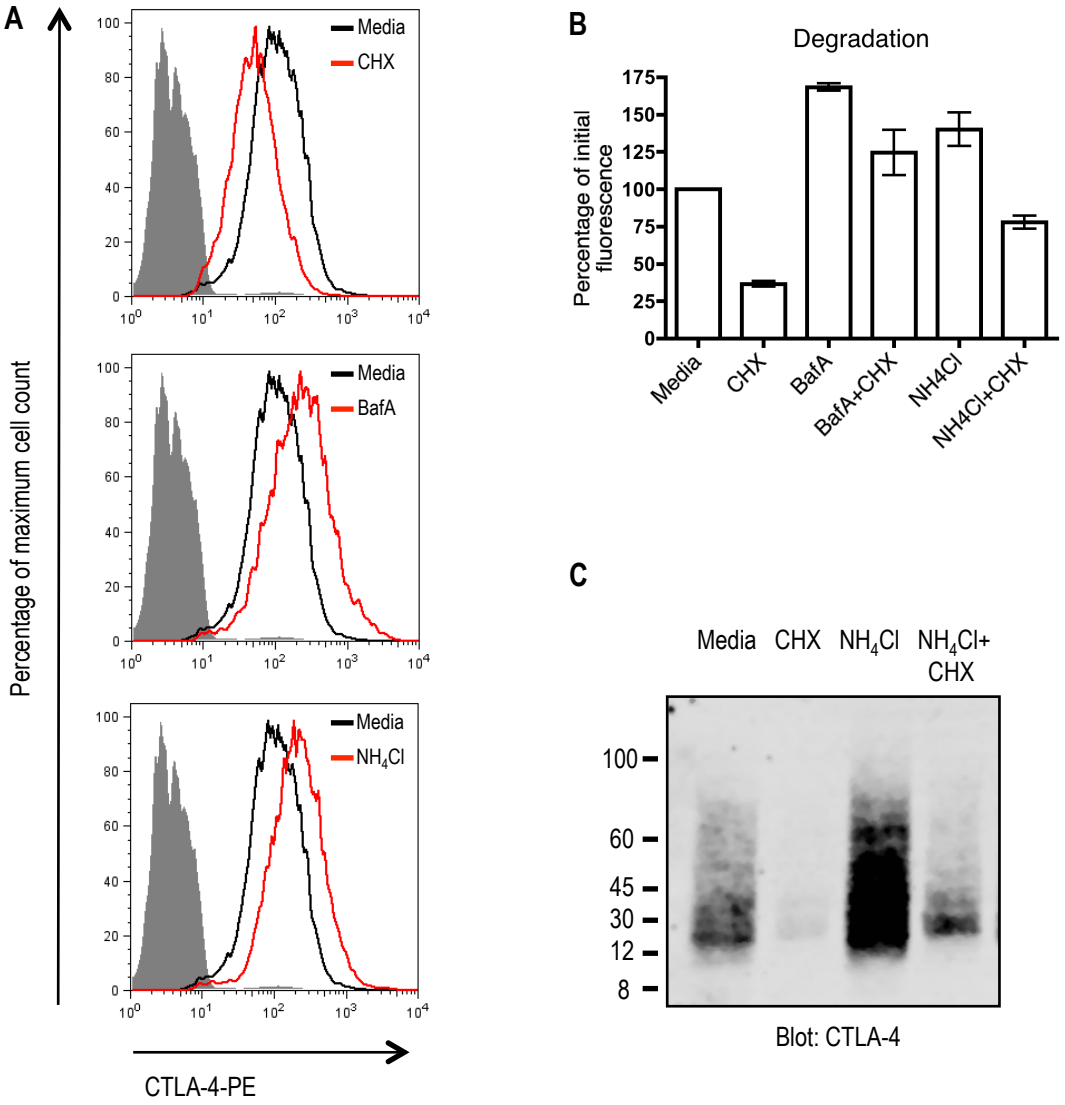

Figure 3.11 Flow cytometry and western blotting verify that human CTLA-4 degradation takes place in lysosomal compartments. (A) CHO cells expressing human CTLA-4 were incubated in medium or medium supplemented with CHX, NH_4Cl or BafA at 37°C for 3hours. Cells were stained for total CTLA-4 expression with a PE-conjugated anti-CTLA-4 Ab and analysed by flow cytometry. Representative FACs plots of one experiment. **(B)** The is MFI plotted as a percentage of initial fluorescence. Error bars show standard error (n>3). **(C)** Cells were treated as shown and CTLA-4 was then immunoprecipitated using an Ab binding to the extracellular region of CTLA-4. Expression of CTLA-4 was analysed by western blotting using a C-19 C-terminal anti-CTLA-4 Ab. This is representative of one independent experiment of n>3.

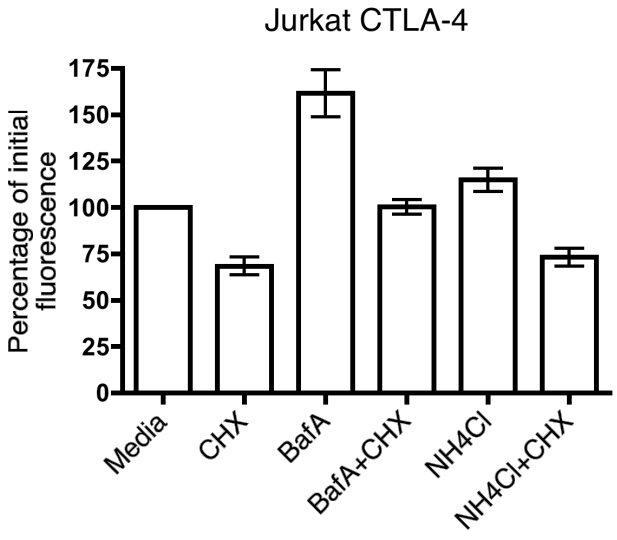

Figure 3.12 Human CTLA-4 degradation in CTLA-4 transfected Jurkat T cells is comparable to CTLA-4 transfected CHO cells. Jurkat T cells expressing CTLA-4 were incubated in medium or medium supplemented with CHX, NH_4Cl or BafA at 37°C for 3hours. Cells were stained for total CTLA-4 expression with a PE-conjugated anti-CTLA-4 Ab and analysed by flow cytometry. The MFI is plotted as a percentage of initial fluorescence. Error bars show standard error (n=3).

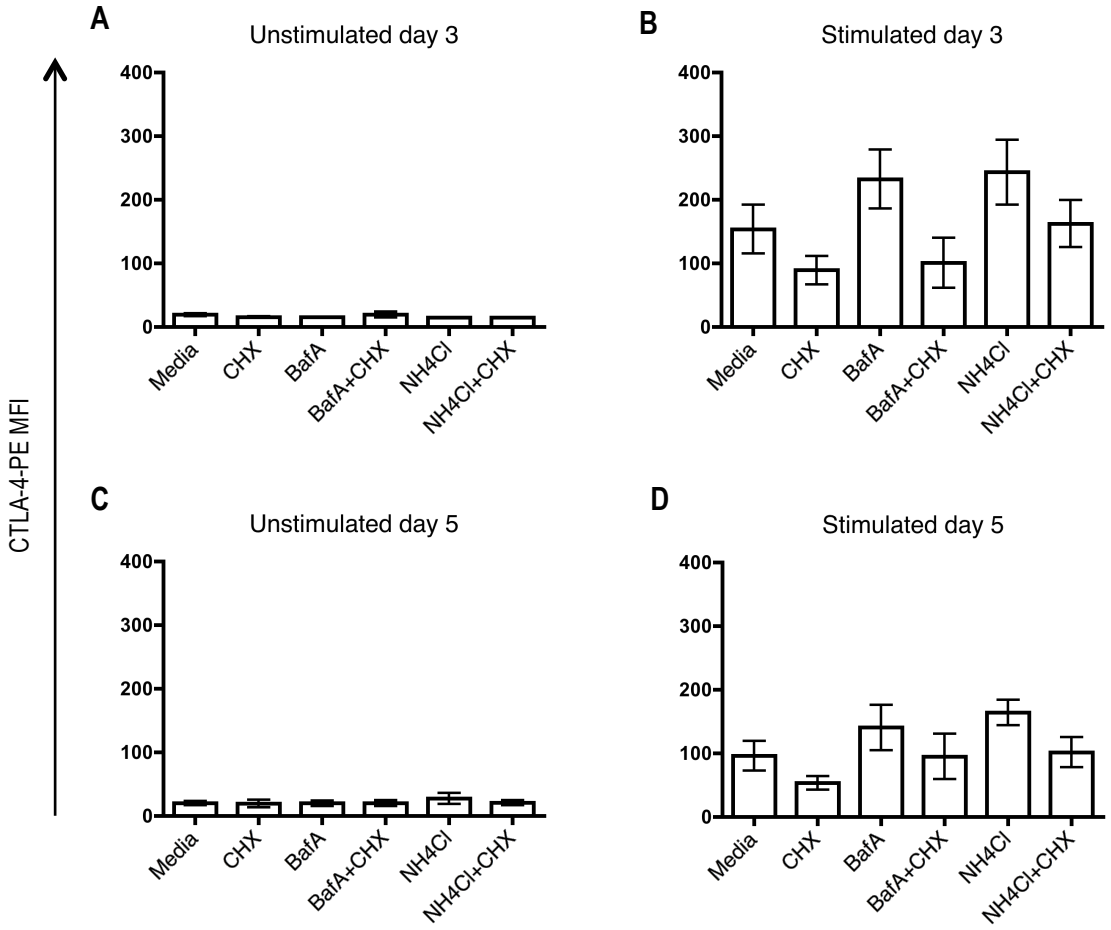

Figure 3.13 Human CTLA-4 degradation in activated T cells is comparable to CTLA-4 transfected CHO and Jurkat T cells. $CD4^{+}CD25^{-}$ T cells were left untreated (unstimulated) or stimulated with anti-CD3/CD28 beads. At three days **(A** and **B)** and five days **(C** and **D)** cells were incubated in medium or medium supplemented with CHX, NH_4Cl or BafA at 37°C for 3hours. Cells were stained for total CTLA-4 expression with a PE-conjugated anti-CTLA-4 Ab and analysed by flow cytometry. Error bars show standard error (n=3).

To determine if CTLA-4 co-localised with markers of late endosomes, CTLA-4 transfected CHO cells were transfected with CD63, fused to GFP, in the presence of NH_4Cl. Notably, human CTLA-4 demonstrated substantial co-localisation with CD63-GFP, suggesting traffic to late endosomes (**figure 3.14**). Collectively these data suggest that degradation in lysosomal compartments may be one mechanism used to regulate the surface expression of CTLA-4 and could explain the decrease seen in the internalised biotinylated CTLA-4 protein in **figure 3.6**.

3.6 CTLA-4 degradation is ubiquitin-dependent

Ubiquitin has long been recognised as an important signal for targeting membrane proteins for destruction in proteasomes and lysosomes (Myung et al., 2001). Intracellular lysine residues serve as targets of ubiquitin attachment in receptor proteins. CTLA-4 has five lysine residues encoded in the cytoplasmic domain. To examine whether ubiquitin regulated CTLA-4 degradation, CTLA-4 was incubated in medium or medium supplemented with NH_4Cl or BafA at 37°C for 3hours. CTLA-4 was then immunoprecipitated from CTLA-4 transfected CHO cells using an antibody binding the extracellular region of CTLA-4. Membranes were then probed for CTLA-4 with a C-19 C-terminus anti-CTLA-4 Ab and for ubiquitin with an anti-ubiquitin Ab, which binds both mono- and polyubiquitin. **Figure 3.15** shows that treatment with NH_4Cl and BafA resulted in an accumulation of CTLA-4, which suggests that by blocking lysosomal function the degradation of CTLA-4 is prevented. Moreover ubiquitinated proteins with molecular masses of ~ 46-58kDa were only detectable after BafA treatment and not with NH_4Cl or the media control. This result could be explained by the fact that NH_4Cl and BafA act at different sites within the cell. NH_4Cl acts to inhibit the acidification of endosomes (Ohkuma and Poole, 1978) whereas BafA is a specific inhibitor of V-type H+-ATPase, which is required for lysosomal function (Yasir et al., 2011). This data therefore suggests that NH_4Cl accumulates CTLA-4 prior to the ubiquitination of the

receptor but BafA accumulates CTLA-4 after receptor ubiquitination. Taken together this data confirms that CTLA-4 degradation in lysosomes is ubiquitin-dependent.

MG132 is an inhibitor of proteasomal degradation but can function to deplete free ubiquitin (Melikova et al., 2006). If CTLA-4 is degraded in lysosomes and this requires ubiquitin CTLA-4 levels should increase in the presence of MG132. To address the requirement of ubiquitin in CTLA-4 trafficking, CHO cells transfected with CTLA-4 were incubated in medium or medium supplemented with MG132 for 2hours at 37°C. Cells were then stained for CTLA-4 expression using a PE-conjugated anti-CTLA-4 Ab at 4°C, 37°C or were fixed and permeabilised for total expression. **Figure 3.16** shows an increase in surface, cycling and total CTLA-4 expression in the presence of MG132. This data suggests that by inhibiting CTLA-4 ubiquitination and degradation, the steady state is altered resulting in an increase of CTLA-4 receptor in the different locations.

In order to maintain steady state when CTLA-4 degradation is blocked, a default pathway could be for the receptor to recycle back to the cell surface. In order to address if CTLA-4 recycling is enhanced after blocking degradation, CHO cells transfected with CTLA-4 were incubated in medium or medium supplemented with MG132 for 2hours at 37°C and the recycling assay as described in section 3.4 was repeated. To quantify any differences in recycling, the fraction of recycled protein was expressed as a percentage of labelled protein. **Figure 3.17A** shows that by depleting free ubiquitin and thereby blocking degradation CTLA-4 recycling is increased.

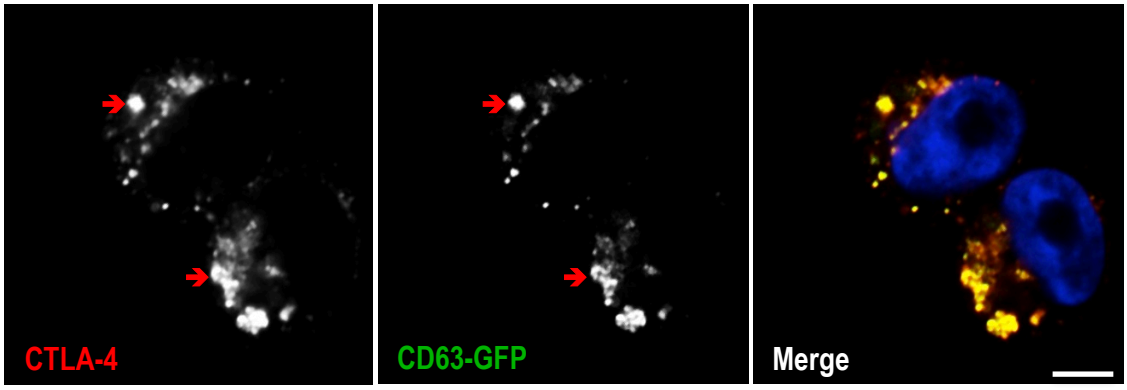

Figure 3.14 Human CTLA-4 co-localises with markers of late endosomes. CHO cells expressing human CTLA-4 were transfected with CD63-GFP. Cells were incubated in medium supplemented with NH_4Cl at 37°C for 3hours. Cells were fixed, permeabilised, and stained with an unlabelled anti-CTLA-4 Ab and Alexa565 anti-human secondary Ab (red) to stain total CTLA-4 protein and analysed by confocal microscopy. The red arrows indicate co-localisation. This is representative of one independent experiment of n=3. Bar indicates scale of 10μm.

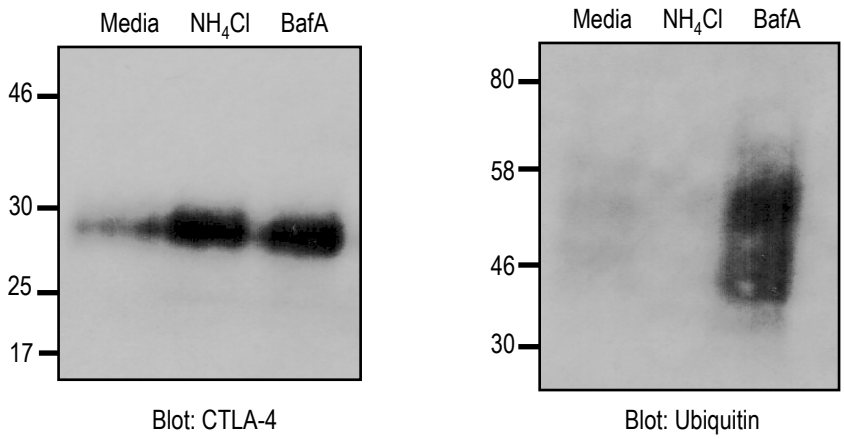

Figure 3.15 Ubiquitination of the CTLA-4 receptor is revealed by blocking lysosomal degradation with BafA. CHO cells transfected with CTLA-4 were incubated in medium or medium supplemented with NH_4Cl or BafA at 37°C for 3hours. CTLA-4 was then immunoprecipitated using an Ab binding to the extracellular region of CTLA-4. Expression of CTLA-4 was analysed by western blotting using a C-19 C-terminal anti-CTLA-4 Ab and an anti-ubiquitin Ab.

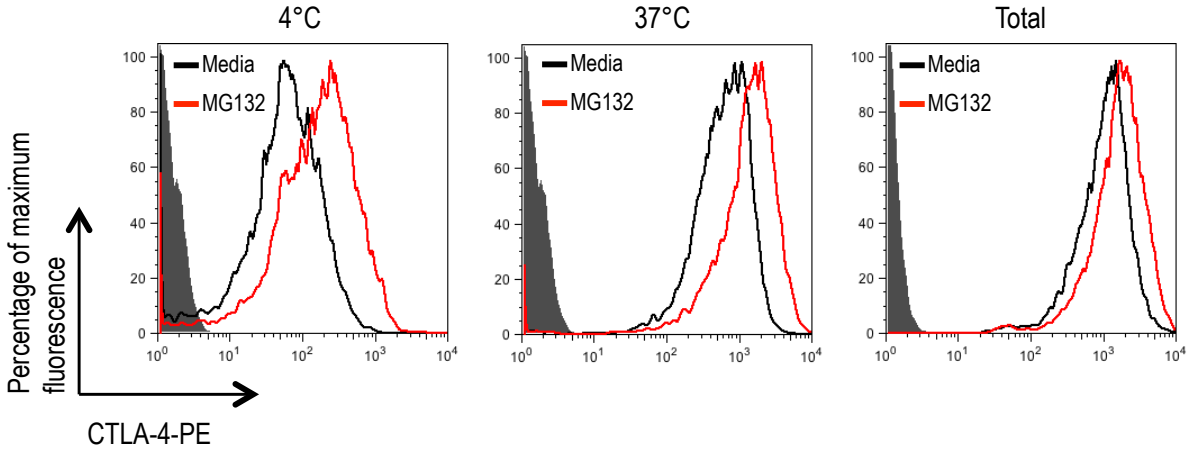

Figure 3.16 The level of surface, cycling and total CTLA-4 expression increases when ubiquitin is depleted. CHO cells transfected with CTLA-4 were incubated with medium or medium supplemented with MG132 for 2hours at 37°C. Cells were then stained for surface, cycling or total CTLA-4 expression using a PE-conjugated anti-CTLA-4 Ab and analysed by flow cytometry. Representative FACs plots of one independent experiment of n=3.

Ubiquitin is attached to intracellular lysine residues via the ubiquitin conjugation cascade. UBEI-41 is an inhibitor of the E1-activating enzyme, which is required to start the cascade (Balut et al., 2011). If this enzyme is inhibited ubiquitin cannot be attached to intracellular lysine residues and this could inhibit CTLA-4 targeting to lysosomes. To address the effect of UBEI-41 on CTLA-4 trafficking, CHO cells transfected with CTLA-4 were incubated in medium or medium supplemented with UBEI-41 for 2hours at 37°C and the recycling assay as described in section 3.4 was repeated. To quantify any differences in recycling, the fraction of recycled protein was expressed as a percentage of labelled protein. **Figure 3.17B** shows a steady increase in CTLA-4 recycling when treated with UBEI-41, further supporting a role for ubiquitin in regulating CTLA-4 degradation.

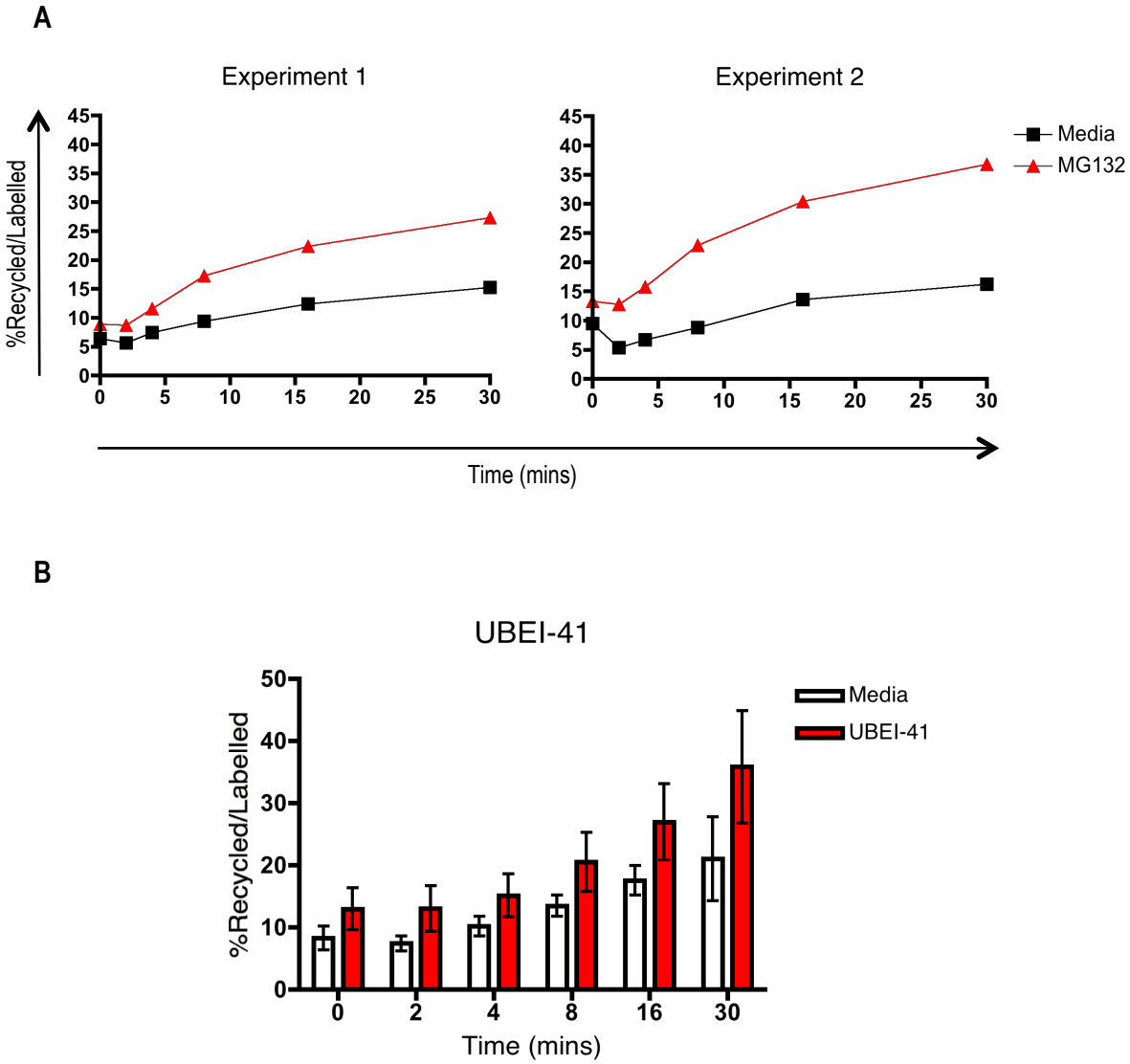

Figure 3.17 Inhibiting CTLA-4 degradation results in an increase in CTLA-4 recycling. CHO cells transfected with CTLA-4 were incubated with medium or medium supplemented with MG132 **(A)** or UBEI-41 **(B)** for 2hours at 37°C. Cells were then labeled with PE-conjugated anti-CTLA-4 Ab at 37°C to detect cycling CTLA-4, washed and any recycling CTLA-4-PE antibody detected by addition of Alexa647 anti-mouse secondary Ab at either 4°C or 37°C. The fraction of recycled protein was expressed as a percentage of labelled protein. (A) Data shown from two independent experiments. (B) Error bars show standard error (n=3).

3.7 CTLA-4 removes ligand from APCs

The importance of CTLA-4 in regulating T cell activation is established but the mechanism under which CTLA-4 inhibition becomes dominant is debatable. As a lab, we have identified a further function for CTLA-4 termed transendocytosis where CTLA-4 binds its ligand at the cell surface, internalises the whole molecule and targets the ligand for degradation in lysosomes (Qureshi et al., 2011). To investigate this CHO cells expressing CTLA-4 were co-cultured with CHO cells stably expressing either CD80 or CD86, fused to GFP, for 3hours at 37°C in medium alone or medium supplemented with NH_4Cl. CD80 or CD86-GFP cells were labelled with CellTrace Violet and accordingly GFP transfer could be quantified by gating CTLA-4 expressing cells that were negative for Violet dye staining. Using flow cytometry, transfer of CD80 and CD86 into CTLA-4-positive cells was observed (**figure 3.18A** and **B**). This transfer was further enhanced after incubation with the lysosomal inhibitor NH_4Cl, which suggests that the ligand is being degraded in the CTLA-4-positive cell. Importantly the capture efficiency of CD80 was greater than CD86, which could relate to the higher affinity of CTLA-4 for CD80 (**figure 3.18C**). Taken together, this data supports the concept that CTLA-4 regulates T cell activation by removing ligand from the surface of APCs and targets the ligand for degradation in lysosomes as reported previously.

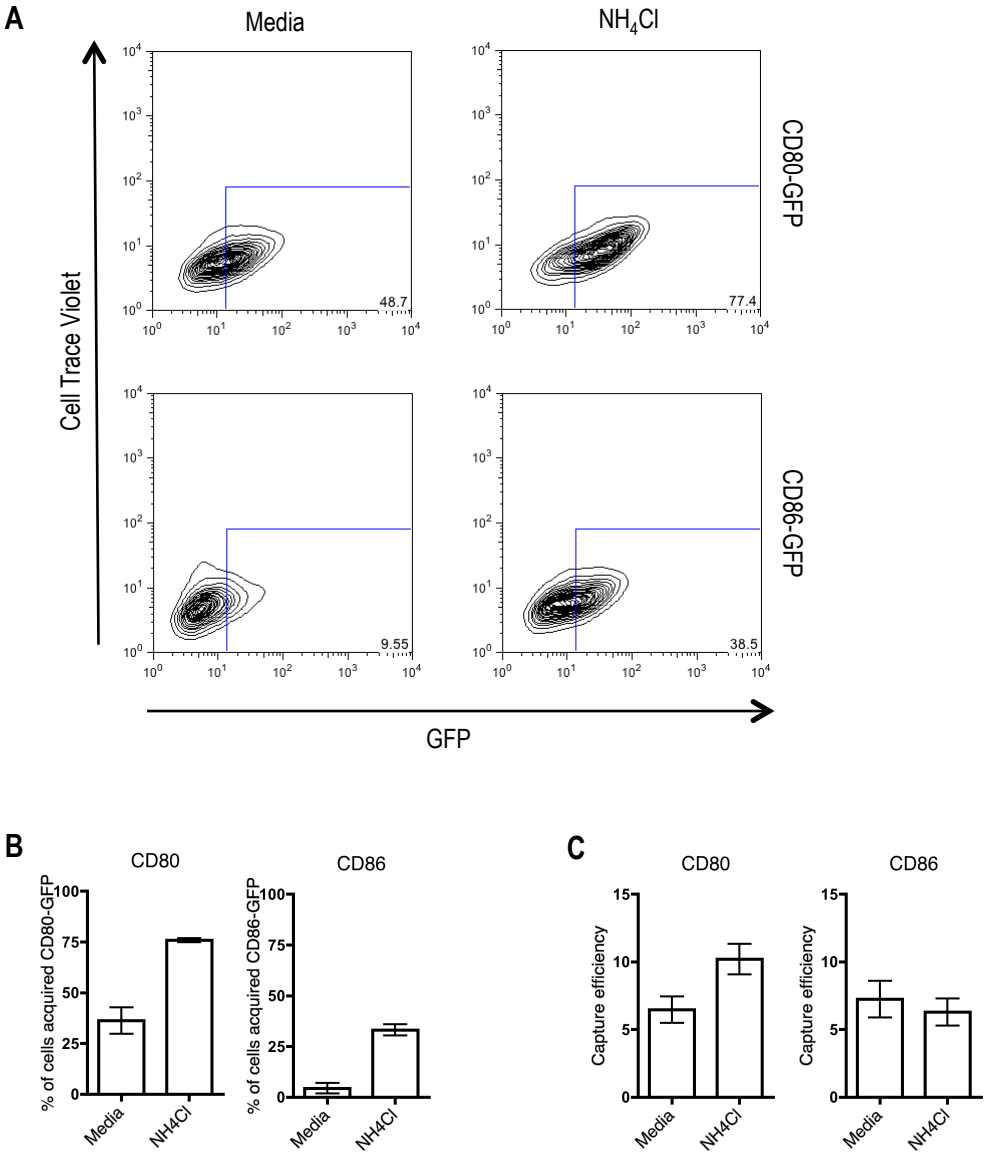

Figure 3.18 CTLA-4 removes CD80 and CD86 and targets the ligand for lysosomal degradation. CD80 and CD86-GFP acquisition by CHO-cells expressing CTLA-4 was determined by flow cytometry. **(A)** Representative FACs plots showing percentage of acquired GFP by CTLA-4 in medium or medium supplemented with NH_4Cl. Data are from a single experiment representative of three performed. **(B)** Error bars show standard error (n=3). **(C)** The capture efficiency was calculated as described in Materials and Methods.

3.8 Discussion

In this chapter the general cell biology of the CTLA-4 receptor was investigated. It is well established that CTLA-4 internalisation from the cell surface is clathrin-mediated following the association of the YVKM motif located in its C-terminus, which associates with the clathrin adaptor AP-2. However the path taken by CTLA-4 post-internalisation and the ultimate fate of the receptor is not well understood. Moreover, how the intracellular trafficking of CTLA-4 and its predominant localisation in intracellular vesicles acts to regulate T cell activation by binding ligands at the cell surface remains controversial. I observed that at steady state CTLA-4 resides in intracellular vesicles in both CTLA-4 transfected cells and in T cells. Following the internalisation of CTLA-4 via clathrin, CTLA-4 either recycled back to the cell surface or was degraded in lysosomes. Importantly both pathways could serve a role in regulating T cell activation by the newly identified function of transendocytosis where CTLA-4 could target the ligand for degradation in lysosomes and recycle back to the surface to further inhibit CD28 co-stimulation.

Using CTLA-4 transfected CHO cells as a model system, work in this thesis has demonstrated that human CTLA-4 is largely located in intracellular vesicles with little surface CTLA-4 expression. Findings were reproducible in transfected Jurkat T cells, activated T cells and in Tregs but the level of total CTLA-4 expression were higher in these cell types when compared to the combined surface and cycling pool. It is interesting to speculate whether once synthesised the CTLA-4 receptor in T cells is stored in a storage compartment and mobilised from these compartments once the T cell encounters antigen. Moreover, although Tregs constitutively express CTLA-4, data presented in this thesis reveals no difference in the localisation and trafficking of CTLA-4 in $CD4^+$ $CD25^-$ T cells or Tregs.

The YVKM motif associates with the μ2 subunit of the AP-2 complex for subsequent inclusion into clathrin-coated pits (Chuang et al., 1997; Shiratori et al., 1997). In our experimental conditions, human CTLA-4 demonstrates rapid internalisation kinetics, where 50% of the surface receptor internalised within 5minutes. Moreover, following internalisation CTLA-4 co-localised with transferrin in intracellular vesicles suggesting that CTLA-4 uses the same pathway as TfR for internalisation. The importance of the YVKM motif in CTLA-4 endocytosis was determined in a previous study by mutating the tyrosine residue in the YVKM motif (Y→F) (Mead et al., 2005). This data revealed that the mutant had increased surface expression, and a slow endocytic rate, but internalisation was only partially inhibited. A likely hypothesis is other residues within the cytoplasmic tail may contribute to inclusion into clathrin pits, and subsequent internalisation (Chuang et al., 1997; Shiratori et al., 1997; Zhang and Allison, 1997).

CTLA-4 trafficking may resemble that of other receptors. For example Protease-activated receptor 1 (PAR1), a GPCR, has a C-tail sequence containing tyrosine-based motifs that appear to mediate distinct trafficking events. The proximal $Y^{383}SIL^{386}$ motif regulates lysosomal sorting whereas the distal $Y^{420}KKL^{423}$ motif controls internalisation (Marchese et al., 2008). Such findings suggest that within the cytoplasmic domain multiple motifs of the same sorting signal may confer distinct endocytic and sorting functions. Interestingly human CTLA-4 contains two tyrosine residues at positions 201 and 218. The proximal $Y^{201}VKM$ motif controls internalisation, whilst to date no functional significance has been identified for tyrosine 218. Thus, it is interesting to hypothesise whether the distal motif, like in PAR1, may have a role that contributes to endocytosis. Furthermore, this could explain the partial internalisation seen with the Y→F mutation in human CTLA-4.

Following internalisation, some internalised receptors are delivered to an early or sorting endosome (Hare and Taylor, 1991). Trafficking receptors such as TfR and EGFR have two fates: to recycle back to the membrane or to be targeted for degradation in lysosomes. Thus, in the absence of specific targeting, one possible route for internalised receptors is recycling back to the cell surface (Hare and Taylor, 1991). The observation of CTLA-4 co-localisation with the TfR raises questions as to whether CTLA-4 can also recycle constitutively back to the plasma membrane (Chuang et al., 1997; Leung et al., 1995). A two-step Ab staining assay revealed that CTLA-4 recycles back to the plasma membrane within a 30minute time period, which was further verified by confocal microscopy. But why does CTLA-4 need to recycle? In the case of EGFR the requirement for recycling can be explained by the requirement for continued signalling by the receptor. If the receptor is degraded, the signal is diminished and the signalling pathway cannot be activated until the number of EGFRs at the surface is re-established by protein synthesis (Roepstorff et al., 2009).

The pH sensitivity of ligand binding further regulates whether EGFR is recycled or degraded. For example TGF-α binding to EGFR is not stable at the pH of endosomes. The receptor dissociates from the ligand, is deubiquitinated and recycled back to the surface. In contrast, EGF binding to EGFR is stable at the endosomal pH, remains ubiquitinated and is targeted for degradation (Roepstorff et al., 2009). Our data has consistently demonstrated that CTLA-4 rips CD80 more efficiently than CD86. This could be explained by the higher affinity of CTLA-4 for CD80 as opposed to CD86. It can therefore be postulated that the lower affinity of CTLA-4 for CD86 could result in CD86 dissociating from CTLA-4 at sorting endosomes, thus allowing the receptor to recycle back to the surface. However our assays have shown that both receptor-ligand pairs are targeted for degradation arguing against the hypothesis that ligands direct CTLA-4 recycling. It is interesting to speculate that the need for CTLA-4 to recycle is to remove ligand from APCs through transendocytosis. In this way, CTLA-4 would be readily available and

the cell-cell contact between the T cell and APC would still be intact for CTLA-4 to remove ligand at the synapse.

The pool of internalised CTLA-4 that does not recycle back to the plasma membrane is targeted to lysosomes for degradation. The rapid turnover rate of CTLA-4 suggests the lysosomal degradation pathway may control CTLA-4 expression and downregulation, and in fact such studies argue against the existence of a recycling pool (Egen and Allison, 2002; Iida et al., 2000). In accordance with Egen & Allison, (2002), a rapid loss of CTLA-4 levels was observed in the absence of new protein translation suggestive of degradation. Moreover the accumulation of CTLA-4 in the presence of lysosomal inhibitors and co-localisation with lysosomal markers suggests trafficking to lysosomes. Again, like recycling it is not completely understood why CTLA-4 needs to be degraded. Receptors involved in signalling are degraded in order to regulate the signalling pathway. Despite earlier studies arguing that CTLA-4 delivers an inhibitory signal, no such signalling pathway has been identified ruling out the possibility that degradation is required to regulate the CTLA-4 negative signal. However, the targeting of ligand for lysosomal degradation provides support for the requirement of this trafficking pathway and further fits the model of CTLA-4 transendocytosis. Moreover if CTLA-4 dissociates from ligand, the receptor could recycle back to the membrane to bind and remove more ligand.

Proteins targeted for lysosomal degradation such as EGFR and PAR2 are ubiquitinated at lysine residues by E3 ligases, where ubiquitin serves as the signal to traffic cargo to lysosomes (Jacob et al., 2005; Levkowitz et al., 1998). Using western blotting and a range of chemical inhibitors the data presented here confirm that CTLA-4 is ubiquitinated. However what needs to be addressed is the site of CTLA-4 ubiquitination. Ubiquitin is now emerging as a potential signal required for internalisation. In fact

in order for Interferon-α receptor 1 subunit (IFNAR1) to undergo efficient internalisation it must be polyubiquitinated (Kumar et al., 2007). The cell surface could therefore serve as the potential site for CTLA-4 ubiquitination, since it is at the cell surface where the receptor binds its ligands, which are targeted for degradation in lysosomes. However in the case of EGFR, ubiquitination is only essential for lysosomal degradation but it is not a requirement for its endocytosis (Huang et al., 2006), which suggests the ubiquitination of CTLA-4 could occur downstream of internalisation.

A question that still needs to be addressed is what are the sorting motifs encoded in CTLA-4 that regulate receptor recycling and degradation? Presumably the YVKM motif plays an important role since CTLA-4 must be internalised first before it is sorted in early endosomes. Moreover, the data shown here reveal a role for lysine residues and ubiquitin in regulating CTLA-4 recycling and degradation. These observations could be confirmed using a lysine-less CTLA-4 mutant. Such a mutant could be used to determine the requirement of lysine residues in internalisation, recycling, degradation and in transendocytosis. Additionally by creating single lysine point mutants of CTLA-4, the lysine residue/s that serve as targets for ubiquitination could be determined. An interesting motif encoded in the CTLA-4 cytoplasmic domain is the proline-based motif PTEP. This motif resembles the PT/SAP motif encoded in viruses required to recruit the ESCRT-I component TSG101 (Dilley et al., 2010). It is interesting to speculate that the PTEP motif in CTLA-4 could be involved in MVB formation prior to the delivery of the receptor to lysosomes.

Central to the role of membrane protein trafficking and degradation are E3 ubiquitin ligases. Two primary classes of E3 ligases have been identified, distinguished by a homologous to E6-AP carboxyl terminus (HECT) domain, and a really interesting new gene (RING) finger domain. The potential

involvement of a HECT type E3 ligase in CTLA-4 ubiquitination arises from the presence of a series of WW domains that recognise proline-rich PPxY motifs (d'Azzo et al., 2005). Such a motif is present in the CTLA-4 extracellular domain. However this would present a problem, as this is same motif required for ligand binding suggesting that if a HECT type E3 ligase was involved in CTLA-4 ubiquitination, ligand must be displaced. Thus it is not yet possible to rule out a role for a HECT type E3 ligase in this process, as the effect of ligand binding on CTLA-4 ubiquitination is not yet clear.

Overall, understanding the localisation, trafficking and function of CTLA-4 could highlight areas that could be manipulated for the treatment of autoimmunity and cancer. I have addressed the mechanisms and pathways required for CTLA-4 intracellular trafficking that could directly impact the function of CTLA-4 as a negative regulator of T cell activation.

4.0 REGULATION OF CTLA-4 RECYCLING AND DEGRADATION

4.1 Introduction

The findings of chapter 3 of this thesis reveal that post-internalisation CTLA-4 either recycles back to the surface or is degraded in lysosomes, a mechanism that involves the ubiquitination of intracellular lysine residues. However other sorting motifs important for such trafficking remain to be identified. Of importance are the two tyrosine-based motifs, the lysine residues and a proline-based motif. By mutating such motifs I considered whether the regulation of CTLA-4 recycling and degradation could be unmasked. In this chapter I have therefore investigated the mechanisms regulating the post-endocytic fate of CTLA-4.

4.2 CTLA-4 localisation in intracellular vesicles is regulated by the YVKM motif

To identify the motifs encoded in the cytoplasmic domain that regulate CTLA-4 localisation in intracellular vesicles, site-directed mutagenesis was used to generate single or multiple point mutants of CTLA-4 as outlined in **figure 4.1**. CHO cells were transfected with the CTLA-4 mutants and expression was compared at 4°C, 37°C or cells were fixed and permeabilised before analysis by confocal microscopy or flow cytometry. KLESS, ATEP and AFIP CTLA-4 showed a comparable localisation to WT CTLA-4 with little or no surface CTLA-4 expression and predominant distribution in intracellular vesicles (**figure 4.2** and **4.3**). In contrast, AVKM and AVKM-AFIP demonstrated predominant surface CTLA-4 expression with far more limited intracellular vesicles (**figure 4.3**). This difference in the amount of surface CTLA-4 relative to the total was quantified by flow cytometry and is shown in **figure 4.4**.

A

```
                190       200       210       220
WT          SKMLKKRSPLTTGVYVKMPPTEPECEKQFQPYFIPIN
KLESS       SRMLRRRSPLTTGVYVRMPPTEPECERQFQPYFIPIN
ATEP        SKMLKKRSPLTTGVYVKMPATEPECEKQFQPYFIPIN
AVKM        SKMLKKRSPLTTGVAVKMPPTEPECEKQFQPYFIPIN
AFIP        SKMLKKRSPLTTGVYVKMPPTEPECEKQFQPAFIPIN
AVKM-AFIP   SKMLKKRSPLTTGVAVKMPPTEPECEKQFQPAFIPIN
```

B

Construct	Mutations
WT	Wild-type human CTLA-4
KLESS	All lysine residues have been mutated to arginine
ATEP	Proline residue in PTEP has been mutated to alanine
AVKM	Tyrosine residue in YVKM has been mutated to alanine
AFIP	Tyrosine residue in YFIP has been mutated to alanine
AVKM-AFIP	Both tyrosine residues in the two tyrosine based hydrophobic motifs have been mutated

Figure 4.1 Generation of CTLA-4 mutants. (A) C-terminal sequence alignments of human CTLA-4. Lysine residues mutated to arginine are shown in blue. Proline and tyrosine mutations to alanine are shown in green. **(B)** Brief description of the CTLA-4 mutants.

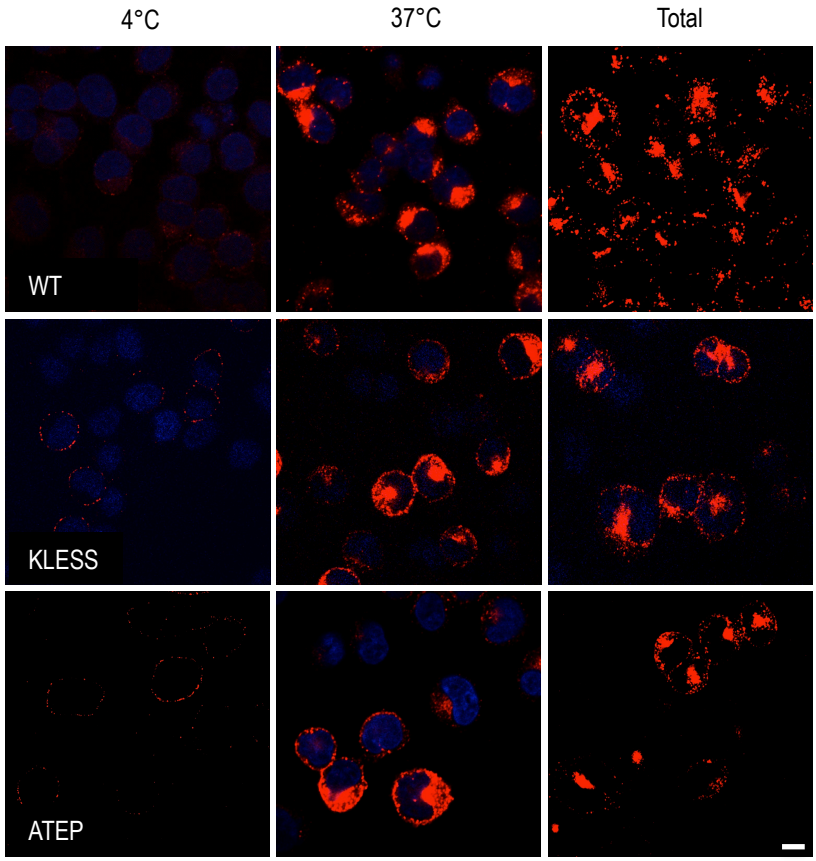

Figure 4.2 Phenotype of CTLA-4 mutants. CHO cells expressing CTLA-4 mutants were stained for surface CTLA-4 expression at 4°C; endocytosed CTLA-4 expression at 37°C; or were fixed and permeabilised prior to staining for total CTLA-4 expression with an unlabelled anti-CTLA-4 Ab and Alexa555 anti-mouse secondary Ab (n≥3). Bar indicates scale of 10μm.

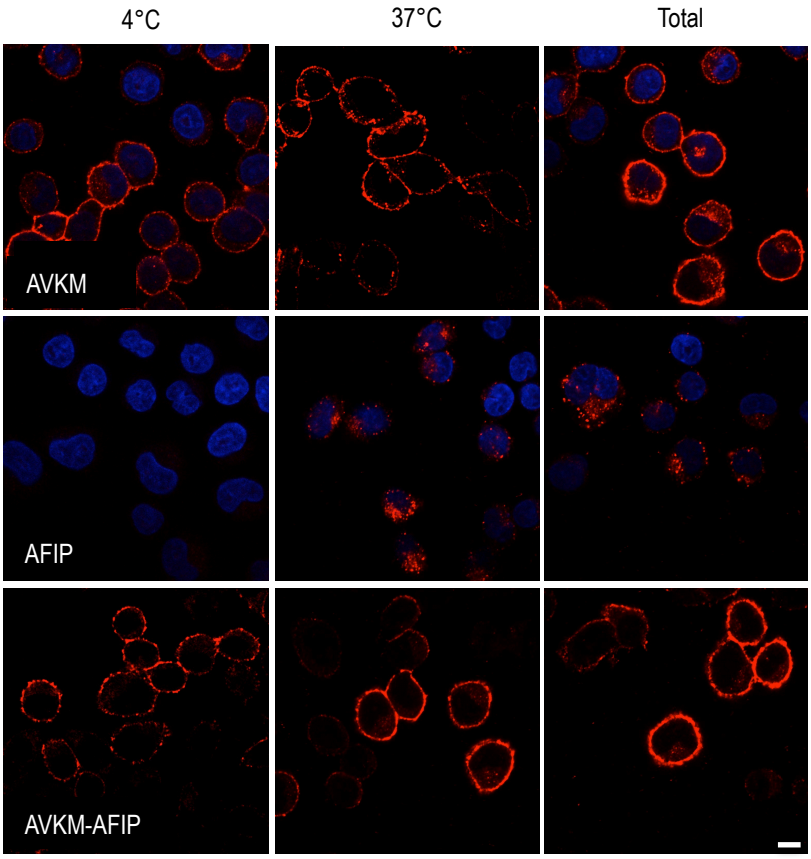

Figure 4.3 Phenotype of CTLA-4 mutants. CHO cells expressing CTLA-4 mutants were stained for surface CTLA-4 expression at 4°C; endocytosed CTLA-4 expression at 37°C; or were fixed and permeabilised prior to staining for total CTLA-4 expression with an unlabelled anti-CTLA-4 Ab and Alexa555 anti-mouse secondary Ab (n≥3). Bar indicates scale of 10μm.

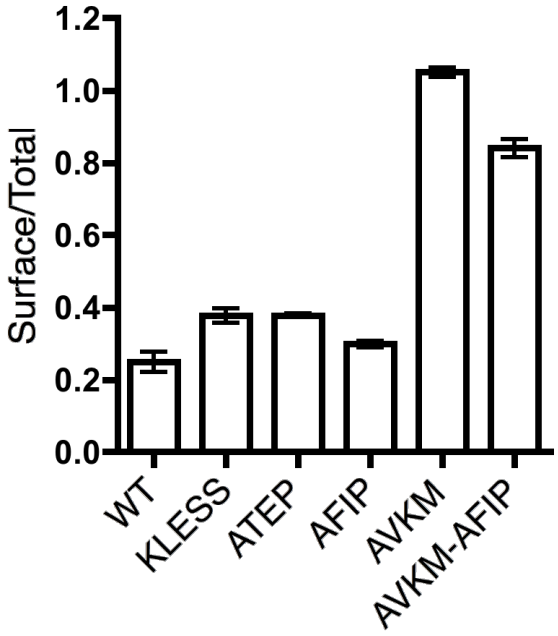

Figure 4.4 Surface to Total ratio of CTLA-4 mutants. CHO cells expressing CTLA-4 mutants were stained for surface CTLA-4 expression at 4°C or were fixed and permeabilised prior to staining for total CTLA-4 expression with PE-conjugated anti-CTLA-4 Ab. Cells were analysed by flow cytometry. The ratio of surface to total CTLA-4 for each mutant is plotted as determined by flow cytometry. Error bars show standard error (n>3).

4.3 CTLA-4 endocytosis is regulated by the YVKM motif

The increased surface expression observed in CTLA-4 mutants deficient in YVKM suggested that the absence of this motif might confer less efficient internalisation. Moreover, although mutations in the lysine residues and in the proline-based motif do not have an effect on CTLA-4 localisation, such mutations could affect the rate of CTLA-4 internalisation from the cell surface. Moreover, it is now emerging that ubiquitination of intracellular lysine residues could serve as an internalisation signal (Kumar et al., 2007). To investigate the importance of these motifs in CTLA-4 internalisation, the cell surface pool of CTLA-4 was stained on ice with a PE-conjugated anti-CTLA-4 Ab. Cells were then warmed to 37°C for the indicated time-points to allow any internalisation of surface CTLA-4 to take place. Cells were then placed on ice, and any CTLA-4 remaining at the cell surface detected with an Alexa647 anti-mouse secondary Ab. Accordingly in this assay loss of Alexa647 staining over time reflects endocytosis of CTLA-4. In the 4°C control, a linear relationship was observed between CTLA-4-PE (y-axis) and Alexa647 (x-axis) for all CTLA-4 mutants (**figure 4.5**). However after 30minute incubation at 37°C a curved plot was generated for WT, KLESS, ATEP and AFIP CTLA-4 where the initial PE-labelled surface CTLA-4 internalised resulting in a minimal surface Alexa647 label, typical of an endocytic protein. In contrast AVKM and AVKM-AFIP showed a more linear relationship between internalised and surface CTLA-4 in the 4°C control and at 37°C suggesting impaired endocytosis.

To quantify this data, the 647 signal was plotted against time as the fraction remaining compared to 4°C. Using this assay WT CTLA-4 showed a comparable rate of endocytosis to KLESS, ATEP and AFIP, internalising 50% or more protein within 15minutes (**figure 4.6A**). In contrast CTLA-4 mutants deficient in YVKM demonstrated a reduced ability to internalise (**figure 4.6B**). Interestingly, AVKM-AFIP was more stable than AVKM suggesting a more stable surface CTLA-4 protein requires both tyrosine

residues to be absent. Taken together, this data suggests CTLA-4 internalisation is regulated by the YVKM motif and is not dependent on lysine residues, the proline-based motif or the YFIP motif.

To confirm the findings identified by flow cytometry, CTLA-4 internalisation in the various mutants was measured by western blotting. Cell surface CTLA-4 was biotinylated at 4°C. Cells were then either kept on ice or warmed to 37°C for the indicated time-points and any remaining surface biotin was reduced. Cells were lysed and internalised CTLA-4 was concentrated by immunoprecipitating biotin using a neutravidin gel. Membranes were then probed for CTLA-4 using a C-19 C-terminus anti-CTLA-4 Ab. For WT CTLA-4 maximal internalisation was seen within 15minutes but after 30minutes this pool decreased over time. Comparable to WT CTLA-4, maximal protection of KLESS and ATEP was seen within 15minutes but the biotinylated pool appeared to be stable throughout the course of the experiment (**figure 4.7**). This data suggests any differences between the trafficking of WT, KLESS and ATEP CTLA-4 are related to their post-endocytic fate. AVKM CTLA-4 was used as a surface control considering the high surface vs. total ratio and impaired endocytosis (**figure 4.4**). However using western blotting it can be confirmed that a fraction of AVKM CTLA-4 internalises and the fate of the internalised pool is comparable to WT (**figure 4.8**).

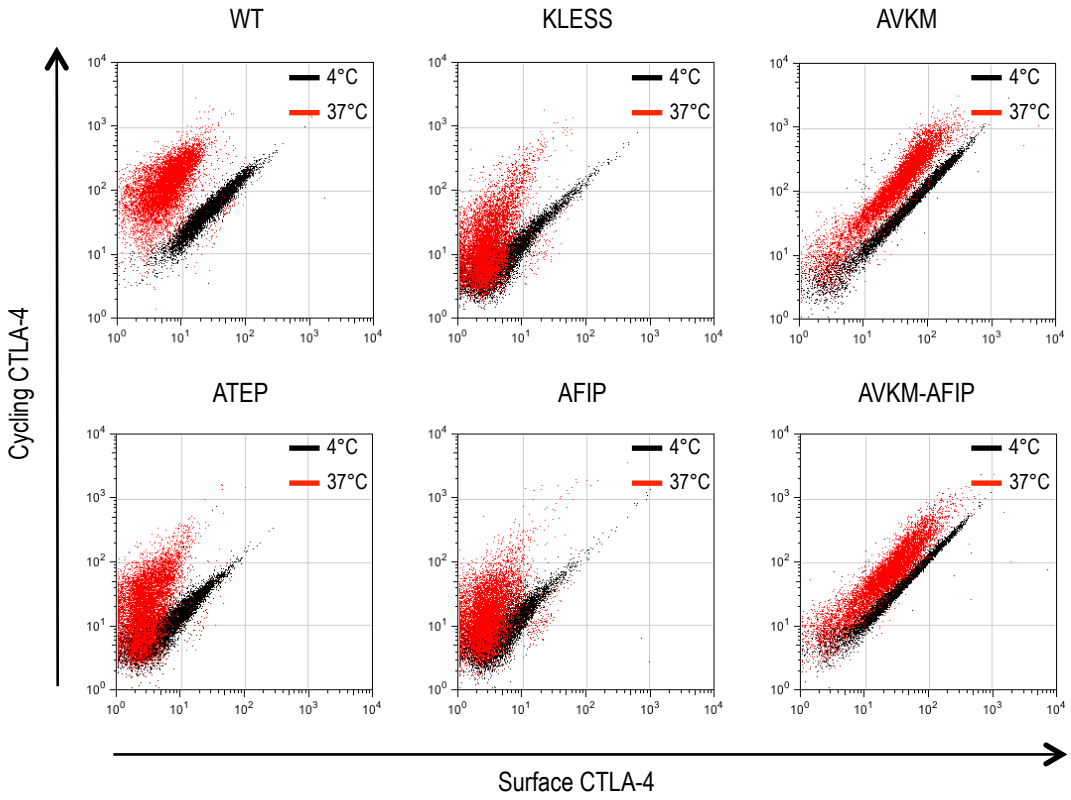

Figure 4.5 CTLA-4 mutants have different endocytic efficiencies. CHO cells expressing CTLA-4 mutants were labelled at 4°C with PE-conjugated anti-CTLA-4 Ab to label surface CTLA-4. Cells were then warmed to 37°C to allow endocytosis. Cells were placed on ice and any remaining surface CTLA-4 detected with Alexa647 anti-mouse secondary Ab. Representative FACs plot of one experiment showing remaining surface CTLA-4 after maximum 37°C incubation (red) compared to 4°C (black).

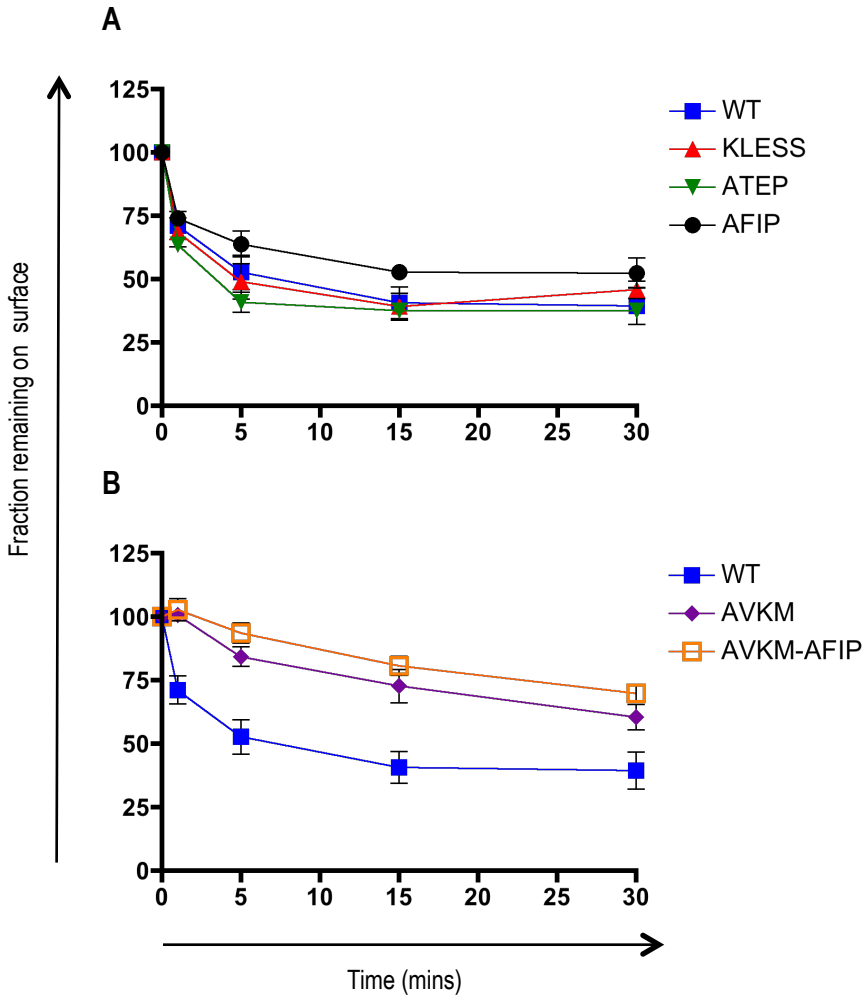

Figure 4.6 CTLA-4 mutants have different endocytic efficiencies. (A and **B)** CHO cells expressing CTLA-4 mutants were labelled at 4°C with PE-conjugated anti-CTLA-4 Ab to label surface CTLA-4. Cells were then warmed to 37°C to allow endocytosis. Cells were placed on ice and any remaining surface CTLA-4 detected with Alexa647 anti-mouse secondary Ab. The 647 signal was plotted against time as a fraction remaining compared to 4°C. Error bars show standard error (n≥3).

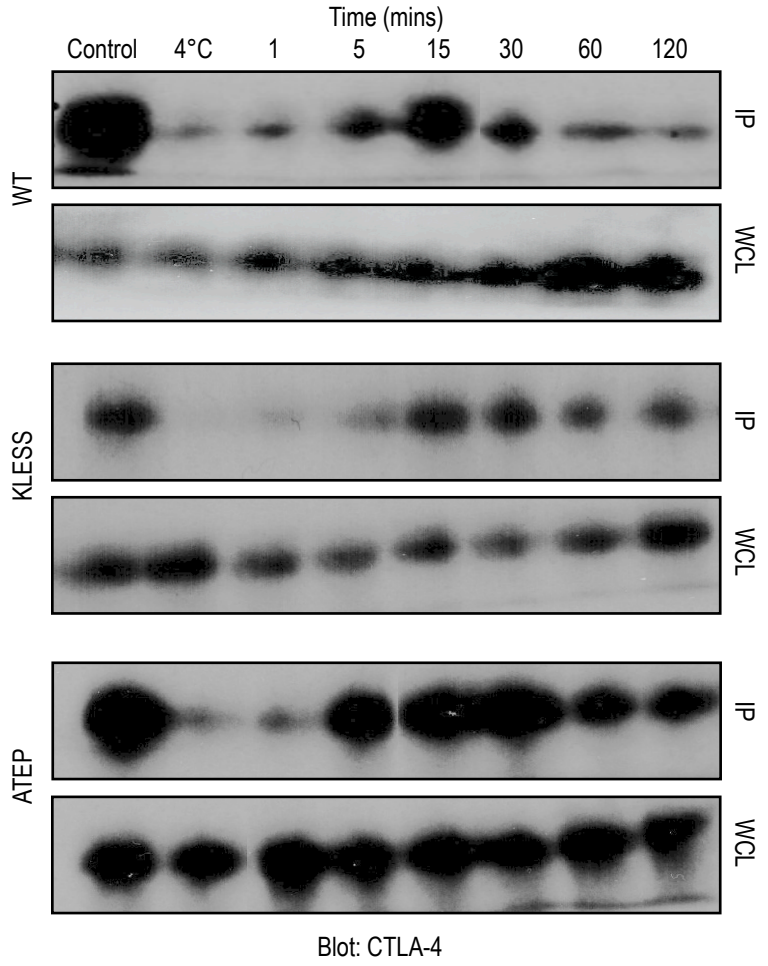

Figure 4.7 Western blotting reveals that KLESS and ATEP CTLA-4 mutants have a different post-endocytic fate to WT CTLA-4. Cell surface CTLA-4 was biotinylated at 4°C. Cells were then either kept on ice or warmed to 37°C for the indicated time-points and any remaining surface biotin was reduced. Cells were lysed and internalised CTLA-4 was concentrated by immunoprecipitating biotin using a neutravidin gel. Membranes were then probed for CTLA-4 using a C-19 C-terminus anti-CTLA-4 Ab. CTLA-4 has a molecular weight of ~ 30kDa. IP, immunoprecipitated CTLA-4 - bands represent CTLA-4 that was internalised and protected. WCL, whole cell lysate - bands represent total amount of CTLA-4 protein present in each condition. This is representative of 3 independent experiments.

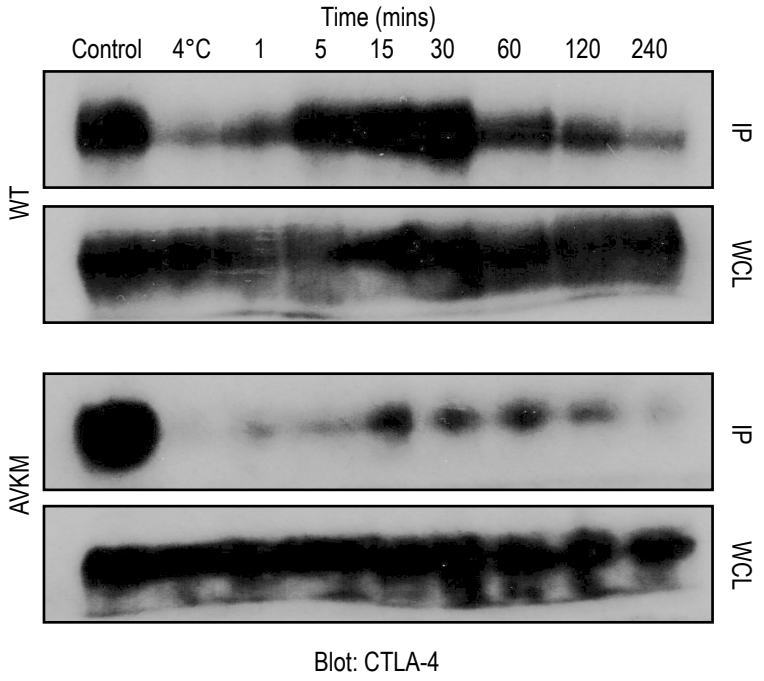

Figure 4.8 Western blotting reveals that AVKM CTLA-4 internalises. Cell surface CTLA-4 was biotinylated at 4°C. Cells were then either kept on ice or warmed to 37°C for the indicated time-points and any remaining surface biotin was reduced. Cells were lysed and internalised CTLA-4 was concentrated by immunoprecipitating biotin using a neutravidin gel. Membranes were then probed for CTLA-4 using a C-19 C-terminus anti-CTLA-4 Ab. CTLA-4 has a molecular weight of ~ 30kDa. IP, immunoprecipitated CTLA-4 - bands represent CTLA-4 that was internalised and protected. WCL, whole cell lysate - bands represent total amount of CTLA-4 protein present in each condition. This is representative of 3 independent experiments.

4.4 CTLA-4 recycling is regulated by lysine residues and a proline motif

We have previously shown that in order to maintain a steady state pool of CTLA-4, a fraction of the internalised receptor either recycles back to the surface or is targeted for degradation (Qureshi et al., 2012). To further address the role of the two tyrosine-based motifs, the lysine residues and the proline-based motif in CTLA-4 intracellular trafficking, CTLA-4 recycling was assayed using flow cytometry. Cells were incubated at 37°C with a PE-conjugated anti-CTLA-4 Ab for 30minutes to label the cycling pool of CTLA-4. Cells were then incubated further at 37°C for various times with an Alexa647 anti-mouse secondary Ab to label any of the primary Ab recycling back to the cell surface. Accordingly, recycling CTLA-4 is seen as an increase in the Alexa647 signal over time.

For WT, KLESS, ATEP and AFIP, after 30minute incubation at 37°C the control re-staining at 4°C revealed that only in a small percentage of cells does CTLA-4 protein remain at the surface to be detected by Alexa647 (**figure 4.9 red**). When cells were stained at 37°C with Alexa647, a greater pool of CTLA-4 for WT, KLESS, ATEP and AFIP was seen (**figure 4.9 black**). This suggests the Alexa647 signal could only have increased if the internalised PE-labelled CTLA-4 recycled back to the plasma membrane. Of note, there were differences in the efficiency of internalisation and recycling of the endocytic mutants as judged by the gradient of the red and black population of cells. KLESS and ATEP internalised and recycled more efficiently than WT and AFIP CTLA-4. In contrast, for AVKM and AVKM-AFIP the control re-staining at 4°C and staining at 37°C revealed a 1:1 relationship between the primary and secondary Ab suggestive of impaired endocytosis and recycling (**figure 4.9**).

To quantify this data, the 647 signal was plotted against time as the fraction recycled compared to 4°C. Using this assay, KLESS and ATEP CTLA-4 recycled more efficiently than WT and AFIP CTLA-4

(**figure 4.10A-D**). In contrast AVKM and AVKM-AFIP demonstrated little or no recycling (**figure 4.10E-F**). Taken together this data suggests that the YVKM motif, lysine residues and a proline motif regulate CTLA-4 recycling, where the absence of YVKM impairs CTLA-4 recycling whilst the absence of lysine residues and PTEP enhances CTLA-4 recycling.

4.5 CTLA-4 degradation is regulated by lysine residues and a proline motif

The increase in CTLA-4 recycling observed for KLESS and the ATEP mutant questions the role of lysine residues and the proline-based motif in regulating CTLA-4 degradation. To address the stability of the CTLA-4 point mutants, new protein synthesis was blocked using CHX to monitor the decay of existing CTLA-4. Moreover, if CTLA-4 was being degraded in lysosomes NH_4Cl or BafA should prevent degradation. After 3hour incubation at 37°C, cells were fixed and permeabilised prior to staining for total CTLA-4 expression and analysed by confocal microscopy. In the absence of new protein synthesis, whilst WT CTLA-4 levels decreased, KLESS and ATEP levels remained relatively constant (**figure 4.11**). Moreover, no accumulation of KLESS or ATEP was seen in the presence of NH_4Cl or BafA but a marked upregulation in the level of WT CTLA-4 was observed, again confirming lysosomes as the site of CTLA-4 degradation. These findings were verified using flow cytometry and a time course revealed that whereas KLESS and ATEP CTLA-4 were stable for up to 5hours, WT CTLA-4 had a half-life of around 2-3hours, in keeping with previous studies (**figure 4.13A-C** and **4.14A-C**). In contrast AVKM and AVKM-AFIP revealed subtle changes in protein expression in the presence of the inhibitors, typical of a surface protein (**figure 4.12, 4.13E-F** and **4.14E-F**). Interestingly, AVKM was less stable than AVKM-AFIP suggesting a more stable surface CTLA-4 protein requires both tyrosine residues to be absent. Collectively this data suggests that intracellular lysine residues and a proline motif regulate CTLA-4 degradation.

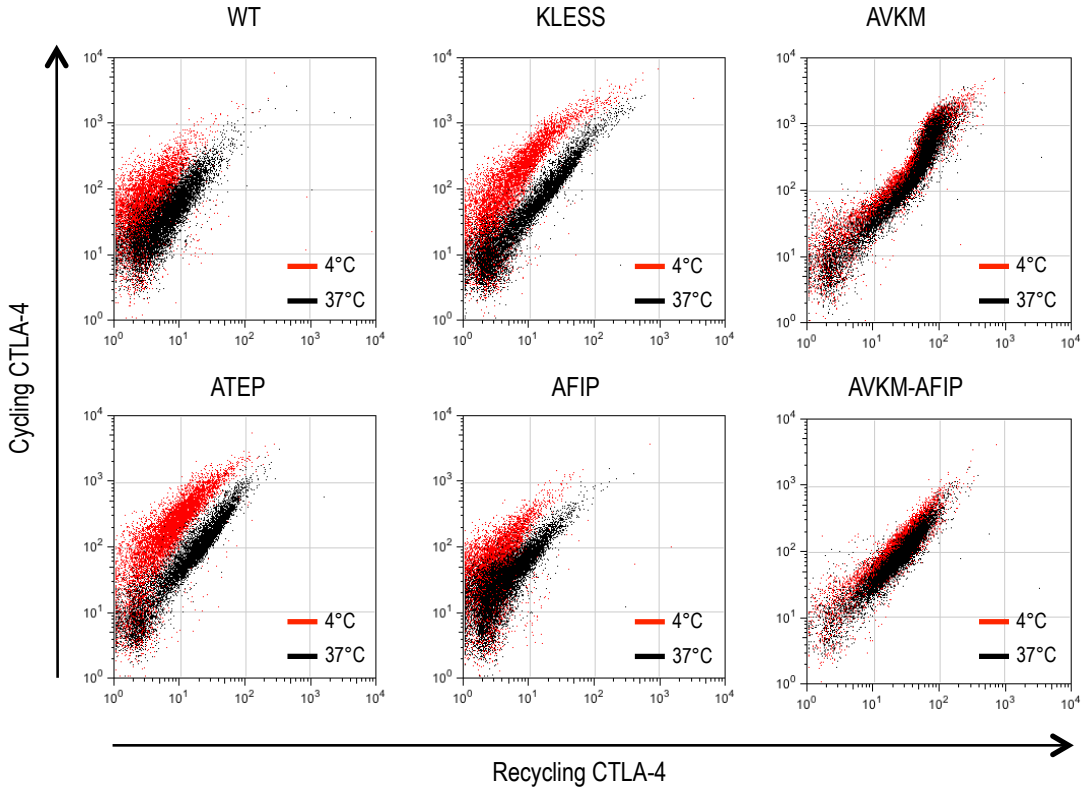

Figure 4.9 CTLA-4 mutants have different recycling efficiencies. CHO cells expressing CTLA-4 mutants were labelled with PE-conjugated anti-CTLA-4 Ab at 37°C to detect cycling CTLA-4, washed and any recycling primary Ab detected by addition of Alexa647 anti-mouse secondary Ab at either 4°C or 37°C. Representative FACS plots are shown for PE-label (cycling CTLA-4) vs Alexa647 label (recycling CTLA-4) of n≥3.

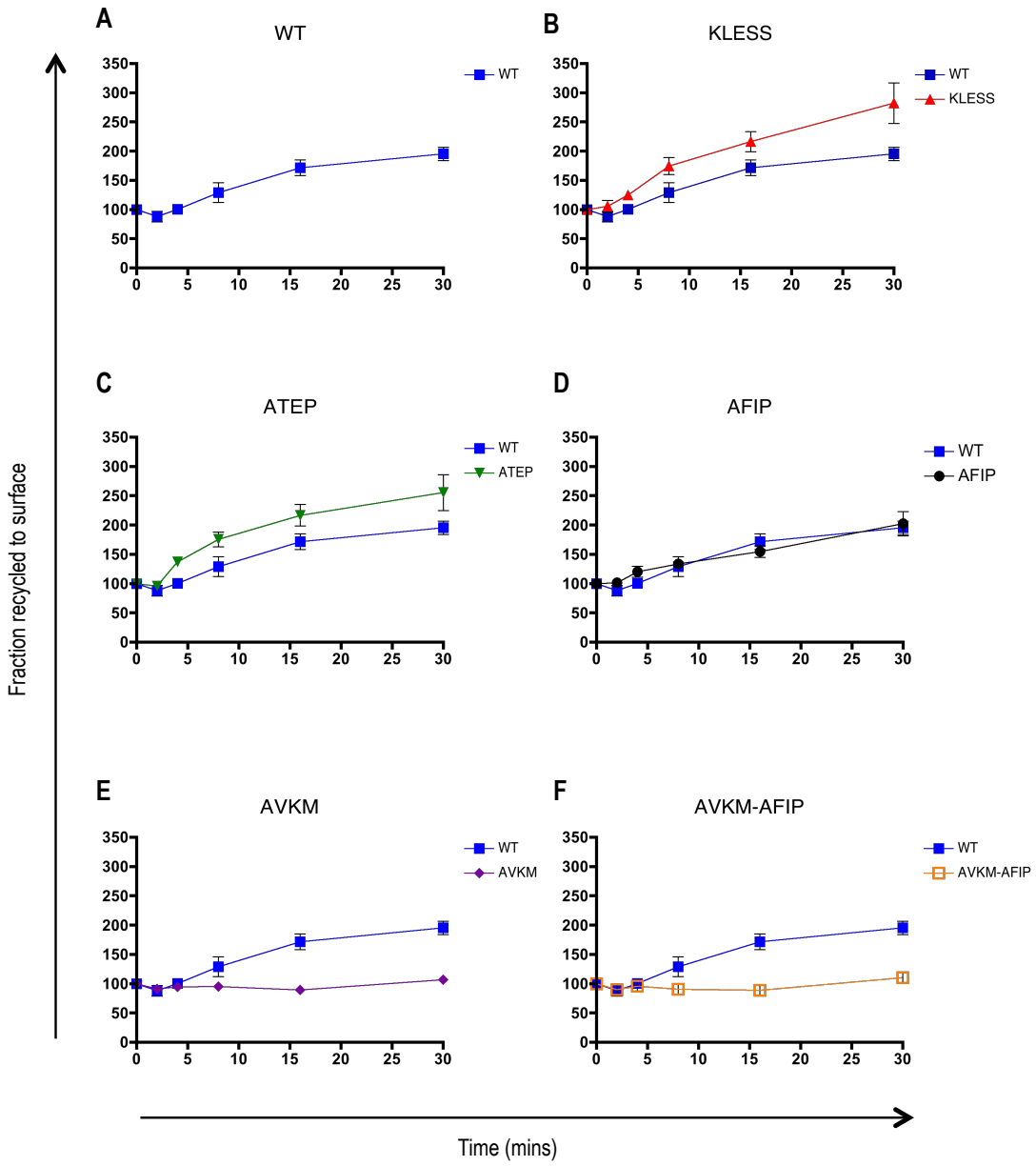

Figure 4.10 CTLA-4 mutants have different recycling efficiencies. CHO cells expressing CTLA-4 mutants were labelled with PE-conjugated anti-CTLA-4 Ab at 37°C to detect cycling CTLA-4, washed and any recycling primary Ab detected by addition of Alexa647 anti-mouse secondary Ab at either 4°C or 37°C. Recycling rates are plotted for CTLA-4 mutants as normalised to the 4°C control. Error bars show standard error (n≥3).

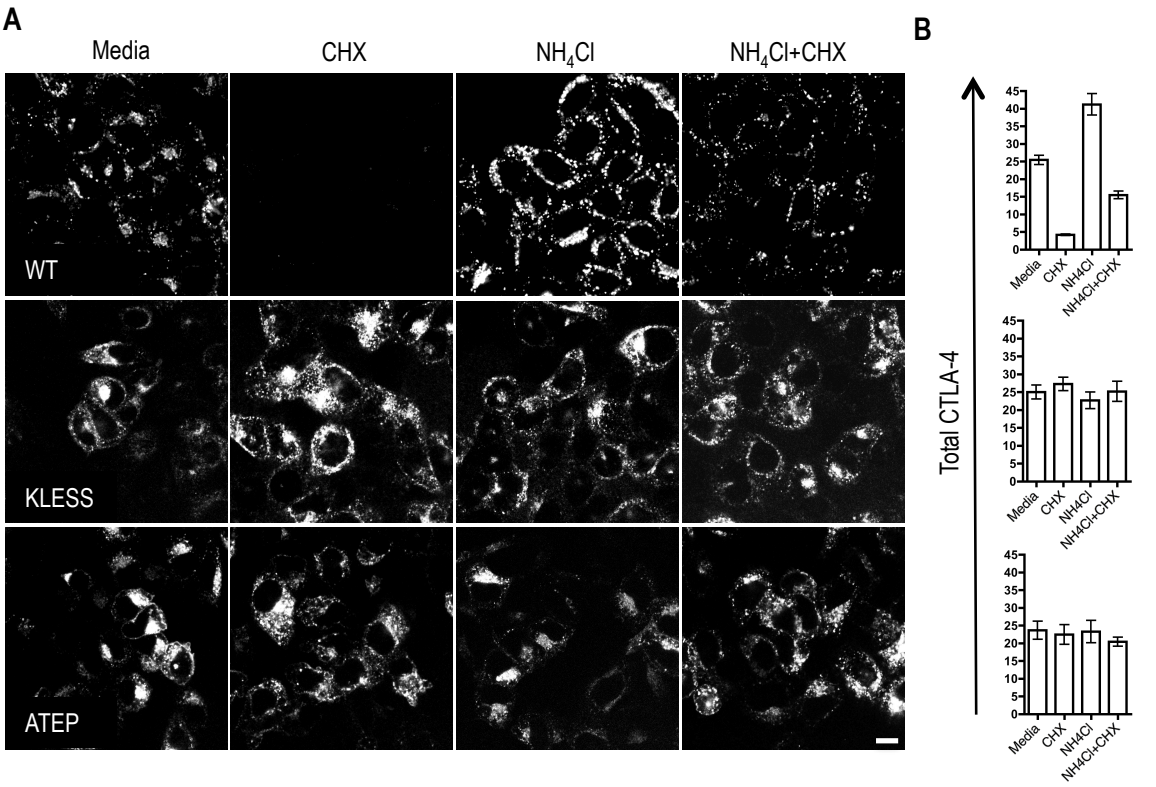

Figure 4.11 CTLA-4 mutants have different degradation efficiencies. (A) CHO cells expressing CTLA-4 mutants were incubated in medium or medium supplemented with CHX, NH_4Cl or NH_4Cl and CHX at 37°C for 3hours. Cells were stained for total CTLA-4 expression with an unlabelled anti-CTLA-4 Ab and Alexa488 anti-mouse secondary Ab and analysed by confocal microscopy. Bar indicates scale of 10μm. **(B)** Total CTLA-4 was quantified by outlining cells in ImageJ and MFI plotted**.** Error bars show standard error (n≥3).

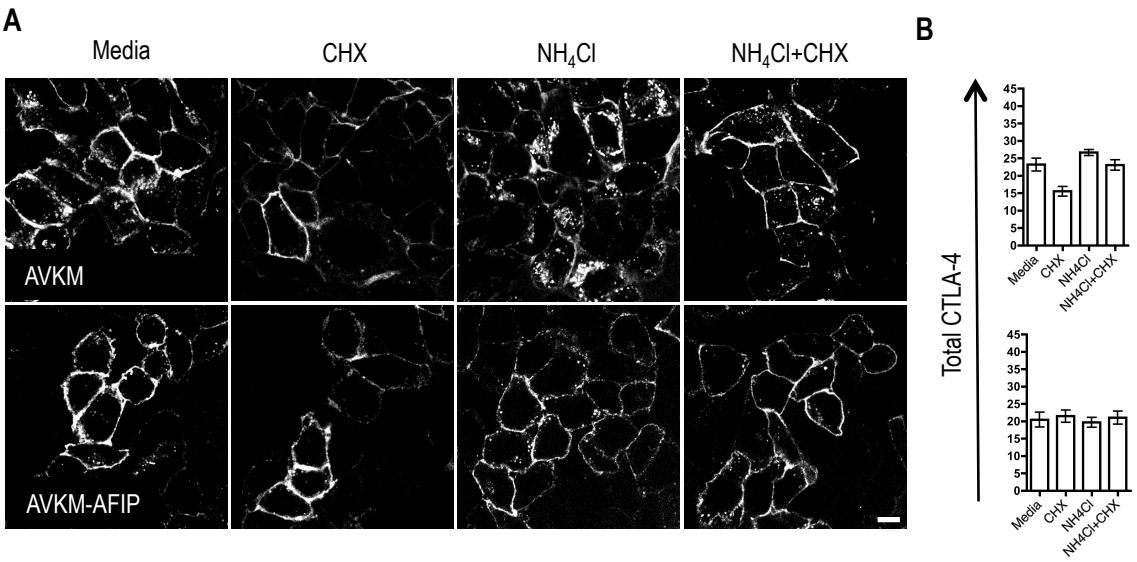

Figure 4.12 CTLA-4 mutants have different degradation efficiencies. (A) CHO cells expressing CTLA-4 mutants were incubated in medium or medium supplemented with CHX, NH_4Cl or NH_4Cl and CHX at 37°C for 3hours. Cells were stained for total CTLA-4 expression with an unlabelled anti-CTLA-4 Ab and Alexa488 anti-mouse secondary Ab and analysed by confocal microscopy. Bar indicates scale of 10µm. **(B)** Total CTLA-4 was quantified by outlining cells in ImageJ and MFI plotted**.** Error bars show standard error (n≥3).

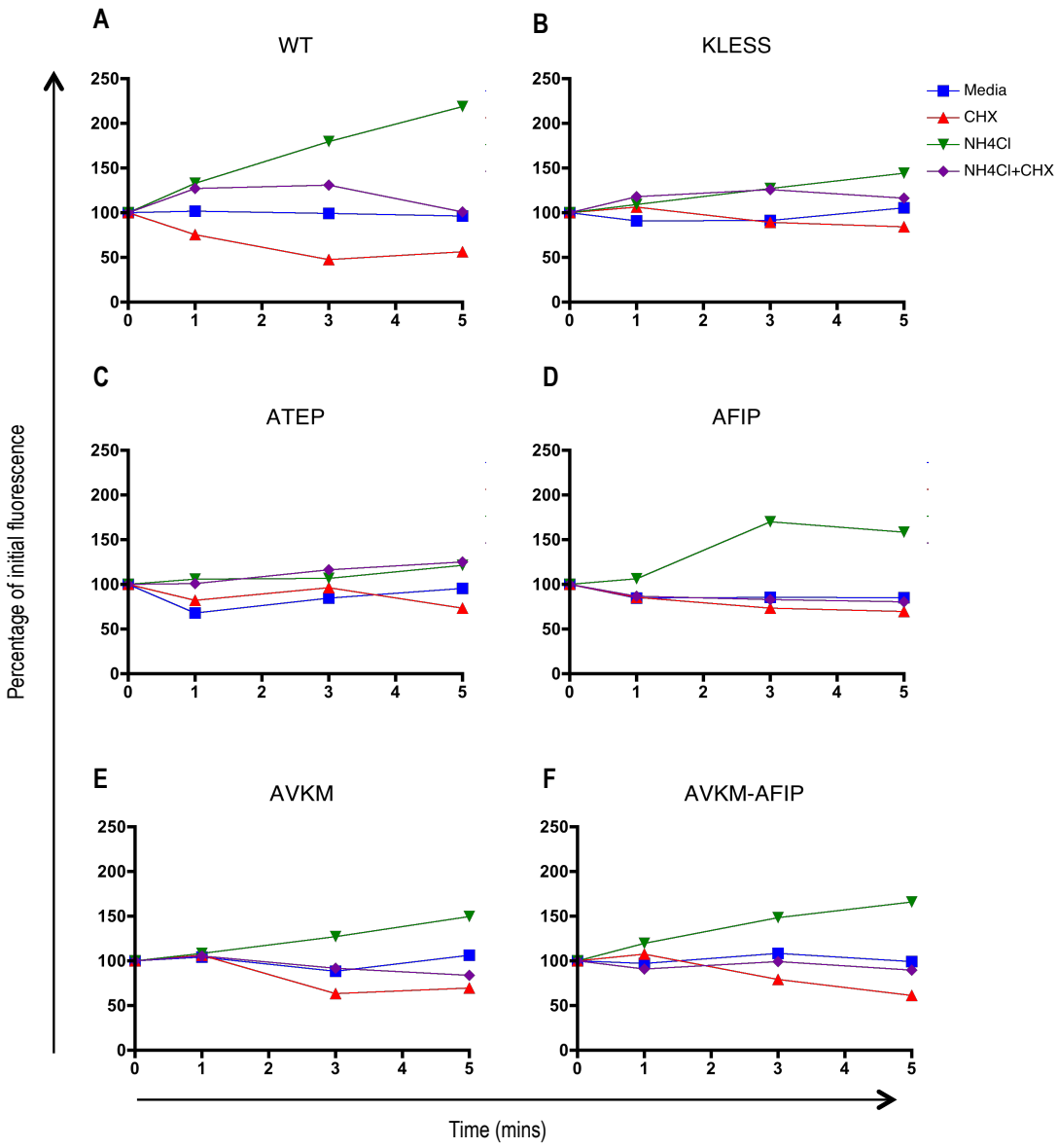

Figure 4.13 Flow cytometry verifies that the CTLA-4 mutants have different degradation efficiencies. CHO cells expressing CTLA-4 mutants were incubated in medium or medium supplemented with CHX, NH_4Cl or NH_4Cl and CHX at 37°C for 1-5hours. Cells were fixed, permeabilised and stained for total CTLA-4 with a PE-conjugated anti-CTLA-4 Ab. Cells were analysed by flow cytometry. The MFI is plotted as a percentage of initial fluorescence (n=1).

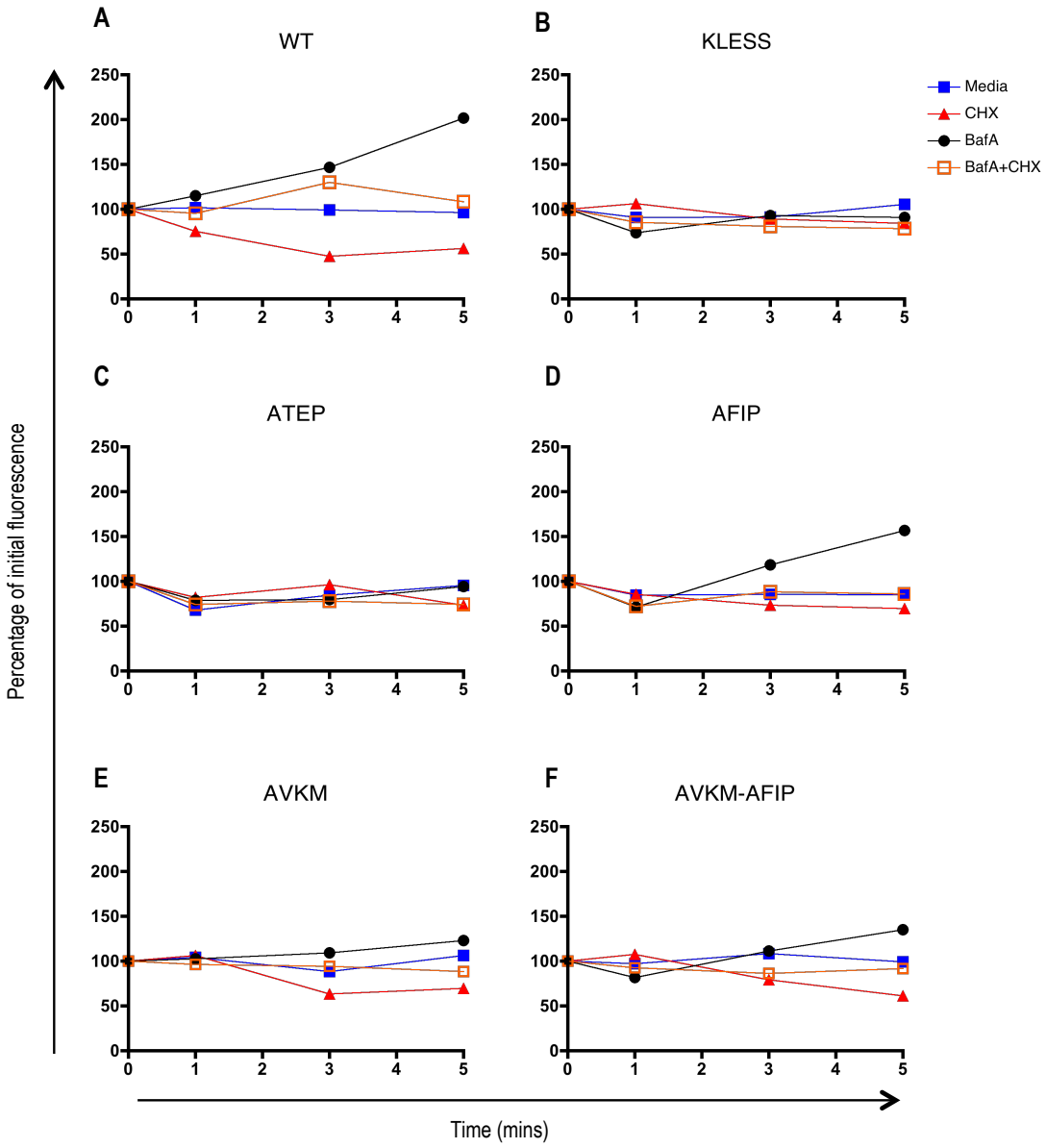

Figure 4.14 Flow cytometry verifies that the CTLA-4 mutants have different degradation efficiencies. CHO cells expressing CTLA-4 mutants were incubated in medium or medium supplemented with CHX, BafA or BafA and CHX at 37°C for 1-5hours. Cells were fixed, permeabilised and stained for total CTLA-4 with a PE-conjugated anti-CTLA-4 Ab. Cells were analysed by flow cytometry. The MFI is plotted as a percentage of initial fluorescence (n=1).

4.6 CTLA-4 ubiquitination is regulated by lysine residues and a proline motif

The increased recycling and stability of KLESS and ATEP CTLA-4 mutants suggests the protein is not being degraded. Receptors such as PAR2 and IFNAR1 have intracellular lysine residues that serve as targets for ubiquitin attachment and thus facilitate their degradation in lysosomes (Jacob et al., 2005; Kumar et al., 2007). Moreover, prior to entry into lysosomes proteins are sorted into MVBs, which requires the ESCRT machinery. Interestingly, the PTEP motif in CTLA-4 cytoplasmic domain could serve as a target site for TSG101 or other components of the ubiquitin conjugation cascade (Dilley et al., 2010).

To address the ubiquitination status of the CTLA-4 mutants, CHO cells transfected with the CTLA-4 mutants were stained for total CTLA-4 expression and analysed by flow cytometry. Cells with approximately equal levels of total protein were incubated in medium or medium supplemented with BafA for 3hours at 37°C. CTLA-4 was then immunoprecipitated using an antibody binding the extracellular region of CTLA-4 and membranes were probed for CTLA-4 with a C-19 C-terminus anti-CTLA-4 Ab and for ubiquitin with an anti-ubiquitin Ab. WT CTLA-4 was accumulated in the presence of BafA, which further revealed ubiquitinated species with molecular masses of ~ 46-58kDa (**figure 4.15**). In contrast, no accumulation of KLESS and ATEP CTLA-4 was observed in the presence of BafA and the two CTLA-4 mutants were not ubiquitinated. AVKM CTLA-4 mutant was accumulated in the presence of BafA, however no ubiquitinated species were detected. This could be explained by the fact that since only a fraction of the protein undergoes internalisation and is targeted for degradation, the ubiquitin signal could be too low for detection. The CTLA-4 signal for the AVKM-AFIP mutant was low most probably due to changes in the site recognised by the C-19 C-terminus anti-CTLA-4 Ab in the cytoplasmic domain. Taken together this data suggests lysine residues and the proline-based motif play a role in the ubiquitination of the CTLA-4 receptor.

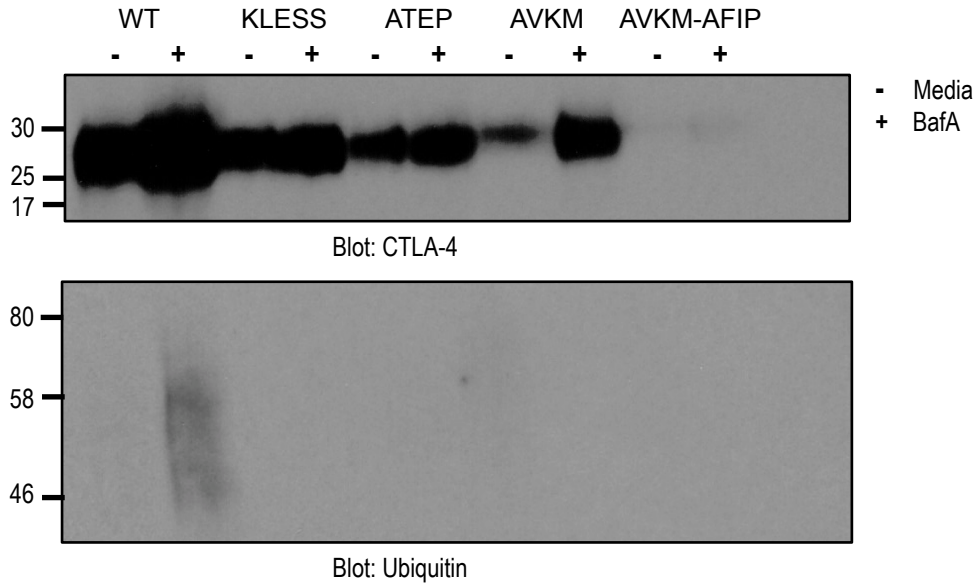

Figure 4.15 CTLA-4 mutants are not ubiquitinated. CHO cells transfected with CTLA-4 mutants were incubated in medium or medium supplemented with BafA at 37°C for 3hours. CTLA-4 was then immunoprecipitated using an Ab binding to the extracellular region of CTLA-4. Expression of CTLA-4 was analysed by western blotting using a C-19 C-terminal anti-CTLA-4 Ab and an anti-ubiquitin Ab. Representative data of one independent experiment of n≥3.

4.7 Inhibition of CTLA-4 ubiquitination affects recycling and degradation

The increased recycling of KLESS and ATEP CTLA-4 mutants suggested that this increase could be due to the lack of receptor ubiquitination, which allows the receptor to escape degradation. To address the effect of inhibiting ubiquitination on CTLA-4 intracellular trafficking, CHO cells transfected with WT and KLESS CTLA-4 were incubated in the presence of MG132 at 37°C, a chemical that depletes free ubiquitin (Melikova et al., 2006). Cells were then stained for surface, cycling and total CTLA-4 with a PE-conjugated anti-CTLA-4 Ab and analysed by flow cytometry. All three pools were increased in WT CTLA-4 following MG132 treatment, which is in keeping with the lack of degradation (**figure 4.16**). However, this effect was not seen for KLESS CTLA-4 consistent with the absence of ubiquitin. To address whether the increase in CTLA-4 protein results in an increase in recycling, cells were pre-incubated with MG132 or UBEI-41, an inhibitor of the E1 enzyme, for 2hours prior to performing the recycling assay described in section 4.4. To quantify any differences in recycling, the fraction of recycled protein was expressed as a percentage of labelled protein. WT CTLA-4 recycled more efficiently after both MG132 and UBEI-41 treatment when compared to the media control (**figure 4.17A** and **C**). Again, this effect was not observed for KLESS CTLA-4 (**figure 4.17B** and **D).** Taken together this data confirms a role for lysine residues and ubiquitin in regulating CTLA-4 recycling and degradation.

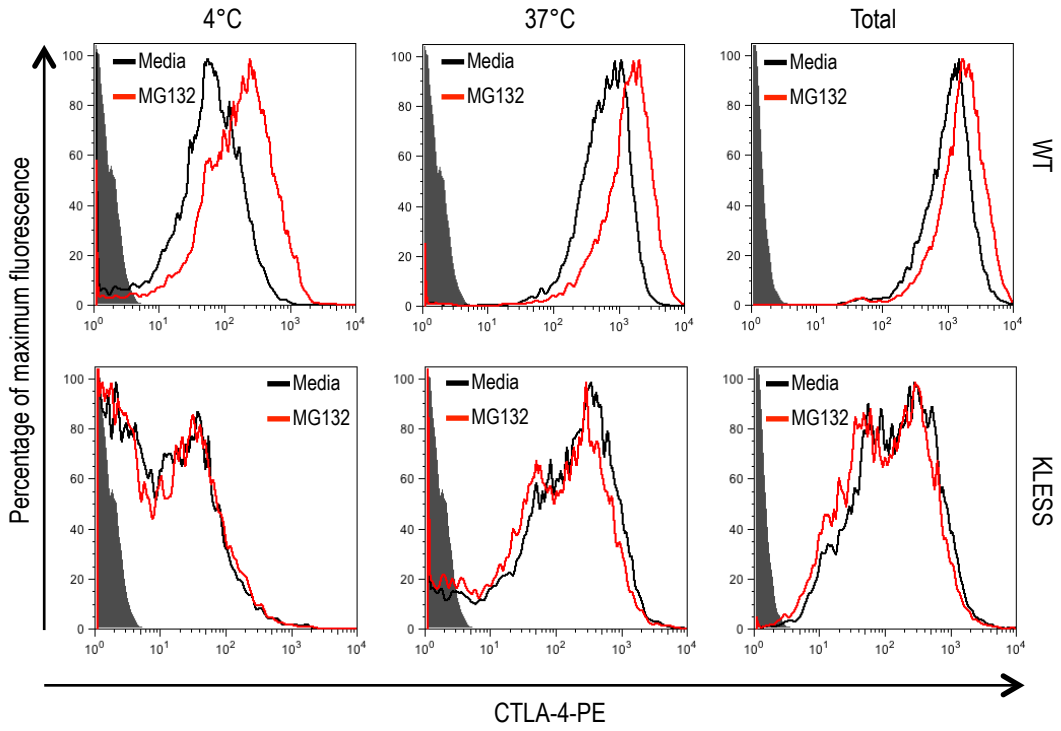

Figure 4.16 Effect of MG132 on WT and KLESS CTLA-4 localisation. CHO cells transfected with WT and KLESS CTLA-4 were incubated with medium or medium supplemented with MG132 for 2hours at 37°C. Cells were then stained for surface, cycling or total CTLA-4 expression and analysed by flow cytometry. Representative FACs plots of one independent experiment of n=3.

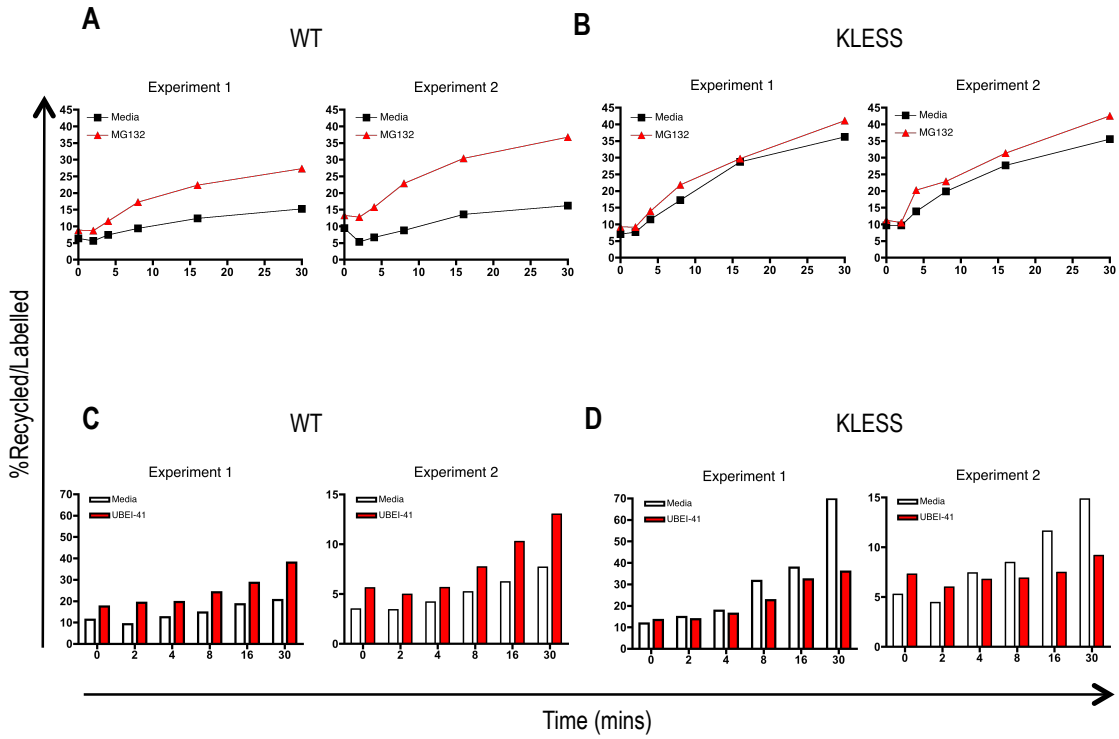

Figure 4.17 MG132 and UBEI-41 have different effects on WT and KLESS CTLA-4 recycling. CHO cells transfected with WT or KLESS CTLA-4 were incubated with medium or medium supplemented with MG132 **(A** and **B)** or UBEI-41 **(C** and **D)** for 2hours at 37°C. Cells were then labelled with PE-conjugated anti-CTLA-4 Ab at 37°C to detect cycling CTLA-4, washed and any recycling CTLA-4-PE antibody detected by addition of Alexa647 anti-mouse secondary Ab at either 4°C or 37°C. The fraction of recycled protein was expressed as a percentage of labelled protein. Data shown from two independent experiments.

4.8 All lysine residues influence CTLA-4 recycling and degradation

Throughout this chapter it is clear that lysine residues regulate CTLA-4 recycling and degradation. However in the case of some receptors such as EGFR and INFAR-1 not all the lysine residues are targets of ubiquitination (Huang et al., 2006; Kumar et al., 2007). In order to address which lysine residues are important for CTLA-4 degradation, single lysine point mutants were generated using site-directed mutagenesis and transfected into CHO cells (**figure 4.18A**). CTLA-4 single lysine point mutants were then characterised to determine their role in the intracellular trafficking of the receptor.

To assess localisation, CHO cells expressing the various CTLA-4 mutants cells were stained for total CTLA-4 expression using an antibody to the human CTLA-4 ectodomain and analysed by confocal microscopy. The data showed that the CTLA-4 single lysine point mutants were predominantly located in intracellular vesicles (**figure 4.18B**). The difference in the amount of surface CTLA-4 relative to cycling CTLA-4 was also quantified by flow cytometry and is shown in **figure 4.19**, further verifying the predominant intracellular localisation of the lysine mutants. To assay internalisation, cells were incubated at 4°C with PE-conjugated anti-CTLA-4 Ab for 30minutes to label the surface pool. Cells were then incubated at 37°C for the indicated time points and remaining surface CTLA-4 was then labelled with Alexa647 anti-mouse secondary Ab. Again this revealed no difference between the internalisation rate of WT CTLA-4, KLESS and the single lysine point mutants (**figure 4.20A**). Taken together this data suggests that the lysine residues do not regulate CTLA-4 localisation and internalisation.

To address which lysine residues are important for regulating CTLA-4 recycling, cells were incubated at 37°C with PE-conjugated anti-CTLA-4 Ab for 30minutes to label the cycling pool. Cells were then either kept on ice or incubated at 37°C for various time points with Alexa647 anti-mouse secondary Ab to label

any of the primary Ab recycling back to the surface. To quantify any differences in recycling, the fraction of recycled protein was expressed as a percentage of labelled protein. An increase in labelled protein that recycled back to the surface was seen for the various CTLA-4 mutants. However, KLESS CTLA-4 recycled more efficiently than any other single lysine point mutant whilst K191R and K192R recycled as efficiently as WT CTLA-4. Importantly a mutation of either one of the two distal lysine residues, K203R or K213R, showed a recycling efficiency that was greater than WT but did not reach the potential of KLESS (**figure 4.20B**). This suggests that both distal lysine residues in the CTLA-4 cytoplasmic domain could regulate the recycling of the CTLA-4 receptor.

To address whether both K203 and K213 residues regulate CTLA-4 recycling, a mutant was generated lacking both of these lysine residues, K203,213R. Again, this mutant was located in intracellular vesicles, internalised as efficiently as WT but the mutant does not recycle as efficiently as KLESS (**figure 4.21**). Collectively, this data therefore suggests all of the lysine residues in the CTLA-4 cytoplasmic domain could regulate recycling.

A

```
                190        200        210     220
WT          SKMLKKRSPLTTGVYVKMPPTEPECEKQFQPYFIPIN
KLESS       SRMLRRRSPLTTGVYVRMPPTEPECERQFQPYFIPIN
K191R       SKMLRKRSPLTTGVYVKMPPTEPECEKQFQPYFIPIN
K192R       SKMLKRRSPLTTGVYVKMPPTEPECEKQFQPYFIPIN
K203R       SKMLKKRSPLTTGVYVRMPPTEPECEKQFQPYFIPIN
K213R       SKMLKKRSPLTTGVYVKMPPTEPECERQFQPYFIPIN
K203,213R   SKMLKKRSPLTTGVYVRMPPTEPECERQFQPYFIPIN
```

B

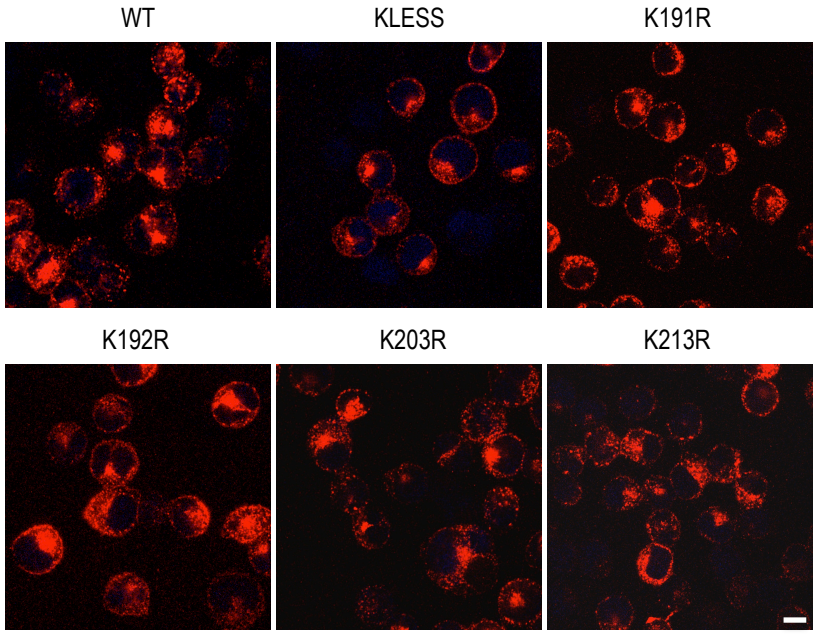

Figure 4.18 Generation and localisation of CTLA-4 single lysine point mutants. (A) C-terminal sequence alignments of human CTLA-4. Lysine residues mutated to arginine are shown in blue. **(B)** CHO cells expressing CTLA-4 lysine mutants were fixed and permeabilised prior to staining for total CTLA-4 expression with an unlabelled anti-CTLA-4 Ab and Alexa555 anti-mouse secondary Ab and analysed by confocal microscopy (n≥ 3). Bar indicates scale of 10μm.

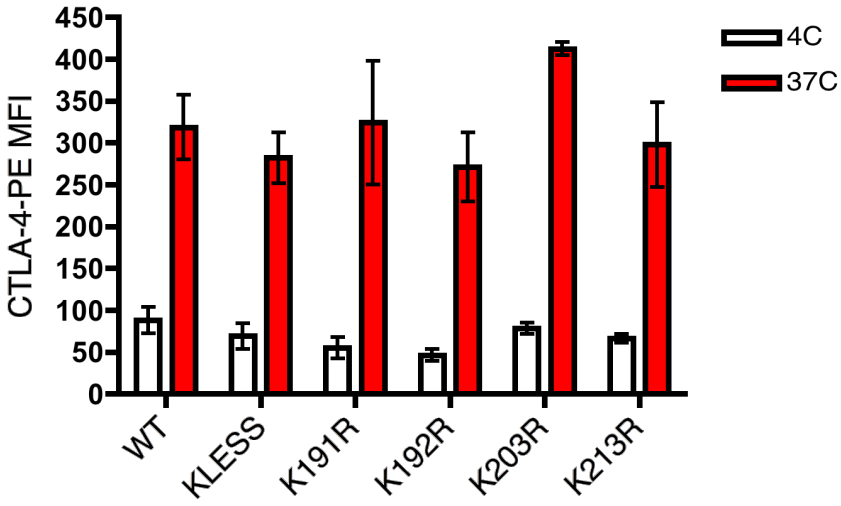

Figure 4.19 Phenotype of CTLA-4 lysine mutants. CHO cells expressing CTLA-4 mutants were stained for surface CTLA-4 expression at 4°C or were fixed and permeabilised prior to staining for total CTLA-4 expression with PE-conjugated anti-CTLA-4 Ab. Cells were analysed by flow cytometry. Error bars show standard error (n>3).

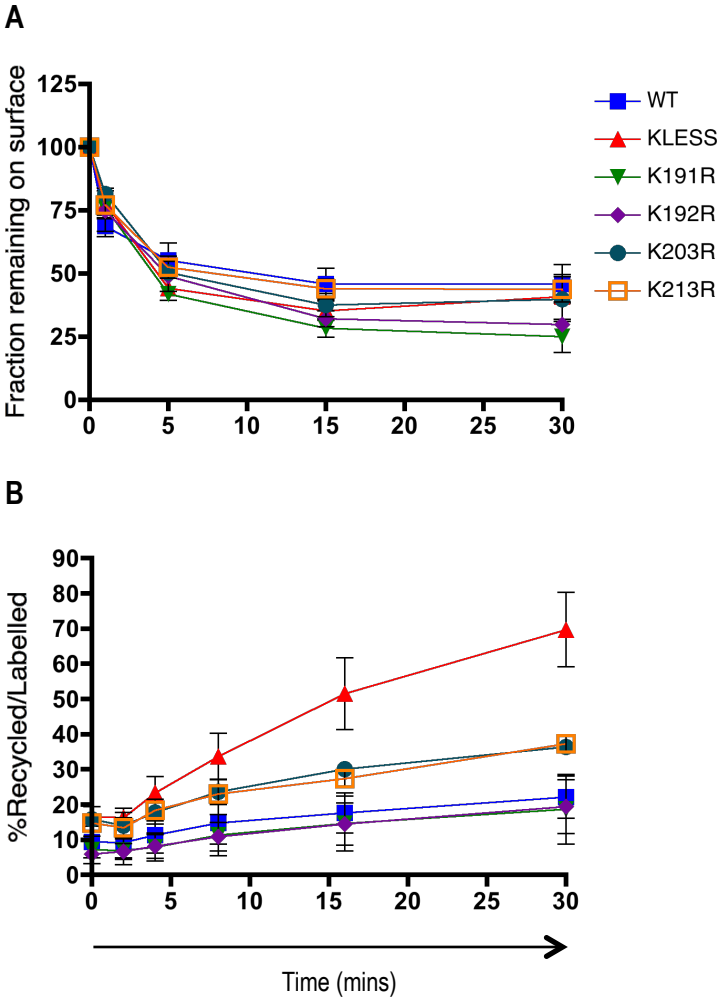

Figure 4.20 CTLA-4 lysine mutants have a comparable internalisation rate to WT but have different recycling efficiencies. (A) CHO cells expressing CTLA-4 lysine mutants were labelled at 4°C with PE-conjugated anti-CTLA-4 Ab. Cells were then warmed to 37°C to allow endocytosis for the times indicated. Cells were then placed on ice and any remaining surface CTLA-4 detected with Alexa647 anti-mouse secondary Ab. The 647 signal was plotted against time as a fraction remaining compared to 4°C. Error bars show standard error (n≥3). **(B)** CHO cells expressing CTLA-4 lysine mutants were labelled with PE-conjugated anti-CTLA-4 Ab at 37°C to detect cycling CTLA-4, washed and any recycling primary Ab detected by addition of Alexa647 anti-mouse secondary Ab at either 4°C or 37°C. The fraction of recycled protein was expressed as a percentage of labelled protein. Error bars show standard error (n≥3).

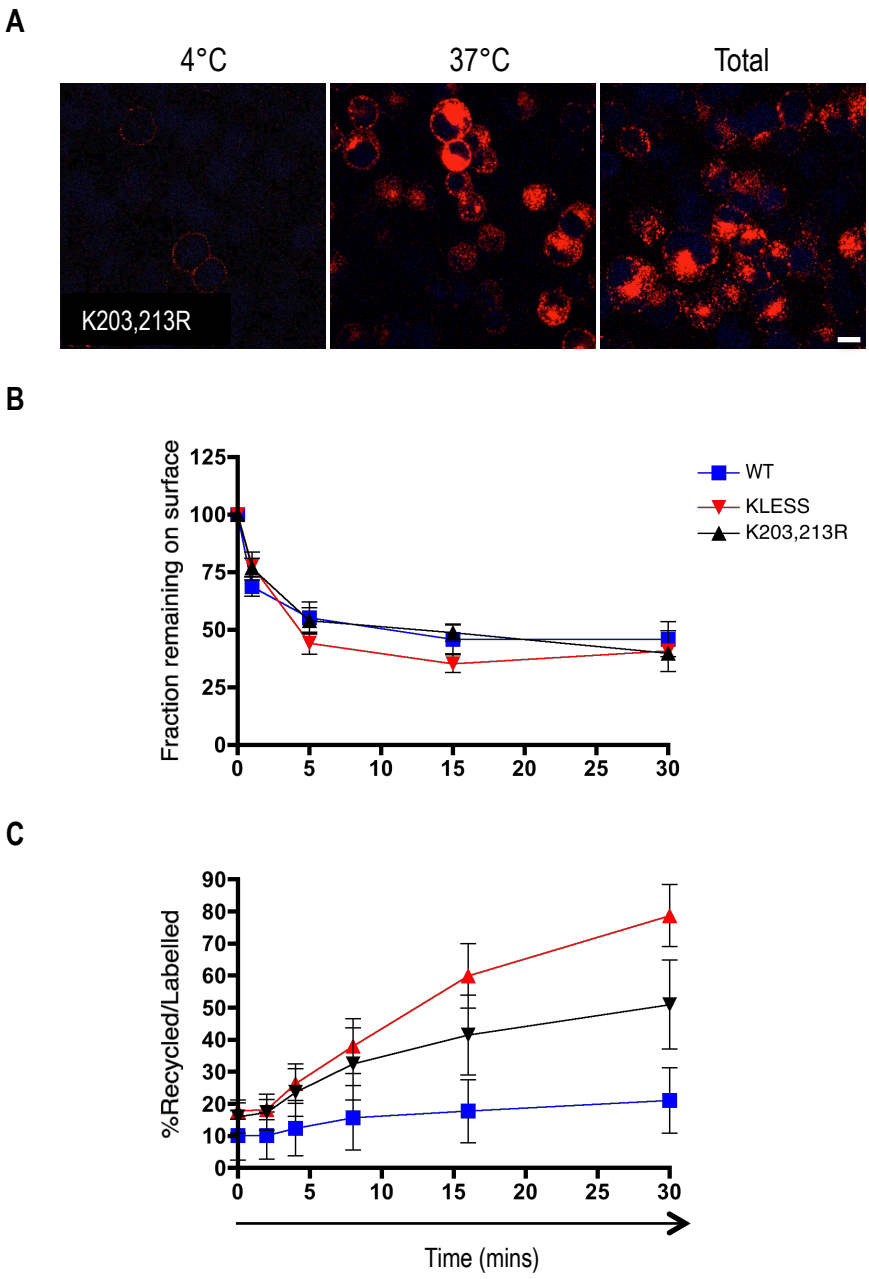

Figure 4.21 K203,213R does not recycle as efficiently as KLESS CTLA-4. (A) CHO cells expressing K203,213R were stained for surface CTLA-4 expression at 4°C; endocytosed CTLA-4 expression at 37°C; or were fixed and permeabilised prior to staining for total CTLA-4 expression with an unlabelled anti-CTLA-4 Ab and Alexa555 anti-mouse secondary Ab and analysed by confocal microscopy (n≥3). Bar indicates scale of 10µm. **(B)** CHO cells expressing WT, KLESS and K203,213R CTLA-4 were labelled at 4°C with PE-conjugated anti-CTLA-4 Ab. Cells were then warmed to 37°C to allow endocytosis for the times indicated. Cells were then placed on ice and any remaining surface CTLA-4 detected with Alexa647 anti-mouse secondary Ab. The 647 signal was plotted against time as a fraction remaining compared to 4°C (n≥3). **(C)** CHO cells expressing WT, KLESS and K203,213R CTLA-4 were labelled with PE-conjugated anti-CTLA-4 Ab at 37°C to detect cycling CTLA-4, washed and any recycling primary Ab detected by addition of Alexa647 anti-mouse secondary Ab at either 4°C or 37°C. The fraction of recycled protein was expressed as a percentage of labelled protein. Error bars show standard error (n≥3).

To address which lysine residues are important for regulating CTLA-4 degradation, CHO cells expressing the lysine mutants were incubated in CHX or NH_4Cl for 3hours at 37°C. Cells were then stained for total CTLA-4 expression and analysed by confocal microscopy or flow cytometry. All single lysine point mutants showed a pattern comparable to WT CTLA-4 with a rapid loss of protein demonstrated in the absence of new protein synthesis and accumulation of protein observed in the presence of NH_4Cl (**figure 4.22-4.24**). K203,213R was much less sensitive to CHX treatment although compared to KLESS CTLA-4 some degradation was still evident (**figure 4.24B** vs **4.24G**). Taken together this data suggests that all lysine residues need to be absent in order for CTLA-4 to escape degradation.

To address the ubiquitination status of CTLA-4 when one or more lysine residues are mutated, CHO cells transfected with the CTLA-4 lysine mutants were stained for total CTLA-4 expression and analysed by flow cytometry. Cells with approximately equal levels of total protein were incubated in medium or medium supplemented with BafA for 3hours at 37°C. CTLA-4 was then immunoprecipitated using an antibody binding the extracellular region of CTLA-4 and membranes were probed for CTLA-4 with a C-19 C-terminus antibody and for ubiquitin with an anti-ubiquitin Ab. The single and double lysine point mutants showed a comparable pattern to WT CTLA-4 where protein was accumulated in the presence of BafA, which further revealed ubiquitinated species with molecular masses of ~ 46-58kDa (**figure 4.25** and **4.26**). This is in contrast to KLESS CTLA-4 where no protein accumulation or ubiquitinated species were detected after BafA incubation. Taken together, this data suggests that all lysine residues in the CTLA-4 cytoplasmic domain serve as targets for ubiquitination.

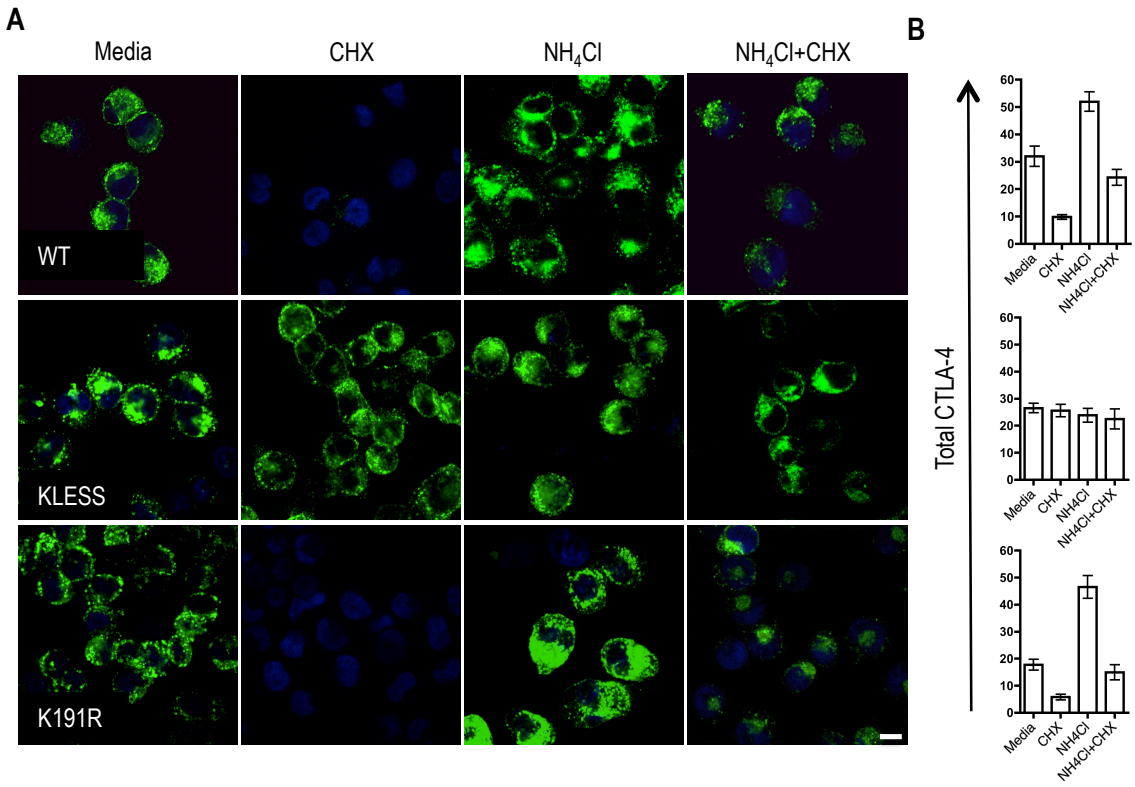

Figure 4.22 CTLA-4 lysine mutants have different degradation efficiencies. (A) CHO cells expressing CTLA-4 lysine mutants were incubated in medium or medium supplemented with CHX, NH_4Cl or NH_4C l and CHX at 37°C for 3hours. Cells were stained for total CTLA-4 expression with an unlabelled anti-CTLA-4 Ab and Alexa488 anti-mouse secondary Ab and analysed by confocal microscopy. Bar indicates scale of 10µm. **(B)** Total CTLA-4 was quantified by outlining cells in ImageJ and MFI plotted**.** Error bars show standard error (n≥3).

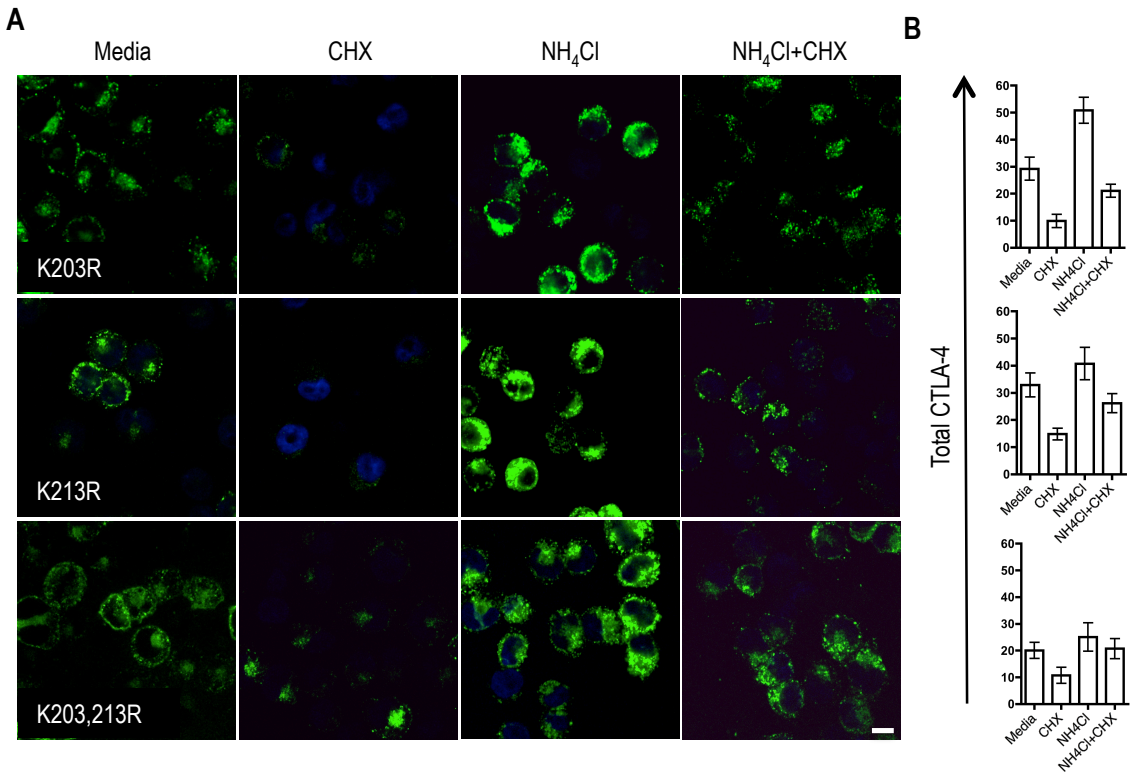

Figure 4.23 CTLA-4 lysine mutants have different degradation efficiencies. (A) CHO cells expressing CTLA-4 lysine mutants were incubated in medium or medium supplemented with CHX, NH_4Cl or NH_4Cl and CHX at 37°C for 3hours. Cells were stained for total CTLA-4 expression with an unlabelled anti-CTLA-4 Ab and Alexa488 anti-mouse secondary Ab and analysed by confocal microscopy. Bar indicates scale of 10μm. **(B)** Total CTLA-4 was quantified by outlining cells in ImageJ and MFI plotted**.** Error bars show standard error (n≥3).

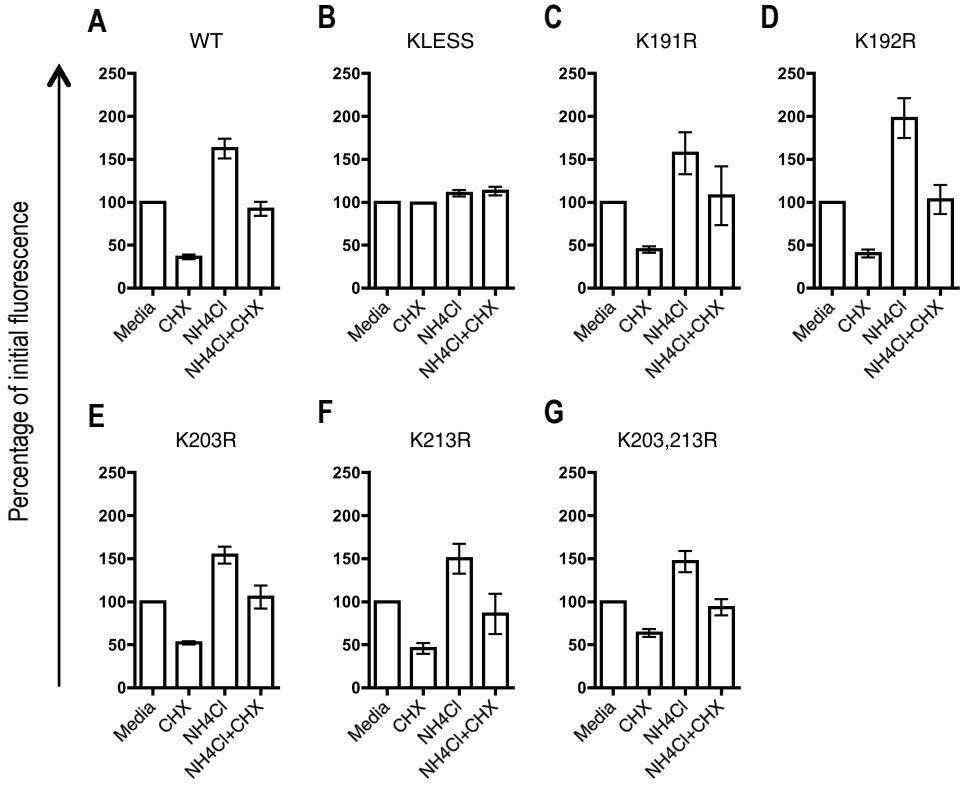

Figure 4.24 Flow cytometry verifies that CTLA-4 lysine mutants have different degradation efficiencies. CHO cells expressing CTLA-4 lysine mutants were incubated in medium or medium supplemented with CHX, NH_4Cl or NH_4Cl and CHX at 37°C for 3hours. Cells were stained for total CTLA-4 expression with a PE-conjugated anti-CTLA-4 Ab and analysed by flow cytometry. The MFI is plotted as a percentage of initial fluorescence. Error bars show standard error (n≥3).

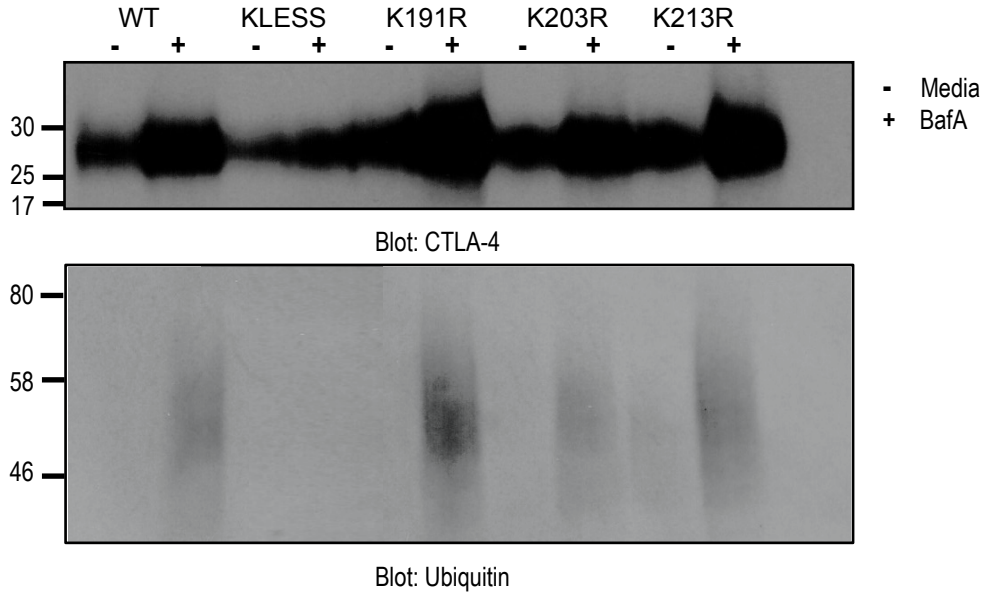

Figure 4.25 CTLA-4 single lysine point mutants are not ubiquitinated. CHO cells transfected with CTLA-4 mutants were incubated in medium or medium supplemented with BafA at 37°C for 3hours. Expression of CTLA-4 was analysed by western blotting using a C-19 C-terminal anti-CTLA-4 Ab and an anti-ubiquitin Ab. Representative data of one independent experiment of n≥3

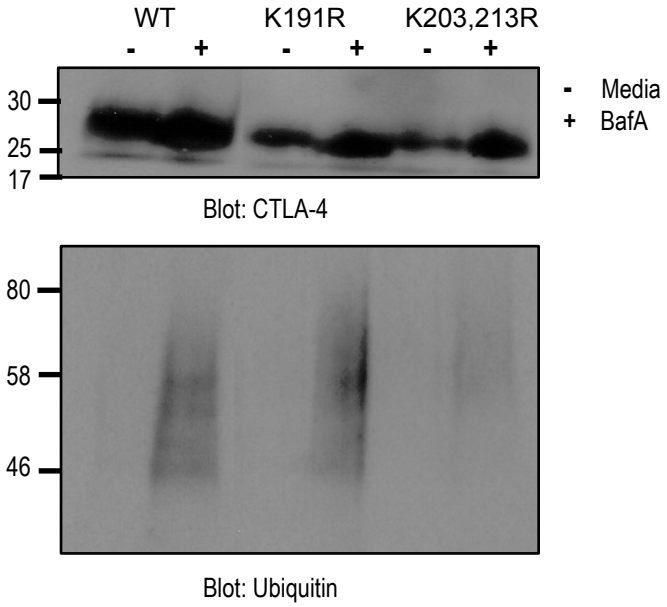

Figure 4.26 CTLA-4 single or double lysine mutants are not ubiquitinated. CHO cells transfected with CTLA-4 mutants were incubated in medium or medium supplemented with BafA at 37°C for 3hours. Expression of CTLA-4 was analysed by western blotting using a C-19 C-terminal anti-CTLA-4 Ab and an anti-ubiquitin Ab. Representative data of one independent experiment of n≥3

4.9 CTLA-4 mutants can transendocytose ligand

Central to the biology of the CTLA-4 receptor is how the receptor functions. Chapter 3 demonstrated that CTLA-4 can transendocytose CD80 or CD86 and then targets the ligand for degradation in lysosomes. Despite CTLA-4 encoding the YVKM motif in the cytoplasmic domain that is important for internalisation, just like CTLA-4 recycling and degradation, the sorting motifs required for transendocytosis are yet unclear. To address the requirements for CTLA-4 transendocytosis CHO cells expressing CTLA-4 mutants were co-cultured with CHO cells stably expressing either CD80 or CD86, fused to GFP, for 3hours at 37°C in medium alone or medium supplemented with NH_4Cl. CD80 or CD86-GFP cells were labelled with CellTrace Violet and accordingly GFP transfer could be quantified by gating CTLA-4 expressing cells that were negative for Violet dye staining. Using flow cytometry, the CTLA-4 mutants demonstrated the ability to capture CD80 or CD86 but the efficiency was lower than WT (**figure 4.27**). Moreover, the capture of CD80 was far greater than CD86. Surprisingly, the CTLA-4 mutant receptors that escaped degradation (KLESS, ATEP and AVKM-AFIP) possessed the ability to target the ligand for lysosomal degradation as revealed by NH_4Cl. Taken together this data suggests the mechanism required for CTLA-4 transendocytosis differs from the mechanism of conventional endocytosis, which is exclusively dependent on a tyrosine-based hydrophobic motif.

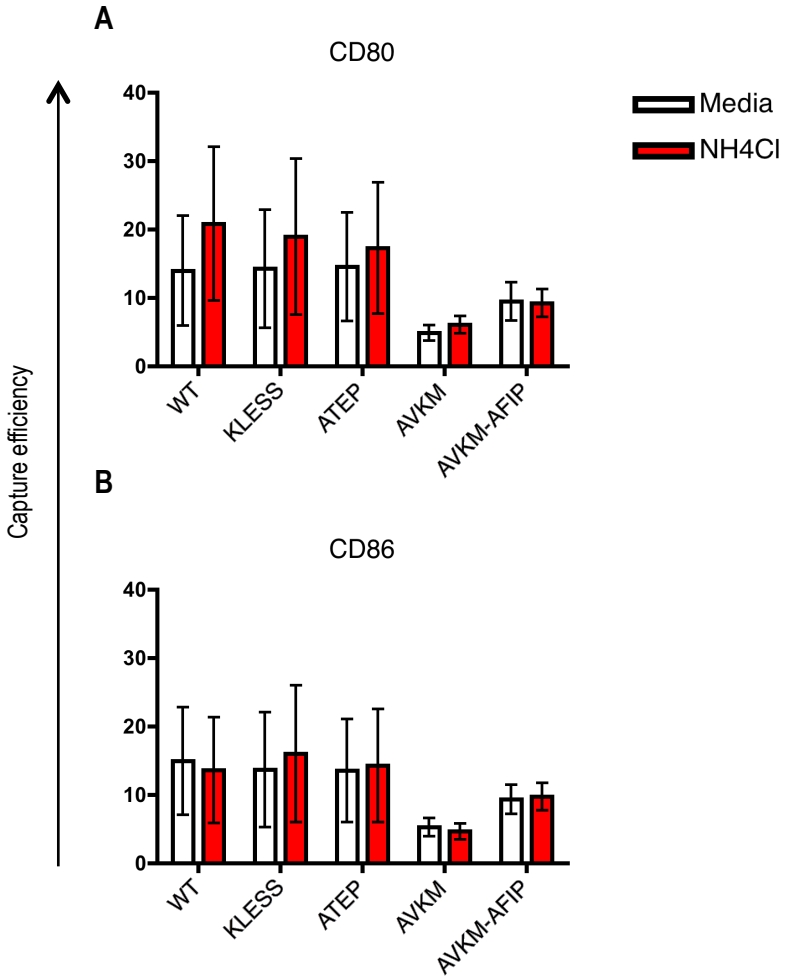

Figure 4.27 CTLA-4 mutants remove CD80 and CD86 and target the ligand for lysosomal degradation. CD80 and CD86-GFP acquisition by CHO-cells expressing CTLA-4 mutants in medium or medium supplemented with NH_4Cl was determined by flow cytometry. Error bars show standard error (n=3). The capture efficiency was calculated as described in Materials and Methods.

4.10 Discussion

The mechanism regulating CTLA-4 internalisation via the clathrin pathway is well described (Chuang et al., 1997; Shiratori et al., 1997). However, despite increased speculation that CTLA-4 can recycle and that it is targeted for lysosomal degradation, the pathways associated with sorting of the receptor to these destinations remains unclear (Chuang et al., 1997; Iida et al., 2000; Leung et al., 1995). Moreover, the uncertainty of the post-endocytic sorting of CTLA-4 adds to the complexity of how a receptor that is predominantly located in intracellular vesicles removes surface transmembrane proteins, internalises them and targets them for degradation. However transendocytosis does provide an answer for some of the unexplained features of the CD28/CTLA-4 system including why CTLA-4 is located in intracellular vesicles and why CD28 and CTLA-4 share ligands.

The CTLA-4 cytoplasmic domain is conserved in mammalian species suggesting there is selective pressure to maintain this region (Bernard et al., 2007; Teft et al., 2006). Multiple motifs are and could be encoded in this region but the precise function of these motifs in CTLA-4 intracellular trafficking remains to be identified. Data presented in this thesis revealed that CTLA-4 internalisation is regulated by the YVKM motif and in keeping with previous studies a Y→A mutation abolished the efficiency of internalisation. Moreover, the YVKM motif appears to be an absolute requirement for CTLA-4 recycling since the receptor must first be internalised prior to being sorted in an intracellular compartment. However this motif does not appear to be an absolute requirement for receptor degradation since the AVKM mutant (where a fraction of receptor is internalised) was susceptible for degradation. This slow turnover rate could explain how stable surface proteins are internalised over time and degraded.

CTLA-4 has five lysine residues in the cytoplasmic domain and the suggestion that the receptor is degraded in lysosomes raised the possibility of ubiquitination being the signal directing the receptor to lysosomes. Although ubiquitination is now emerging as a signal for internalisation (Kumar et al., 2007), the data presented here shows that CTLA-4 internalisation is not ubiquitin-dependent using a lysine-less mutant of CTLA-4 (KLESS). However, lysine residues do regulate CTLA-4 recycling and degradation and this regulation resembles that of other receptors such as PAR2 (Jacob et al., 2005) and Neurokinin-1 receptor (Cottrell et al., 2006) where enhanced recycling is observed in the absence of lysine residues. This suggests that the mutation of intracellular lysine residues allows CTLA-4 to escape from lysosomal degradation and return to the plasma membrane. Moreover, in the presence of lysosomal inhibitors no accumulation of KLESS CTLA-4 was observed and no ubiquitinated species were detected. The lack of KLESS targeting to lysosomes suggests the step at which ubiquitination is essential for post-internalisation sorting could be absent. The size of ubiquitinated CTLA-4 indicates that the receptor is mono- or multi-ubiquitinated thus resulting in molecular sizes of 46-58kDa. Such a finding could prove to be significant when developing therapeutic vaccines for the treatment of autoimmune disease or cancers. The ubiquitin attachment checkpoint could be manipulated so as to increase CTLA-4 levels by preventing ubiquitination or decreasing CTLA-4 levels by promoting ubiquitination accordingly. However, further work is required to address what effect ligand binding has on CTLA-4 ubiquitination. It is also interesting to speculate whether the CTLA-4 receptor undergoes deubiquitination after disposing of ligand in lysosomes, a process that should free up the receptor to recycle back to the cell surface. Such a process has been described for EGFR (Berlin et al., 2010) and thus further work could help us identify the deubiquitinating enzyme responsible for this activity.

Work in this thesis concluded that all five lysine residues play a role in CTLA-4 recycling and degradation and in the absence of one or more of these residues other lysines could compensate for

the loss. This was surprising considering how for other receptors such as EGFR (Huang et al., 2006) and IFNAR1 (Kumar et al., 2004) not all lysine residues are targets of ubiquitination. Importantly further work is required to address which E3 ligase is responsible for attaching ubiquitin molecules to the intracellular lysine residues in CTLA-4. Focus on T cell specific E3 ligases places GRAIL (gene related to anergy in lymphocytes) (Anandasabapathy et al., 2003), Cbl-b (Bachmaier et al., 2000) and Itch (Perry et al., 1998) as possible candidates. Previous studies have shown that all three E3 ligases are upregulated in anergic $CD4^+$ $CD25^-$ T cells during ionomycin-induced anergy (Heissmeyer et al., 2004), a phenotype that often results when a T cell is activated via the TCR without appropriate co-stimulatory signals. In particular the hyperproliferative and activated phenotype of T cells deficient in Cbl-b and Itch resembles the phenotype seen in CTLA-4 knockout mice, further questioning whether these ligases have a role in CTLA-4 ubiquitination.

A role for lysine residues in CTLA-4 degradation could be explained by a requirement for the receptor to undergo ubiquitination prior to lysosomal degradation. However the phenotype of the CTLA-4 receptor where the proline residue in a PTEP motif was mutated was surprising. By removing the candidate lysine residues, ubiquitin can no longer be attached to the CTLA-4 receptor and enhanced recycling of the KLESS mutant was observed. But what role does the proline-based motif play in this process? In the ATEP mutant, the targets of ubiquitin are still intact yet the receptor escapes ubiquitination and degradation. Thus, it is interesting to speculate whether the step prior to ubiquitin attachment could be blocked. This particular motif could be the binding site of the E3 ligase mediating ubiquitin attachment to lysine residues or of an intermediate protein that recruits the ligase. Of interest is TSG101, which is part of the ESCRT complex and co-ordinates MVB formation (Dilley et al., 2010). TSG101 binds to PT/SAP motifs similar to the PTEP motif in CTLA-4 and could facilitate its recruitment into MVBs prior to receptor degradation in lysosomes. Further work is required to identify the specific role of TSG101 in CTLA-4

intracellular trafficking possibly through knockdown or overexpression of this protein. In fact, this would fill in the missing blanks as to how CTLA-4 is trafficking from sorting endosomes to lysosomes.

The range of CTLA-4 mutants generated allowed a differentiation to be made between the sorting motifs important for internalisation, recycling and degradation. However for transendocytosis, all CTLA-4 mutants captured ligand albeit less efficiently than WT. Although transendocytosis has been reported for other receptor-ligand pairs (Cagan et al., 1992; Klueg et al., 1998; Kusakari et al., 2008), a detailed mechanistic pathway for the requirements of such a pathway remains to be identified. Recent data in our lab suggests that the actin machinery is important in clustering the receptor and ligand, leading to membrane deformation and subsequent endocytosis (Omar Qureshi; personal communication). Such a mechanism could therefore bypass the endocytosis machinery and could explain how surface CTLA-4 mutants AVKM and AVKM-AFIP capture and degrade ligand.

Taken together, this chapter details the mechanisms regulating CTLA-4 intracellular trafficking; in particular highlighting the sorting motifs encoded in the cytoplasmic domain important for CTLA-4 recycling and degradation. Such data could help our understanding when therapies are being developed in controlling autoimmune disease and conditions where the CD28/CTLA-4 pathway plays a key role.

5.0 COMPARISON OF THE INTRACELLULAR TRAFFICKING ITINERARY OF CTLA-4 ORTHOLOGUES

5.1 Introduction

The CD28/CTLA-4 pathway has been well characterised in mammals and is vital for regulating effective T cell responses. Interestingly, the CTLA-4 receptor has been identified in rainbow trout, amphibians and birds, that although require functional characterisation, could provide an insight into the evolution of the CTLA-4 receptor (Bernard et al., 2007; Bernard et al., 2006; Teft et al., 2006). Sequence alignments of the CTLA-4 extracellular domain reveal that the proline-based motif required for ligand binding, M(L)YPPPY, is well conserved across species. In contrast, whilst the cytoplasmic domain shows a striking degree of conservation in mammals, it is much less well conserved in non-mammals.

In mammals, CTLA-4 is constitutively internalised from the plasma membrane, which is dependent on the association of the YVKM motif encoded in the CTLA-4 cytoplasmic domain associating with the clathrin adaptor AP-2 (Chuang et al., 1997; Shiratori et al., 1997). At steady state, the receptor is predominantly located in intracellular compartments raising the question of how intracellular trafficking may affect the function of CTLA-4. Our lab has recently proposed a model that this endocytic ability may play an important role in CTLA-4 function by facilitating the capture of its transmembrane co-stimulatory ligands from opposing cells by a process of transendocytosis (Qureshi et al., 2011). This chapter therefore addressed whether CTLA-4 intracellular trafficking is conserved during evolution and if any differences in receptor trafficking affect CTLA-4 function across species.

5.2 Comparison of the intracellular distribution of CTLA-4 orthologues

In mammals, there is essentially 100% amino acid sequence conservation of the CTLA-4 cytoplasmic tail (**figure 5.1A**) (Bernard et al., 2007; Bernard et al., 2006; Teft et al., 2006). This supports the view that any protein sorting signals encoded within this region are likely to be of functional importance. In contrast, in species such as chicken, *xenopus* and trout, there is considerable variation in this region (**figure 5.1A**), which may provide insights into CTLA-4 trafficking and the regulation of co-stimulation. Chimeric versions of human CTLA-4 were therefore generated where the C-terminus was replaced with that of chicken, *xenopus*, or trout CTLA-4 (**figure 5.1B**). Chinese hamster ovary (CHO) cell lines were transfected with the CTLA-4 chimeras, the cell surface was labelled with wheat germ agglutinin (WGA) at 4°C and then cells were stained for total CTLA-4 expression using an Ab to the human CTLA-4 ectodomain to assess localisation (**figure 5.2A**)**.** *Xenopus* and chicken chimeras revealed a pattern similar to human CTLA-4 with a punctate intracellular distribution. In contrast, the chimera with the trout C-terminus showed robust surface expression with far more limited intracellular vesicles. This difference in the amount of surface CTLA-4 relative to the total was quantified by flow cytometry and is shown in **figure 5.2B**.

A

```
                 190        200        210        220
Human        SKMLKKRSPLTTGVYVKMPPTEPECEKQFQPYFIPIN
Chimp        SKMLKKRSPLTTGVYVKMPPTEPECEKQFQPYFIPIN
Dog          SKMLKKRSPLTTGVYVKMPPTEPECEKQFQPYFIPIN
Cow          SKMLKKRSPLTTGVYVKMPPTEPECEKQFQPYFIPIN
Mouse        SKMLKKRSPLTTGVYVKMPPTEPECEKQFQPYFIPIN
Rat          NRTLKKRSPLTTGVYVKMPPTEPECEKQFQPYFIPIN
Platypus     SKMIKKRSLLTTGVYVKMPPPEPEHEKQFQPYFIPIN
```

B

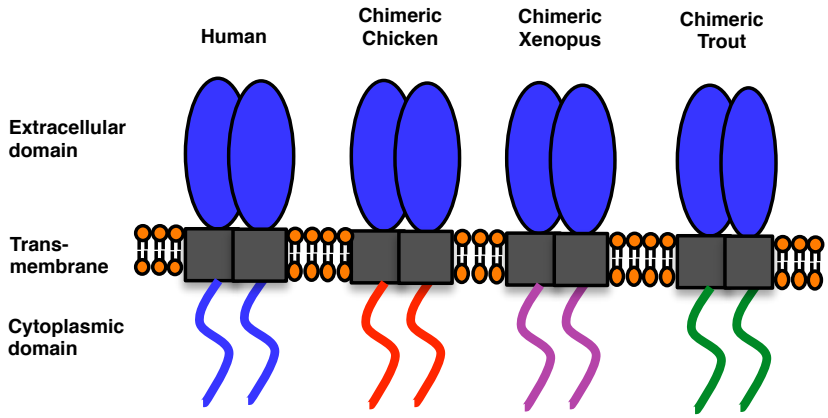


```
                 190        200        210        220
Human        SKMLKKRSPLTTGVYVKMPPTEPECEKQFQPYFIPIN
Chicken      GKAIQRRQRLTTGVYVKMP.SE.KLEKKVIPFHITVN
Xenopus      . CGKQRKKFTVGNYEKMLESD..QGNGFSPYYIRVN
Trout           QRKRRFEA..IVPMMSKN...DGRFD..YGNFQ
```

Figure 5.1 Generation of CTLA-4 chimeras. (A) C-terminal sequence alignments of selected mammalian CTLA-4 based on sequence data from Ensembl and in reference Bernard et al., (1997). **(B)** Diagram of human CTLA-4 chimeras containing the extracellular and transmembrane domain of human CTLA-4 and the C-terminus of species shown. C-terminal amino acid sequence alignments of human, chicken, *xenopus* and trout CTLA-4 are shown below, based on alignments using Clustal W.

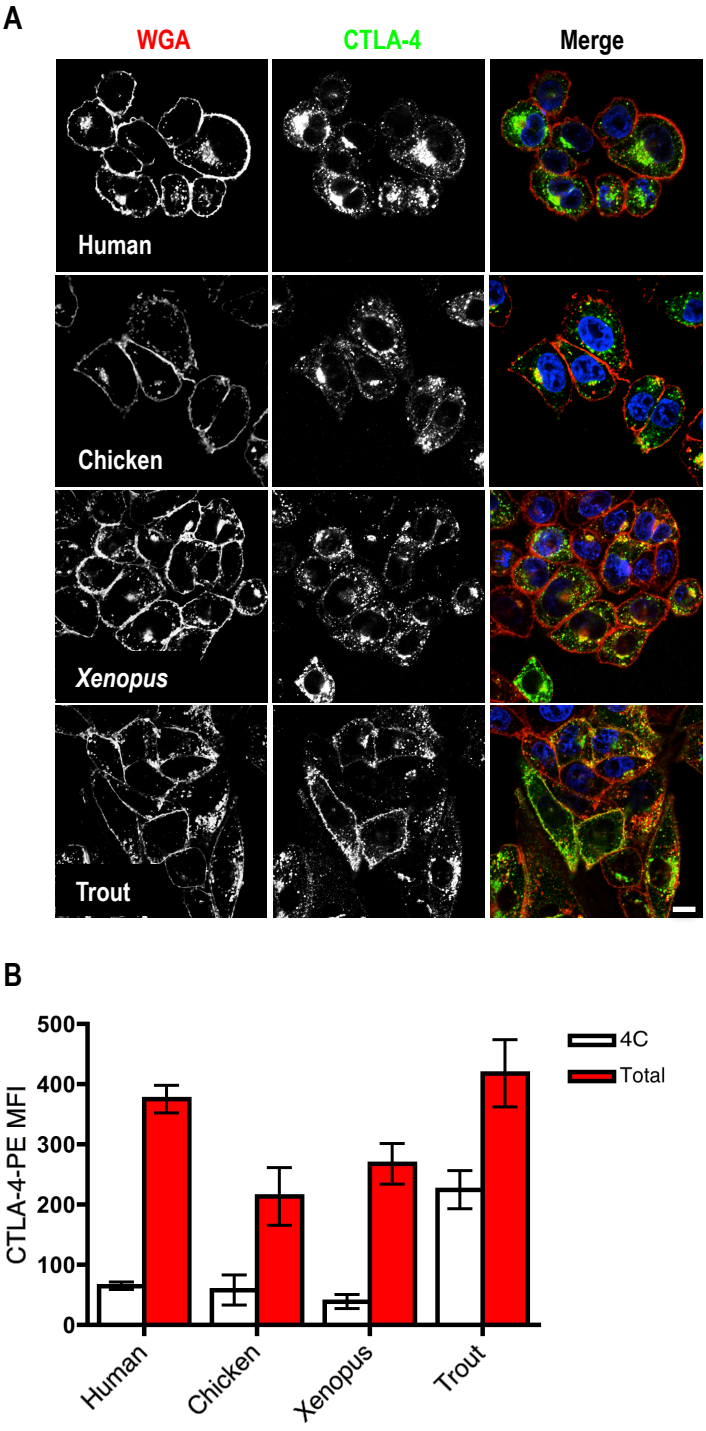

Figure 5.2 Localisation of CTLA-4 chimeras. (A) CHO cells expressing CTLA-4 chimeras were incubated with WGA-tetramethylrhodamine at 4°C. Cells were subsequently fixed, permeabilised, and stained with an unconjugated anti-CTLA-4 Ab followed by Alexa488 anti-human secondary Ab (green) to stain total CTLA-4 protein. Cells were analysed by confocal microscopy. Confocal images shown are representative of at least 40 cells taken from one independent experiment of n=3. Bar indicates scale of 10µm. **(B)** Relative expression of surface (4°C) and total CTLA-4 for each chimera as determined by flow cytometry. Error bars show standard error (n>3).

5.3 Comparison of the endocytic ability of CTLA-4 orthologues

The increased surface expression observed with chimeric trout CTLA-4 suggested that the C-terminus of trout CTLA-4 might confer less efficient internalisation consistent with its lack of a YXKM motif. To assay internalisation directly, cells were labelled at 37°C with an unlabelled anti-CTLA-4 Ab so as to label CTLA-4 protein cycling from the plasma membrane. Cells were subsequently placed on ice to prevent further trafficking and receptors remaining at the cell surface labeled with Alexa555 anti-mouse secondary Ab (red). Cells were then fixed and permeabilised and internalised CTLA-4 protein detected with Alexa488 anti-mouse secondary Ab (green) before analysing cells by confocal microscopy (**figure 5.3A).** To quantify these differences, internalisation was also measured as a ratio of surface (red) to internalised (green) CTLA-4 (**figure 5.3B**). Human CTLA-4 possessed the lowest surface to internalised ratio reflecting that CTLA-4 is predominantly localised in intracellular vesicles, which was similar to chimeric constructs from *xenopus* and chicken CTLA-4. In contrast, the C-terminus of trout CTLA-4 showed a greater surface to internalised ratio suggesting relatively poor endocytosis consistent with its more obvious surface phenotype.

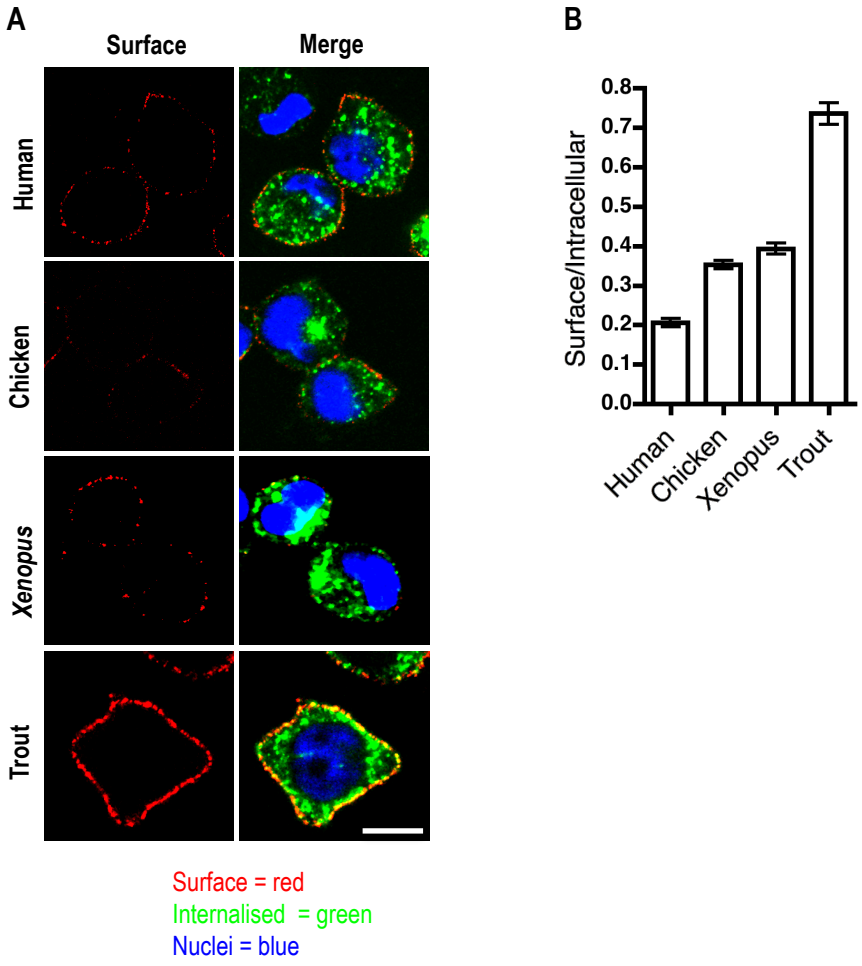

Figure 5.3 Cellular localisation of CTLA-4 chimeras. (A) CHO cells expressing CTLA-4 chimeras were incubated with unconjugated anti-CTLA-4 Ab at 37°C for 1hour, cooled to 4°C and surface CTLA-4 stained red with Alexa555 anti-mouse secondary Ab. Cells were subsequently fixed, permeabilised and stained with Alexa488 anti-mouse secondary Ab (green) and imaged by confocal microscopy. Confocal images shown are representative of at least 40 cells taken from one independent experiment of n=3. Bar indicates scale of 10µm. **(B)** The ratio of surface to internalised CTLA-4 fluorescence was calculated by outlining cells in ImageJ. Error bars show standard error. Representative data of one independent experiment of n=3.

To assay the efficiency of CTLA-4 internalisation more quantitatively in multiple cells, a flow cytometric approach was used. Cycling CTLA-4 was labelled with a PE-conjugated anti-CTLA-4 Ab at 37°C. Cells were subsequently washed and placed on ice and any residual surface primary antibody was detected using an Alexa647 anti-mouse secondary Ab (**figure 5.4A**). For WT CTLA-4 this generates a curved plot where the extensive cycling label at 37°C (Y-axis) is greater than the minimal surface label (x-axis), typical of an endocytic protein. Whilst both chicken and *xenopus* CTLA-4 chimeras showed a similar pattern to human the chimeric trout CTLA-4 displayed an almost linear relationship between cycling and surface CTLA-4 (**figure 5.4B**) typical of a cell surface protein, again suggesting impaired CTLA-4 endocytosis in trout.

To directly measure the rates of endocytosis the cell surface pool of CTLA-4 was stained on ice with an unlabelled anti-CTLA-4 Ab. Cells were then warmed to 37ºC for the indicated time-points to allow any internalisation of surface CTLA-4 to take place. Cells were then placed on ice, and any CTLA-4 remaining at the cell surface detected with an Alexa647 anti-mouse secondary Ab. Accordingly, in this assay the loss of Alexa647 staining over time reflects endocytosis of CTLA-4. Using this assay, human CTLA-4 showed a comparable rate of endocytosis to the chimeric *xenopus* and chicken constructs (**figure 5.5A**), internalising 50% or more within 5minutes. In contrast, chimeric trout CTLA-4 showed a much slower rate of endocytosis taking at least 30minutes to achieve 50% internalisation. Nevertheless, chimeric trout CTLA-4 did internalise compared to a control CTLA-4 chimera with a cytoplasmic domain from CD86, which is a plasma membrane resident in CHO cells (**figure 5.5A**)**.** However, it was clear that even for surface proteins (CTLA-4-CD86) there was a small decrease in signal over time in this assay, which was not due to endocytosis, further emphasising the much reduced endocytic nature of the trout chimera.

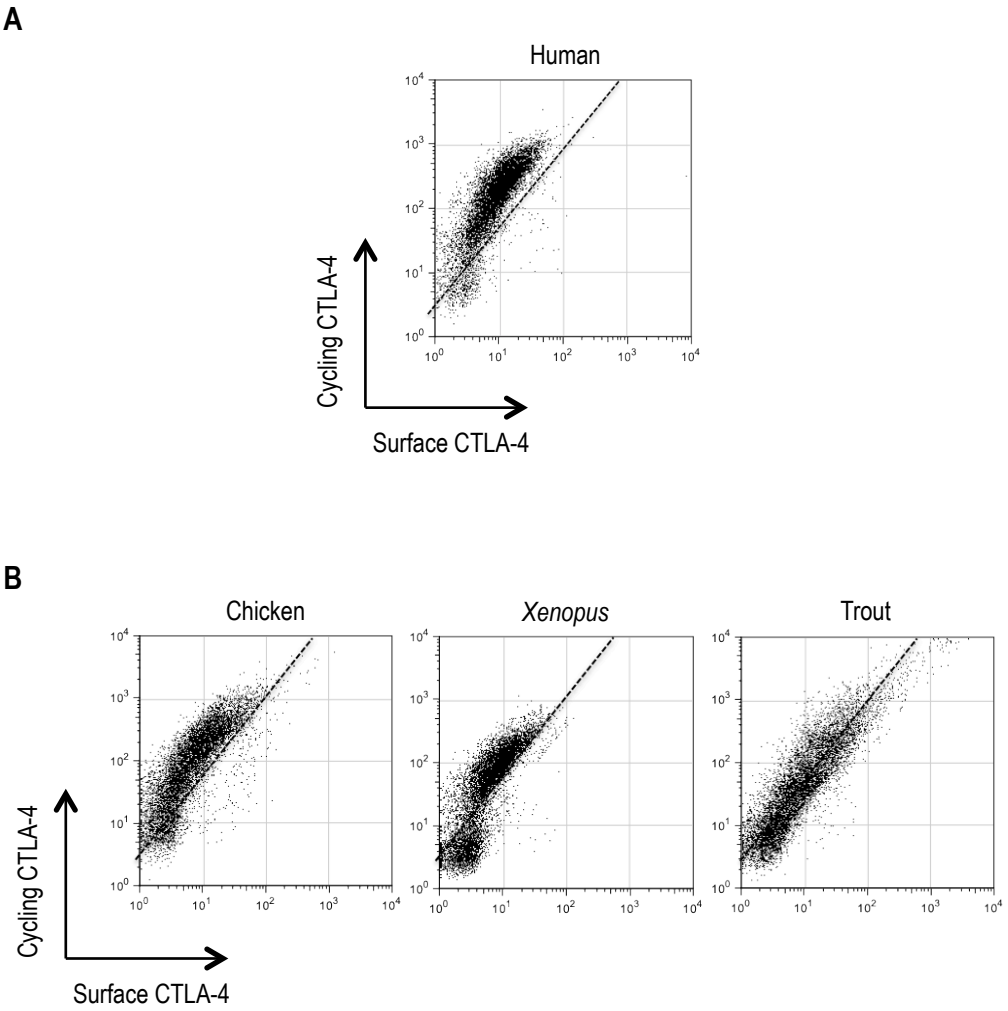

Figure 5.4 Flow cytometry identifies different cellular trafficking in the CTLA-4 chimeras. (A) CHO cells expressing human CTLA-4 were labelled with PE-conjugated anto-CTLA-4 Ab at 37°C for 30 minutes followed by labelling surface CTLA-4 on ice (4°C) with Alexa647 anti-mouse secondary Ab. Cells were analysed by flow cytometry and data are plotted as cycling CTLA-4 (37°C label) vs surface CTLA-4 (4°C label). **(B)** CHO cells expressing the CTLA-4 chimeras were labelled as described in A. and analysed by flow cytometry. Dotted line provides a standard gradient for reference purposes. Representative FACS plots are shown of one independent experiment of n≥3.

Experiments in chapter 3 revealed that in the presence of hypertonic sucrose CTLA-4 internalisation is inhibited. The effect of sucrose treatment was therefore tested on the chimeric constructs to determine their clathrin dependence. As shown in **figure 5.5B** sucrose treatment inhibited the endocytosis of CTLA-4 molecules. In particular the more rapid endocytosis seen in chicken, *xenopus* and human CTLA-4 chimeras (relative to trout) was prevented by sucrose treatment. Overall, this data suggests that the chimeras internalise via a clathrin dependent pathway.

To further verify that the chimeras internalise using clathrin, the co-localisation of the CTLA-4 chimeras with transferrin was compared. Cells were incubated with transferrin AlexaFluor633 and PE-conjugated anti-CTLA-4 Ab at 37°C for 45minutes and subsequently fixed and analysed by confocal microscopy. This revealed that human, chicken and *xenopus* CTLA-4 co-localised with transferrin in intracellular vesicles, suggesting internalisation in the chimeras is clathrin-dependent (**figure 5.6**). Additionally, this assay revealed limited but detectable co-localisation between trout CTLA-4 and transferrin, further suggesting that trout CTLA-4 does internalise via clathrin albeit at a reduced rate.

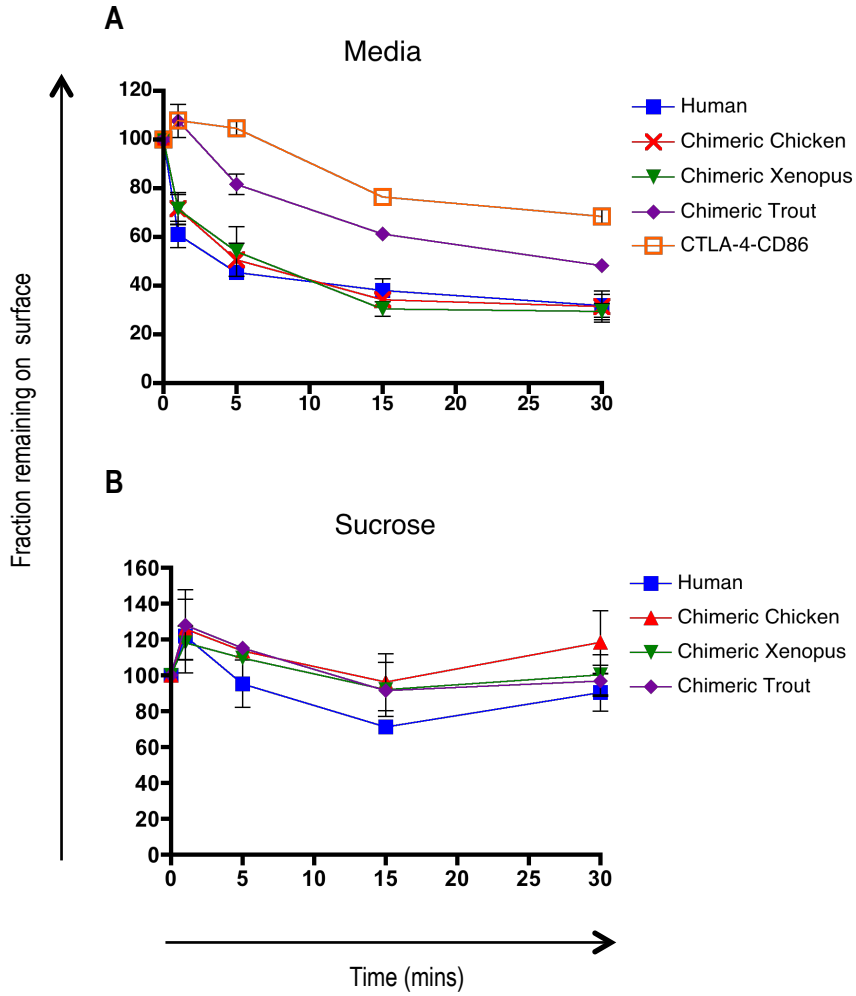

Figure 5.5 CTLA-4 chimeras show different endocytic efficiencies. (A) CHO cells expressing CTLA-4 chimeras were labeled at 4°C with an unlabelled anti-CTLA-4 Ab to label surface CTLA-4. Cells were then warmed to 37°C to allow endocytosis for the times indicated. Cells were then placed on ice and any remaining surface CTLA-4 detected with Alexa647 anti-mouse secondary Ab. The 647 signal was plotted against time as the fraction remaining compared to 4°C. **(B)** CHO cells expressing CTLA-4 chimeras were labeled as in A. but in medium supplemented with sucrose (0.45M) to prevent endocytosis. Error bars show standard error (n≥3).

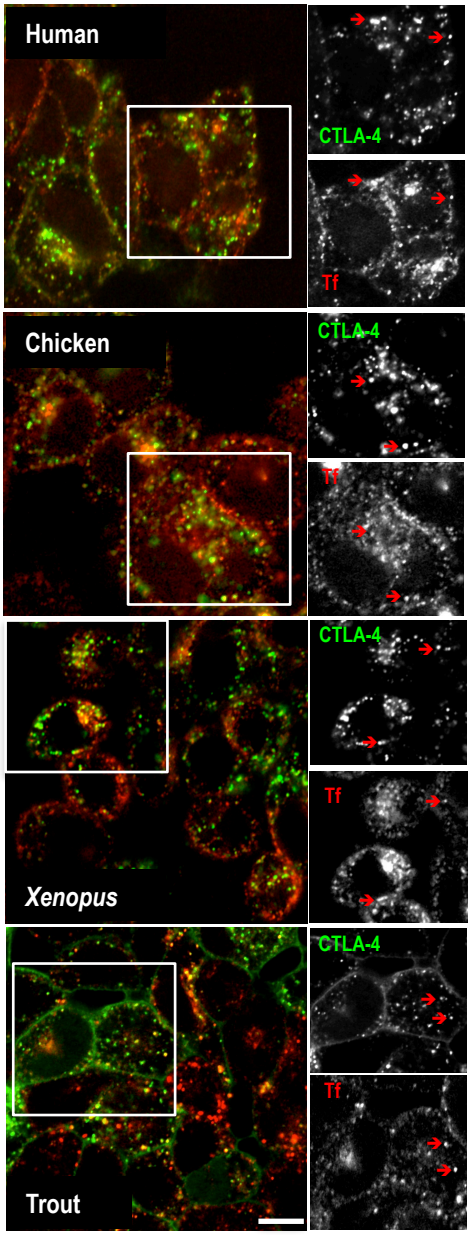

Figure 5.6 CTLA-4 chimeras internalise using a clathrin-dependent pathway. CHO cells expressing the chimeric CTLA-4 constructs were incubated with a transferrin AlexaFluor633 and PE-conjugated anti-CTLA-4 at 37°C for 45minutes. Cells were subsequently fixed and analysed by confocal microscopy. The red arrows indicate co-localisation. Confocal images shown are representative of at least 40 cells taken from one independent experiment of n=3. Bar indicates scale of 10µm.

Whilst trout CTLA-4 lacked the conserved YVKM internalisation motif found in mammals, it did appear to have a putative YxxF motif (Bernard et al., 2007), which could possibly mediate endocytosis. To address whether this motif contributed to the internalisation observed with the chimeric trout CTLA-4, the tyrosine residue was mutated to a valine and the behaviour of this mutant was monitored in CHO cells. A comparison of internalisation rates indicated the VGNF mutant had further impaired endocytosis compared to the YGNF control and now resembled the behavior of non-endocytic proteins seen using sucrose or with the surface CD86 chimera (**figure 5.7A**). In contrast to chimeric trout CTLA-4 containing YGNF, the VGNF mutant demonstrated no co-localisation with transferrin (**figure 5.7B**). Together, these results confirmed the presence of a functional tyrosine-based endocytic motif in trout CTLA-4 albeit one that functions with reduced efficiency.

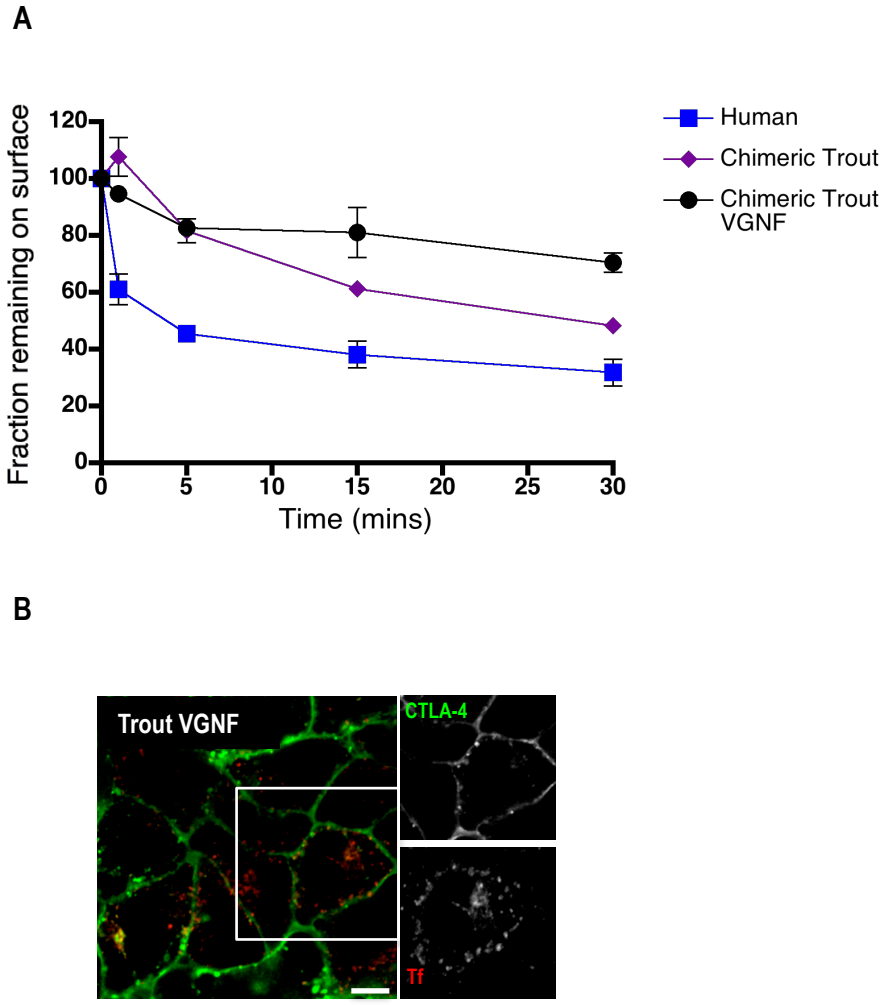

Figure 5.7 Trout CTLA-4 has a rudimentary endocytic motif. (A) CHO cells expressing CTLA-4 chimeras were labeled at 4°C with an unlabelled anti-CTLA-4 Ab to label surface CTLA-4. Cells were then warmed to 37°C to allow endocytosis for the times indicated. Cells were then placed on ice and any remaining surface CTLA-4 detected with Alexa647 anti-mouse secondary Ab. The 647 signal was plotted against time as the fraction remaining compared to 4°C. Error bars show standard error (n≥3). **(B)** CHO cells expressing the chimeric CTLA-4 constructs were incubated with a transferrin AlexaFluor633 and PE-conjugated anti-CTLA-4 at 37°C for 45minutes. Cells were subsequently fixed and analysed by confocal microscopy. Confocal image shown is representative of at least 40 cells taken from one independent experiment of n=3. Bar indicates scale of 10μm.

5.4 Degradation of CTLA-4 orthologues correlates with endocytic ability

Chapter 3 revealed that human CTLA-4 is degraded in lysosomes. To address the stability of the CTLA-4 chimeras, new protein synthesis was blocked using CHX and the decay of existing CTLA-4 was monitored. In addition, if CTLA-4 was being degraded via a lysosomal pathway then NH_4Cl should prevent degradation. CTLA-4 protein stability was therefore monitored in the presence of CHX or NH_4Cl for 3hours at 37°C. After treatment, cells were fixed and permeabilised prior to staining for total CTLA-4 expression and analysed by confocal microscopy or flow cytometry. In the absence of new protein synthesis, rapid loss of human, chicken and *xenopus* CTLA-4 was observed (**figure 5.8A**) indicating that CTLA-4 was degraded rapidly. Degradation was quantified by both confocal analysis (**figure 5.8B**) and by flow cytometry (**figure 5.9**). Moreover, NH_4Cl resulted in an accumulation of CTLA-4 (predominantly in human, xenopus and chicken chimeras) suggesting that blocking lysosomal function prevents CTLA-4 degradation. Whilst human CTLA-4, chimeric *xenopus* and chicken showed comparable degradation, the trout CTLA-4 chimera was much less affected by CHX although compared to the non-endocytic variants (trout VGNF and CTLA-4-CD86 chimera) some degradation was still evident (**figure 5.8** and **5.9E-F**).

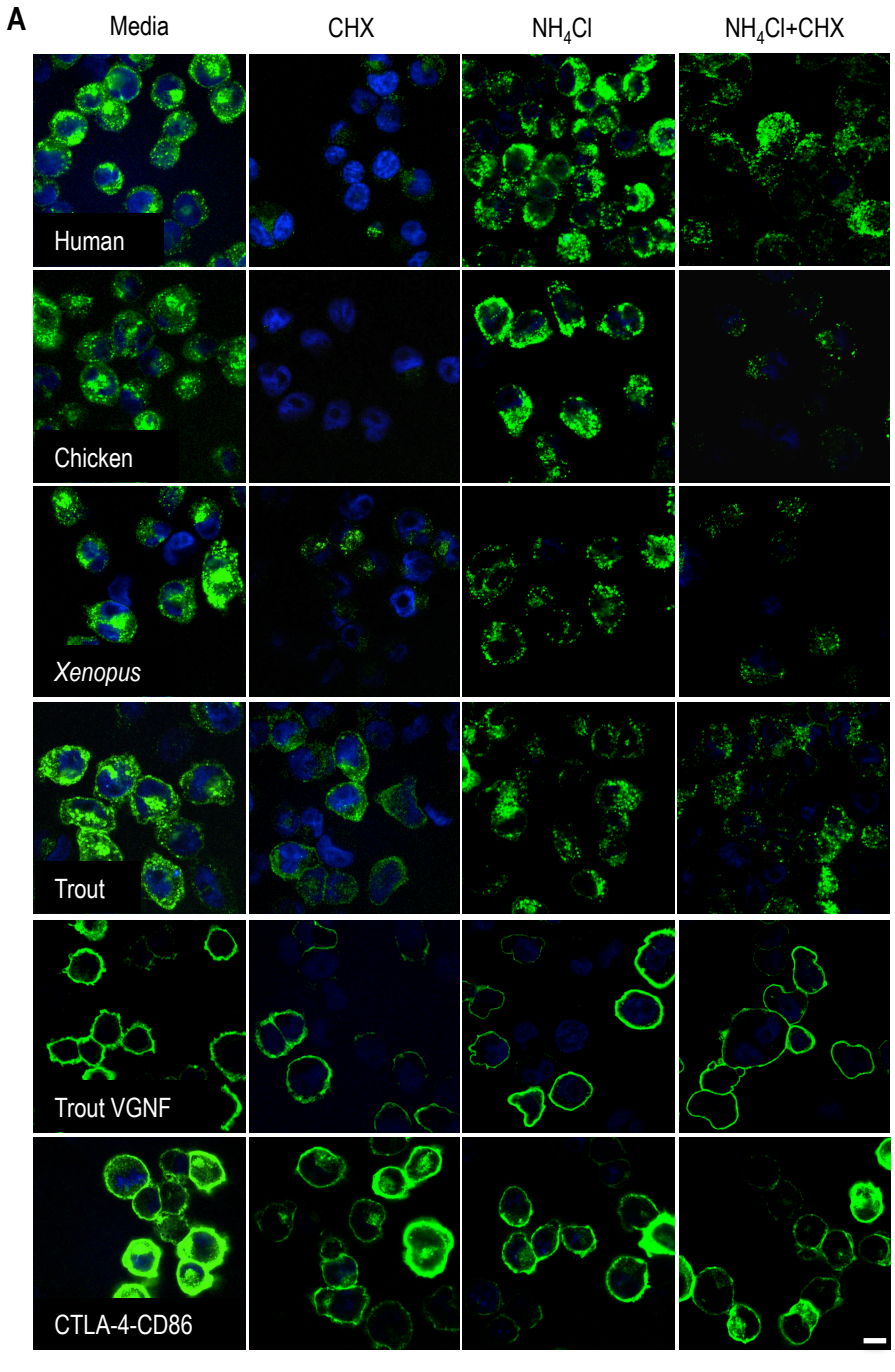

Figure 5.8 Degradation efficiency of the CTLA-4 chimeras correlates with their endocytic potential. (A) CHO cells expressing CTLA-4 chimeras were incubated in medium or medium supplemented with CHX, NH_4Cl or NH_4Cl and CHX at 37°C for 3hours. Cells were fixed, permeabilised and stained for total CTLA-4 with an unlabelled anti-CTLA-4 Ab followed by Alexa488 anti-mouse secondary Ab (green) and nuclei counterstained using DAPI (blue). Cells were analysed by confocal microscopy. Bar indicates scale of 10µm. **(B)** Total CTLA-4 was quantified by outlining cells in ImageJ and MFI plotted. Error bars shows standard error (n≥3).

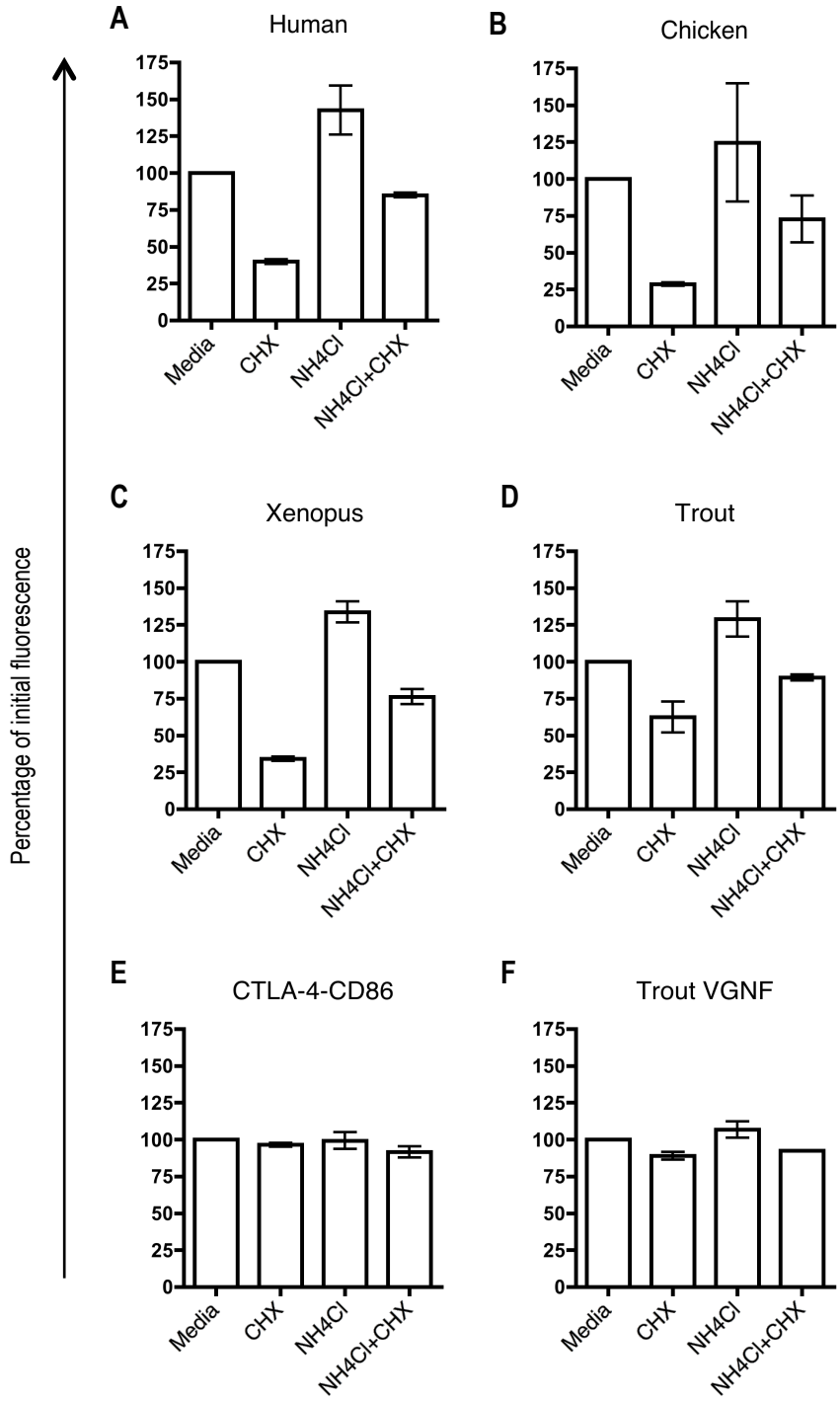

Figure 5.9 Flow cytometry verifies the degradation efficiency of the CTLA-4 chimeras correlates with their endocytic potential. CHO cells expressing CTLA-4 chimeras were incubated in medium or medium supplemented with CHX, NH_4Cl or NH_4Cl and CHX at 37°C for 3hours. Cells were fixed, permeabilised and stained for total CTLA-4 with a PE-conjugated anti-CTLA-4 Ab. Cells were analysed by flow cytometry. The MFI is plotted as a percentage of initial fluorescence. Error bars show standard error (n≥3).

To determine if CTLA-4 co-localised with markers of late endosomes, the CTLA-4 chimeras were transfected with CD63, fused to GFP, in the presence of NH_4Cl. Notably, human, chicken and *xenopus* CTLA-4 all demonstrated substantial co-localisation with CD63-GFP, suggesting traffic to late endosomes (**figure 5.10**). In contrast, the non-endocytic trout VGNF mutant and the cell surface CTLA-4-CD86 chimera demonstrated no obvious co-localisation with CD63. Collectively these data suggest that degradation of CTLA-4 is related to its endocytic capacity and that the presence of YV/EKM motif promotes both internalisation and sensitivity to lysosomal degradation. Moreover, trout CTLA-4 contains an alternate tyrosine-based motif that has a reduced efficiency of endocytosis and has a more stable cell surface phenotype when compared to CTLA-4 from human, chicken and *xenopus*.

5.5 CTLA-4 orthologues differ in their ability to recycle

Chapter 3 revealed that once internalised a proportion of human CTLA-4 molecules recycle back to the plasma membrane. Since variation in endocytic motifs may also affect recycling, this property was assessed in the chimeras (Obermuller et al., 2002). To assay CTLA-4 recycling, cells were incubated at 37°C with a PE-conjugated anti-CTLA-4 Ab for 30 minutes to label the cycling pool of CTLA-4. Cells were then incubated further at 37°C for various times with an Alexa647 anti-mouse secondary Ab to label any of the primary antibody recycling back to the cell surface. Accordingly, recycling CTLA-4 is seen as an increase in the Alexa647 signal over time. Notably, human CTLA-4 and chimeric chicken CTLA-4 (YVKM containing proteins) showed a comparable rate of recycling (**figure 5.11**) whereas chimeric *xenopus* and trout CTLA-4, which lacked YVKM motif were notably less efficient.

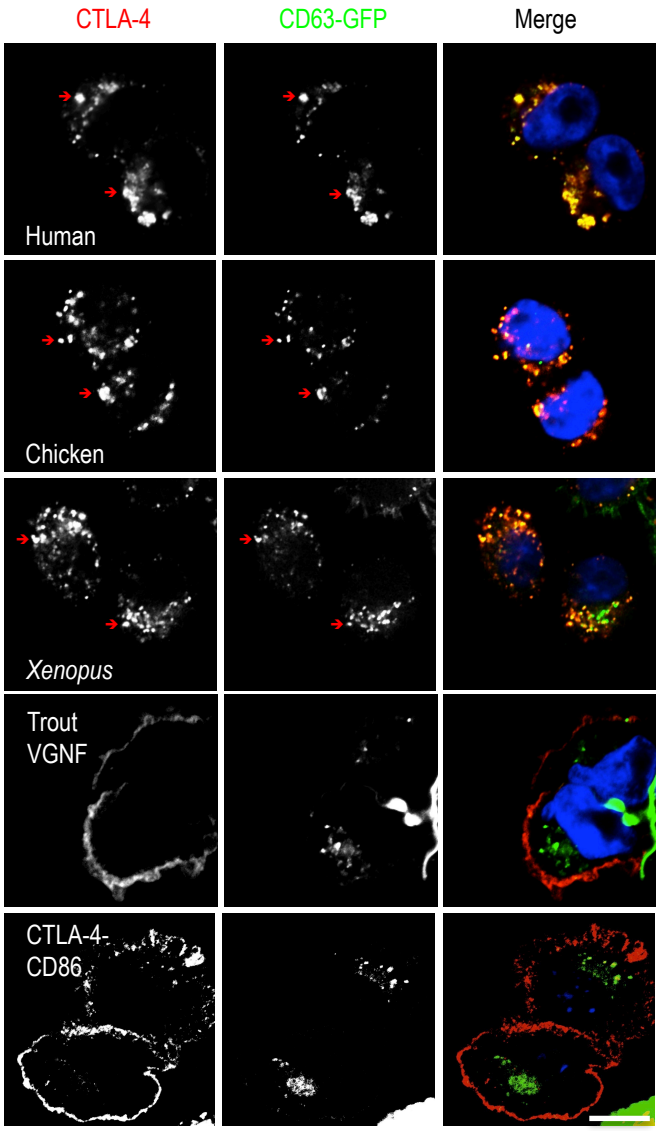

Figure 5.10 CTLA-4 chimeras co-localise with markers of late endosomes. CHO cells expressing CTLA-4 chimeras were transfected with CD63-GFP. Cells were incubated in medium supplemented with NH_4Cl at 37°C for 3 hours. Cells were fixed, permeabilised, and stained with an unconjugated anti-CTLA-4 Ab and Alexa565 anti-human secondary Ab (red) to stain total CTLA-4 protein and analysed by confocal microscopy. The red arrows indicate co-localisation. Confocal images shown are representative of at least 40 cells taken from one independent experiment of n=3. Bar indicates scale of 10µm.

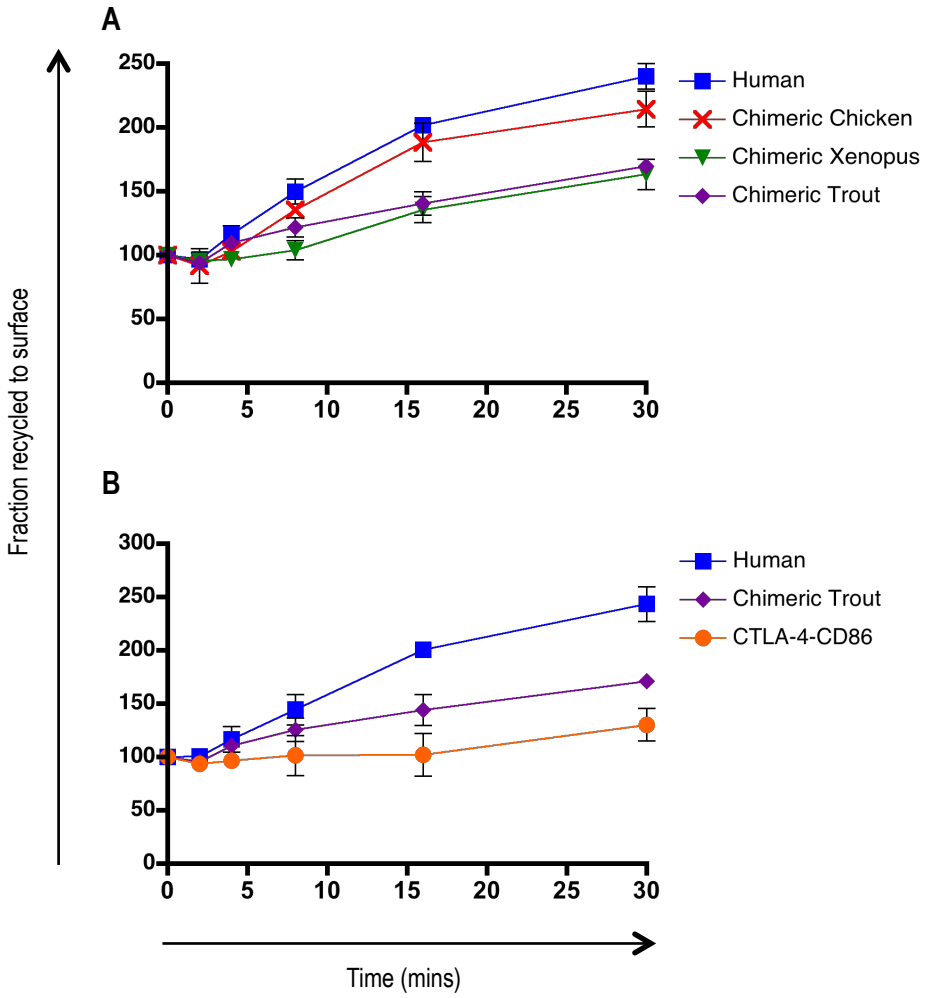

Figure 5.11 CTLA-4 chimeras differ in their ability to recycle. CHO cells expressing CTLA-4 chimeras were labeled with PE-conjugated anti-CTLA-4 Ab at 37°C to detect cycling CTLA-4, washed and any recycling CTLA-4-PE antibody detected by addition of Alexa647 anti-mouse secondary Ab at either 4°C or 37°C. Recycling rates are plotted for the chimeras as normalised to the 4°C control (**A** and **B**). Error bars shown standard error (n=3).

Since an acidic residue (E) at the +1 position of YxxM has been suggested to favour an interaction with the lysosomal sorting adaptor AP-3 (Ohno et al., 1998), the YVKM motif in human CTLA-4 was mutated to YEKM and assayed for the efficiency of internalisation and recycling. The CTLA-4 YEKM construct remained endocytic albeit with slightly reduced efficiency compared to CTLA-4 YVKM (**figure 5.12A**). However, recycling by CTLA-4 YEKM was impaired (**figure 5.12B**)**,** which was reminiscent of the lower recycling observed for the *xenopus* CTLA-4 chimera (**figure 5.12C**)**.** Taken together these data suggest that the YVKM motif found in mammalian CTLA-4 is optimised for both endocytosis and recycling of CTLA-4 and that even relatively subtle variations as found in *xenopus* CTLA-4 can compromise these functions.

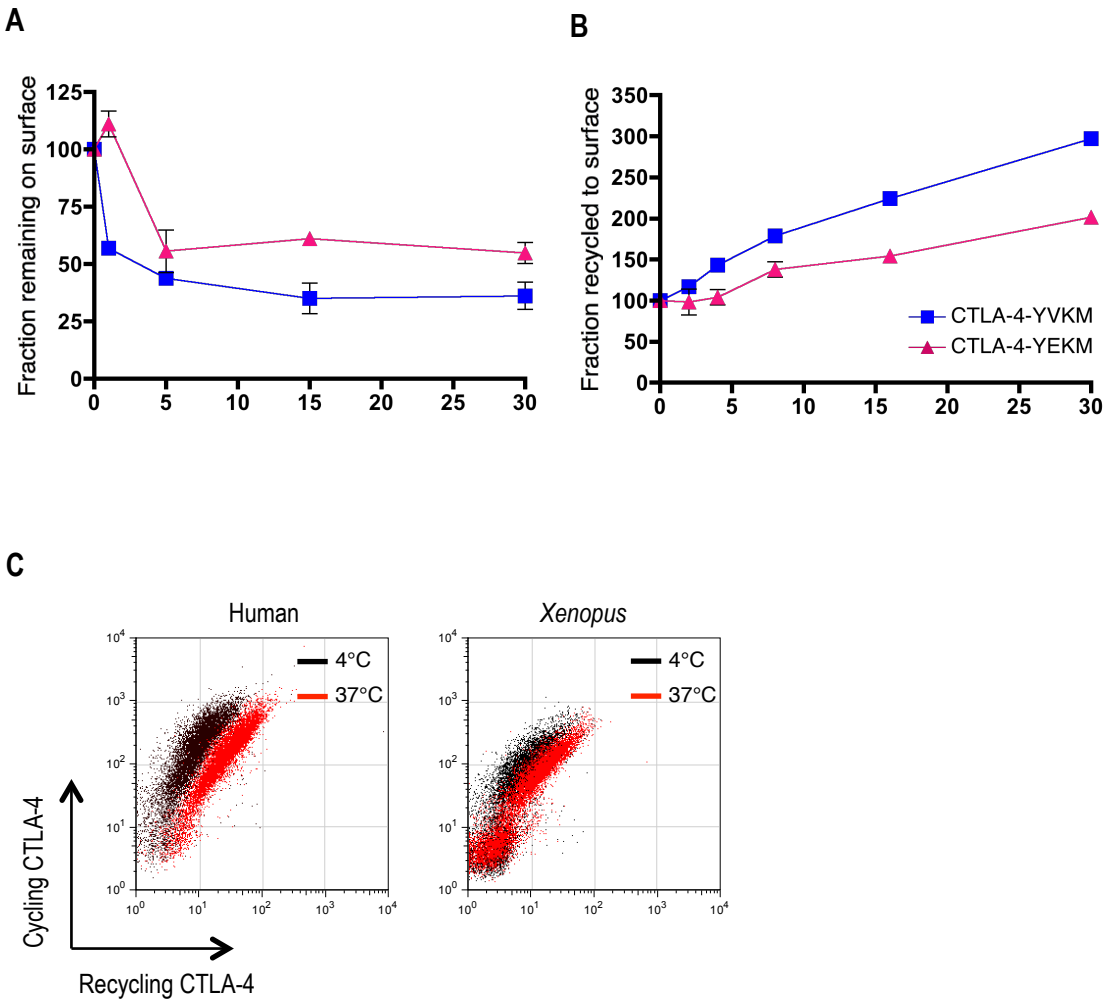

Figure 5.12 Recycling efficiency is regulated by the YVKM motif. (A) CHO cells expressing WT human CTLA-4 YVKM or YEKM motif were labelled at 4°C with anti-CTLA-4 to label surface CTLA-4. Cells were warmed to 37°C for the time indicated. Cells were then placed on ice and the remaining surface CTLA-4 detected with Alexa647 anti-mouse secondary Ab and plotted over time. Error bars show standard error (n=3). **(B)** CHO cells expressing WT human CTLA-4 YVKM or a point mutant YEKM motif were labelled with PE-conjugated anti-CTLA-4 Ab at 37°C to detect cycling CTLA-4. Recycling protein was detected with Alexa647 anti-mouse secondary Ab at 37°C for the indicated time points. Recycling rates are plotted for the CTLA-4 variants normalised to the 4°C control. Error bars show standard error (n=3). **(C)** Representative data comparing human and *xenopus* CTLA-4 recycling after 30minutes is shown (n≥3).

5.6 CTLA-4 orthologues can transendocytose ligand

The significant variation in the CTLA-4 cytoplasmic domain between species suggests there could be a difference in the function and the ability of the CTLA-4 in these species to transendocytose ligand. To address transendocytosis, CHO cells expressing CTLA-4 chimeras were co-cultured with CHO cells stably expressing either CD80 or CD86, fused to GFP, for 3hours at 37°C in medium alone or medium supplemented with NH_4Cl. CD80 or CD86-GFP cells were labelled with CellTrace Violet and accordingly GFP transfer could be quantified by gating CTLA-4 expressing cells that were negative for Violet dye staining. Using flow cytometry, the CTLA-4 chimeras demonstrated the ability to capture CD80 or CD86 albeit at a reduced efficiency when compared to human CTLA-4 (**figure 5.13**). The ability to capture CD80 was higher for all chimeras when compared to the capture of CD86. Importantly, this ability was diminished in the trout VGNF mutant, suggesting the YxxF motif could direct transendocytosis in trout CTLA-4. Importantly, the trend in the pattern of ligand capture, (human>chicken>*xenopus*>trout) demonstrates that the efficiency of ligand capture has improved as a result of evolution but may also require other sorting motifs encoded within the CTLA-4 cytoplasmic domain.

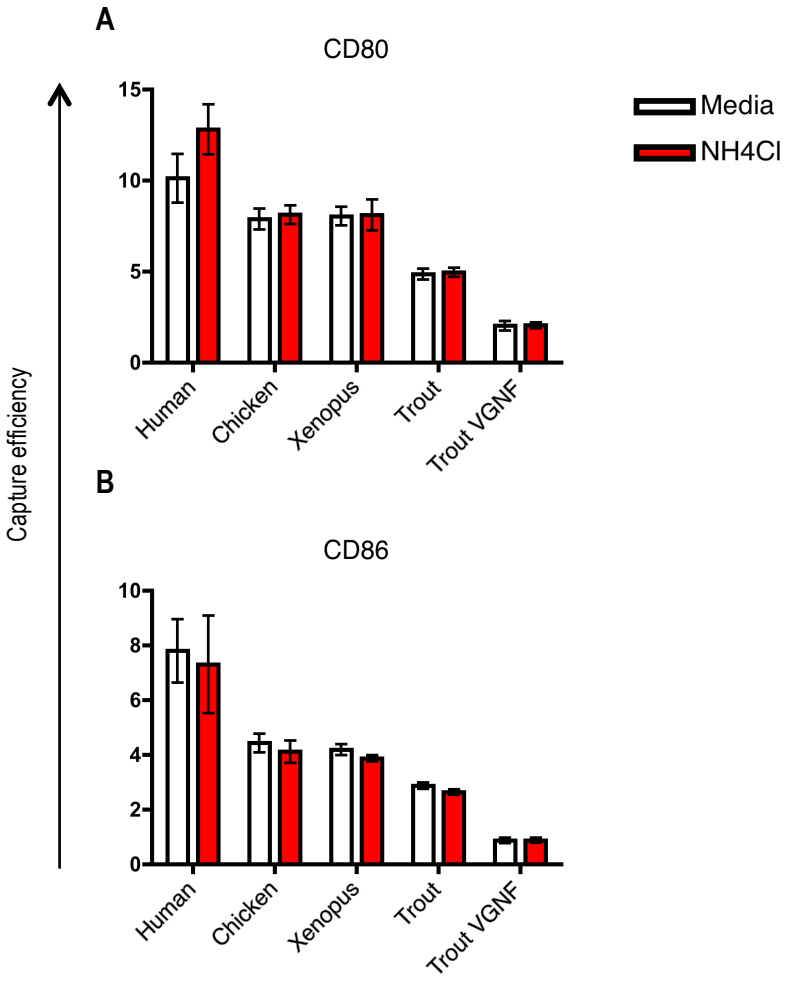

Figure 5.13 CTLA-4 chimeras show a difference in their ability to capture ligand. CD80-GFP **(A)** and CD86-GFP **(B)** acquisition by CHO cells expressing CTLA-4 chimeras was determined by flow cytometry. The capture efficiency of ligand by the CTLA-4 chimeras was calculated as described in Materials and Methods in medium or medium supplemented with NH_4Cl. Error bars show standard error (n=3).

5.7 Discussion

The high degree of conservation in the CTLA-4 cytoplasmic domain amongst mammalian species suggests there is selective pressure to maintain the functional regulation mediated via motifs encoded in this region (Bernard et al., 2007; Teft et al., 2006). As a lab we have identified a new function of CTLA-4 termed transendocytosis that takes its highly endocytic nature into account (Qureshi et al., 2011). Moreover after binding and internalising ligand, CTLA-4 disposes of the ligand in lysosomal compartments. However in non-mammals the CTLA-4 cytoplasmic domain varies considerably from that encoded in mammals. This therefore raises questions as to whether the intracellular trafficking of CTLA-4 is conserved through evolution and whether these differences impact CTLA-4 function. In this chapter I found that the location of the tyrosine-based hydrophobic motif in the CTLA-4 cytoplasmic domain contributes greatly to localisation, endocytosis and recycling across species. Moreover, the sensitivity to lysosomal degradation correlates with the endocytic potential of the CTLA-4 receptor and is conserved through evolution evident since the emergence of fish.

The YVKM motif in human CTLA-4 is important in regulating the internalising of the receptor from the cell surface. Chicken and *xenopus* CTLA-4 encode a tyrosine-based hydrophobic motif that align well with the mammalian YVKM motif and both chimeras demonstrated comparable characteristics to human CTLA-4 being present in intracellular vesicles. The absence of a conserved YXXM motif in trout CTLA-4 is interesting since without this motif some of the specialised trafficking features we observe in human CTLA-4 should be absent. However, emphasis has been placed on YxxF motif located further downstream in the trout CTLA-4 cytoplasmic domain (Bernard et al., 2007). Work in this thesis confirmed that despite the trout CTLA-4 chimera exhibiting a greater surface to internalised ratio when compared to other endocytic chimeras, internalisation was taking place but at a reduced rate.

Mutagenesis of the YxxF motif in trout CTLA-4 did in fact confirm that this motif was regulating its internalisation. This was surprising and not only from the point of view of the CTLA-4 receptor. Work in other receptors has demonstrated that location of the tyrosine residue in the cytoplasmic tail of receptors is critical to the movement of a receptor into coated pits (Lazarovits and Roth, 1988). Likewise, CD28 has YMNM motif similar to the YVKM motif in CTLA-4. However whereas CTLA-4 is endocytic CD28 is a surface resident receptor. Alignment of the cytoplasmic domain sequences reveals that the YMNM motif in CD28 is located further downstream of the YVKM motif in CTLA-4. Moreover transfer of the YVKM motif in CTLA-4 to CD28 does not trigger endocytosis but endocytosis is preserved in a CTLA-4 mutant encoding the YMNM motif of CD28 (Omar Qureshi; personal communication). Thus, it appears that the location of the tyrosine-based hydrophobic motif in the cytoplasmic domain is key to the efficiency of CTLA-4 endocytosis. In the case of trout CTLA-4 the location of the YxxF motif further downstream could prevent rapid and efficient internalisation but the presence of this motif in trout CTLA-4 suggests that this could represent the initial emergence of CTLA-4 endocytosis.

The degradation of CTLA-4 in lysosomal compartments has been suggested to be a mechanism used to regulate the expression of the receptor at the cell surface (Iida et al., 2000). Work in this thesis demonstrates that the sensitivity to lysosomal degradation in the various CTLA-4 chimeras correlates with their endocytic potential and in the ability to transendocytose ligand. Although these features were less well developed in trout CTLA-4 they do exist. It is therefore interesting to speculate whether the specialised intracellular trafficking of mammalian CTLA-4 and the transendocytosis function is the direct result of mutation and selection of cytoplasmic domain variants. The greater surface expression of trout CTLA-4 suggests that the receptor could largely function at the cell surface. Once the receptor binds ligand only does it then internalise and dispose of the ligand in lysosomes. This would explain the slow internalisation rate of trout CTLA-4 and little sensitivity to degradation. In the case of the endocytic

chimeras since internalisation from the cell surface is constitutive, the chance of interacting with components regulating lysosomal degradation is increased and thus the receptor undergoes degradation in the presence or absence of ligand.

Work in this thesis has confirmed that once internalised a fraction of the CTLA-4 receptor is recycled back to the cell surface. The C-terminus of chicken CTLA-4 demonstrated a comparable rate of recycling as human CTLA-4 suggesting that the recycling function is regulated by the YVKM motif. Importantly the residue in the +1 position of the YXXM motif also plays a role in regulating recycling as demonstrated by the lack of recycling seen for *xenopus* CTLA-4 that encodes a YEKM motif. This finding is consistent with the trafficking of other membrane receptors. The lysosomal membrane proteins LAMP1 and LAP (lysosomal acid phosphatase) are both trafficked to lysosomes from the TGN (Honing et al., 1996; Peters et al., 1990). However the route taken to lysosomes is determined by the tyrosine based hydrophobic motifs encoded in the cytoplasmic domain (Obermuller et al., 2002). LAP encodes a YRHV motif which regulates recycling of the protein between endosomes and the plasma membrane and is delivered via an indirect route to lysosomes. LAMP1 however encodes a YQTI motif which delivers the protein directly from the TGN to lysosomes. These may represent subtle differences in the tyrosine-based hydrophobic motif but these changes have a direct effect on which clathrin adaptor protein binds to the motif and thus the trafficking pathway in which the receptor is sorted. In the case of human CTLA-4, the recycling efficiency was reduced when the valine residue in the YVKM motif was mutated to glutaminc acid further demonstrating the tight regulation of this mechanism.

Taken together data in this chapter has demonstrated that CTLA-4 function as a cell-extrinsic regulator of the immune system is conserved through evolution. However, the CTLA-4 cytoplasmic domain has

undergone major changes since the emergence of fish. Fish have a simple immune system and do not require the specialised immune features present in mammals. Thus it is interesting to speculate that CTLA-4 in fish could function as a cell-extrinsic regulator and remove ligand efficiently by predominantly remaining at the cell surface. In the case of mammals, the cell-extrinsic function of CTLA-4 in Tregs requires CTLA-4 to traffic continuously to the plasma membrane and remove ligand from the surface of APCs.

6.0 GENERAL DISCUSSION

The regulation of T cell activation is vital for controlling immune responses against foreign pathogens and in preventing the development of autoimmune disease (Murphy, 2008). To control this on/off switch T cells require two signals for activation. Of importance is the second co-stimulatory signal provided by the CD28 receptor or the CTLA-4 receptor. Both receptors share 30% homology at the amino acid level and bind the same ligands expressed on APCs but the outcome of ligand engagement leads to different outcomes (Carreno and Collins, 2002; Sharpe and Freeman, 2002). CD28 binding to CD80 or CD86 drives T cell activation, proliferation and differentiation (Carreno and Collins, 2002; Lenschow et al., 1996). However, once T cells are activated they upregulate CTLA-4, which acts to compete with CD28 to bind the ligands and inhibit T cell activation. Over the years there has been a long-standing debate as to how CTLA-4 functions and importantly how this function is related to its predominant localisation in intracellular vesicles (Rudd, 2008; Walker and Sansom, 2011). CTLA-4 endocytosis via the clathrin-pathway has been well described (Chuang et al., 1997; Shiratori et al., 1997). However our understanding of the intracellular trafficking pathways used by CTLA-4 is not complete. This thesis therefore set out to identify the post-internalisation fate of CTLA-4 with particular emphasis in identifying the sorting signals encoded in the cytoplasmic domain important for trafficking.

The location of CTLA-4 in intracellular vesicles has been the most dominating aspect of its biology yet the receptor functions at the cell surface. One aim of this PhD was to address the localisation of the CTLA-4 receptor at steady state in activated T cells and Tregs. Most trafficking receptors are predominantly located at the cell surface and only once the receptor binds ligand does the receptor internalise. CTLA-4 is unusual as its internalisation is constitutive and ligand binding is not an absolute

requirement for its internalisation. As such we found that in both activated T cells and Tregs CTLA-4 was located in intracellular compartments with minimal cell surface expression. Previous studies suggest that T cell activation by Src kinases results in the stabilisation of the CTLA-4 receptor at the plasma membrane (Bradshaw et al., 1997; Chuang et al., 1997; Hu et al., 2001; Shiratori et al., 1997). For this to occur the tyrosine residue of the YVKM motif encoded the CTLA-4 cytoplasmic domain is phosphorylated and can no longer associate with the clathrin adaptor AP-2 therefore preventing endocytosis. However, recent findings in our lab have shown that after T cell activation, CTLA-4 is mobilised to the plasma membrane but the receptor is not stabilised at the surface and continues to undergo endocytosis (Qureshi et al., 2012).

Work in this thesis shows that in activated T cells and regulatory T cells the total CTLA-4 expression is greater than the pool of surface and cycling CTLA-4. This indicates that CTLA-4 like GLUT4 could be stored in a storage compartment and could be mobilised from these compartments once the T cell encounters antigen (Slot et al., 1991). This could explain how effector T cells in the periphery are able to regulate the immune response with limited damage to self. In this instance, CTLA-4 is already available in a T cell ready to be trafficked to the surface and bind ligand.

The mechanism for CTLA-4 internalisation was first investigated when it was identified that following T cell activation most of the receptor resides in intracellular compartments and that any surface CTLA-4 is rapidly re-internalised (Chuang et al., 1997; Shiratori et al., 1997). It was concluded that CTLA-4 internalises via the clathrin pathway and relies on a tyrosine-based hydrophobic motif encoded in the cytoplasmic domain associating with the clathrin adaptor AP-2 (Chuang et al., 1997). The work in this thesis confirmed these findings where a mutation of the YVKM motif to AVKM abolished CTLA-4

internalisation providing evidence that this motif is directing endocytosis of CTLA-4 from the cell surface. Moreover, a transferrin uptake assay confirmed that CTLA-4 utilises the same internalisation pathway as TfR, a well-established receptor that uses clathrin. Importantly, the ability of CTLA-4 to endocytose appears to be evolutionary conserved evident since the emergence of fish, however the efficiency to internalise was greater in humans and least efficient in fish. The YxxF motif in trout CTLA-4 aligns well with the second tyrosine based motif YFIP in human CTLA-4 and the finding that some human CTLA-4 can internalise in the absence of YVKM could indicate that YFIP is mediating this poor and less efficient internalisation. Taken together this data could therefore suggest that the complex intracellular trafficking itinerary of mammalian CTLA-4 may have resulted from mutation and selection of cytoplasmic domain variants.

Another aim of this thesis was to address the post-internalisation fate of the CTLA-4 receptor. Once endocytic receptors are internalised they are sorted in intracellular compartments, where receptors are first delivered to early endosomes and from here a decision is made about whether the receptor will be recycled back to the surface or targeted for degradation (Trowbridge et al., 1993). We have previously shown that fraction of internalised CTLA-4 is recycled back to the cell surface and co-localises with Rab11 positive compartments (Qureshi et al., 2012). Work in this thesis confirms that CTLA-4 does recycle and that recycling is driven by the YVKM motif, which appears to be optimised for this function. Moreover even subtle changes in the YVKM motif as identified in *xenopus* CTLA-4, which encodes a YEKM motif, can impair recycling. An acidic residue in the +1 position of YXXM has been suggested to favor interaction with the lysosomal sorting adaptor AP-3 (Ohno et al., 1998) and this could explain the reduced receptor recycling we observed in human CTLA-4 when the YVKM motif was mutated to YEKM.

Most trafficking receptors such as EGFR are recycled back to the surface so as to maintain the signal transmitted by the receptor (Roepstorff et al., 2009; Waterman et al., 1998). The requirement for recycling would fit in well with the model of CTLA-4 function where the receptor has been suggested to deliver an inhibitory signal in T cells, as similar to EGFR, recycling would be the mechanism by which CTLA-4 prolongs its signal. However despite years of research, no such signalling cascade for CTLA-4 has been identified and it has now been suggested that CTLA-4 actually functions in a cell-extrinsic manner as opposed to a cell-intrinsic manner (Walker and Sansom, 2011). It is therefore interesting to speculate whether for the newly identified function of CTLA-4, transendocytosis, recycling is required to continuously remove ligand from the surface of APCs. CTLA-4 would therefore act like a pump to internalise ligand from the synapse between a T cell and an APC, target the ligand for degradation and recycle back to the cell surface to remove more ligand.

In keeping with previous findings, work in this thesis confirms that CTLA-4 is degraded in lysosomes. CTLA-4 co-localised with lysosomal markers in the presence of NH_4Cl. Moreover a rapid loss of protein was detected in the presence of CHX, which could explain why co-localisation of CTLA-4 with markers of lysosomal compartments has been difficult to detect in other studies. Previous studies suggest that degradation could be used as a mechanism to regulate the surface expression of CTLA-4 (Iida et al., 2000; Schneider et al., 1999), but the exact requirement for degradation remains to be identified. Work in this thesis has confirmed that the sensitivity to degradation is related to the endocytic potential of the receptor. However it is interesting to speculate whether for transendocytosis trafficking to lysosomal compartments could be used to dispose of ligand allowing CTLA-4 to recycle back to the cell surface.

EGFR like CTLA-4 binds to more than one ligand, each of which has a different affinity for the receptor (Henriksen et al., 2013; Roepstorff et al., 2009). As such depending on which ligand binds EGFR, the receptor undergoes a different fate. For instance TGF-α binding to EGFR results in receptor recycling because the receptor-ligand binding is not stable at the endosomal pH and so become dissociated. This frees up EGFR to recycle back to the surface whilst targeting TGF-α for degradation. In contrast, EGF binding to EGFR is stable at the endosomal pH and so both receptor and ligand are degraded (Hu et al., 2001). CD80 has a higher affinity for CTLA-4 compared to CD86 thus raising speculation that CTLA-4 fate could also be determined by ligand binding. However work in this thesis has shown that CTLA-4 can target both ligands for lysosomal degradation and the endocytic machinery may not solely be responsible for this function (Omar Qureshi; personal communication). Despite considerable variation between the cytoplasmic domain of human and trout CTLA-4, the trout CTLA-4 chimera could also transendocytose ligand further suggesting that other mechanisms contribute to this function of CTLA-4. Thus it appears that the function of transendocytosis appears to be evolutionary conserved, which could partly explain why the ligand-binding site is also conserved across species (Bernard et al., 2007; Teft et al., 2006).

Finally the work in this thesis addressed the mechanism regulating CTLA-4 recycling and the degradation of the receptor in lysosomes. Ubiquitination is recognised as an important signal for targeting trafficking receptors to lysosomes (Kumar et al., 2007). The process involves the attachment of ubiquitin to intracellular lysine residues of the receptor (Myung et al., 2001). CTLA-4 encodes five lysine residues in the cytoplasmic domain and the mutation of these residues to arginine (KLESS) produced a stable trafficking receptor that was resistant to lysosomal degradation. Moreover assessment of the ubiquitination status revealed that human CTLA-4 is ubiquitinated and the loss of ubiquitination in the KLESS mutant confirmed that the lysine residues are targets of ubiquitin attachment.

The lack of degradation resulted in an increase in CTLA-4 recycling as has been described for other trafficking receptors such as PAR2 (Jacob et al., 2005). The point at which ubiquitin is attached to CTLA-4 could be used as a checkpoint to vary CTLA-4 levels in Tregs depending on whether expression needs to be increased or decreased. By modulating CTLA-4 levels there could be a possibility to enhance the weak immune responses against tumor antigens in cancer or decrease the strong immune responses observed in graft rejection. Thus, targeting CTLA-4 in Tregs could prove pivotal when designing vaccines and treatment for autoimmune disease, cancers and in facilitating organ transplantation. Further work however is required to determine the effect ligand binding has on CTLA-4 ubiquitination. However, it is interesting to speculate whether after CTLA-4 targets the ligand for degradation, the receptor itself becomes deubiquitinated and recycles back to the plasma membrane to remove more ligand. Such a mechanism has been described for EGFR (Berlin et al., 2010) and moreover provides an additional explanation for why CTLA-4 would need to recycle.

More importantly further work is required to identify the E3 ligase responsible for ubiquitin attachment. Cbl-b is a candidate E3 ligase for TCR ubiquitination, which raises speculation if the same ligases could be associated with CTLA-4 downregulation and degradation in lysosomes. Moreover, the upregulation of Cbl-b in anergic $CD4^+$ $CD25^+$ T cells, a phenotype resulting from a lack of appropriate T cell co-stimulation, and the marked similarity between the phenotype of Cbl-b deficient and CTLA-4 deficient mice makes this E3 ligase an ideal candidate. Other candidates include GRAIL and Itch. Again both these ligases are upregulated in anergic T cells and in particular Itch, a HECT type E3 ligase, binds to PPxY motifs via WW domains (Ishihara et al., 2011). Thus it is interesting to speculate whether Itch binds to the PPPY motif encoded in the CTLA-4 extracellular domain and thereby regulates CTLA-4 ubiquitination. However, in order to facilitate ubiquitin attachment the E3 ubiquitin ligase should be recruited close to the intracellular lysine residues. Thus, the distance between the PPPY motif in the

CTLA-4 extracellular domain and the cytoplasmic lysine residues may rule out the involvement of a HECT type E3 ligase.

Most trafficking receptors targeted for lysosomal degradation are ubiquitinated and subsequently sorted into MVBs (Wollert and Hurley, 2010). CTLA-4 has been reported to be present in non-lysosomal, perinuclear vesicles, which could represent MVBs or late endosomes (Mead et al., 2005). Interestingly TSG101, a component of the ESCRT complex that regulates MVB formation binds to ubiquitinated cargo and to PT/SAP motifs (Dilley et al., 2010). CTLA-4 encodes a PTEP motif the significance of which remains to be identified. However, work in this thesis has shown that a mutation of the proline residue to arginine resulted in a stable CTLA-4 receptor that exhibited the same characteristics as KLESS. The fact that the ubiquitin targets are still intact in the ATEP mutant suggests this could be the binding site for a protein required prior to the attachment of ubiquitin to the lysine residues. This protein could either act as an intermediate recruiting the E3 ubiquitin ligase or could be the binding site for the E3 ubiquitin ligase. Moreover the close proximity of the PTEP motif to the cytoplasmic lysine residues makes this site a more ideal candidate to recruit or bind an E3 ubiquitin ligase than the PPPY motif located in the extracellular domain.

In summary, the work in this thesis has provided further insight into the intracellular trafficking of the CTLA-4 receptor demonstrating in particular how the receptors ability to undergo constitutive internalisation and how its post-endocytic sorting could be related to the recently identified function of transendocytosis. The findings are novel and exciting since by increasing our understanding on how CTLA-4 traffics in activated T cells or Tregs provides us with the opportunity to possibly manipulate CTLA-4 levels in certain intracellular compartments, which could prove to be invaluable therapeutically.

Work in this thesis also investigated the mechanisms responsible for CTLA-4 recycling and degradation with a particular emphasis on the sorting motifs encoded in the cytoplasmic domain. Since single or double point lysine mutants could not identify which lysine residue/s are targets of ubiquitination, it is concluded that in the absence of one or more lysine residues, other lysine residues could compensate. To strengthen this conclusion, more work would be required and the most obvious step to take would be to perform mass spectrometry. This technique has been used successfully to identify lysine residues that serve as targets of ubiquitin attachment for other receptors such as EGFR. Moreover, a second advantage of using mass spectrometry would be to identify the E3 ligase responsible for ubiquitin attachment. This would be more difficult as the E3 ligase would bind to the receptor transiently but nevertheless this is not impossible. Moreover, it would be worthwhile investigating if ligand binding has an effect on CTLA-4 receptor ubiquitination to see if the susceptibility of CTLA-4 towards lysosomal degradation is increased or decreased.

The vertebrate immune system has evolved considerably with the development of lymph nodes (Boehm et al., 2012) and the emergence of a specialised subset of T cells, Tregs, which regulate enhanced effector functions (Sansom and Walker, 2006). Clearing up longstanding issues of how the biology of the CTLA-4 receptor and its function are related could prove crucial in the treatment of autoimmune disease and cancers where Tregs are known to play an important role. Moreover, further detailed mechanisms into how CTLA-4 is sorted into various intracellular compartments could be used as checkpoints in regulating the level of CTLA-4 when designing vaccines.

7.0 REFERENCES

Aderem, A., and Underhill, D.M. (1999). Mechanisms of phagocytosis in macrophages. Annu Rev Immunol *17*, 593-623.

Ajioka, R.S., and Kaplan, J. (1986). Intracellular pools of transferrin receptors result from constitutive internalization of unoccupied receptors. Proc Natl Acad Sci U S A *83*, 6445-6449.

Alegre, M.L., Frauwirth, K.A., and Thompson, C.B. (2001). T-cell regulation by CD28 and CTLA-4. Nat Rev Immunol *1*, 220-228.

Anandasabapathy, N., Ford, G.S., Bloom, D., Holness, C., Paragas, V., Seroogy, C., Skrenta, H., Hollenhorst, M., Fathman, C.G., and Soares, L. (2003). GRAIL: an E3 ubiquitin ligase that inhibits cytokine gene transcription is expressed in anergic CD4+ T cells. Immunity *18*, 535-547.

Anderson, R.G., and Jacobson, K. (2002). A role for lipid shells in targeting proteins to caveolae, rafts, and other lipid domains. Science *296*, 1821-1825.

Annacker, O., Asseman, C., Read, S., and Powrie, F. (2003). Interleukin-10 in the regulation of T cell-induced colitis. Journal of autoimmunity *20*, 277-279.

Babst, M., Katzmann, D.J., Snyder, W.B., Wendland, B., and Emr, S.D. (2002). Endosome-associated complex, ESCRT-II, recruits transport machinery for protein sorting at the multivesicular body. Dev Cell *3*, 283-289.

Bache, K.G., Stuffers, S., Malerod, L., Slagsvold, T., Raiborg, C., Lechardeur, D., Walchli, S., Lukacs, G.L., Brech, A., and Stenmark, H. (2006). The ESCRT-III subunit hVps24 is required for degradation but not silencing of the epidermal growth factor receptor. Mol Biol Cell *17*, 2513-2523.

Bachmaier, K., Krawczyk, C., Kozieradzki, I., Kong, Y.Y., Sasaki, T., Oliveira-dos-Santos, A., Mariathasan, S., Bouchard, D., Wakeham, A., Itie, A.*, et al.* (2000). Negative regulation of lymphocyte activation and autoimmunity by the molecular adaptor Cbl-b. Nature *403*, 211-216.

Bachmann, M.F., Kohler, G., Ecabert, B., Mak, T.W., and Kopf, M. (1999). Cutting edge: lymphoproliferative disease in the absence of CTLA-4 is not T cell autonomous. J Immunol *163*, 1128-1131.

Baier-Bitterlich, G., Uberall, F., Bauer, B., Fresser, F., Wachter, H., Grunicke, H., Utermann, G., Altman, A., and Baier, G. (1996). Protein kinase C-theta isoenzyme selective stimulation of the transcription factor complex AP-1 in T lymphocytes. Molecular and cellular biology *16*, 1842-1850.

Balut, C.M., Loch, C.M., and Devor, D.C. (2011). Role of ubiquitylation and USP8-dependent deubiquitylation in the endocytosis and lysosomal targeting of plasma membrane KCa3.1. FASEB journal : official publication of the Federation of American Societies for Experimental Biology *25*, 3938-3948.

Baumann, H., and Doyle, D. (1978). Turnover of plasma membrane glycoproteins and glycolipids of hepatoma tissue culture cells. J Biol Chem *253*, 4408-4418.

Berlin, I., Schwartz, H., and Nash, P.D. (2010). Regulation of epidermal growth factor receptor ubiquitination and trafficking by the USP8.STAM complex. J Biol Chem *285*, 34909-34921.

Bernard, D., Hansen, J.D., Du Pasquier, L., Lefranc, M.P., Benmansour, A., and Boudinot, P. (2007). Costimulatory receptors in jawed vertebrates: conserved CD28, odd CTLA4 and multiple BTLAs. Dev Comp Immunol *31*, 255-271.

Bernard, D., Riteau, B., Hansen, J.D., Phillips, R.B., Michel, F., Boudinot, P., and Benmansour, A. (2006). Costimulatory receptors in a teleost fish: typical CD28, elusive CTLA4. J Immunol *176*, 4191-4200.

Boasso, A., Herbeuval, J.P., Hardy, A.W., Winkler, C., and Shearer, G.M. (2005). Regulation of indoleamine 2,3-dioxygenase and tryptophanyl-tRNA-synthetase by CTLA-4-Fc in human CD4+ T cells. Blood *105*, 1574-1581.

Boehm, M., and Bonifacino, J.S. (2001). Adaptins: the final recount. Mol Biol Cell *12*, 2907-2920.

Boehm, T., Hess, I., and Swann, J.B. (2012). Evolution of lymphoid tissues. Trends Immunol.

Borriello, F., Sethna, M.P., Boyd, S.D., Schweitzer, A.N., Tivol, E.A., Jacoby, D., Strom, T.B., Simpson, E.M., Freeman, G.J., and Sharpe, A.H. (1997). B7-1 and B7-2 have overlapping, critical roles in immunoglobulin class switching and germinal center formation. Immunity *6*, 303-313.

Bradshaw, J.D., Lu, P., Leytze, G., Rodgers, J., Schieven, G.L., Bennett, K.L., Linsley, P.S., and Kurtz, S.E. (1997). Interaction of the cytoplasmic tail of CTLA-4 (CD152) with a clathrin-associated protein is negatively regulated by tyrosine phosphorylation. Biochemistry *36*, 15975-15982.

Brodsky, F.M., Chen, C.Y., Knuehl, C., Towler, M.C., and Wakeham, D.E. (2001). Biological basket weaving: formation and function of clathrin-coated vesicles. Annual review of cell and developmental biology *17*, 517-568.

Burgos, P.V., Mardones, G.A., Rojas, A.L., daSilva, L.L., Prabhu, Y., Hurley, J.H., and Bonifacino, J.S. (2010). Sorting of the Alzheimer's disease amyloid precursor protein mediated by the AP-4 complex. Dev Cell *18*, 425-436.

Cagan, R.L., Kramer, H., Hart, A.C., and Zipursky, S.L. (1992). The bride of sevenless and sevenless interaction: internalization of a transmembrane ligand. Cell *69*, 393-399.

Carreno, B.M., Carter, L.L., and Collins, M. (2005). Therapeutic opportunities in the B7/CD28 family of ligands and receptors. Current opinion in pharmacology *5*, 424-430.

Carreno, B.M., and Collins, M. (2002). The B7 family of ligands and its receptors: new pathways for costimulation and inhibition of immune responses. Annu Rev Immunol *20*, 29-53.

Chambers, C.A., Sullivan, T.J., Truong, T., and Allison, J.P. (1998). Secondary but not primary T cell responses are enhanced in CTLA-4-deficient CD8+ T cells. Eur J Immunol *28*, 3137-3143.

Chen, W., Jin, W., and Wahl, S.M. (1998). Engagement of cytotoxic T lymphocyte-associated antigen 4 (CTLA-4) induces transforming growth factor beta (TGF-beta) production by murine CD4(+) T cells. J Exp Med *188*, 1849-1857.

Chen, W.J., Goldstein, J.L., and Brown, M.S. (1990). NPXY, a sequence often found in cytoplasmic tails, is required for coated pit-mediated internalization of the low density lipoprotein receptor. J Biol Chem *265*, 3116-3123.

Chen, X., and Jensen, P.E. (2008). The role of B lymphocytes as antigen-presenting cells. Archivum immunologiae et therapiae experimentalis *56*, 77-83.

Chi, S., Cao, H., Wang, Y., and McNiven, M.A. (2011). Recycling of the epidermal growth factor receptor is mediated by a novel form of the clathrin adaptor protein Eps15. J Biol Chem *286*, 35196-35208.

Chien, Y.H., Gascoigne, N.R., Kavaler, J., Lee, N.E., and Davis, M.M. (1984). Somatic recombination in a murine T-cell receptor gene. Nature *309*, 322-326.

Chikuma, S., Abbas, A.K., and Bluestone, J.A. (2005). B7-independent inhibition of T cells by CTLA-4. J Immunol *175*, 177-181.

Chikuma, S., Imboden, J.B., and Bluestone, J.A. (2003). Negative regulation of T cell receptor-lipid raft interaction by cytotoxic T lymphocyte-associated antigen 4. J Exp Med *197*, 129-135.

Chu, F.F., and Doyle, D. (1985). Turnover of plasma membrane proteins in rat hepatoma cells and primary cultures of rat hepatocytes. J Biol Chem *260*, 3097-3107.

Chuang, E., Alegre, M.L., Duckett, C.S., Noel, P.J., Vander Heiden, M.G., and Thompson, C.B. (1997). Interaction of CTLA-4 with the clathrin-associated protein AP50 results in ligand-independent endocytosis that limits cell surface expression. J Immunol *159*, 144-151.

Clague, M.J., and Hammond, D.E. (2006). Membrane traffic: catching the lysosome express. Curr Biol *16*, R416-418.

Clevers, H., Alarcon, B., Wileman, T., and Terhorst, C. (1988). The T cell receptor/CD3 complex: a dynamic protein ensemble. Annu Rev Immunol *6*, 629-662.

Collins, A.V., Brodie, D.W., Gilbert, R.J., Iaboni, A., Manso-Sancho, R., Walse, B., Stuart, D.I., van der Merwe, P.A., and Davis, S.J. (2002). The interaction properties of costimulatory molecules revisited. Immunity *17*, 201-210.

Conner, S.D., and Schmid, S.L. (2003). Regulated portals of entry into the cell. Nature *422*, 37-44.

Cooper, G.M. (2000). The Cell: A Molecular Approach (Sinauer Associates, Inc).

Cottrell, G.S., Padilla, B., Pikios, S., Roosterman, D., Steinhoff, M., Gehringer, D., Grady, E.F., and Bunnett, N.W. (2006). Ubiquitin-dependent down-regulation of the neurokinin-1 receptor. J Biol Chem *281*, 27773-27783.

Darlington, P.J., Baroja, M.L., Chau, T.A., Siu, E., Ling, V., Carreno, B.M., and Madrenas, J. (2002). Surface cytotoxic T lymphocyte-associated antigen 4 partitions within lipid rafts and relocates to the immunological synapse under conditions of inhibition of T cell activation. J Exp Med *195*, 1337-1347.

Davis, M.M., Boniface, J.J., Reich, Z., Lyons, D., Hampl, J., Arden, B., and Chien, Y. (1998). Ligand recognition by alpha beta T cell receptors. Annu Rev Immunol *16*, 523-544.

Davis, P.M., Abraham, R., Xu, L., Nadler, S.G., and Suchard, S.J. (2007). Abatacept binds to the Fc receptor CD64 but does not mediate complement-dependent cytotoxicity or antibody-dependent cellular cytotoxicity. The Journal of rheumatology *34*, 2204-2210.

d'Azzo, A., Bongiovanni, A., and Nastasi, T. (2005). E3 ubiquitin ligases as regulators of membrane protein trafficking and degradation. Traffic *6*, 429-441.

de Felipe, P. (2004). Skipping the co-expression problem: the new 2A "CHYSEL" technology. Genetic vaccines and therapy *2*, 13.

Deinhardt, K., Berninghausen, O., Willison, H.J., Hopkins, C.R., and Schiavo, G. (2006). Tetanus toxin is internalized by a sequential clathrin-dependent mechanism initiated within lipid microdomains and independent of epsin1. J Cell Biol *174*, 459-471.

Delves, P.J., and Roitt, I.M. (2000a). The immune system. First of two parts. The New England journal of medicine *343*, 37-49.

Delves, P.J., and Roitt, I.M. (2000b). The immune system. Second of two parts. The New England journal of medicine *343*, 108-117.

Deneka, M., Neeft, M., Popa, I., van Oort, M., Sprong, H., Oorschot, V., Klumperman, J., Schu, P., and van der Sluijs, P. (2003). Rabaptin-5alpha/rabaptin-4 serves as a linker between rab4 and gamma(1)-adaptin in membrane recycling from endosomes. Embo J *22*, 2645-2657.

Dilley, K.A., Gregory, D., Johnson, M.C., and Vogt, V.M. (2010). An LYPSL late domain in the gag protein contributes to the efficient release and replication of Rous sarcoma virus. Journal of virology *84*, 6276-6287.

Doherty, G.J., and McMahon, H.T. (2009). Mechanisms of endocytosis. Annual review of biochemistry *78*, 857-902.

Doyotte, A., Russell, M.R., Hopkins, C.R., and Woodman, P.G. (2005). Depletion of TSG101 forms a mammalian "Class E" compartment: a multicisternal early endosome with multiple sorting defects. Journal of cell science *118*, 3003-3017.

Drake, M.T., Shenoy, S.K., and Lefkowitz, R.J. (2006). Trafficking of G protein-coupled receptors. Circulation research *99*, 570-582.

Edidin, M. (2001). Shrinking patches and slippery rafts: scales of domains in the plasma membrane. Trends Cell Biol *11*, 492-496.

Egen, J.G., and Allison, J.P. (2002). Cytotoxic T lymphocyte antigen-4 accumulation in the immunological synapse is regulated by TCR signal strength. Immunity *16*, 23-35.

Egen, J.G., Kuhns, M.S., and Allison, J.P. (2002). CTLA-4: new insights into its biological function and use in tumor immunotherapy. Nat Immunol *3*, 611-618.

Genovese, M.C., Becker, J.C., Schiff, M., Luggen, M., Sherrer, Y., Kremer, J., Birbara, C., Box, J., Natarajan, K., Nuamah, I.*, et al.* (2005). Abatacept for rheumatoid arthritis refractory to tumor necrosis factor alpha inhibition. The New England journal of medicine *353*, 1114-1123.

Glenney, J.R., Jr., Chen, W.S., Lazar, C.S., Walton, G.M., Zokas, L.M., Rosenfeld, M.G., and Gill, G.N. (1988). Ligand-induced endocytosis of the EGF receptor is blocked by mutational inactivation and by microinjection of anti-phosphotyrosine antibodies. Cell *52*, 675-684.

Godfrey, W.R., Spoden, D.J., Ge, Y.G., Baker, S.R., Liu, B., Levine, B.L., June, C.H., Blazar, B.R., and Porter, S.B. (2005). Cord blood CD4(+)CD25(+)-derived T regulatory cell lines express FoxP3 protein and manifest potent suppressor function. Blood *105*, 750-758.

Goh, L.K., and Sorkin, A. (2013). Endocytosis of receptor tyrosine kinases. Cold Spring Harbor perspectives in biology *5*, a017459.

Goodnow, C.C., Sprent, J., Fazekas de St Groth, B., and Vinuesa, C.G. (2005). Cellular and genetic mechanisms of self tolerance and autoimmunity. Nature *435*, 590-597.

Gough, S.C., Walker, L.S., and Sansom, D.M. (2005). CTLA4 gene polymorphism and autoimmunity. Immunol Rev *204*, 102-115.

Grant, B.D., and Donaldson, J.G. (2009). Pathways and mechanisms of endocytic recycling. Nature reviews. Molecular cell biology *10*, 597-608.

Gray, D.H., Ueno, T., Chidgey, A.P., Malin, M., Goldberg, G.L., Takahama, Y., and Boyd, R.L. (2005). Controlling the thymic microenvironment. Current opinion in immunology *17*, 137-143.

Green, E.G., Ramm, E., Riley, N.M., Spiro, D.J., Goldenring, J.R., and Wessling-Resnick, M. (1997). Rab11 is associated with transferrin-containing recycling compartments in K562 cells. Biochemical and biophysical research communications *239*, 612-616.

Grohmann, U., Orabona, C., Fallarino, F., Vacca, C., Calcinaro, F., Falorni, A., Candeloro, P., Belladonna, M.L., Bianchi, R., Fioretti, M.C., and Puccetti, P. (2002). CTLA-4-Ig regulates tryptophan catabolism in vivo. Nat Immunol *3*, 1097-1101.

Gross, J.A., St John, T., and Allison, J.P. (1990). The murine homologue of the T lymphocyte antigen CD28. Molecular cloning and cell surface expression. J Immunol *144*, 3201-3210.

Gruenberg, J., and Maxfield, F.R. (1995). Membrane transport in the endocytic pathway. Current opinion in cell biology *7*, 552-563.

Haigler, H.T., McKanna, J.A., and Cohen, S. (1979). Direct visualization of the binding and internalization of a ferritin conjugate of epidermal growth factor in human carcinoma cells A-431. J Cell Biol *81*, 382-395.

Hall, A., and Nobes, C.D. (2000). Rho GTPases: molecular switches that control the organization and dynamics of the actin cytoskeleton. Philosophical transactions of the Royal Society of London. Series B, Biological sciences *355*, 965-970.

Hare, J.F., and Taylor, K. (1991). Mechanisms of plasma membrane protein degradation: recycling proteins are degraded more rapidly than those confined to the cell surface. Proc Natl Acad Sci U S A *88*, 5902-5906.

Henriksen, L., Grandal, M.V., Knudsen, S.L., van Deurs, B., and Grovdal, L.M. (2013). Internalization mechanisms of the epidermal growth factor receptor after activation with different ligands. PloS one *8*, e58148.

Heissmeyer, V., Macian, F., Im, S.H., Varma, R., Feske, S., Venuprasad, K., Gu, H., Liu, Y.C., Dustin, M.L., and Rao, A. (2004). Calcineurin imposes T cell unresponsiveness through targeted proteolysis of signaling proteins. Nat Immunol *5*, 255-265.

Heuser, J.E., and Anderson, R.G. (1989). Hypertonic media inhibit receptor-mediated endocytosis by blocking clathrin-coated pit formation. J Cell Biol *108*, 389-400.

Hirst, J., Barlow, L.D., Francisco, G.C., Sahlender, D.A., Seaman, M.N., Dacks, J.B., and Robinson, M.S. (2011). The fifth adaptor protein complex. PLoS biology *9*, e1001170.

Honing, S., Griffith, J., Geuze, H.J., and Hunziker, W. (1996). The tyrosine-based lysosomal targeting signal in lamp-1 mediates sorting into Golgi-derived clathrin-coated vesicles. Embo J *15*, 5230-5239.

Hu, H., Rudd, C.E., and Schneider, H. (2001). Src kinases Fyn and Lck facilitate the accumulation of phosphorylated CTLA-4 and its association with PI-3 kinase in intracellular compartments of T-cells. Biochemical and biophysical research communications *288*, 573-578.

Huang, D.T., Miller, D.W., Mathew, R., Cassell, R., Holton, J.M., Roussel, M.F., and Schulman, B.A. (2004a). A unique E1-E2 interaction required for optimal conjugation of the ubiquitin-like protein NEDD8. Nature structural & molecular biology *11*, 927-935.

Huang, D.T., Walden, H., Duda, D., and Schulman, B.A. (2004b). Ubiquitin-like protein activation. Oncogene *23*, 1958-1971.

Huang, F., Kirkpatrick, D., Jiang, X., Gygi, S., and Sorkin, A. (2006). Differential regulation of EGF receptor internalization and degradation by multiubiquitination within the kinase domain. Mol Cell *21*, 737-748.

Huotari, J., and Helenius, A. (2011). Endosome maturation. Embo J *30*, 3481-3500.

Iacopetta, B.J., Rothenberger, S., and Kuhn, L.C. (1988). A role for the cytoplasmic domain in transferrin receptor sorting and coated pit formation during endocytosis. Cell *54*, 485-489.

Iida, T., Ohno, H., Nakaseko, C., Sakuma, M., Takeda-Ezaki, M., Arase, H., Kominami, E., Fujisawa, T., and Saito, T. (2000). Regulation of cell surface expression of CTLA-4 by secretion of CTLA-4-containing lysosomes upon activation of CD4+ T cells. J Immunol *165*, 5062-5068.

Ikemizu, S., Gilbert, R.J., Fennelly, J.A., Collins, A.V., Harlos, K., Jones, E.Y., Stuart, D.I., and Davis, S.J. (2000). Structure and dimerization of a soluble form of B7-1. Immunity *12*, 51-60.

Inaba, K., Steinman, R.M., Van Voorhis, W.C., and Muramatsu, S. (1983). Dendritic cells are critical accessory cells for thymus-dependent antibody responses in mouse and in man. Proc Natl Acad Sci U S A *80*, 6041-6045.

Ishihara, T., Inoue, J., Kozaki, K., Imoto, I., and Inazawa, J. (2011). HECT-type ubiquitin ligase ITCH targets lysosomal-associated protein multispanning transmembrane 5 (LAPTM5) and prevents LAPTM5-mediated cell death. J Biol Chem *286*, 44086-44094.

Jacob, C., Cottrell, G.S., Gehringer, D., Schmidlin, F., Grady, E.F., and Bunnett, N.W. (2005). c-Cbl mediates ubiquitination, degradation, and down-regulation of human protease-activated receptor 2. J Biol Chem *280*, 16076-16087.

Jones, M.E., and Zhuang, Y. (2007). Acquisition of a functional T cell receptor during T lymphocyte development is enforced by HEB and E2A transcription factors. Immunity *27*, 860-870.

Kashles, O., Szapary, D., Bellot, F., Ullrich, A., Schlessinger, J., and Schmidt, A. (1988). Ligand-induced stimulation of epidermal growth factor receptor mutants with altered transmembrane regions. Proc Natl Acad Sci U S A *85*, 9567-9571.

Katzmann, D.J., Babst, M., and Emr, S.D. (2001). Ubiquitin-dependent sorting into the multivesicular body pathway requires the function of a conserved endosomal protein sorting complex, ESCRT-I. Cell *106*, 145-155.

Katzmann, D.J., Odorizzi, G., and Emr, S.D. (2002). Receptor downregulation and multivesicular-body sorting. Nature reviews. Molecular cell biology *3*, 893-905.

Kibbey, R.G., Rizo, J., Gierasch, L.M., and Anderson, R.G. (1998). The LDL receptor clustering motif interacts with the clathrin terminal domain in a reverse turn conformation. J Cell Biol *142*, 59-67.

Kirchhausen, T., Bonifacino, J.S., and Riezman, H. (1997). Linking cargo to vesicle formation: receptor tail interactions with coat proteins. Current opinion in cell biology *9*, 488-495.

Klueg, K.M., Parody, T.R., and Muskavitch, M.A. (1998). Complex proteolytic processing acts on Delta, a transmembrane ligand for Notch, during Drosophila development. Mol Biol Cell *9*, 1709-1723.

Kouranti, I., Sachse, M., Arouche, N., Goud, B., and Echard, A. (2006). Rab35 regulates an endocytic recycling pathway essential for the terminal steps of cytokinesis. Curr Biol *16*, 1719-1725.

Kozik, P., Francis, R.W., Seaman, M.N., and Robinson, M.S. (2010). A screen for endocytic motifs. Traffic *11*, 843-855.

Kremer, J.M., Dougados, M., Emery, P., Durez, P., Sibilia, J., Shergy, W., Steinfeld, S., Tindall, E., Becker, J.C., Li, T.*, et al.* (2005). Treatment of rheumatoid arthritis with the selective costimulation modulator abatacept: twelve-month results of a phase iib, double-blind, randomized, placebo-controlled trial. Arthritis and rheumatism *52*, 2263-2271.

Krummel, M.F., and Allison, J.P. (1995). CD28 and CTLA-4 have opposing effects on the response of T cells to stimulation. J Exp Med *182*, 459-465.

Kumar, K.G., Barriere, H., Carbone, C.J., Liu, J., Swaminathan, G., Xu, P., Li, Y., Baker, D.P., Peng, J., Lukacs, G.L., and Fuchs, S.Y. (2007). Site-specific ubiquitination exposes a linear motif to promote interferon-alpha receptor endocytosis. J Cell Biol *179*, 935-950.

Kumar, K.G., Krolewski, J.J., and Fuchs, S.Y. (2004). Phosphorylation and specific ubiquitin acceptor sites are required for ubiquitination and degradation of the IFNAR1 subunit of type I interferon receptor. J Biol Chem *279*, 46614-46620.

Kusakari, S., Ohnishi, H., Jin, F.J., Kaneko, Y., Murata, T., Murata, Y., Okazawa, H., and Matozaki, T. (2008). Trans-endocytosis of CD47 and SHPS-1 and its role in regulation of the CD47-SHPS-1 system. Journal of cell science *121*, 1213-1223.

Lamaze, C., Dujeancourt, A., Baba, T., Lo, C.G., Benmerah, A., and Dautry-Varsat, A. (2001). Interleukin 2 receptors and detergent-resistant membrane domains define a clathrin-independent endocytic pathway. Molecular cell *7*, 661-671.

Larsen, C.P., Pearson, T.C., Adams, A.B., Tso, P., Shirasugi, N., Strobert, E., Anderson, D., Cowan, S., Price, K., Naemura, J.*, et al.* (2005). Rational development of LEA29Y (belatacept), a high-affinity variant of CTLA4-Ig with potent immunosuppressive properties. American journal of transplantation : official journal of the American Society of Transplantation and the American Society of Transplant Surgeons *5*, 443-453.

Laufer, T.M. (2008). Tolerance to self: which cells kill? PLoS biology *6*, e241.

Lavezzari, G., McCallum, J., Dewey, C.M., and Roche, K.W. (2004). Subunit-specific regulation of NMDA receptor endocytosis. The Journal of neuroscience : the official journal of the Society for Neuroscience *24*, 6383-6391.

Lazarovits, J., and Roth, M. (1988). A single amino acid change in the cytoplasmic domain allows the influenza virus hemagglutinin to be endocytosed through coated pits. Cell *53*, 743-752.

Le Roy, C., and Wrana, J.L. (2005). Clathrin- and non-clathrin-mediated endocytic regulation of cell signalling. Nature reviews. Molecular cell biology *6*, 112-126.

Lenschow, D.J., Walunas, T.L., and Bluestone, J.A. (1996). CD28/B7 system of T cell costimulation. Annu Rev Immunol *14*, 233-258.

Lenschow, D.J., Zeng, Y., Thistlethwaite, J.R., Montag, A., Brady, W., Gibson, M.G., Linsley, P.S., and Bluestone, J.A. (1992). Long-term survival of xenogeneic pancreatic islet grafts induced by CTLA4lg. Science *257*, 789-792.

Letourneur, F., and Klausner, R.D. (1992). A novel di-leucine motif and a tyrosine-based motif independently mediate lysosomal targeting and endocytosis of CD3 chains. Cell *69*, 1143-1157.

Leung, H.T., Bradshaw, J., Cleaveland, J.S., and Linsley, P.S. (1995). Cytotoxic T lymphocyte-associated molecule-4, a high-avidity receptor for CD80 and CD86, contains an intracellular localization motif in its cytoplasmic tail. J Biol Chem *270*, 25107-25114.

Levings, M.K., Sangregorio, R., Sartirana, C., Moschin, A.L., Battaglia, M., Orban, P.C., and Roncarolo, M.G. (2002). Human CD25+CD4+ T suppressor cell clones produce transforming growth factor beta, but not interleukin 10, and are distinct from type 1 T regulatory cells. J Exp Med *196*, 1335-1346.

Levkowitz, G., Waterman, H., Zamir, E., Kam, Z., Oved, S., Langdon, W.Y., Beguinot, L., Geiger, B., and Yarden, Y. (1998). c-Cbl/Sli-1 regulates endocytic sorting and ubiquitination of the epidermal growth factor receptor. Genes & development *12*, 3663-3674.

Li, M.O., Wan, Y.Y., Sanjabi, S., Robertson, A.K., and Flavell, R.A. (2006). Transforming growth factor-beta regulation of immune responses. Annu Rev Immunol *24*, 99-146.

Li, S., Seitz, R., and Lisanti, M.P. (1996). Phosphorylation of caveolin by src tyrosine kinases. The alpha-isoform of caveolin is selectively phosphorylated by v-Src in vivo. J Biol Chem *271*, 3863-3868.

Lin, H., Bolling, S.F., Linsley, P.S., Wei, R.Q., Gordon, D., Thompson, C.B., and Turka, L.A. (1993). Long-term acceptance of major histocompatibility complex mismatched cardiac allografts induced by CTLA4Ig plus donor-specific transfusion. J Exp Med *178*, 1801-1806.

Lindsten, T., Lee, K.P., Harris, E.S., Petryniak, B., Craighead, N., Reynolds, P.J., Lombard, D.B., Freeman, G.J., Nadler, L.M., Gray, G.S., and et al. (1993). Characterization of CTLA-4 structure and expression on human T cells. J Immunol *151*, 3489-3499.

Linsley, P.S., Bradshaw, J., Greene, J., Peach, R., Bennett, K.L., and Mittler, R.S. (1996). Intracellular trafficking of CTLA-4 and focal localization towards sites of TCR engagement. Immunity *4*, 535-543.

Linsley, P.S., Brady, W., Urnes, M., Grosmaire, L.S., Damle, N.K., and Ledbetter, J.A. (1991). CTLA-4 is a second receptor for the B cell activation antigen B7. J Exp Med *174*, 561-569.

Luzio, J.P., Rous, B.A., Bright, N.A., Pryor, P.R., Mullock, B.M., and Piper, R.C. (2000). Lysosome-endosome fusion and lysosome biogenesis. Journal of cell science *113 (Pt 9)*, 1515-1524.

Madshus, I.H., and Stang, E. (2009). Internalization and intracellular sorting of the EGF receptor: a model for understanding the mechanisms of receptor trafficking. J Cell Sci *122*, 3433-3439.

Malmstrom, V., Trollmo, C., and Klareskog, L. (2005). Modulating co-stimulation: a rational strategy in the treatment of rheumatoid arthritis? Arthritis research & therapy *7 Suppl 2*, S15-20.

Marchese, A., Paing, M.M., Temple, B.R., and Trejo, J. (2008). G protein-coupled receptor sorting to endosomes and lysosomes. Annual review of pharmacology and toxicology *48*, 601-629.

Marotti, L.A., Jr., Newitt, R., Wang, Y., Aebersold, R., and Dohlman, H.G. (2002). Direct identification of a G protein ubiquitination site by mass spectrometry. Biochemistry *41*, 5067-5074.

Martin, M., Schneider, H., Azouz, A., and Rudd, C.E. (2001). Cytotoxic T lymphocyte antigen 4 and CD28 modulate cell surface raft expression in their regulation of T cell function. J Exp Med *194*, 1675-1681.

Masteller, E.L., Chuang, E., Mullen, A.C., Reiner, S.L., and Thompson, C.B. (2000). Structural analysis of CTLA-4 function in vivo. J Immunol *164*, 5319-5327.

Mayor, S., and Pagano, R.E. (2007). Pathways of clathrin-independent endocytosis. Nature reviews. Molecular cell biology *8*, 603-612.

McAdam, A.J., Schweitzer, A.N., and Sharpe, A.H. (1998). The role of B7 co-stimulation in activation and differentiation of CD4+ and CD8+ T cells. Immunol Rev *165*, 231-247.

Mead, K.I., Zheng, Y., Manzotti, C.N., Perry, L.C., Liu, M.K., Burke, F., Powner, D.J., Wakelam, M.J., and Sansom, D.M. (2005). Exocytosis of CTLA-4 is dependent on phospholipase D and ADP ribosylation factor-1 and stimulated during activation of regulatory T cells. J Immunol *174*, 4803-4811.

Melikova, M.S., Kondratov, K.A., and Kornilova, E.S. (2006). Two different stages of epidermal growth factor (EGF) receptor endocytosis are sensitive to free ubiquitin depletion produced by proteasome inhibitor MG132. Cell biology international *30*, 31-43.

Mellman, I. (1996). Endocytosis and molecular sorting. Annual review of cell and developmental biology *12*, 575-625.

Mellor, A.L., Chandler, P., Baban, B., Hansen, A.M., Marshall, B., Pihkala, J., Waldmann, H., Cobbold, S., Adams, E., and Munn, D.H. (2004). Specific subsets of murine dendritic cells acquire potent T cell regulatory functions following CTLA4-mediated induction of indoleamine 2,3 dioxygenase. Int Immunol *16*, 1391-1401.

Mellor, A.L., and Munn, D.H. (2004). IDO expression by dendritic cells: tolerance and tryptophan catabolism. Nat Rev Immunol *4*, 762-774.

Merrill, J.T., Burgos-Vargas, R., Westhovens, R., Chalmers, A., D'Cruz, D., Wallace, D.J., Bae, S.C., Sigal, L., Becker, J.C., Kelly, S.*, et al.* (2010). The efficacy and safety of abatacept in patients with non-life-threatening manifestations of systemic lupus erythematosus: results of a twelve-month, multicenter, exploratory, phase IIb, randomized, double-blind, placebo-controlled trial. Arthritis and rheumatism *62*, 3077-3087.

Milich, D.R., Linsley, P.S., Hughes, J.L., and Jones, J.E. (1994). Soluble CTLA-4 can suppress autoantibody production and elicit long term unresponsiveness in a novel transgenic model. J Immunol *153*, 429-435.

Miranda, M., and Sorkin, A. (2007). Regulation of receptors and transporters by ubiquitination: new insights into surprisingly similar mechanisms. Molecular interventions *7*, 157-167.

Misra, N., Bayry, J., Lacroix-Desmazes, S., Kazatchkine, M.D., and Kaveri, S.V. (2004). Cutting edge: human CD4+CD25+ T cells restrain the maturation and antigen-presenting function of dendritic cells. J Immunol *172*, 4676-4680.

Miyatake, S., Nakaseko, C., Umemori, H., Yamamoto, T., and Saito, T. (1998). Src family tyrosine kinases associate with and phosphorylate CTLA-4 (CD152). Biochemical and biophysical research communications *249*, 444-448.

Mukherjee, S., Ghosh, R.N., and Maxfield, F.R. (1997). Endocytosis. Physiological reviews *77*, 759-803.

Munn, D.H., Shafizadeh, E., Attwood, J.T., Bondarev, I., Pashine, A., and Mellor, A.L. (1999). Inhibition of T cell proliferation by macrophage tryptophan catabolism. J Exp Med *189*, 1363-1372.

Munn, D.H., Sharma, M.D., and Mellor, A.L. (2004). Ligation of B7-1/B7-2 by human CD4+ T cells triggers indoleamine 2,3-dioxygenase activity in dendritic cells. J Immunol *172*, 4100-4110.

Murphy, K., Travers, P. and Walport, M. (2008). Janeway's Immunobiology (Garland Science).

Myung, J., Kim, K.B., and Crews, C.M. (2001). The ubiquitin-proteasome pathway and proteasome inhibitors. Med Res Rev *21*, 245-273.

Naramura, M., Jang, I.K., Kole, H., Huang, F., Haines, D., and Gu, H. (2002). c-Cbl and Cbl-b regulate T cell responsiveness by promoting ligand-induced TCR down-modulation. Nat Immunol *3*, 1192-1199.

Nichols, B.J., and Lippincott-Schwartz, J. (2001). Endocytosis without clathrin coats. Trends Cell Biol *11*, 406-412.

Oberle, N., Eberhardt, N., Falk, C.S., Krammer, P.H., and Suri-Payer, E. (2007). Rapid suppression of cytokine transcription in human CD4+CD25 T cells by CD4+Foxp3+ regulatory T cells: independence of IL-2 consumption, TGF-beta, and various inhibitors of TCR signaling. J Immunol *179*, 3578-3587.

Obermuller, S., Kiecke, C., von Figura, K., and Honing, S. (2002). The tyrosine motifs of Lamp 1 and LAP determine their direct and indirect targetting to lysosomes. Journal of cell science *115*, 185-194.

Oderup, C., Cederbom, L., Makowska, A., Cilio, C.M., and Ivars, F. (2006). Cytotoxic T lymphocyte antigen-4-dependent down-modulation of costimulatory molecules on dendritic cells in CD4+ CD25+ regulatory T-cell-mediated suppression. Immunology *118*, 240-249.

Ohkuma, S., and Poole, B. (1978). Fluorescence probe measurement of the intralysosomal pH in living cells and the perturbation of pH by various agents. Proc Natl Acad Sci U S A *75*, 3327-3331.

Ohno, H. (2006a). Clathrin-associated adaptor protein complexes. Journal of cell science *119*, 3719-3721.

Ohno, H. (2006b). Physiological roles of clathrin adaptor AP complexes: lessons from mutant animals. Journal of biochemistry *139*, 943-948.

Ohno, H., Aguilar, R.C., Yeh, D., Taura, D., Saito, T., and Bonifacino, J.S. (1998). The medium subunits of adaptor complexes recognize distinct but overlapping sets of tyrosine-based sorting signals. J Biol Chem *273*, 25915-25921.

Onishi, Y., Fehervari, Z., Yamaguchi, T., and Sakaguchi, S. (2008). Foxp3+ natural regulatory T cells preferentially form aggregates on dendritic cells in vitro and actively inhibit their maturation. Proc Natl Acad Sci U S A *105*, 10113-10118.

Orabona, C., Belladonna, M.L., Vacca, C., Bianchi, R., Fallarino, F., Volpi, C., Gizzi, S., Fioretti, M.C., Grohmann, U., and Puccetti, P. (2005). Cutting edge: silencing suppressor of cytokine signaling 3 expression in dendritic cells turns CD28-Ig from immune adjuvant to suppressant. J Immunol *174*, 6582-6586.

Owen, D.J., Collins, B.M., and Evans, P.R. (2004). Adaptors for clathrin coats: structure and function. Annual review of cell and developmental biology *20*, 153-191.

Owen, D.J., and Evans, P.R. (1998). A structural explanation for the recognition of tyrosine-based endocytotic signals. Science *282*, 1327-1332.

Pandey, K.N. (2009). Functional roles of short sequence motifs in the endocytosis of membrane receptors. Frontiers in bioscience : a journal and virtual library *14*, 5339-5360.

Patino-Lopez, G., Dong, X., Ben-Aissa, K., Bernot, K.M., Itoh, T., Fukuda, M., Kruhlak, M.J., Samelson, L.E., and Shaw, S. (2008). Rab35 and its GAP EPI64C in T cells regulate receptor recycling and immunological synapse formation. J Biol Chem *283*, 18323-18330.

Pearse, B.M. (1976). Clathrin: a unique protein associated with intracellular transfer of membrane by coated vesicles. Proc Natl Acad Sci U S A *73*, 1255-1259.

Peggs, K.S., Quezada, S.A., and Allison, J.P. (2008). Cell intrinsic mechanisms of T-cell inhibition and application to cancer therapy. Immunol Rev *224*, 141-165.

Pelkmans, L., and Helenius, A. (2002). Endocytosis via caveolae. Traffic *3*, 311-320.

Perry, W.L., Hustad, C.M., Swing, D.A., O'Sullivan, T.N., Jenkins, N.A., and Copeland, N.G. (1998). The itchy locus encodes a novel ubiquitin protein ligase that is disrupted in a18H mice. Nature genetics *18*, 143-146.

Peters, C., Braun, M., Weber, B., Wendland, M., Schmidt, B., Pohlmann, R., Waheed, A., and von Figura, K. (1990). Targeting of a lysosomal membrane protein: a tyrosine-containing endocytosis signal in the cytoplasmic tail of lysosomal acid phosphatase is necessary and sufficient for targeting to lysosomes. Embo J *9*, 3497-3506.

Piper, R.C., and Luzio, J.P. (2001). Late endosomes: sorting and partitioning in multivesicular bodies. Traffic *2*, 612-621.

Qureshi, O.S., Kaur, S., Hou, T.Z., Jeffery, L.E., Poulter, N.S., Briggs, Z., Kenefeck, R., Willox, A.K., Royle, S.J., Rappoport, J.Z., and Sansom, D.M. (2012). Constitutive clathrin-mediated endocytosis of CTLA-4 persists during T cell activation. J Biol Chem *287*, 9429-9440.

Qureshi, O.S., Zheng, Y., Nakamura, K., Attridge, K., Manzotti, C., Schmidt, E.M., Baker, J., Jeffery, L.E., Kaur, S., Briggs, Z.*, et al.* (2011). Trans-endocytosis of CD80 and CD86: a molecular basis for the cell-extrinsic function of CTLA-4. Science *332*, 600-603.

Rajendran, L., Knolker, H.J., and Simons, K. (2010). Subcellular targeting strategies for drug design and delivery. Nature reviews. Drug discovery *9*, 29-42.

Razi, M., and Futter, C.E. (2006). Distinct roles for Tsg101 and Hrs in multivesicular body formation and inward vesiculation. Mol Biol Cell *17*, 3469-3483.

Ren, M., Xu, G., Zeng, J., De Lemos-Chiarandini, C., Adesnik, M., and Sabatini, D.D. (1998). Hydrolysis of GTP on rab11 is required for the direct delivery of transferrin from the pericentriolar recycling compartment to the cell surface but not from sorting endosomes. Proc Natl Acad Sci U S A *95*, 6187-6192.

Robinson, M.S. (2004). Adaptable adaptors for coated vesicles. Trends Cell Biol *14*, 167-174.

Roepstorff, K., Grandal, M.V., Henriksen, L., Knudsen, S.L., Lerdrup, M., Grovdal, L., Willumsen, B.M., and van Deurs, B. (2009). Differential effects of EGFR ligands on endocytic sorting of the receptor. Traffic *10*, 1115-1127.

Rudd, C.E. (2008). The reverse stop-signal model for CTLA4 function. Nat Rev Immunol *8*, 153-160.

Ruperto, N., Lovell, D.J., Quartier, P., Paz, E., Rubio-Perez, N., Silva, C.A., Abud-Mendoza, C., Burgos-Vargas, R., Gerloni, V., Melo-Gomes, J.A.*, et al.* (2008). Abatacept in children with juvenile idiopathic arthritis: a randomised, double-blind, placebo-controlled withdrawal trial. Lancet *372*, 383-391.

Russell, M.R., Nickerson, D.P., and Odorizzi, G. (2006). Molecular mechanisms of late endosome morphology, identity and sorting. Current opinion in cell biology *18*, 422-428.

Sabharanjak, S., Sharma, P., Parton, R.G., and Mayor, S. (2002). GPI-anchored proteins are delivered to recycling endosomes via a distinct cdc42-regulated, clathrin-independent pinocytic pathway. Dev Cell *2*, 411-423.

Sadowski, M., and Sarcevic, B. (2010). Mechanisms of mono- and poly-ubiquitination: Ubiquitination specificity depends on compatibility between the E2 catalytic core and amino acid residues proximal to the lysine. Cell division *5*, 19.

Saito, T., and Yamasaki, S. (2003). Negative feedback of T cell activation through inhibitory adapters and costimulatory receptors. Immunol Rev *192*, 143-160.

Sakaguchi, S. (2000). Regulatory T cells: key controllers of immunologic self-tolerance. Cell *101*, 455-458.

Sakaguchi, S., Wing, K., and Miyara, M. (2007). Regulatory T cells - a brief history and perspective. Eur J Immunol *37 Suppl 1*, S116-123.

Sandvig, K., and van Deurs, B. (2002). Membrane traffic exploited by protein toxins. Annual review of cell and developmental biology *18*, 1-24.

Sansom, D.M., and Walker, L.S. (2006). The role of CD28 and cytotoxic T-lymphocyte antigen-4 (CTLA-4) in regulatory T-cell biology. Immunol Rev *212*, 131-148.

Schlessinger, J. (1988). The epidermal growth factor receptor as a multifunctional allosteric protein. Biochemistry *27*, 3119-3123.

Schmidt, A., Oberle, N., and Krammer, P.H. (2012). Molecular mechanisms of treg-mediated T cell suppression. Front Immunol *3*, 51.

Schmidt, O., and Teis, D. (2012). The ESCRT machinery. Curr Biol *22*, R116-120.

Schneider, H., Martin, M., Agarraberes, F.A., Yin, L., Rapoport, I., Kirchhausen, T., and Rudd, C.E. (1999). Cytolytic T lymphocyte-associated antigen-4 and the TCR zeta/CD3 complex, but not CD28, interact with clathrin adaptor complexes AP-1 and AP-2. J Immunol *163*, 1868-1879.

Schwartz, J.C., Zhang, X., Fedorov, A.A., Nathenson, S.G., and Almo, S.C. (2001). Structural basis for co-stimulation by the human CTLA-4/B7-2 complex. Nature *410*, 604-608.

Schwartz, R.H. (1992). Costimulation of T lymphocytes: the role of CD28, CTLA-4, and B7/BB1 in interleukin-2 production and immunotherapy. Cell *71*, 1065-1068.

Schwartz, R.H. (1996). Models of T cell anergy: is there a common molecular mechanism? J Exp Med *184*, 1-8.

Schwarz, B.A., and Bhandoola, A. (2006). Trafficking from the bone marrow to the thymus: a prerequisite for thymopoiesis. Immunol Rev *209*, 47-57.

Seabra, M.C., and Wasmeier, C. (2004). Controlling the location and activation of Rab GTPases. Current opinion in cell biology *16*, 451-457.

Shahinian, A., Pfeffer, K., Lee, K.P., Kundig, T.M., Kishihara, K., Wakeham, A., Kawai, K., Ohashi, P.S., Thompson, C.B., and Mak, T.W. (1993). Differential T cell costimulatory requirements in CD28-deficient mice. Science *261*, 609-612.

Sharpe, A.H., and Freeman, G.J. (2002). The B7-CD28 superfamily. Nat Rev Immunol *2*, 116-126.

Shaw, J.P., Utz, P.J., Durand, D.B., Toole, J.J., Emmel, E.A., and Crabtree, G.R. (1988). Identification of a putative regulator of early T cell activation genes. Science *241*, 202-205.

Sheff, D.R., Daro, E.A., Hull, M., and Mellman, I. (1999). The receptor recycling pathway contains two distinct populations of early endosomes with different sorting functions. J Cell Biol *145*, 123-139.

Shiratori, T., Miyatake, S., Ohno, H., Nakaseko, C., Isono, K., Bonifacino, J.S., and Saito, T. (1997). Tyrosine phosphorylation controls internalization of CTLA-4 by regulating its interaction with clathrin-associated adaptor complex AP-2. Immunity *6*, 583-589.

Slot, J.W., Geuze, H.J., Gigengack, S., James, D.E., and Lienhard, G.E. (1991a). Translocation of the glucose transporter GLUT4 in cardiac myocytes of the rat. Proc Natl Acad Sci U S A *88*, 7815-7819.

Slot, J.W., Geuze, H.J., Gigengack, S., Lienhard, G.E., and James, D.E. (1991b). Immuno-localization of the insulin regulatable glucose transporter in brown adipose tissue of the rat. J Cell Biol *113*, 123-135.

Sorkin, A. (2000). The endocytosis machinery. J Cell Sci *113 Pt 24*, 4375-4376.

Sorkin, A., and von Zastrow, M. (2009). Endocytosis and signalling: intertwining molecular networks. Nature reviews. Molecular cell biology *10*, 609-622.

Stamper, C.C., Zhang, Y., Tobin, J.F., Erbe, D.V., Ikemizu, S., Davis, S.J., Stahl, M.L., Seehra, J., Somers, W.S., and Mosyak, L. (2001). Crystal structure of the B7-1/CTLA-4 complex that inhibits human immune responses. Nature *410*, 608-611.

Stenmark, H. (2009). Rab GTPases as coordinators of vesicle traffic. Nature reviews. Molecular cell biology *10*, 513-525.

Swanson, J.A., and Watts, C. (1995). Macropinocytosis. Trends Cell Biol *5*, 424-428.

Tadokoro, C.E., Shakhar, G., Shen, S., Ding, Y., Lino, A.C., Maraver, A., Lafaille, J.J., and Dustin, M.L. (2006). Regulatory T cells inhibit stable contacts between CD4+ T cells and dendritic cells in vivo. J Exp Med *203*, 505-511.

Tang, Q., Adams, J.Y., Tooley, A.J., Bi, M., Fife, B.T., Serra, P., Santamaria, P., Locksley, R.M., Krummel, M.F., and Bluestone, J.A. (2006). Visualizing regulatory T cell control of autoimmune responses in nonobese diabetic mice. Nat Immunol *7*, 83-92.

Teft, W.A., Kirchhof, M.G., and Madrenas, J. (2006). A molecular perspective of CTLA-4 function. Annu Rev Immunol *24*, 65-97.

Tivol, E.A., Borriello, F., Schweitzer, A.N., Lynch, W.P., Bluestone, J.A., and Sharpe, A.H. (1995). Loss of CTLA-4 leads to massive lymphoproliferation and fatal multiorgan tissue destruction, revealing a critical negative regulatory role of CTLA-4. Immunity *3*, 541-547.

Toda, A., and Piccirillo, C.A. (2006). Development and function of naturally occurring CD4+CD25+ regulatory T cells. Journal of leukocyte biology *80*, 458-470.

Traub, L.M. (2003). Sorting it out: AP-2 and alternate clathrin adaptors in endocytic cargo selection. J Cell Biol *163*, 203-208.

Traub, L.M. (2005). Common principles in clathrin-mediated sorting at the Golgi and the plasma membrane. Biochim Biophys Acta *1744*, 415-437.

Trowbridge, I.S., Collawn, J.F., and Hopkins, C.R. (1993). Signal-dependent membrane protein trafficking in the endocytic pathway. Annu Rev Cell Biol *9*, 129-161.

Ueda, H., Howson, J.M., Esposito, L., Heward, J., Snook, H., Chamberlain, G., Rainbow, D.B., Hunter, K.M., Smith, A.N., Di Genova, G.*, et al.* (2003). Association of the T-cell regulatory gene CTLA4 with susceptibility to autoimmune disease. Nature *423*, 506-511.

Ullrich, O., Reinsch, S., Urbe, S., Zerial, M., and Parton, R.G. (1996). Rab11 regulates recycling through the pericentriolar recycling endosome. J Cell Biol *135*, 913-924.

Urbanowski, J.L., and Piper, R.C. (2001). Ubiquitin sorts proteins into the intralumenal degradative compartment of the late-endosome/vacuole. Traffic *2*, 622-630.

Valitutti, S., Muller, S., Salio, M., and Lanzavecchia, A. (1997). Degradation of T cell receptor (TCR)-CD3-zeta complexes after antigenic stimulation. J Exp Med *185*, 1859-1864.

van der Aa, M.A., Huth, U.S., Hafele, S.Y., Schubert, R., Oosting, R.S., Mastrobattista, E., Hennink, W.E., Peschka-Suss, R., Koning, G.A., and Crommelin, D.J. (2007). Cellular uptake of cationic polymer-DNA complexes via caveolae plays a pivotal role in gene transfection in COS-7 cells. Pharmaceutical research *24*, 1590-1598.

Vardhana, S., Choudhuri, K., Varma, R., and Dustin, M.L. (2010). Essential role of ubiquitin and TSG101 protein in formation and function of the central supramolecular activation cluster. Immunity *32*, 531-540.

Vendruscolo, M., Zurdo, J., MacPhee, C.E., and Dobson, C.M. (2003). Protein folding and misfolding: a paradigm of self-assembly and regulation in complex biological systems. Philosophical transactions. Series A, Mathematical, physical, and engineering sciences *361*, 1205-1222.

Verstreken, P., Kjaerulff, O., Lloyd, T.E., Atkinson, R., Zhou, Y., Meinertzhagen, I.A., and Bellen, H.J. (2002). Endophilin mutations block clathrin-mediated endocytosis but not neurotransmitter release. Cell *109*, 101-112.

Walker, L.S., and Sansom, D.M. (2011). The emerging role of CTLA4 as a cell-extrinsic regulator of T cell responses. Nat Rev Immunol *11*, 852-863.

Walunas, T.L., Bakker, C.Y., and Bluestone, J.A. (1996). CTLA-4 ligation blocks CD28-dependent T cell activation. J Exp Med *183*, 2541-2550.

Wang, L.H., Sudhof, T.C., and Anderson, R.G. (1995). The appendage domain of alpha-adaptin is a high affinity binding site for dynamin. J Biol Chem *270*, 10079-10083.

Watanabe, N., and Nakajima, H. (2012). Coinhibitory molecules in autoimmune diseases. Clinical & developmental immunology *2012*, 269756.

Waterhouse, P., Penninger, J.M., Timms, E., Wakeham, A., Shahinian, A., Lee, K.P., Thompson, C.B., Griesser, H., and Mak, T.W. (1995). Lymphoproliferative disorders with early lethality in mice deficient in Ctla-4. Science *270*, 985-988.

Waterman, H., Sabanai, I., Geiger, B., and Yarden, Y. (1998). Alternative intracellular routing of ErbB receptors may determine signaling potency. J Biol Chem *273*, 13819-13827.

Wing, K., Onishi, Y., Prieto-Martin, P., Yamaguchi, T., Miyara, M., Fehervari, Z., Nomura, T., and Sakaguchi, S. (2008). CTLA-4 control over Foxp3+ regulatory T cell function. Science *322*, 271-275.

Wollert, T., and Hurley, J.H. (2010). Molecular mechanism of multivesicular body biogenesis by ESCRT complexes. Nature *464*, 864-869.

Wollert, T., Wunder, C., Lippincott-Schwartz, J., and Hurley, J.H. (2009). Membrane scission by the ESCRT-III complex. Nature *458*, 172-177.

Xing, Y., and Hogquist, K.A. (2012). T-cell tolerance: central and peripheral. Cold Spring Harbor perspectives in biology *4*.

Yasir, M., Pachikara, N.D., Bao, X., Pan, Z., and Fan, H. (2011). Regulation of chlamydial infection by host autophagy and vacuolar ATPase-bearing organelles. Infect Immun *79*, 4019-4028.

Yudowski, G.A., Puthenveedu, M.A., Henry, A.G., and von Zastrow, M. (2009). Cargo-mediated regulation of a rapid Rab4-dependent recycling pathway. Mol Biol Cell *20*, 2774-2784.

Zhang, Y., and Allison, J.P. (1997). Interaction of CTLA-4 with AP50, a clathrin-coated pit adaptor protein. Proc Natl Acad Sci U S A *94*, 9273-9278.

APPENDIX

Published in final edited form as:
J Immunol. 2012 December 1; 189(11): 5155–5164. doi:10.4049/jimmunol.1200786.

Availability of 25-hydroxyvitamin D_3 to antigen presenting cells controls the balance between regulatory and inflammatory T cell responses

Louisa E. Jeffery[*], **Alice M. Wood**[†], **Omar S Qureshi**[*], **Tie Zheng Hou**[*], **David Gardner**[*], **Zoe Briggs**[*], **Satdip Kaur**[*], **Karim Raza**[*,‡], and **David M. Sansom**[*]

[*]MRC Centre for Immune Regulation, School of Immunity and Infection, Institute of Biomedical Research, University of Birmingham College of Medical and Dental Sciences, Birmingham, B15 2TT, UK

[†]School of Clinical and Experimental Medicine University of Birmingham College of Medical and Dental Sciences, Birmingham, B15 2TT, UK

[‡]Department of Rheumatology, Sandwell and West Birmingham Hospitals NHS Trust, Birmingham, B18 7QH, UK

Abstract

1,25-dihydroxyvitamin D_3 ($1,25(OH)_2D_3$), the active form of vitamin D, exerts potent effects on several tissues including cells of the immune system, where it affects T cell activation, differentiation and migration. The circulating, inactive form of vitamin D, $25(OH)D_3$, is generally used as an indication of "vitamin D status". However, utilization of this precursor depends on its uptake by cells and subsequent conversion by the enzyme $25(OH)D_3$-1α-hydroxylase (CYP27B1) into active $1,25(OH)_2D_3$. Using human T cells, we now show that addition of inactive $25(OH)D_3$ is sufficient to alter T cell responses only when dendritic cells (DCs) are present. Mechanistically, CYP27B1 is induced in DCs upon maturation with LPS or upon T cell contact resulting in the generation and release of $1,25(OH)_2D_3$ which subsequently affects T cell responses. In most tissues, vitamin D binding protein (DBP) acts as a carrier to enhance the utilization of vitamin D. However, we show that DBP modulates T cell responses by restricting the availability of inactive $25(OH)D_3$ to DC. These data indicate that the level of "free" $25(OH)D_3$ available to DCs determines the inflammatory/regulatory balance of ensuing T cell responses.

Introduction

Besides its longstanding association with calcium regulation and bone density, more widespread physiological roles for vitamin D are now acknowledged. This is consistent with the broad distribution of the vitamin D receptor throughout the body[1] and the association of low vitamin D status with numerous diseases in epidemiological studies[2]. Interestingly, low vitamin D appears to increase the risk of immune related diseases, including multiple sclerosis[3,4], rheumatoid arthritis (RA)[5], type 1 diabetes[6] and inflammatory bowel disease[7]. Thus, vitamin D appears to have an important immune-regulatory function, which may have implications for the treatment of many conditions. Consistent with this, vitamin D supplementation in mouse models of autoimmunity has been demonstrated to have prophylactic and therapeutic benefit[8-13]. *In-vitro* studies have also identified profound immunological effects of 1,25-dihydroxyvitamin D_3 ($1,25(OH)_2D_3$), the biologically active

Correspondence to: Professor David M. Sansom, School of Immunity and Infection, IBR building, Room 430, College of Medical and Dental Sciences, University of Birmingham, B15 2TT, UK, Tel (44) 121 414 2268, Fax (44)121 414 3599, d.m.sansom@bham.ac.uk.

Europe PMC Funders Author Manuscripts

Published in final edited form as:
Science. 2011 April 29; 332(6029): 600–603. doi:10.1126/science.1202947.

Trans-endocytosis of CD80 and CD86: a molecular basis for the cell extrinsic function of CTLA-4 **

Omar S. Qureshi[1], **Yong Zheng**[1], **Kyoko Nakamura**[1], **Kesley Attridge**[1], **Claire Manzotti**[1], **Emily M. Schmidt**[1], **Jennifer Baker**[1], **Louisa E. Jeffery**[1], **Satdip Kaur**[1], **Zoe Briggs**[1], **Tie Z. Hou**[1], **Clare E. Futter**[2], **Graham Anderson**[1], **Lucy S.K. Walker**[1], and **David M. Sansom**[1,*]

[1]MRC Centre for Immune Regulation, School of Immunity and Infection, Institute of Biomedical Research, University of Birmingham Medical School, Birmingham, B15 2TT, UK.

[2]Department of Cell Biology, University College London Institute of Ophthalmology, University College London, London, EC1V 9EL, UK.

Abstract

CTLA-4 is an essential negative regulator of T cell immune responses whose mechanism of action is the subject of debate. CTLA-4 also shares two ligands (CD80 and CD86) with a stimulatory receptor, CD28. Here we show that CTLA-4 can capture its ligands from opposing cells by a process of trans-endocytosis. Following removal, these costimulatory ligands are degraded inside CTLA-4-expressing cells resulting in impaired costimulation via CD28. Acquisition of CD86 from antigen presenting cells is stimulated by TCR engagement and observed *in vitro* and *in vivo*. These data reveal a mechanism of immune regulation whereby CTLA-4 acts as an effector molecule to inhibit CD28 costimulation by the cell-extrinsic depletion of ligands, accounting for many of the known features of the CD28-CTLA-4 system.

Keywords

CTLA-4; CD86; T cell; dendritic cell; suppression

The T cell protein CTLA-4 is essential to the prevention of autoimmune disease (1-3). Although the molecular basis for CTLA-4 action has been suggested to be a cell-intrinsic inhibitory signal(4) possibly mediated by the cytoplasmic domain (5), a cell-extrinsic function for CTLA-4 is clearly evident from *in vivo* models (6-13). Therefore a molecular explanation of CTLA-4 function compatible with such a cell-extrinsic mechanism is needed. The intercellular transfer of a ligand from one cell to its receptor on a different cell is observed in both immune settings and elsewhere (14-19). Because of its highly endocytic behaviour, we tested whether CTLA-4 could potentially act in such a manner in order to deplete its ligands and thereby extrinsically inhibit T cell activation via CD28. We cultured CTLA-4-expressing (CTLA-4$^+$) CHO cells with donor CHO cells expressing a C-terminally tagged CD86 protein (CD86-GFP). Using a flow cytometric assay we observed substantial transfer of CD86 into CTLA-4$^+$ cells (Fig. 1A and fig. S1). This finding was confirmed by confocal microscopy where acquisition of ligand by CTLA-4 caused the appearance of CD86 containing vesicles within the CTLA-4$^+$ cell (Fig. 1B). Treatment with the lysosomal inhibitor bafilomycin A caused an increase in detectable CD86-GFP after transfer (Fig 1A),

*To whom correspondence should be addressed. D.M.Sansom@bham.ac.uk.

Europe PMC Funders Author Manuscripts

Cell Biology:

Constitutive Clathrin-mediated Endocytosis of CTLA-4 Persists during T Cell Activation

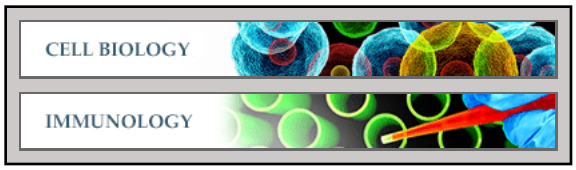

Omar S. Qureshi, Satdip Kaur, Tie Zheng Hou, Louisa E. Jeffery, Natalie S. Poulter, Zoe Briggs, Rupert Kenefeck, Anna K. Willox, Stephen J. Royle, Joshua Z. Rappoport and David M. Sansom

J. Biol. Chem. 2012, 287:9429-9440.
doi: 10.1074/jbc.M111.304329 originally published online January 19, 2012
